UNIVERSIDAD AUTÓNOMA DE MADRID

FACULTAD DE CIENCIAS

Departamento de Química-Física Aplicada

UNA EVALUACIÓN ALIMENTÓMICA DE LA ACTIVIDAD ANTICANCERÍGENA DE POLIFENOLES DE ORIGEN ALIMENTARIO

ALBERTO VALDÉS TABERNERO

Tesis doctoral

Mención internacional

INSTITUTO DE INVESTIGACIÓN EN CIENCIAS DE LA ALIMENTACIÓN (CIAL)

Madrid, 2016

UNIVERSIDAD AUTÓNOMA DE MADRID

FACULTAD DE CIENCIAS

Departamento de Química-Física Aplicada

UNA EVALUACIÓN ALIMENTÓMICA DE LA ACTIVIDAD ANTICANCERÍGENA DE POLIFENOLES DE ORIGEN ALIMENTARIO

Memoria presentada por:

ALBERTO VALDÉS TABERNERO

Para optar al grado de

DOCTOR EN BIOLOGÍA Y CIENCIAS DE LA ALIMENTACIÓN

(MENCIÓN INTERNACIONAL)

Directores del trabajo:	Dr. Alejandro Cifuentes Gallego
	Dra. Virginia García Cañas
	Instituto de Investigación en Ciencias de la Alimentación (CIAL-CSIC)
Tutor académico:	Dr. Guillermo Reglero Rada
	Universidad Autónoma de Madrid (UAM)

D. Alejandro Cifuentes Gallego, Dr. en Ciencias Químicas, Profesor de Investigación en el Instituto de Investigación en Ciencias de la Alimentación del C.S.I.C., y

Dª. Virginia García Cañas, Dra. en Ciencia y Tecnología de los Alimentos, Científico Titular en el Instituto de Investigación en Ciencias de la Alimentación del C.S.I.C.

CERTIFICAN:

Que el presente trabajo, titulado "**UNA EVALUACIÓN ALIMENTÓMICA DE LA ACTIVIDAD ANTICANCERÍGENA DE POLIFENOLES DE ORIGEN ALIMENTARIO**", y que constituye la Memoria que presenta D. Alberto Valdés Tabernero para optar al grado de Doctor en Biología y Ciencias de la Alimentación, ha sido realizada en el Departamento de Bioactividad y Análisis de Alimentos en el Instituto de Investigación en Ciencias de la Alimentación del C.S.I.C., bajo nuestra dirección.

Y para que así conste, firman el presente certificado en Madrid a 25 de mayo de 2016.

Fdo. D. Alejandro Cifuentes Gallego **Fdo. Dª. Virginia García Cañas**

A mis padres…

AGRADECIMIENTOS

En primer lugar, me gustaría agradecer a mis directores de tesis, Alejandro y Virginia, por haberme dado la oportunidad de incorporarme a su grupo de investigación hace más de cinco años. Muchas gracias por vuestro apoyo, paciencia, confianza, y facilidades que me habéis dado. Me siento muy afortunado de haber aprendido de investigadores como vosotros. Particularmente Virginia, me gustaría agradecerte toda la ayuda que me has prestado, tanto científica como personal, y por hacerme ver las cosas de forma positiva cuando he pasado momentos difíciles.

También me gustaría agradecer a la Prof. Elena Ibáñez toda su ayuda y sus consejos durante estos años, y por haberme "traído" al mundo de la investigación.

Gracias al Dr. Guillermo Reglero, por ser mi tutor académico y por ofrecerme siempre su ayuda y disponibilidad.

Me gustaría agradecer a la Universidad Autónoma de Madrid y a la Fundación de la Universidad Autónoma de Madrid las becas que me concedieron durante el primer año y medio de tesis, y al Ministerio de Economía y Competitividad la beca predoctoral FPI que he percibido durante los últimos cuatro años, y la ayuda a las estancias breves en el extranjero que disfruté en el laboratorio de Jonas Bergquist.

Gracias a los doctores Carolina Simó, Miguel Herrero y José Antonio Mendiola, por ofrecerme siempre su ayuda cuando lo he necesitado. Y al resto de los integrantes del grupo Foodomics o que en algún momento lo fueron (Lidia, Andrea, Tanize, Bienve, Clara, María, Marina, Peppe, Joana, Luci, Engin), con quienes he tenido la suerte de compartir laboratorio durante estos años.

I would like to thank Dr. Jonas Bergquist and Dr. Konstantin A. Artemenko to kindly accept my short-term stay in their lab (Biomedical Centre-Analytical Chemistry Department, Uppsala University, Sweden), and for all their help.

También me gustaría agradecer al resto de compañeros del CIAL (Marta, Dani, Carlos, Alba, Tomas, Elvira, Pilar, Dani, Cris, Bea, Marta, Laura, Pablo) con quien comer, tomar un café, salir a correr o tomar una cerveza es un placer. Asimismo, me gustaría dedicar un agradecimiento a la dirección del CIAL, y al personal de administración y mantenimiento; Vivi, Tiziana, Macarena, Josefina, Julia, Rubén, José, Pedro, Isidoro…gracias por la ayuda y la amabilidad con la que he contado en todo momento.

Como no, también quiero dar las gracias a mis amigos, por apoyarme, aunque no sepan qué hago y por qué voy al laboratorio a las 3 de la mañana…Gracias por todos los buenos momentos que hemos pasado ¡y por los que quedan!

Por último, quiero dedicar esta tesis a mis padres Miguel Ángel y Ana Isabel, por todo lo que nos habéis dado y enseñado. Llegar hasta aquí hubiera sido imposible sin vosotros. Y a mis hermanos Patricia y Miguel, por aconsejarme, soportarme, quererme e incluso, seguirme. Miguel, me alegra que hayas decidido hacer el doctorado y te vaya todo genial. ¡Te lo mereces!

A todos vosotros, **¡muchísimas gracias!**

ÍNDICE

ÍNDICE

ABREVIATURAS

ABREVIATURAS

2-DE (*two-dimensional gel electrophoresis*): electroforesis bidimensional en gel.

APC (*adenomatous polyposis coli*): poliposis adenomatosa coli o familiar.

AQUA (*absolute quantification*): cuantificación absoluta.

ATP (*adenosine 5′-triphosphate*): adenosina 5′-trifosfato.

BCR-ABL (*breakpoint cluster region/Abelson tyrosine-protein kinase*).

CE (*capillary electrophoresis*): electroforesis capilar.

DML (*dimethyl labeling*): marcaje isotópico con dimetilo.

EMT (*epithelial–mesenchymal transition*): transición epitelio-mesénquima.

DNA (*deoxyribonucleic acid*): ácido desoxirribonucleico.

DNAc (*complementary DNA*): ADN complementario.

ERAD (e*ndoplasmic-reticulum-associated protein degradation*): degradación de proteínas asociadas al retículo endoplasmático.

ESI (*electrospray ionization*): ionización por electrospray.

FDA (*food and drug administration*): Administración para alimentos y fármacos.

FDR (*false discovery rate*): tasa de falsos positivos.

FT-ICR (*Fourier transform ion cyclotron resonance*): resonancia de ión ciclotrón con transformada de Fourier.

GC (*gas chromatography*): cromatografía de gases.

GCNT3 (*glucosaminyl (N-acetyl) transferase-3*): N-acetil-glucosaminil transferasa-3.

GI50 (*50% growth inhibition*): concentración inhibitoria del 50% del crecimiento.

GO (*gene ontology*): onlotogía génica.

GRAS (*generally recognized as safe*): generalmente reconocido como seguro.

GSEA (*gene set enrichment analysis*): análisis de enriquecimiento del conjunto de genes.

IPA (*Ingenuity pathway analysis*): análisis de rutas por Ingenuity.

iTRAQ (*isobaric tags for relative and absolute quantification*): marcaje isobárico para la cuantificación relativa y absoluta.

KEAP1 (*kelch-like ECH-associated protein-1*): proteína asociada a ECH-1 similar a kelch.

KEGG (*Kyoto encyclopedia of genes and genomes*): enciclopedia de genes y genomas de Kyoto.

LC (*liquid chromatography*): cromatografía de líquidos.

LC50 (*50% lethal concentration*): concentración letal del 50% de las células.

LTQ (*linear ion trap*): trampa de iones lineal.

m/z (*mass-to-charge ratio*): relación masa-carga.

MALDI (*matrix-assisted laser desorption/ionization*): desorción/ionización láser asistida por matriz.

MAS 5 (*microarray suite 5.0*).

MMP-2 (*matrix metalloproteinase-2*): metaloproteinasa de matriz-2.

MMP-9 (*matrix metalloproteinase-9*): metaloproteinasa de matriz-9.

MPSS (*massively parallel signature sequencing*): determinación masiva de secuencias en paralelo.

MRM (*multiple-reaction monitoring*): monitorización de múltiples reacciones.

MS (*mass spectrometry*): espectrometría de masas.

mTOR (*mammalian target of rapamycin*): diana de rapamicina en células de mamífero.

MTT (*3-(4,5-dimethylthiazol-2-yl)-2,5-diphenyltetrazolium bromide*).

NADPH (*nicotinamide adenine dinucleotide phosphate*): nicotinamida adenina dinucleótido fosfato.

NRF2 (*nuclear factor (erythroid-derived 2)-like 2*): factor de transcripción nuclear eritroide-2.

PARP1 (*poly (ADP-ribose) polymerase-1*): poli ADP ribosa polimerasa-1.

PCR (*polymerase chain reaction*): reacción en cadena de la polimerasa.

PLE (*pressurized liquid extraction*): extracción con fluidos presurizados.

PLIER (*probe logarithmic error estimation*).

Q (*quadrupole*): cuadrupolo.

RMA (*robust multi-array analysis*).

RMN (*nuclear magnetic resonance*): resonancia magnética nuclear.

RNA (*ribonucleic acid*): ácido ribonucleico.

RNAm (*messenger RNA*): ARN mensajero.

RNA-Seq (*RNA sequencing*): secuenciación del ARN.

RPKM (*reads per kilobase per million mapped reads*): lecturas por kilobase por millón de lecturas mapeadas.

RT-qPCR (*quantitative reverse transcription PCR*): retrotranscripción PCR cuantitativa.

SAGE (*serial analysis of gene expression*): análisis seriado de la expresión génica.

SFE (*supercritical fluid extraction*): extracción con fluidos supercríticos.

SILAC (*stable isotope labeling by amino acids in cell culture*): marcaje de aminoácidos con isótopos estables en medio de cultivo.

SNP (*single nucleotide polymorphism*): polimorfismo de nucleótidos simples.

SRM (*selected-reaction monitoring*): monitorización de la reacción seleccionada.

STAT3 (*signal transducer and activator of transcription-3*): transductor de señal y activador de la transcripción-3.

TGI (*total growth inhibition*): concentración inhibitoria del 100% del crecimiento.

TIMP-2 (*metallopeptidase inhibitor-2*): inhibidor de metalopeptinasa-2.

TKI (*tyrosine kinase inhibitor*): inhibidor de la tirosin-quinasa.

TNT (*tandem mass tags*): marcaje de masas en tándem.

TOF (*time of flight*): tiempo de vuelo.

TSC2 (*tuberous sclerosis complex-2*): complejo de esclerosis tuberosa-2.

UHPLC: (*ultra high performance liquid chromatography*): cromatografía de líquidos de ultra alta resolución.

uPA (*urokinase-type plasminogen activator*): activador de plasminógeno tipo uroquinasa.

RESUMEN/

SUMMARY

RESUMEN

Aunque el cáncer es una enfermedad genética que representa una de las mayores causas de morbilidad y mortalidad en el mundo, numerosos estudios epidemiológicos indican una menor incidencia de esta enfermedad en poblaciones que siguen preferentemente una "Dieta Mediterránea". Dentro de los alimentos contenidos en esta dieta se encuentra el romero, una planta rica en polifenoles que ha demostrado tener efectos anticancerígenos debido a su actividad quimioprotectora, antiproliferativa y antimetastásica. Tradicionalmente, la determinación de la actividad anticancerígena del romero se ha llevado a cabo mediante metodologías analíticas dirigidas al estudio de un grupo reducido de marcadores moleculares. Sin embargo, la integración de metodologías avanzadas de análisis en Nutrición y en Ciencia y Tecnología de los Alimentos ha permitido el desarrollo de nuevas estrategias como, por ejemplo, la Alimentómica, que permiten el estudio de los alimentos desde una perspectiva más global. Esta estrategia se basa en el empleo de técnicas ómicas (fundamentalmente Transcriptómica, Proteómica y Metabolómica) para investigar los alimentos y sus múltiples conexiones con la Nutrición y la salud. El enfoque alimentómico dirigido al estudio del efecto de los componentes de la dieta en el tratamiento y prevención de enfermedades crónicas permite obtener información detallada acerca de los cambios moleculares que se producen en los sistemas biológicos. En la presente Tesis doctoral se ha utilizado esta estrategia Alimentómica con el objetivo de estudiar, siguiendo una aproximación global, el efecto antiproliferativo de polifenoles de romero en distintos modelos celulares de leucemia y cáncer de colon.

En primer lugar, se estudió el efecto antiproliferativo y el efecto en la progresión del ciclo celular de varios extractos de romero en las células de leucemia y cáncer de colon. De todos los extractos ensayados, aquel obtenido mediante fluidos supercríticos empleando

CO_2 a 40 ºC, 150 bares de presión y 7% de etanol presentó un efecto antiproliferativo mayor, por lo que se seleccionó este extracto enriquecido en polifenoles para estudiar sus efectos en el transcriptoma, el proteoma y el metaboloma de los distintos modelos celulares. Estos estudios se llevaron a cabo utilizando tecnologías de análisis de alto rendimiento, como son los microarrays de expresión génica y la electroforesis capilar/cromatografía de líquidos acopladas a espectrometría de masas, y herramientas bioinformáticas avanzadas, que permiten la interpretación y la integración de la enorme cantidad de datos generados. Los resultados obtenidos en estos estudios indican que el tratamiento con los polifenoles de romero activa la *Respuesta al Estrés Oxidativo* mediante la activación del factor de transcripción NRF2. Además, estos estudios demuestran que el tratamiento con el extracto de romero (especialmente con ácido carnósico) induce la activación temprana de la *Respuesta a Proteínas Desplegadas*, altera la homeostasis proteica, induce la acumulación de colesterol y reprime la actividad del factor de transcripción E2F1 en las células de cáncer de colon HT-29. Por otro lado, se ha demostrado por primera vez que el carnosol inhibe de forma directa la actividad catalítica del proteasoma (IC50 = 16.5 μM), un complejo multi-enzimático utilizado como diana terapéutica en el tratamiento del cáncer.

En resumen, el estudio llevado a cabo en esta Tesis doctoral ha demostrado que los polifenoles de romero tienen actividad antiproliferativa en distintos modelos celulares de cáncer. Además, el empleo de una estrategia Alimentómica ha permitido estudiar el efecto de estos compuestos a nivel molecular, así como establecer los posibles mecanismos de acción responsables de la actividad antiproliferativa observados.

SUMMARY

Although cancer is a genetic disease that represents one of the major causes of morbidity and mortality worldwide, several epidemiological studies have demonstrated a lower incidence of this disease in populations that follow a “Mediterranean Diet”. This diet includes the consumption of several vegetables, such as Rosemary, a Mediterranean herb rich in polyphenols that has shown anticancer effects due to its chemoprotective, antiproliferative and antimetastatic activities. Rosemary anticancer effects have commonly been investigated using analytical methodologies focused on a limited group of molecular markers. However, the use of advanced methodologies in Nutrition and Food Science has allowed the development of new strategies, such as Foodomics, that enables the study of food from a global perspective. This strategy is based on the use of omics techniques (mainly transcriptomics, proteomics and metabolomics) to investigate food and its multiple connections with nutrition and health. The Foodomics approach aimed at studying the effect of dietary components in the treatment and prevention of chronic diseases provides detailed information about the molecular changes that occur in a biological system. In this PhD Thesis work, we have applied a Foodomics method to study, following a global approach, the antiproliferative activity of rosemary polyphenols against different leukemia and colon cancer cells.

Firstly, the antiproliferative activity and the effect of various rosemary extracts on the cell cycle progression were studied in the different leukemia and colon cancer cells. Among the various tested rosemary extracts, the extract obtained using supercritical CO_2 at 40 ºC, 150 bars and 7% of ethanol showed the highest antiproliferative activity, and this extract (enriched in polyphenols) was selected to study its effect on the transcriptome, proteome and metabolome of the different cell culture models. These studies were carried

out using high throughput technologies, such as gene expression microarray and capillary electrophoresis/liquid chromatography coupled to mass spectrometry, and advanced bioinformatics tools, for interpretation and integration of the information. The results obtained in these studies indicate that rosemary polyphenols activate the *Oxidative Stress Response* through the activation of NRF2 transcription factor. Furthermore, these studies also demonstrate that rosemary extract and carnosic acid treatment induce early activation of *Unfolded Protein Response*, alter protein homeostasis, induce cholesterol accumulation and repress the activity of E2F1 transcription factor in HT-29 colon cancer cells. Moreover, it has been demonstrated for the first time that carnosol directly inhibits the catalytic activity of the proteasome (IC50 = 16.5 μM), a multi-enzymatic complex used as a therapeutic target in cancer treatment.

In summary, the study carried out in this PhD Thesis work has demonstrated that rosemary polyphenols have antiproliferative activity in different cancer cell models. In addition, the Foodomics approach applied has allowed us to study the effect of these compounds at molecular level and to establish the possible mechanisms of action responsible of the observed antiproliferative activity.

ESTRUCTURA DE LA MEMORIA

ESTRUCTURA DE LA MEMORIA

La presente Memoria se encuentra estructurada en cinco secciones, detalladas a continuación:

Introducción: presentación de los fundamentos y antecedentes correspondientes a los trabajos realizados.

Objetivos y plan de trabajo: planteamiento de los objetivos generales y parciales de esta Memoria, así como la descripción de la metodología, los procedimientos aplicados, y las tareas realizadas para alcanzar los objetivos planteados.

Resultados y discusión: exposición de los resultados obtenidos divididos en dos secciones encabezadas cada una por un prefacio, donde se explica de forma general y resumida el contenido de cada sección. En estos prefacios se justifican y enlazan las publicaciones derivadas de esta Memoria, las que se incluyen a continuación, en el formato original en que se encuentran publicadas.

Discusión general: se presenta una discusión general de los trabajos presentados en la Memoria, relacionando los resultados obtenidos en las distintas secciones.

Conclusiones: presentación de las conclusiones generales más relevantes obtenidas de los trabajos expuestos y discutidos en las secciones anteriores.

1. INTRODUCCIÓN

1. INTRODUCCIÓN

1.1 Alimentómica: alimentos, salud y tecnologías ómicas

La ciencia que estudia la Nutrición Humana ha avanzado enormemente en la última década, periodo en el que ha pasado de considerar los alimentos como simple fuente de energía, al reconocimiento de su papel en el mantenimiento de la salud y la reducción del riesgo de padecer determinadas enfermedades. En paralelo, la Ciencia y Tecnología de los Alimentos también ha evolucionado considerablemente en los últimos años, permitiendo el desarrollo de nuevos productos alimenticios, el diseño de nuevos procesos de producción y materiales de empaquetado, y la mejora de la vida útil de los alimentos y de sus características sensoriales. Además, tanto la Ciencia de la Nutrición como la Ciencia y Tecnología de los Alimentos han integrado en sus estudios metodologías avanzadas de análisis previamente establecidas en áreas como la farmacología, la medicina y la biotecnología. La adopción de tales metodologías ha permitido el desarrollo de nuevas estrategias para el estudio de los alimentos desde una perspectiva más global. Dentro de las nuevas metodologías de análisis se encuentran las tecnologías "ómicas" (de alto rendimiento) y las herramientas bioinformáticas asociadas a ellas. Las tecnologías de análisis de alto rendimiento son aquellas que permiten la obtención de gran cantidad de datos en un periodo de tiempo corto. El sufijo "ómica" deriva del término "genome" acuñado por Hans Winkler en 1920 (Winkler, 1920), y aunque las principales tecnologías ómicas sean la Genómica, la Transcriptómica, la Proteómica y la Metabolómica, se han desarrollado otras tecnologías ómicas que se encargan del estudio específico de algunos de los componentes celulares, como la Epigenómica o la Lipidómica.

La aplicación de estas técnicas avanzadas de análisis al estudio de los alimentos ha dado lugar a la definición de una nueva disciplina denominada Alimentómica (*Foodomics*

en inglés, ver Figura 1.1) (Cifuentes, 2009; Herrero y col., 2010a; Herrero y col., 2012; García-Cañas y col., 2012). La Alimentómica emplea técnicas ómicas (fundamentalmente Transcriptómica, Proteómica y Metabolómica) para investigar los alimentos incluyendo sus múltiples conexiones con la Nutrición y la salud. El objetivo último de la Alimentómica es mejorar la salud y el bienestar de los consumidores a través de su dieta, elevando la calidad y seguridad de los alimentos y proporcionando una base científica sólida a las alegaciones de salud de nuevos alimentos o ingredientes funcionales. El empleo del enfoque alimentómico al estudio del efecto de los componentes de la dieta en el tratamiento y prevención de enfermedades crónicas permite por tanto obtener información detallada acerca de los cambios que se producen en los sistemas biológicos, mejorando así nuestro conocimiento sobre los efectos de la dieta en la salud.

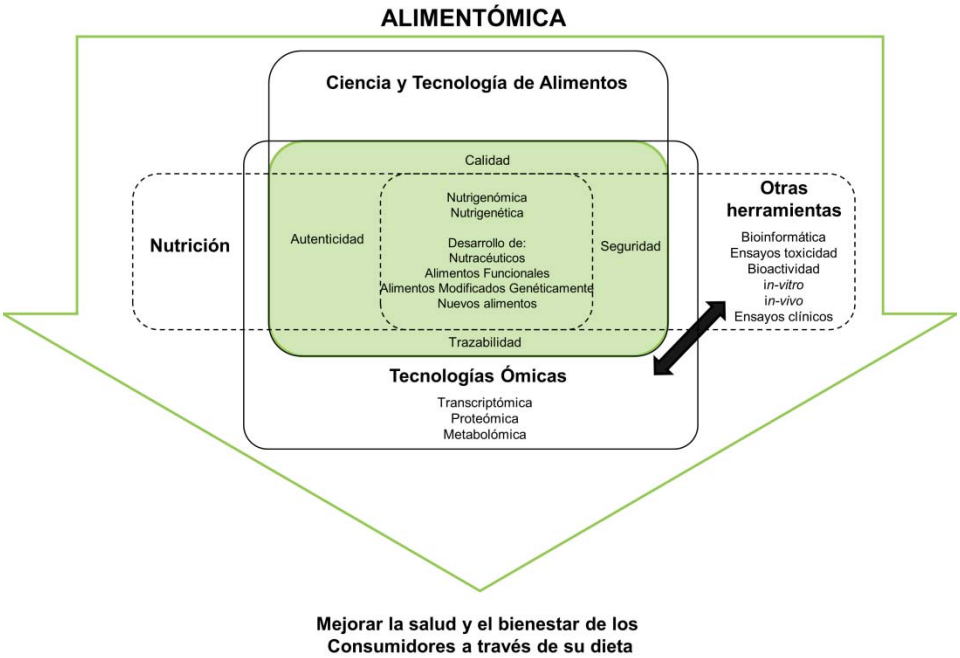

Figura 1.1 Esquema de la Alimentómica.

1.1.1 Transcriptómica

La Transcriptómica es el conjunto de técnicas y metodologías dirigidas al estudio del transcriptoma, o conjunto completo del RNA (del inglés *Ribonucleic Acid*) transcrito a partir de un genoma en un determinado momento. La expresión génica es el proceso por el cual la información codificada en el genoma es transformada en las proteínas necesarias para el desarrollo y funcionamiento de un sistema biológico, por lo que el estudio del transcriptoma permite investigar la relación entre el fenotipo y la información codificada en el DNA (del inglés *Deoxyribonucleic Acid*). Así, el objetivo final de la Transcriptómica abarca:

- La anotación de todas las especies de transcritos, incluyendo (RNA mensajero, RNA no codificante y RNA pequeño).
- La determinación de la estructura de los transcritos y los fenómenos de "edición alternativa" (una misma secuencia génica puede dar lugar a distintos transcritos).
- La cuantificación de los niveles de expresión de cada transcrito en un sistema biológico sometido a distintas condiciones.

A pesar de que el objetivo de la presente sección no es entrar en excesivos detalles sobre la Transcriptómica (una descripción detallada de las tecnologías más empleadas en estudios transcriptómicos puede consultarse en varios libros publicados recientemente, sirva de ejemplo los dos títulos siguientes: "Applications of Advanced Omics Technologies: From Genes to Metabolites" de V. García-Cañas, A. Cifuentes y C. Simó, 2014, y "Fundamentals of Advanced Omics Technologies" de C. Simó, A. Cifuentes y V. García-Cañas, 2014), a continuación se describirán las técnicas analíticas más utilizadas en los estudios transcriptómicos.

El estudio de las secuencias transcritas puede abordarse mediante el empleo de técnicas clásicas como el Northern blot o la reacción en cadena de la polimerasa (PCR, *Polymerase Chain Reaction*) cuantitativa, que permiten determinar la expresión de un número limitado de transcritos. Otras técnicas como el análisis seriado de la expresión génica (SAGE, *Serial Analysis of Gene Expression*) (Velculescu y col., 1995) o la determinación masiva de secuencias en paralelo (MPSS, *Massively Parallel Signature Sequencing*) (Brenner y col., 2000) permiten la secuenciación del transcriptoma completo, aunque con un coste elevado. Por otro lado, el gran avance producido en los últimos años en las técnicas de microfluídica y miniaturización ha permitido el desarrollo de técnicas como el microarray de expresión génica y la secuenciación masiva del RNA (RNA-Seq, *RNA Sequencing*), que posibilitan el análisis de miles de secuencias transcritas de RNA en muestras biológicas de manera rápida y eficaz (Morozova y Marra, 2008).

1.1.1.1 Microarray de expresión génica

El empleo de microarrays de expresión génica se ha extendido en los últimos años y ha encontrado diversas aplicaciones como, por ejemplo, la investigación de nuevas enfermedades, el desarrollo de nuevas herramientas de diagnóstico o la identificación de los mecanismos de respuesta frente a fármacos. La expansión de esta técnica se ha visto favorecida por la continua optimización de los instrumentos y la estandarización de los protocolos. Además, el desarrollo de nuevos métodos de fabricación de microchips ha permitido reducir los costes de cada análisis. La tecnología de los microarrays de expresión génica está basada en la hibridación específica de ácidos nucleicos y permite medir simultáneamente la cantidad relativa de miles de secuencias entre dos o más muestras. Existen dos tipos de microarrays de expresión génica en función de su diseño, los

microarrays en sustratos planos y los microarrays en sustratos esféricos (Trachtenberg y col., 2012).

Los microarrays en sustratos planos (o microchips) más modernos se caracterizan por tener secuencias cortas de DNA (oligonucleótidos o sondas) inmovilizadas en un sustrato sólido en localizaciones conocidas (Stafford, 2009). Estos microarrays pueden diferenciarse en función del sistema de impresión *in situ* que se emplee en su fabricación. Por un lado, la tecnología SurePrint (o "ink-jet"), empleada por la compañía Agilent, se basa en la microinyección secuencial de las distintas bases nucleotídicas de modo similar al que lo hacen las impresoras de tinta. Esta tecnología permite la síntesis de más de 250.000 secuencias distintas de hasta 60 nucleótidos en cada chip (Hughes y col., 2001). Por otro lado, la tecnología basada en máscaras fotolitográficas, empleada por la compañía Affymetrix, es similar a la utilizada en la fabricación de circuitos integrados. Esta tecnología ha permitido aumentar la densidad de secuencias, pudiendo sintetizarse más de 750.000 secuencias de 25 nucleótidos en cada chip (Barczak y col., 2003). En estos microchips, cada secuencia de RNA mensajero (RNAm, *Messenger RNA*) está representada por 10 secuencias distintas de oligonucleótidos. El uso de un mayor número de oligonucleótidos permite aumentar la cobertura de la secuencia del transcrito analizado, y posibilita el estudio de procesos de "edición alternativa", y/o la presencia de polimorfismos de nucleótidos simples (SNPs, *Single Nucleotide Polymorphism*) (Stafford, 2009).

En los microarrays de partículas, las secuencias de DNA son inmovilizadas en esferas de sílice de 3 μm y estas son distribuidas aleatoriamente sobre un sustrato sólido. En cada esfera se sintetizan más de 100.000 secuencias de 50 nucleótidos, lo que permite obtener una mayor densidad de secuencias que con los sistemas de síntesis *in situ* (Gunderson y col., 2004).

El procedimiento de análisis en microarrays requiere de la extracción previa del RNA de las células o tejidos, su marcaje con distintos reactivos y su incubación sobre el microarray en condiciones controladas que permitan la hibridación específica de las secuencias de RNAm (Figura 1.2).

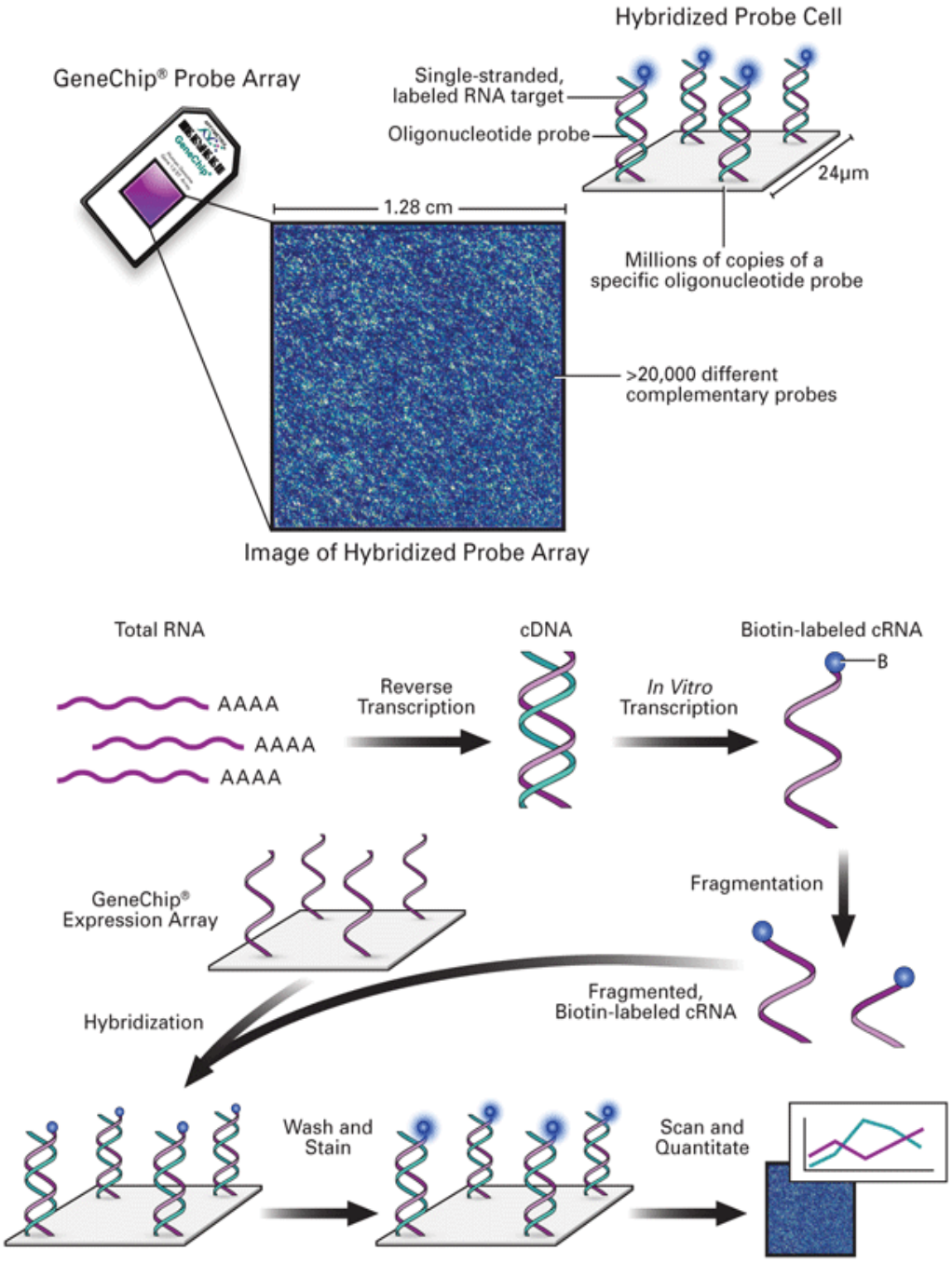

Figura 1.2 Procedimiento de análisis mediante el uso de microarrays de expresión génica. Figura obtenida de Affymetrix, Inc, 2009.

Una vez hibridada la muestra sobre el microarray, se realizan una serie de lavados y se lleva a cabo la detección de las señales mediante un escáner de alta resolución y sensibilidad. Finalmente, la señal adquirida es transformada en un valor numérico (Nambiar y col., 2005).

Generalmente, el marcaje de las muestras se lleva a cabo mediante fluoróforos derivados de la cianina. El procedimiento de marcaje varía en función del esquema de detección que se vaya a utilizar, pudiendo utilizarse uno o dos canales. En el caso de usar el sistema de dos canales, cada muestra se marca con un fluoróforo diferente, y las muestras se hibridan simultáneamente sobre el mismo microarray, de modo que la señal de ambos fluoróforos se adquiere simultáneamente. Uno de los inconvenientes de este esquema es que el empleo de dos fluoróforos normalmente genera desviaciones en la adquisición de las señales fluorescentes como consecuencia de las diferentes eficiencias de marcado de cada fluoróforo. En estos casos, normalmente es necesario realizar un segundo análisis en otro microarray con las muestras marcadas inversamente para compensar tales desviaciones (Dombkowski y col., 2004). En el caso de la detección por un canal, todas las muestras del experimento son marcadas con el mismo fluoróforo, lo cual elimina posibles sesgos en la detección de las señales asociados al empleo de fluoróforos distintos (Churchill, 2002). Tras la detección, las señales adquiridas son procesadas para calcular los niveles de expresión génica relativa de cada transcrito entre las distintas muestras analizadas. Este procesado de las señales varía en función de la plataforma y de la estrategia de marcaje utilizada, y requiere el uso de herramientas bioinformáticas avanzadas, como se verá más adelante en la sección de bioinformática. Finalmente, los datos son analizados estadísticamente con el fin de identificar aquellos genes expresados diferencialmente entre las distintas condiciones experimentales estudiadas (Burton y McGehee, 2004).

A pesar de las numerosas ventajas del microarray de expresión génica, esta tecnología presenta algunas limitaciones como, por ejemplo, la necesidad de conocer previamente la secuencia del transcriptoma a analizar, el elevado ruido de fondo, el limitado intervalo dinámico, y el carácter relativo de la cuantificación (Wang y col., 2009). Estas debilidades se han intentado solventar con el desarrollo de nuevas técnicas basadas en la secuenciación masiva, denominadas RNA-seq.

1.1.1.2 RNA-seq

Las técnicas de RNA-seq están basadas en las tecnologías de secuenciación de nueva generación (ultrasecuenciación o secuenciación masiva) y tienen como objetivo la secuenciación completa del transcriptoma (Wang y col., 2009). A diferencia del microarray de expresión, las técnicas de RNA-seq permiten la caracterización completa de cualquier transcriptoma sin conocerlo *a priori*. Además, desde un punto de vista cuantitativo, las técnicas de RNA-seq proporcionan una mayor sensibilidad e intervalo dinámico lineal, y permiten la cuantificación absoluta de los transcritos identificados (Wilhelm y Landry, 2009). Unido a estas ventajas, la alta competición entre las empresas desarrolladoras ha propiciado que estas técnicas avancen rápidamente. Actualmente, existe un gran número de plataformas de secuenciación. Aunque cada plataforma presenta prestaciones técnicas distintas, todas ellas tienen la característica común de utilizar sistemas miniaturizados que posibilitan el uso de pequeñas cantidades de muestra y de reactivos (Wang y col., 2009). Además, la mayoría de las plataformas de ultrasecuenciación siguen el procedimiento general de análisis que se esquematiza en la Figura 1.3 (Zeng y Mortazavi, 2012).

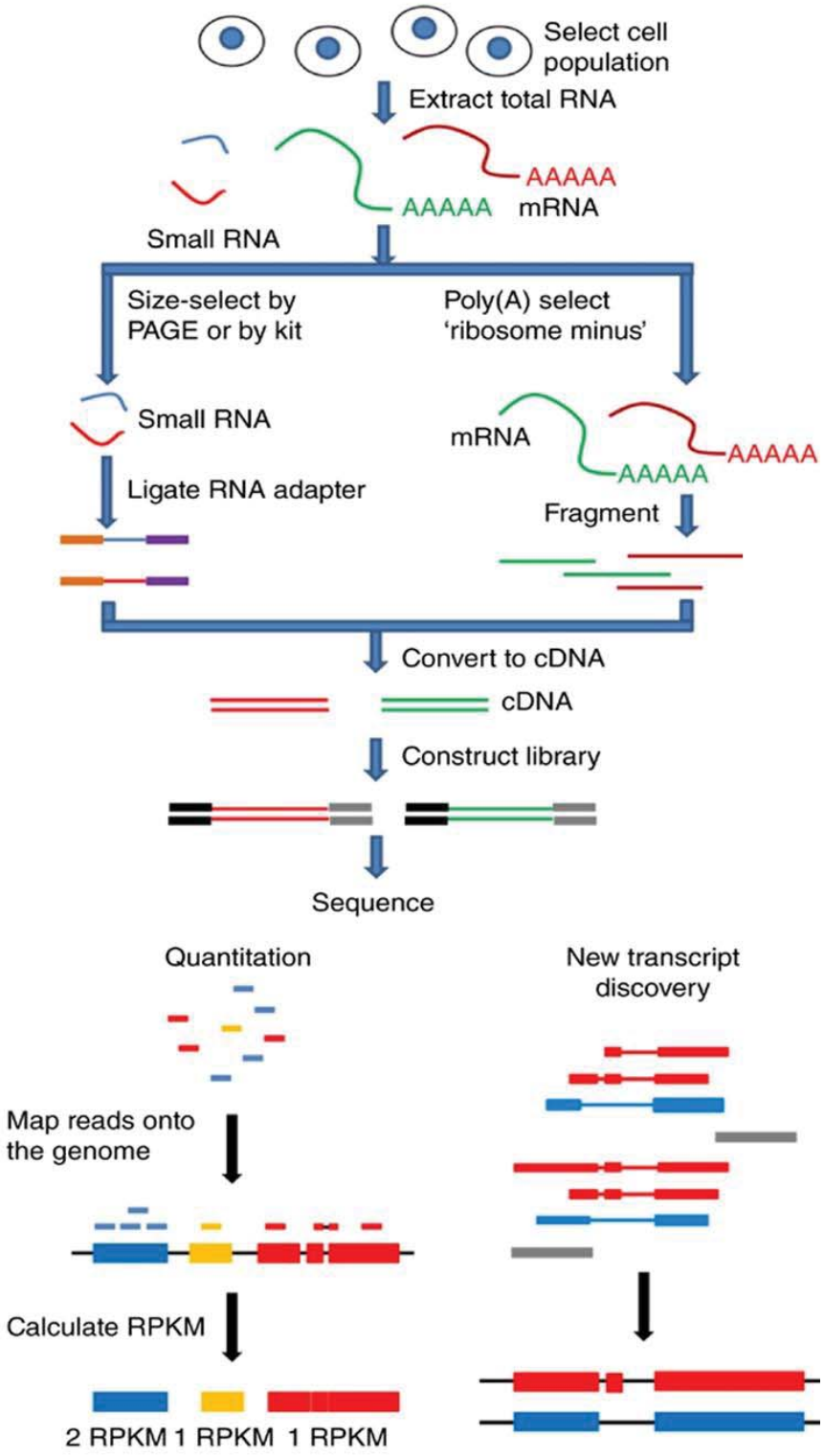

Figura 1.3 Procedimiento de análisis mediante el uso de las técnicas de RNA-seq. Figura modificada de Zeng y Mortazavi, 2012.

En cuanto a este procedimiento de análisis, el primer paso consiste en extraer el RNA total de las células o los tejidos. Tras la extracción, la muestra se somete a un tratamiento de purificación para la eliminación del RNA ribosómico (no codificante) con el fin de obtener una muestra enriquecida en RNAm (codificante). Una vez aislado el RNAm, se procede a la preparación de las "librerías" de RNA. La preparación de las "librerías" de RNA consiste en la fragmentación del RNAm y su hibridación con distintos oligonucleótidos (oligo dT o hexámeros aleatorios). Estos oligonucleótidos permiten la retrotranscripción del RNAm a DNA complementario (DNAc, *Complementary DNA*). Una vez sintetizado, el DNAc requiere la unión de adaptadores específicos para su inmovilización a un soporte sólido que puede ser plano o esférico (dependiendo de cada plataforma). La inmovilización del DNAc permite su amplificación posterior, una etapa imprescindible ya que la mayoría de los sistemas de imagen no pueden detectar la fluorescencia de una sola molécula (Wilhelm y Landry, 2009). Por último, el DNAc amplificado es sometido a varios ciclos en los que sucesivamente se adicionan los reactivos de secuenciación y seguidamente se lavan y se adquieren las señales mediante un sistema de detección (Egan y col., 2012).

A pesar de las similitudes entre las distintas plataformas de secuenciación, existen diferencias notables entre ellas como, por ejemplo, la longitud de los fragmentos amplificados, el tiempo de análisis o la "profundidad" de las lecturas (Valdés y col., 2013b). La longitud de los fragmentos amplificados puede variar entre 25 y 800 nucleótidos, y cuanto menor sea la longitud, menor será la tasa de error en la secuenciación. Sin embargo, una menor la longitud de los fragmentos genera un mayor número de lecturas, dificultando su posterior ensamblaje. El tiempo de análisis también es muy variable, y en el caso de la plataforma Genome Analyzer II de Illumina, el tiempo de análisis puede durar varias semanas. Por último, otro factor diferenciador es la "profundidad" de las lecturas, o el

número de veces que una determinada base nucleotídica es secuenciada. El aumento en la profundidad de lectura está asociado a un incremento en el coste de los análisis, y cuanto mayor sea este parámetro, mayor es la sensibilidad y el intervalo dinámico de la técnica (Wang y col., 2009).

Tras la detección de las señales, el RNAm secuenciado puede ser alineado a un genoma (o transcriptoma) de referencia o ensamblado *de novo* mediante el uso de herramientas bioinformáticas para producir un mapa transcriptómico con información estructural y cuantitativa de la expresión génica (Egan y col., 2012). En el caso de llevar a cabo tal alineamiento con un genoma (o transcriptoma) de referencia, un parámetro muy importante es la "cobertura" obtenida tras la secuenciación. La "cobertura" se define como el número de lecturas (secuencias) medio que contienen un determinado nucleótido del transcriptoma objeto de estudio. Así, cuanto mayor sea el número de veces que un nucleótido es secuenciado (mayor cobertura de secuenciación), mayor fiabilidad se logra en la secuenciación (Steijger y col., 2013).

Una vez identificados los genes, se lleva a cabo el cálculo de los valores de expresión utilizando herramientas bioinformáticas avanzadas. El método de cálculo más utilizado se basa en el recuento de las lecturas obtenidas de cada gen, corregido por la longitud del gen al que pertenecen y el número total de lecturas del análisis (RPKM, *Reads Per Kilobase per Million mapped reads*, Mortazavi y col., 2008). Por último, y al igual que ocurre con los datos de microarray de expresión, es necesario llevar a cabo el análisis estadístico para determinar los genes expresados diferencialmente entre las muestras.

La secuenciación del RNA también presenta algunas limitaciones como, por ejemplo, la dificultad para almacenar la gran cantidad de datos generados, la necesidad de herramientas bioinformáticas avanzadas que permitan el análisis de datos complejos, o la

falta de estandarización de los métodos para el procesado de los datos (García-Cañas y col., 2010). Además, el coste de esta tecnología es aún muy elevado y pueden introducirse sesgos en la secuenciación como consecuencia de los posibles errores producidos durante la amplificación del DNAc (Maitra y col., 2012).

1.1.1.3 Aplicación de la Transcriptómica en ciencias de la alimentación

La Transcriptómica se ha utilizado ampliamente en el campo de la Ciencia y Tecnología de los Alimentos y Nutrición, y tiene una gran importancia en áreas como la producción de alimentos, la seguridad alimentaria o en el estudio de los efectos de los compuestos de la dieta en la salud (revisado por Valdés y col., 2013a). En lo referente a la producción de los alimentos, el estudio del transcriptoma de determinadas especies con importancia agronómica ha permitido conocer: (1) los genes implicados en el aumento de la producción y la tolerancia a condiciones ambientales adversas (Lodha y Basak, 2012); (2) los genes responsables de la síntesis de nutrientes y compuestos bioactivos (Annadurai y col., 2013); (3) los mecanismos moleculares que se producen durante los procesos de almacenaje y tratamiento tras las cosechas (Chope y col., 2012); y (4) los posibles efectos no deseados derivados de las transformaciones genéticas en los organismos modificados genéticamente (Valdés y col., 2013a). En cuanto a la seguridad alimentaria, la Transcriptómica se ha utilizado para investigar los mecanismos de producción de ciertas toxinas (Brown y col., 2012) o para identificar los genes responsables de la formación de biofilms por especies patógenas (Tirumalai y Prakash, 2011). Por último, esta tecnología también se ha utilizado ampliamente para estudiar los efectos de los nutrientes de la dieta en la prevención y el desarrollo de enfermedades crónicas como, por ejemplo, el cáncer (Valdés y col., 2013a).

1.1.2 Proteómica

La Proteómica es el conjunto de técnicas y metodologías dirigidas al estudio del proteoma. El proteoma se define como el conjunto completo de las proteínas expresadas en un sistema biológico en un momento determinado (Wasinger y col., 1995). Así, la Proteómica se encarga tanto de la identificación y la cuantificación de las proteínas, como del estudio de la estructura primaria, la conformación, y la localización de esas proteínas en un lugar, espacio o tiempo determinado. La diversidad estructural de las proteínas y el amplio intervalo dinámico de su expresión (hasta 6 órdenes de magnitud), hacen del estudio del proteoma una tarea compleja. Además de estas dificultades, la Proteómica tiene que hacer frente a otros problemas como son: (1) la "edición alternativa" (una misma molécula de RNA puede dar lugar a distintas proteínas); (2) las modificaciones post-traduccionales, o modificaciones químicas que afectan a la funcionalidad de las proteínas en términos de actividad, localización e interacción con otros componentes celulares como proteínas, ácidos nucleicos, lípidos o cofactores; (3) la relación entre los niveles de expresión de los transcritos y las proteínas en un determinado momento.

El objetivo de la presente sección es dar una visión general de la Proteómica, y a continuación se describirán las dos etapas más relevantes en los estudios proteómicos (la identificación y la cuantificación de proteínas). Una información más completa de las tecnologías más empleadas en Proteómica puede encontrarse en los libros "Applications of Advanced Omics Technologies: From Genes to Metabolites" de V. García-Cañas, A. Cifuentes y C. Simó, 2014, y "Fundamentals of Advanced Omics Technologies" de C. Simó, A. Cifuentes y V. García-Cañas, 2014.

1.1.2.1 Identificación de proteínas

En los primeros estudios proteómicos, las mezclas complejas de proteínas se separaban mediante electroforesis bidimensional en gel (2-DE, *Two-Dimensional Gel Electrophoresis*), pero la identificación y caracterización posterior se llevaban a cabo mediante métodos lentos y poco sensibles, como el método de Edman (Edman, 1950). El método de Edman es una técnica que permite la secuenciación de los aminoácidos contenidos en un péptido. Esta técnica está basada en el marcaje del residuo N-terminal del péptido con fenilisotiocianato en condiciones básicas, y la posterior eliminación del residuo marcado al someterlo a condiciones ácidas. El residuo N-terminal eliminado es identificado por cromatografía de líquidos (LC, *Liquid Chromatography*) o electroforesis capilar (CE, *Capillary Electrophoresis*), y el nuevo residuo N-terminal es marcado, eliminado e identificado por repetición de la misma serie de reacciones. Este procedimiento se repite hasta la determinación completa de la secuencia del péptido.

En los últimos años, el desarrollo y mejora de las técnicas analíticas instrumentales, unido a los avances en la secuenciación del genoma, han impulsado el progreso de la Proteómica. Entre los avances analíticos más importantes dentro de este campo se encuentra el desarrollo de los métodos de ionización suave: MALDI (del inglés *Matrix-Assisted Laser Desorption/Ionization*) (Tanaka y col., 1988) y ESI (del inglés *Electrospray Ionization*) (Fenn y col., 1989). Estos métodos permiten la ionización de las proteínas/péptidos, y su posterior análisis mediante las técnicas de espectrometría de masas (MS, *Mass Spectrometry*), lo que ha propiciado que la MS sea el método de elección para la identificación de las proteínas.

Tal y como se ha comentado previamente, la naturaleza de las proteínas es muy diversa, por lo que para su estudio son necesarios uno o varios pasos de purificación y/o

separación previos al análisis por MS. En función del método elegido, existen dos estrategias analíticas diferentes (Figura 1.4):

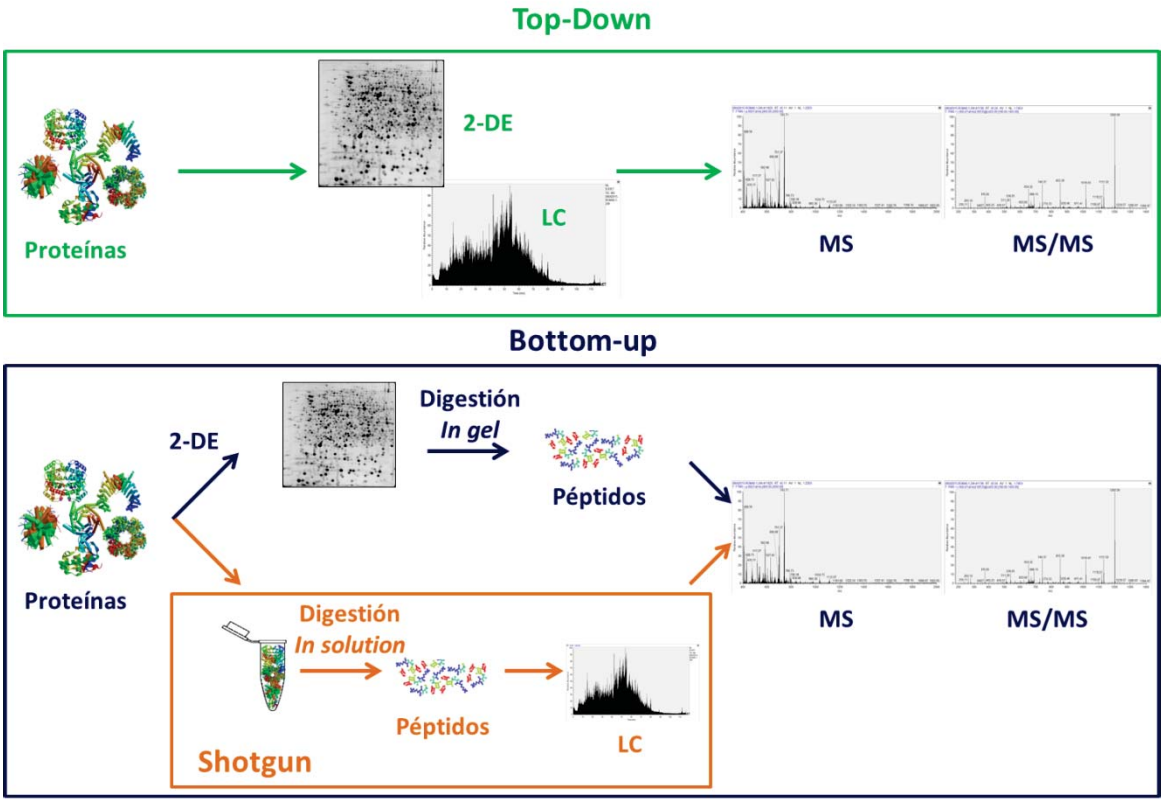

Figura 1.4 Principales estrategias analíticas utilizadas en Proteómica.

Top-down: se basa en el estudio de las proteínas intactas. Las proteínas son separadas previamente (2-DE o LC), y posteriormente son ionizadas para su análisis por MS. Una vez en el espectrómetro, las proteínas se fragmentan en la celda de colisión y los fragmentos son detectados mediante MS/MS (McLafferty y col., 1999).

Bottom-up: se caracteriza por la digestión enzimática de las proteínas en sus respectivos péptidos antes del análisis mediante MS. La enzima más utilizada en esta aproximación es la tripsina, aunque diversos estudios han demostrado que el uso de otras proteasas como Lys-C, Lys-N o quimiotripsina aumenta la cobertura en el estudio del proteoma (Peng y

col., 2012; Tsiatsiani y Heck, 2015). Esta digestión puede llevarse a cabo antes o después de la separación.

- Cuando la digestión de las proteínas es posterior a la separación, la técnica de separación más utilizada es la 2-DE. En este método, las proteínas se separan en una primera etapa en función de su punto isoeléctrico, y posteriormente en función de su peso molecular. Una vez separadas, las proteínas se extraen del gel individualmente, se digieren enzimáticamente y se analizan mediante MS.
- Si la digestión es previa a la separación, también conocido como "shotgun", todas las proteínas de la muestra son digeridas simultáneamente y los péptidos se analizan normalmente mediante LC acoplada a MS (Yates, 2013).

Tanto en la aproximación "top-down", como en la "bottom-up", la identificación de la proteína original se determina por comparación de los espectros de masas experimentales de los péptidos con las masas teóricas de los péptidos almacenadas en bases de datos proteómicos. Para llevar a cabo esta comparación, existen a su vez dos estrategias, la huella peptídica y la secuenciación peptídica (desarrolladas en mayor profundidad en la sección de bioinformática). Si la proteína no se encuentra en las bases de datos, es necesaria la secuenciación *de novo* de los péptidos. La secuenciación peptídica consiste en la interpretación manual de los espectros de masas de los péptidos, y la comparación posterior frente a las masas de los aminoácidos individuales que los constituyen (Bartels, 1990).

1.1.2.2 Cuantificación de proteínas

Además de la identificación de las proteínas, la Proteómica también se centra en la cuantificación de las mismas. Para ello, se han diseñado diversas aproximaciones que permiten cuantificar absoluta o relativamente las proteínas (Wasinger y col., 2013). En la

Tabla 1.1 se muestran las ventajas y los inconvenientes de los métodos de cuantificación de proteínas más utilizados. La cuantificación de las proteínas puede ser dirigida (se mide la concentración de una o varias proteínas previamente seleccionadas) o no dirigida (cuando se quiere cuantificar el mayor número posible de proteínas de una muestra).

La cuantificación dirigida puede llevarse a cabo utilizando algoritmos matemáticos para calcular la concentración de las proteínas, como el método emPAI (Ishihama y col., 2005). Este método es sencillo y económico, pero su uso está limitado debido a su baja precisión. Otro método utilizado es AQUA (del inglés *Absolute Quantification*) (Gerber y col., 2003), que consiste en la selección de determinadas proteínas y la adición de patrones internos que permitan cuantificarlas. Los patrones internos utilizados son péptidos específicos de las proteínas que se quieran cuantificar, pero marcados con isótopos estables. Tanto el péptido de la muestra, como el péptido marcado co-eluyen y son detectados, seleccionados y fragmentados por el espectrómetro de masas. Al haberse seleccionado previamente las proteínas que se quieren cuantificar, este tipo de cuantificación permite el uso de modos de adquisición que aumentan la reproducibilidad, la sensibilidad y la selectividad de los análisis. De entre todos los modos de adquisición disponibles, los más utilizados en los estudios proteómicos dirigidos son el SRM (del inglés *Selected-Reaction Monitoring*) y el MRM (del inlgés *Multiple-Reaction Monitoring*). Estos modos consisten en la monitorización de la señal de uno o más fragmentos correspondientes a la transición de uno o más péptidos previamente seleccionados.

La cuantificación no dirigida absoluta se lleva a cabo habitualmente mediante algoritmos matemáticos mientras que, en la cuantificación no dirigida relativa, se pueden emplear isótopos estables o no. En el caso de emplear isótopos, esta estrategia se basa en la combinación de isótopos ligeros o pesados de ^{13}C, ^{2}H, ^{15}N o ^{18}O. El procedimiento general consiste en mezclar las muestras a estudiar e identificar los péptidos marcados por

Tabla 1.1 Principales métodos de cuantificación absoluta y relativa utilizados en Proteómica.

Cuantificación absoluta				
Método	**Descripción**	**Ventajas**	**Inconvenientes**	**Referencia**
AQUA (absolute quantification)	Adición de péptidos con isótopos sintetizados químicamente a la muestra, en concentraciones conocidas	Gran precisión en la cuantificación	Coste elevado. Se necesita información previa de los péptidos que se quiere cuantificar	Gerber y col., 2003
emPAI	Cálculo del emPAI usando el número de péptidos observados y los observables	Simple. No requiere marcaje	Baja precisión en la cuantificación	Ishihama y col., 2005
Top3	Cálculo de la relación entre la respuesta de la señal de los tres péptidos trípticos más abundantes y la concentración de proteína	Gran precisión. No requiere marcaje	Se necesita añadir una proteína estándar a la muestra antes de la digestión	Silva y col., 2006
Cuantificación relativa				
Método	**Descripción**	**Ventajas**	**Inconvenientes**	**Referencia**
ICAT (Isotope-Coded Affinity Tag)	Marcaje químico específico de cisteína	Reduce la complejidad de la muestra al enriquecer la muestra en los péptidos marcados	Se necesitan péptidos con residuos de cisteína. Las cadenas laterales con cisteína pueden reaccionar	Gygi y col., 1999
ICPL (Isotope-Coded Protein Label)	Marcaje químico de los grupos amino libres	Se marcan todos los péptidos de la muestra. Las cadenas laterales no reaccionan	Los péptidos resultantes de la digestión son relativamente grandes	Schmidt y col., 2005
Dimethyl Labeling	Marcaje químico de los grupos amino libres	Se marcan todos los péptidos de la muestra. Las cadenas laterales no reaccionan. Es barato. Las etiquetas son pequeñas	Reactivos tóxicos	Hsu y col., 2003
iTRAQ (Isobaric Tags for Relative and Absolute Quantification) **TMT** (Tandem Mass Tags)	Marcaje químico específico de los grupos amino. La cuantificación se lleva a cabo en modo MS/MS	Marcaje eficiente. Permite analizar hasta 8 muestras juntas	Requiere fragmentación efectiva y tiene un coste elevado	Ross y col., 2004 Thompson y col., 2003
Marcaje con ^{15}N	Marcaje metabólico con medio enriquecido en ^{15}N	Marcaje eficiente	El análisis de datos es complejo	Oda y col., 1999
SILAC	Marcaje metabólico con aminoácidos que contienen isótopos pesados	Marcaje eficiente, una etiqueta por cada péptido.	Es caro	Ong y col., 2002
Marcaje con $H_2{}^{18}O$	Marcaje enzimático con $H_2{}^{18}O$	Simple, relativamente barato	El marcaje incompleto dificulta el análisis de los datos	Mirgorodskaya y col., 2000
Contaje de espectros/péptidos	Comparación relativa de muestras diferentes basada en el número de espectros MS/MS o péptidos identificados	No requiere marcaje. El procesado de los datos es simple. Se pueden comparar muchas muestras	Menos robusto que los métodos de marcaje. Requiere alta reproducibilidad entre las muestras	Liu y col., 2004
Ion current	Basado en la intensidad de los iones	No requiere marcaje. Se pueden comparar muchas muestras	Requiere alta reproducibilidad entre las muestras	Wiener y col., 2004

parejas en base a su espectro de MS, o usando un ion "informador" del espectro de MS^2. El ion informador es una etiqueta añadida a los péptidos mediante reacciones químicas, y que es detectada cuando los péptidos se fragmentan. La modificación o marcaje de la muestra con isótopos puede llevarse a cabo química, metabólica o enzimáticamente. Algunos de los métodos de marcaje químico más utilizados son iTRAQ (del inglés *Isobaric Tags for Relative and Absolute Quantification*) (Ross y col., 2004) y DML (del inglés *Dimethyl labeling*) (Hsu y col., 2003). Para el marcaje enzimático normalmente se utiliza $H_2{}^{18}O$ durante la digestión de las proteínas (Mirgorodskaya y col., 2000). En el caso del marcaje metabólico de muestras de cultivo celular, normalmente se emplean medios de cultivo con aminoácidos marcados con isótopos estables, de modo que las células puedan incorporarlos en las proteínas (SILAC, *Stable Isotope Labeling by Amino Acids in Cell Culture*) (Ong y col., 2002). Por otro lado, en el caso de no utilizar isótopos para llevar a cabo la cuantificación relativa, se realiza la comparación de las muestras en base a la intensidad normalizada del ion del mismo péptido, o en el número de veces que aparece el mismo patrón de fragmentación (Liu y col., 2004). El modo de adquisición más utilizado en los estudios proteómicos no dirigidos es el análisis dependiente de los datos. Este modo de adquisición consiste en que una vez que los péptidos más abundantes han sido seleccionados para su fragmentación, estos son excluidos durante un tiempo determinado, lo que permite que los péptidos menos abundantes también sean seleccionados (Mann y col., 2001). Este modo permite la detección de un mayor número de péptidos presentes en la muestra.

Por último, una vez identificadas y cuantificadas las proteínas, es necesario llevar a cabo el análisis estadístico para determinar aquellas proteínas expresadas diferencialmente entre los distintos grupos estudiados.

1.1.2.3 Aplicación de la Proteómica en ciencias de la alimentación

Al igual que la Transcriptómica, la Proteómica ha demostrado ser una herramienta potente dentro del campo de la Ciencia y Tecnología de los Alimentos y la Nutrición (Cunsolo y col., 2014). A modo de ejemplo, la Proteómica ha permitido la monitorización de los cambios producidos en los alimentos tras su conservación y su procesado (Sayd y col., 2012), el estudio de las propiedades de las proteínas y péptidos bioactivos (Udenigwe y Aluko, 2012), o la investigación del efecto que los alimentos pueden tener sobre la salud (Kussmann y col., 2010). En cuanto a la seguridad alimentaria, la Proteómica se ha utilizado para autentificar alimentos, ya que permite caracterizar, detectar y cuantificar numerosas proteínas y péptidos en especies poco caracterizadas genéticamente (Gallardo y col., 2013). Además, dada su elevada especificidad y fiabilidad, se ha utilizado para identificar y cuantificar proteínas alergénicas en matrices alimentarias, y para estudiar el efecto de los distintos procesados de los alimentos sobre estas proteínas (Anđelković y col., 2015). Por otro lado, numerosos estudios proteómicos han puesto de manifiesto las propiedades beneficiosas de las proteínas y los péptidos bioactivos, atribuyéndoles efectos antihipertensivos, antioxidantes, hipercolesterolémicos, inmunomoduladores, antimicrobianos o anticancerígenos (Panchaud y col., 2012). Por último, la Proteómica también se ha utilizado para estudiar los efectos de los nutrientes en el proteoma de células, tejidos u organismos (Ganesh y Hettiarachchy, 2012).

1.1.3 Metabolómica

La Metabolómica es el conjunto de técnicas y metodologías dirigidas al estudio del metaboloma, o conjunto de metabolitos de un determinado sistema biológico. Los metabolitos son las moléculas de bajo peso molecular (normalmente < 1.500 Da) resultantes de la actividad enzimática durante el metabolismo celular y extracelular. Al igual que el proteoma y el transcriptoma, los niveles de los metabolitos varían en el tiempo, el espacio, o el sistema biológico, y en función de los diferentes estímulos a los que esté sometido el sistema biológico (condiciones ambientales, alimentación, etc.). Al tratarse de los productos resultantes de las actividades enzimáticas (o reacciones bioquímicas), el estudio de los metabolitos permite investigar la relación entre el genotipo y el fenotipo. Aunque el objetivo de esta sección no es profundizar en el estudio de la Metabolómica (una descripción más detallada puede encontrarse en los libros "Applications of Advanced Omics Technologies: From Genes to Metabolites" de V. García-Cañas, A. Cifuentes y C. Simó, 2014, y "Fundamentals of Advanced Omics Technologies" de C. Simó, A. Cifuentes y V. García-Cañas, 2014) a continuación se presentan las principales aproximaciones, así como de las técnicas más utilizadas en Metabolómica.

Desde un punto de vista analítico, el estudio de los metabolitos puede llevarse a cabo siguiendo cuatro aproximaciones:

- Análisis dirigido. Se centra en el análisis de un metabolito o un grupo limitado de metabolitos previamente seleccionados.
- Análisis del "perfil metabólico". Se basa en el análisis de un grupo de metabolitos que han sido seleccionados previamente y que están relacionados bioquímicamente entre sí, y/o que participan en una determinada ruta metabólica.

- Análisis de la "huella metabólica". Consiste en la identificación o cuantificación del máximo número de metabolitos en la muestra. Esta aproximación permite la separación entre las muestras, por lo que es la más apropiada para el descubrimiento de biomarcadores, el diagnóstico de enfermedades y para identificar diferencias y/o similitudes entre muestras (Fiehn, 2002).
- Análisis de "flujo metabólico". Se basa en la monitorización de determinados elementos (normalmente carbono), a través de las distintas rutas metabólicas para la caracterización detallada del metabolismo de los compuestos que contienen ese elemento.

Independientemente de la aproximación seleccionada, la gran variabilidad de las propiedades físico-químicas de los metabolitos y su amplio intervalo de concentraciones, hacen del estudio del metaboloma una tarea muy compleja. En Metabolómica, la selección del método de preparación de la muestra (debido a la distinta naturaleza de los metabolitos), y de la técnica analítica, es muy importante a la hora de obtener una mayor o menor cobertura del metaboloma, ya que actualmente no existe una única técnica capaz de caracterizar adecuadamente todos los metabolitos.

El análisis del metaboloma se lleva a cabo principalmente mediante la resonancia magnética nuclear (RMN, *Nuclear Magnetic Resonance*) y la MS, técnicas que se describirán a continuación.

1.1.3.1 Resonancia magnética nuclear (RMN)

La RMN fue la primera técnica de alto rendimiento utilizada en Metabolómica. Esta técnica se puede emplear tanto para la identificación de metabolitos como para caracterizar su estructura y cuantificar su abundancia en mezclas complejas de manera rápida y poco

sesgada. Esto se debe a que la RMN tiene la misma sensibilidad para un elemento (hidrógeno, carbono, fósforo) independientemente de las propiedades del metabolito que lo contenga, por lo que la cuantificación puede llevarse a cabo incluyendo un sencillo patrón interno o externo. Además, la RMN requiere un escaso tratamiento de la muestra, es una técnica no destructiva y permite la identificación de nuevos compuestos. Esta técnica analítica ha sido frecuentemente empleada en la obtención de perfiles y huellas metabólicas (Zhang y Powers, 2012), así como en la evaluación de la calidad de los alimentos (Trimigno y col., 2015). A pesar de las ventajas que presenta y de las mejoras instrumentales que se han producido en los últimos años (mejora de la sensibilidad, resolución e interpretación de los espectros mediante el uso de herramientas bioinformáticas), la sensibilidad relativamente baja de la RMN en comparación con la MS ha hecho que esta última sea la técnica más empleada en los estudios metabolómicos.

1.1.3.2 Espectrometría de masas (MS)

La MS permite el análisis de compuestos en función de su relación masa-carga (m/z), por lo que se ha utilizado para la determinación de la masa y de la fórmula molecular, así como para la identificación y cuantificación de metabolitos. El empleo de espectrómetros de masas de alta resolución como el de tiempo de vuelo (TOF, *Time Of Flight*) y el de resonancia de ion ciclotrón con transformada de Fourier (FT-ICR, *Fourier Transform Ion Cyclotron Resonance*), así como el uso de analizadores de masa en tándem (cuadrupolo TOF, qTOF; TOF/TOF; trampa lineal-Orbitrap, LTQ-Orbitrap), han permitido obtener la selectividad, sensibilidad, resolución e información estructural necesarias para la determinación de los valores de m/z y los patrones de fragmentación, para su uso posterior en el proceso de identificación de los metabolitos de interés.

El análisis de los metabolitos por MS puede realizarse de manera directa o en dos o más etapas mediante el acoplamiento a una técnica de separación previa a MS. Los acoplamientos entre la cromatografía de gases (GC, *Gas Chromatography*), la LC o la CE con MS son los más utilizados en el campo de la Ciencia y Tecnología de los Alimentos y la Nutrición (Fernandes y col., 2011; Rogachev y Aharoni, 2012; García-Cañas y col., 2014).

1.1.3.2.1 Acoplamientos GC-MS, LC-MS y CE-MS

El acoplamiento GC-MS se caracteriza por poseer una gran capacidad de separación, además de robustez y reproducibilidad en la adquisición de los espectros de masas. Además, la disponibilidad de librerías con tiempos de retención y espectros de masas (obtenidos mediante la interfase de impacto electrónico trabajando en condiciones estandarizadas) permite la identificación de los metabolitos por comparación con los espectros obtenidos experimentalmente. La técnica GC-MS es particularmente apropiada para el análisis de compuestos de bajo peso molecular, compuestos orgánicos volátiles y otros compuestos no volátiles previamente derivatizados. El acoplamiento GC-MS se ha utilizado de forma extensiva en la evaluación de compuestos del aroma (Bryant y col., 2011; Pennazza y col., 2013), lípidos (Sathe y col., 2008; Fatima y col., 2012), contaminantes en alimentos (Fernandes y col., 2011), en el estudio de enfermedades relacionadas con la alimentación (Zeng y col., 2010), etc.

El acoplamiento LC-MS es la técnica más utilizada en los estudios metabolómicos, a pesar de tener un poder de resolución menor que la GC-MS. Esta técnica permite la separación de compuestos con mayor peso molecular y polaridad sin necesidad de una etapa previa de derivatización. Dentro de la LC, el modo de separación más utilizado es el de

fase inversa, especialmente indicado para el análisis de metabolitos con media/baja polaridad. La LC-MS se ha empleado ampliamente en el estudio de la composición y calidad de los alimentos (Rogachev y Aharoni, 2012), en la evaluación de la seguridad alimentaria (Tengstrand y col., 2013), en el estudio del efecto de los alimentos en enfermedades como la obesidad (Lee y col., 2015) o el cáncer (Guertin y col., 2015), etc.

El acoplamiento CE-MS permite el análisis de metabolitos iónicos, ligeramente iónicos o muy polares con una elevada resolución y utilizando volúmenes de reactivos y de muestras pequeños. Esta técnica no es tan robusta como el acoplamiento GC-MS o LC-MS, por lo que aún siguen investigándose posibles mejoras en el diseño de la interfase entre CE y MS. El acoplamiento CE-MS ha sido muy utilizado en el campo de las ciencias de la alimentación, para estudiar la composición, la calidad y las interacciones entre los alimentos (García-Cañas y col., 2014), para el estudio de los efectos de los nutrientes de la dieta en la prevención de enfermedades como el cáncer (Celebier y col., 2012), etc.

1.1.4 La bioinformática: herramienta imprescindible para los estudios ómicos

La bioinformática es un campo interdisciplinar, donde las ciencias computacionales, la estadística y las matemáticas confluyen para desarrollar métodos y herramientas informáticas que permitan el almacenamiento, la obtención, el análisis y la interpretación de datos obtenidos de sistemas biológicos (Brains, 1996). La bioinformática ha sido imprescindible para el desarrollo de las tecnologías ómicas previamente descritas, ya que ha permitido diseñar, manejar y/o interpretar la cantidad masiva de datos generados por las técnicas ómicas. Al igual que en las secciones anteriores, el objetivo de esta sección no es entrar en excesivos detalles (para obtener información más completa el lector puede acudir al libro "Bioinformatics for Omics Data" de Bernd Mayer, 2011).

A continuación, se describen las características principales de los procedimientos bioinformáticos más utilizados en el campo de la Transcriptómica, la Proteómica y la Metabolómica, entre las que se encuentran las herramientas bioinformáticas usadas en el desarrollo de la presente Tesis doctoral.

En el campo de la **Transcriptómica**, la bioinformática ha sido fundamental para el diseño de los microarrays de expresión, ya que las secuencias de DNA impresas en los microarrays se seleccionan computacionalmente a partir de la información del transcriptoma en estudio. Además, tras la etapa de adquisición de la señal de fluorescencia durante el proceso de análisis, se pueden emplear distintos algoritmos matemáticos que permiten: (1) diferenciar entre el ruido de fondo y las señales útiles, así como compensar las señales obtenidas en el caso de utilizar dos canales de adquisición; (2) normalizar las señales entre los microarrays de un mismo experimento, con el fin de reducir los errores sistemáticos (Niculescu y col., 2007); (3) agrupar las señales de los oligonucleótidos que

representan un mismo gen, con el objetivo de calcular la intensidad media de expresión de cada gen. Para el procesado de los datos obtenidos utilizando los microarrays de Affymetrix, los principales algoritmos matemáticos son MAS 5 (MicroArray Suite 5.0), PLIER (Probe Logarithmic Error Estimation) y RMA (Robust Multi-array Analysis) (Cahan y col., 2007), siendo RMA el más utilizado en la actualidad. El algoritmo RMA: (1) calcula el ruido de fondo a partir de la deconvolución de todas las señales, asumiendo que las señales obtenidas son una combinación de la señal válida y del ruido de fondo; (2) transforma los valores a escala logarítmica en base 2; (3) normaliza las señales utilizando la información de todos los microarrays del experimento; (4) combina los valores de intensidad de los oligonucleótidos que representan cada gen para dar un valor medio, utilizando para ello el cálculo de la mediana (Carvalho e Irizarry, 2010).

Una vez procesados los datos y obtenidos los valores de intensidad de cada gen, se lleva a cabo el cálculo de la expresión génica relativa para cada gen entre las distintas condiciones experimentales estudiadas. Asociado al cálculo de la expresión génica, se realiza un test estadístico de contraste de hipótesis para cada gen. La realización de múltiples contrastes de hipótesis (tantos como genes se están comparando) puede dar lugar a la aceptación de genes identificados como diferencialmente expresados sin que realmente lo sean. Existen varias funciones estadísticas que permiten calcular y minimizar la aparición de estos falsos positivos como, por ejemplo, el método FDR (del inglés *False Discovery Rate*) (Benjamini and Hochberg, 1995). La corrección de los datos mediante este método ha demostrado aumentar la potencia estadística de los análisis de expresión génica (Shaffer, 1995). Una vez realizado el análisis estadístico, es necesario asignar a cada identificador de Affymetrix el nombre del gen y su identificador (Gene Symbol, EntrezID, Ensembl ID), utilizando para ello las base de datos públicas (por ejemplo, GenBank www.ncbi.nlm.nih.gov/genbank/).

En la actualidad, la disponibilidad de entornos de programación gratuitos ha propiciado que la bioinformática haya experimentado un avance muy rápido. En este sentido, el entorno de programación gratuito R está basado en paquetes que permiten llevar a cabo las funciones anteriormente mencionadas. En esta Tesis doctoral, R ha sido una herramienta fundamental para llevar a cabo los estudios transcriptómicos presentados en esta Memoria.

En lo referente a la **Proteómica**, la estructura de los datos proteómicos es multidimensional (valor m/z de los iones, intensidad, espectro de fragmentación y en el caso de la aproximación "shotgun", tiempo de retención), y el uso de espectrómetros de masas de última generación ha hecho que se genere una gran cantidad de espectros MS^2 por análisis. La complejidad y el tamaño de los datos proteómicos hacen que su tratamiento siga siendo el cuello de botella de esta tecnología, y actualmente se siguen desarrollando herramientas bioinformáticas que permitan su tratamiento (Kumar y Mann, 2009). En el caso de la aproximación "shotgun", el primer paso en el tratamiento de estos datos es la extracción de los picos de los cromatogramas mediante algoritmos matemáticos. Posteriormente, la masa experimental de cada compuesto y su patrón de fragmentación son comparadas con los datos almacenados en bases de datos proteómicos utilizando diversos motores de búsqueda. Los motores de búsqueda de péptidos y proteínas más utilizados en los estudios proteómicos son Mascot (Perkins y col., 1999), SEQUEST (Eng y col., 1994) y Andromeda (Cox y col., 2011). La comparación entre los datos experimentales y teóricos se puede llevar a cabo mediante dos estrategias:

- Huella peptídica: Se compara la lista de masas peptídicas experimentales con la lista de masas peptídicas teóricas almacenadas en las bases de datos. Cuanto mayor sea el número de coincidencias entre masas experimentales y masas teóricas, mayor será la probabilidad de identificar correctamente la proteína.

- Secuenciación peptídica: Se compara la masa molecular y el espectro de fragmentación de cada uno de los péptidos generados en la digestión de las proteínas, con las masas moleculares y los espectros de fragmentación teóricos contenidos en las bases de datos proteómicos (Figura 1.5).

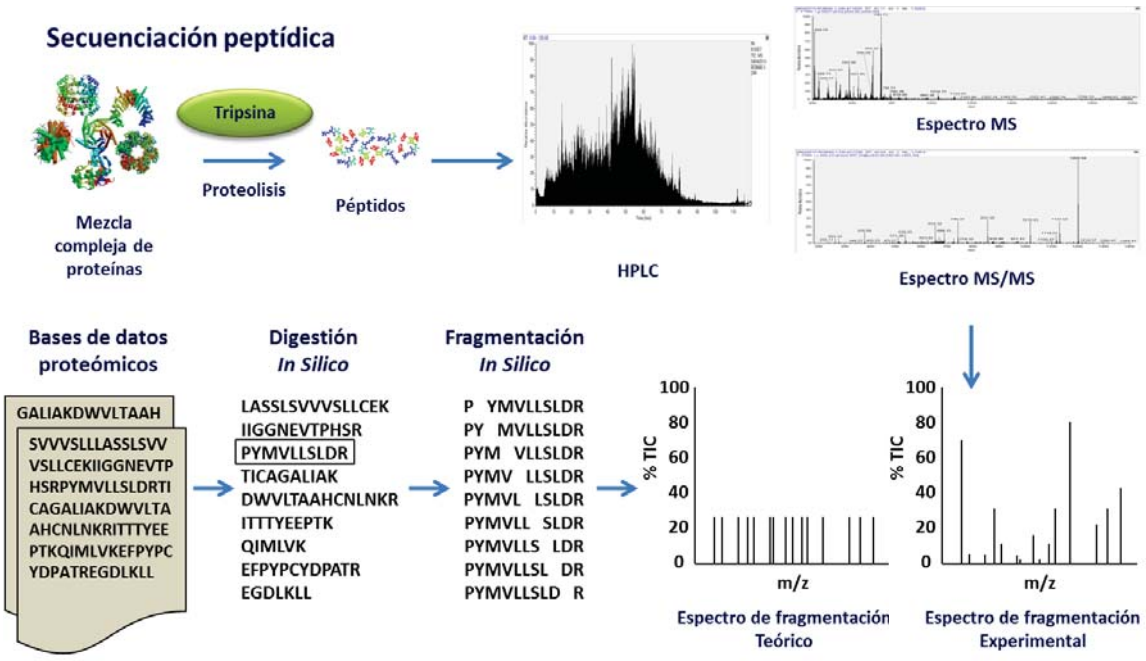

Figura 1.5 Estrategia basada en la secuenciación peptídica para la identificación de proteínas.

Los algoritmos matemáticos empleados por los diversos motores de búsqueda dan como resultado una lista de las proteínas identificadas, y un valor de probabilidad o tasa de falsos positivos (Kumar y Mann, 2009). Tras la identificación de las proteínas, y tal y como se ha comentado anteriormente, la cuantificación puede llevarse a cabo utilizando diversos métodos. En los estudios proteómicos de tipo "shotgun" llevados a cabo en esta Tesis doctoral se ha utilizado la herramienta MaxQuant, un software de libre acceso que permite trabajar con los archivos generados por espectrómetros de masas de distintas casas

comerciales (Thermo, Bruker u otros) (Cox y Mann, 2008). Este software permite la extracción de los picos, y haciendo uso del motor de búsqueda Andromeda, lleva a cabo la identificación de los péptidos y sus correspondientes proteínas, así como su cuantificación.

En el campo de la **Metabolómica**, y al igual que en Proteómica, los datos obtenidos se caracterizan por ser altamente complejos, por lo que para su procesado también se requieren herramientas bioinformáticas especializadas (Mehrotra y Mendes, 2006). En primer lugar, los datos deben transformarse a formatos compatibles para procesarse con estas herramientas. En general, el procesado consiste en la detección de las especies iónicas, la eliminación de las señales que no proceden de la muestra, el alineamiento de los tiempos de migración/retención y la anotación de los picos detectados. Las herramientas bioinformáticas seleccionadas para el procesado de los datos variarán en función de la plataforma utilizada para el análisis. Posteriormente es necesario hacer un análisis estadístico de las señales para identificar aquellas señales significativas entre las distintas muestras. Por último, se identifican los metabolitos comparando la masa, el perfil isotópico y el patrón de fragmentación con los contenidos en distintas bases de datos de metabolitos. Las bases de datos de metabolitos más utilizados en los estudios metabolómicos son Human Metabolome Database (Wishart y col., 2009), KEEG (Kanehisa, 1997), METLIN (Smith y col., 2005) o PubChem (http://pubchem.ncbi.nlm.nih.gov/). Para llevar a cabo los estudios metabolómicos presentados en esta Tesis doctoral se ha utilizado la herramienta bioinformática MZmine (Katajamaa y Oresic, 2005) y el paquete XCMS (Smith y col., 2006) del entorno de programación R.

1.1.4.1 Análisis exploratorio de los datos

Además de las herramientas bioinformáticas específicas para cada plataforma, también se han desarrollado herramientas que asisten al investigador en la interpretación de los datos ómicos. Estas herramientas conocidas como "técnicas de enriquecimiento funcional" tienen como objetivo identificar las funciones biológicas o rutas metabólicas alteradas entre las distintas situaciones estudiadas. Para la interpretación de los resultados, las herramientas de enriquecimiento funcional hacen uso de bases de datos públicas como Gene Ontology (GO) (Ashburner y col., 2000), KEGG (del inglés *Kyoto Encyclopedia of Genes and Genomes*) o Reactome (Joshi-Tope y col., 2003). La base de datos GO se creó con el objetivo de generar una terminología universal y dinámica, teniendo en cuenta que nuestro conocimiento de las funciones de las proteínas y los genes cambia con el tiempo. En la base de datos GO, los genes y proteínas responsables de las principales funciones biológicas están organizados en tres grandes grupos: procesos biológicos, funciones moleculares y componentes celulares. Por otro lado, en las bases de datos KEGG y Reactome está almacenada la información de los genes, proteínas y metabolitos involucrados en las distintas rutas metabólicas.

Las herramientas de enriquecimiento funcional más utilizadas en los estudios ómicos pueden dividirse en tres grandes grupos:

Herramientas de primera generación, o basadas en el método de "solapamiento". Estas herramientas utilizan las listas de genes o proteína expresadas diferencialmente obtenidas tras los análisis ómicos. El método de "solapamiento" consiste en la superposición de los genes o proteínas contenidos en las listas, sobre los genes o proteínas que conforman los términos de la GO o las rutas metabólicas contenidas en las bases de datos como KEGG o Reactome. Tras la superposición de los datos, estas herramientas

llevan a cabo distintos test estadísticos para determinar los términos y/o funciones/procesos más representados entre las distintas condiciones experimentales estudiadas. La herramienta de primera generación Ingenuity Pathway Analysis (IPA) ha sido utilizada en la presente Tesis doctoral. Además de permitir el análisis de datos transcriptómicos, proteómicos y metabolómicos, IPA permite inferir el estado de los factores de transcripción (activación o inactivación), analizando el patrón de expresión de los genes/proteínas que están bajo su control.

Herramientas de segunda generación, o basadas en el método de "puntuación de las funciones". Estas herramientas son específicas para el análisis de datos transcriptómicos, y permiten evaluar si un grupo de genes (seleccionado por el analista o no) está enriquecido en relación al total de genes analizados. El primer paso del método de "puntuación de las funciones" consiste en el cálculo de la expresión de todos los genes entre las distintas condiciones experimentales estudiadas. Posteriormente, se selecciona un grupo de genes y se mapea su valor de expresión entre los distintos términos y/o funciones/procesos biológicos. Finalmente, se "puntúan" o analizan estadísticamente cada uno de estos términos y/o funciones/procesos biológicos con el objetivo de determinar cuáles están más representados. Al tener en cuenta la información de todos los genes, y no solo de un conjunto, los resultados obtenidos utilizando este método han demostrado ser más consistentes que los obtenidos mediante las herramientas de primera generación (Pavlidis y col., 2004). La herramienta de segunda generación de libre acceso Gene Set Enrichment Analysis (GSEA), ha sido utilizada en la presente Tesis doctoral para analizar los datos transcriptómicos obtenidos mediante la técnica del microarray de expresión génica.

Herramientas de tercera generación, o de "rutas topológicas". Algunas de las herramientas de tercera generación trabajan con listas de genes o proteínas, y otras utilizan todos los genes representados en los microarrays. En cualquiera de los dos casos, estas

herramientas utilizan la tasa de expresión de los genes/proteínas entre las distintas condiciones experimentales estudiadas, y superponen los valores de expresión sobre los genes o proteínas que conforman los términos y/o funciones/procesos biológicos. Las herramientas de tercera generación se diferencian de las de primera y segunda generación en que tienen en cuenta la importancia que los genes/proteínas tienen en los términos o las funciones/procesos biológicos donde están representados.

1.1.5 Integración de las tecnologías ómicas: Biología de sistemas

La biología de sistemas se ha definido como la ciencia que estudia los principios que permiten la aparición de las propiedades funcionales de los organismos vivos, a partir de las interacciones entre las macromoléculas que los constituyen (Westerhoff y Alberghina 2005).

La biología de sistemas considera cada sistema biológico como un todo, centrándose en: (1) la cuantificación de los distintos niveles de información biológica; (2) la integración de la información, analizando tanto el metabolismo y la fisiología celular, como la función y los cambios generados por el ambiente; (3) el estudio dinámico de los cambios, teniendo en cuenta no solo el estado celular actual y su relación con el ambiente, sino su posible cambio en el tiempo; (4) la generación de modelos causales que permitan desarrollar relaciones biológicas jerárquicas; (5) la comprobación de hipótesis y el establecimiento de modelos de predicción (Figura 1.6).

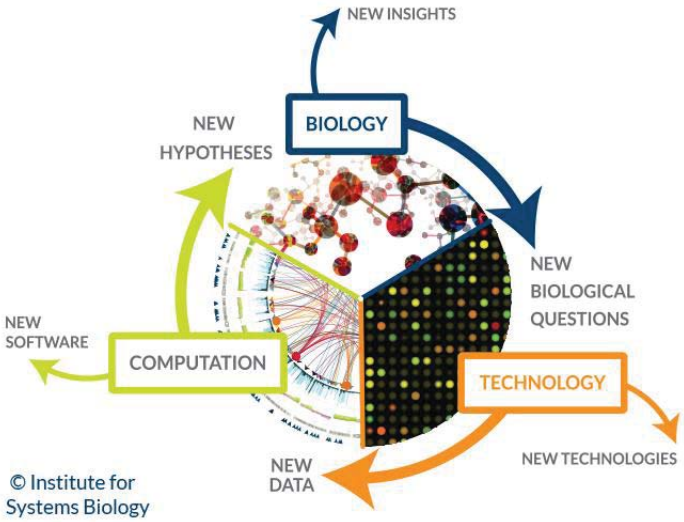

Figura 1.6 Esquema de la biología de sistemas. Figura obtenida del Insitute for Systems Biology.

Actualmente, los esfuerzos de la biología de sistemas se centran en la conversión de los datos masivos obtenidos por las tecnologías de alto rendimiento en información relevante. Con el objetivo de almacenar y manejar esta información, se han creado distintas bases de datos como GenBank (genes), UniProt (proteinas) (Apweiler y col., 2004) o HMDB (metabolitos), y repositorios de datos transcriptómicos (Gene Expression Omnibus, Edgar y col., 2002) o datos proteómicos (PRIDE, Martens y col., 2005). En los repositorios de datos, los investigadores pueden depositar tanto los datos como la información referente a las técnicas utilizadas en sus experimentos, y así poder ser comparados y validados con resultados obtenidos en otros laboratorios. Los datos contenidos en estos repositorios pueden utilizarse como bases de datos para realizar búsquedas, permiten a otros investigadores utilizar metodologías diferentes a las que se usaron en un primer momento y son una fuente muy importante para el desarrollo del "data mining" o minería de datos (Vizcaíno y col., 2010). La creación de las bases de datos y los repositorios, unido a la creación de las bases de datos donde está almacenada la información biológica (GO, KEGG, Reactoma), ha requerido el desarrollo de herramientas bioinformáticas capaces de organizar toda la información, y así aumentar el valor de los datos existentes. Sin embargo, la comprensión de un sistema biológico desde el punto de vista de la biología de sistemas, requiere la integración de todos los datos mediante modelos matemáticos (Gomez-Cabrero y col., 2014). Los modelos matemáticos tratan de describir mecanísticamente las relaciones existentes entre todos los componentes de un sistema biológico. El objetivo final es la comprensión minuciosa de las funciones biológicas, para la posterior aplicación de este conocimiento en el diagnóstico de enfermedades, la identificación de dianas terapéuticas, y el diseño de fármacos y terapias (Lappe y Holm, 2004). Sin embargo, y a pesar de los esfuerzos que se han hecho en el desarrollo de herramientas como IPA, aún no se han desarrollado herramientas computacionales suficientemente potentes que permitan

comprender el funcionamiento de los sistemas biológicos desde un punto de vista holístico. La falta de estas herramientas y nuestro conocimiento limitado de los procesos celulares a nivel molecular son las principales limitaciones encontradas en los estudios en los que se intenta integrar información procedente de los distintos niveles de expresión (transcriptoma, proteoma y metaboloma), como los estudios alimentómicos presentados en esta Tesis.

1.2 Dieta mediterránea

La "Dieta Mediterránea", o patrones dietéticos propios de las zonas geográficas de la cuenca Mediterránea, ha ganado popularidad en los últimos años (Sofi y Casini, 2014; Estruch y col., 2013). Esto se debe al elevado número de estudios epidemiológicos que sugieren una menor incidencia de enfermedades crónicas en poblaciones que consumen preferentemente este tipo de dieta, caracterizada por el consumo elevado de frutas, verduras, aceite de oliva virgen, etc. Las propiedades saludables de esta dieta se han atribuido en parte a la gran cantidad y diversidad de compuestos bioactivos contenidos en estos alimentos (Gerber y Hoffman, 2015). Además, en los últimos años se han llevado a cabo muchos estudios *in vitro* e *in vivo* que han demostrado las distintas propiedades biológicas de estos compuestos, siendo los polifenoles el grupo más estudiado (Iriti y Vitalini, 2012).

Los polifenoles es el grupo de compuestos bioactivos más abundante, y actualmente se han descrito más de 8000 compuestos diferentes (Manach y col., 2004). Existen varias clases y subclases, que se definen en función del número de anillos fenólicos que poseen y de los grupos funcionales que presentan estos anillos. Los principales grupos de polifenoles son los ácidos fenólicos (derivados del ácido hidroxibenzoico o del ácido hidroxicinámico), estilbenos, lignanos, alcoholes fenólicos y flavonoides, siendo estos últimos los más numerosos. Los polifenoles se originan principalmente como productos del metabolismo secundario de las plantas. Estos compuestos pueden desempeñar diversas funciones fisiológicas, actuando como antioxidantes, modulando el crecimiento o captando las radiaciones UV, impidiendo así sus efectos nocivos en los tejidos vegetales (Manach y col., 2004). Además, estos compuestos forman parte de la composición de esencias y pigmentos,

y pueden proteger a las plantas generando sabores o texturas que resultan desagradables para los herbívoros.

El consumo de los polifenoles en la dieta es muy variable y está afectado por los hábitos alimentarios y las preferencias individuales. Se ha calculado que el consumo medio es de aproximadamente 1 g por persona y día (Scalbert y Williamson, 2000). Una vez incorporados a la dieta humana, los polifenoles tienen propiedades fisiológicas variadas, pudiendo actuar como antialergénicos, anticancerígenos, antiaterogénicos, antiinflamatorios, antimicrobianos, antioxidantes, antitrombóticos, cardioprotectores y vasodilatadores (Quiñones y col., 2013). Una de las propiedades más estudiadas es su actividad antioxidante. Esta actividad confiere a los polifenoles un efecto protector, al ser capaces de secuestrar radicales libres y así paliar el estrés oxidativo generado por las especies reactivas del oxígeno durante el desarrollo de algunas enfermedades crónicas como el cáncer. En este sentido, distintos estudios aseguran que las terapias basadas en el uso de polifenoles con alta capacidad antioxidante son capaces de disminuir los niveles de las especies reactivas del oxígeno (Lee y Lee, 2006). Otros estudios han demostrado que la combinación de antioxidantes con diferentes modos de acción aumenta la eficacia frente a las dietas suplementadas con un solo antioxidante, debido a los posibles efectos aditivos o sinérgicos entre los distintos compuestos (Liu, 2004).

Algunos de los alimentos más estudiados debido a su alto contenido en polifenoles son el té verde, el aceite de oliva, la soja, la uva, o especias como el romero. En el té verde, el principal compuesto bioactivo es el epigalocatequin-3-galato. Este compuesto ha demostrado ser un agente quimioprotector frente al cáncer de pulmón, hígado, piel y próstata (Khan y Mukhtar, 2010; Klaus y col., 2005). El aceite de oliva también se ha estudiado en profundidad, y su consumo dentro de la dieta mediterránea se ha asociado con un efecto protector frente al desarrollo de varios tipos de cáncer (colon, endometrio,

estómago, mama y ovario) (Perez-Jiménez y col., 2005). Dentro del aceite de oliva, el polifenol principal es el hidroxitirosol, al que además se le han atribuido propiedades como reductor de enfermedades coronarias y ateroesclerosis (Tuck y Hayball, 2002). También hay evidencias suficientes de estudios epidemiológicos y experimentales de los efectos protectores de la soja y sus isoflavonas frente a enfermedades crónicas como el cáncer (colon, mama, próstata, o pulmón), la osteoporosis, o desórdenes cardiovasculares (Franke y col., 2010; Levis y col., 2010). Otro alimento que ha sido muy estudiado es la uva. El compuesto bioactivo principal de este alimento es el resveratrol, un polifenol con una potente actividad antioxidante. El resveratrol ha demostrado tener propiedades beneficiosas para la salud, ya que protege frente a la aparición de enfermedades como la diabetes tipo 2, las enfermedades cardiovasculares o el cáncer (Marques y col., 2009; Markus y Morris, 2008). Por otro lado, también se han estudiado distintas especias utilizadas en la dieta mediterránea, como el romero (*Rosmarinus officinalis*). Esta planta es muy rica en polifenoles, y se le han atribuido propiedades antimicrobianas, antiinflamatorias, o antioxidantes, entre otras. Además de estas propiedades, también se ha demostrado que el romero protege frente a la aparición de enfermedades crónicas como el cáncer (González-Vallinas y col., 2015a) y la diabetes (Bakirel y col., 2008).

1.3 Romero

El romero es una planta aromática que pertenece a la familia de las Lamiaceae. Es un arbusto de hoja perenne que puede llegar a los dos metros de altura, y posee hojas curvadas y coriáceas. Estas hojas tienen la superficie superior de color verde oscuro y la inferior de color gris, y pueden medir hasta 3 cm de longitud y 3 mm de grosor. El romero es una planta xeromórfica que crece de forma espontánea en la arena, acantilados y pedregales, y se da de forma natural y abundante en la cuenca Mediterránea. Debido a sus características organolépticas y antioxidantes, el romero se ha utilizado desde la antigüedad con fines culinarios, como aromatizante y conservante. Además, al romero también se le han atribuido diversas propiedades medicinales, tales como actividad antimicrobiana (Hussain y col., 2010), antiinflamatoria (Arranz y col., 2015) o antioxidante (Naciye y col., 2008). Además de estas propiedades, el romero también tiene efectos beneficiosos para la salud, ya que ayuda en la protección y el tratamiento de enfermedades como la diabetes (Bakirel y col., 2008), el cáncer (González-Vallinas y col., 2015a) o las enfermedades cardiovasculares (Afonso y col., 2013).

La composición química del romero varía en función de la especie, la variedad, las condiciones de crecimiento, el momento de la recolección, las propiedades del suelo, el clima y la localización geográfica. Dentro de los compuestos presentes en esta planta, los más importantes son los compuestos fenólicos y los compuestos volátiles, ambos responsables de las características funcionales de esta planta. Los compuestos fenólicos mayoritarios son el ácido carnósico, el ácido rosmarínico y sus productos de degradación, como el carnosol, el rosmanol, el epirosmanol, el epiisorosmanol, el rosmadial o el carnosato de metilo, entre otros (Schwarz y Ternes, 1992) (Figura 1.7). Los compuestos volátiles conforman el aceite esencial de romero, y puede representar hasta el 2.5% de la

composición de la hoja. Los compuestos volátiles principales son el acetato de borneol, el canfor, el eucaliptol, el α-pineno, el β-pineno, el β-cariofileno, la verbenona, el mirceno, el borneol y el 1,8-cineol (Salido y col., 2003) (Figura 1.8).

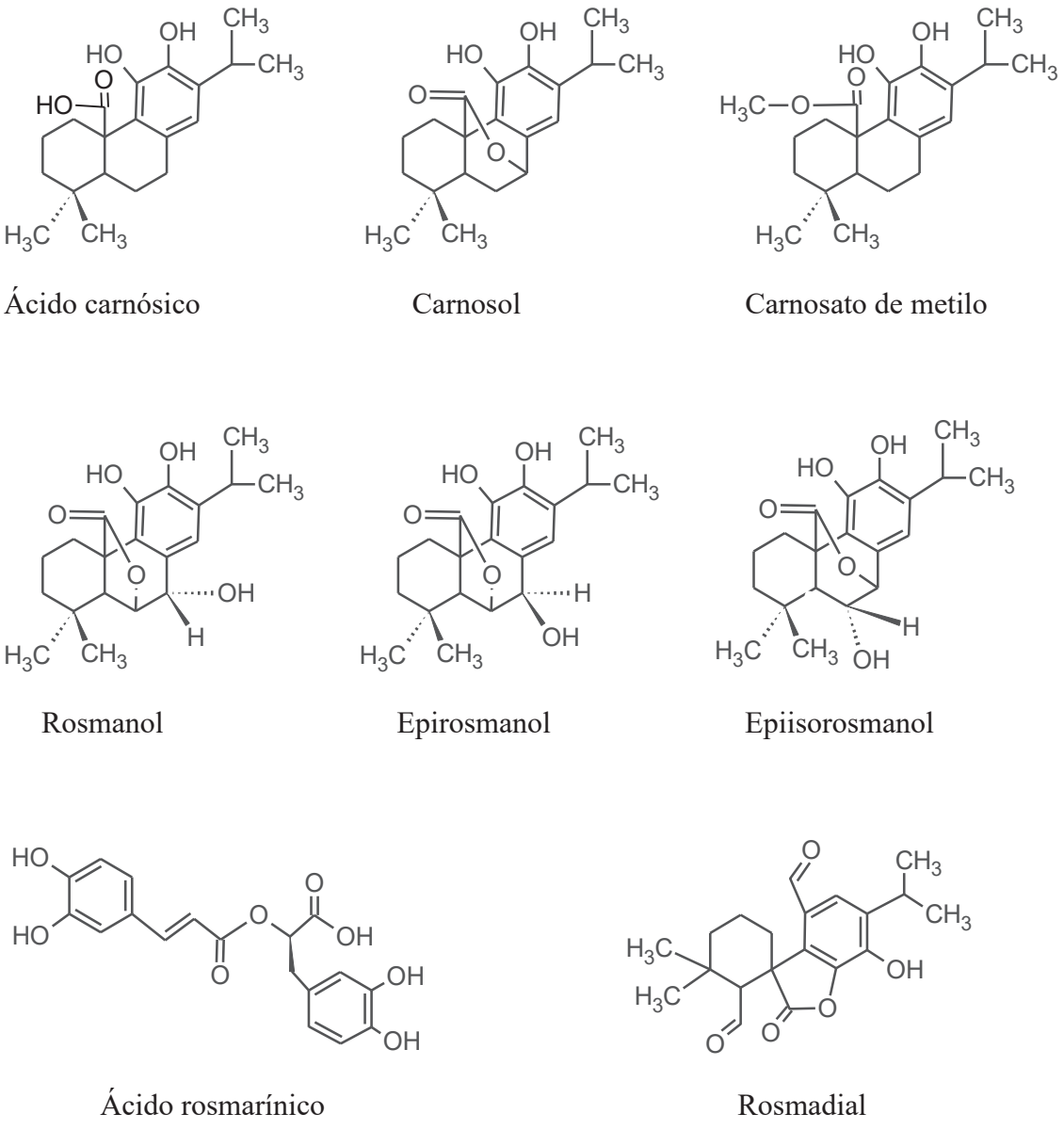

Figura 1.7 Principales compuestos fenólicos del romero.

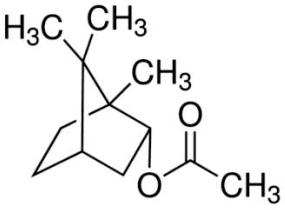

Acetato de borneol

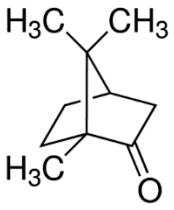

Canfor

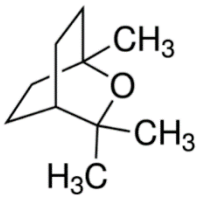

Eucaliptol

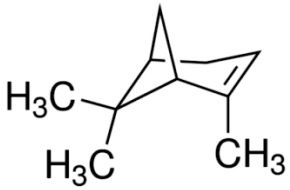

α-pineno

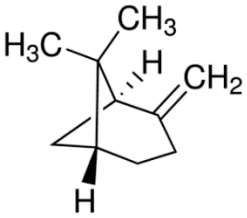

β-pineno

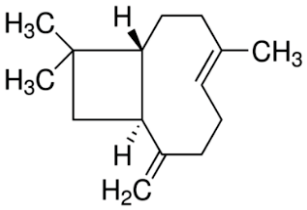

β-cariofileno

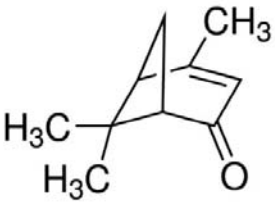

Verbenona

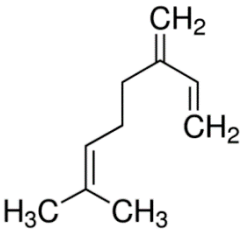

Mirceno

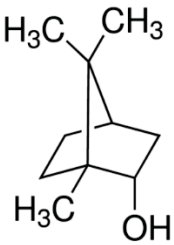

Borneol

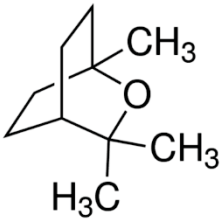

1,8-cineol

Figura 1.8 Principales compuestos volátiles del romero.

1.3.1 Almacenamiento, procesado y extracción de romero

Además de las variaciones biológicas/geológicas/climatológicas, varios estudios han demostrado que la composición y la cantidad de los polifenoles y los compuestos volátiles del romero está condicionada por el tipo de almacenamiento tras su recolección, las condiciones de procesado, así como el método de extracción (Szumni y col., 2010; Dumbravă y col., 2012; Herrero y col., 2010b).

El romero se ha utilizado tanto en forma sólida (fresco o desecado) como líquida tras una etapa de extracción (aceite esencial o extracto de romero). En el romero fresco, el ácido carnósico es el polifenol mayoritario, pero dependiendo de las condiciones en las que se almacene, se procese o se extraiga, el ácido carnósico puede degradarse a otros compuestos. Estos, en su mayoría, son compuestos fenólicos con estructuras de lactona, como el carnosol, rosmanol, epirosmanol y 7-metil-epirosmanol, siendo el carnosol el producto resultante mayoritario (Almela y col., 2006).

En el caso del almacenamiento, se han llevado a cabo diversos estudios que demuestran que la conservación de las hojas de romero frescas o congeladas favorece la oxidación del ácido rosmarínico, algo que no ocurre cuando estas son desecadas. Los investigadores atribuyen este efecto al agua contenida en las hojas, que posibilita la actividad oxidante de ciertas enzimas (Bellumori y col., 2015, Mulinacci y col., 2011).

El secado de las hojas puede llevarse a cabo de muchas formas: bajo el sol, con aire a temperatura ambiente, por corriente convectiva, en horno, por microondas, etc. Estos métodos pueden alterar la composición del romero, y por tanto su actividad biológica, y algunos de ellos (por corriente convectiva, por microondas o una combinación de ambos) han sido comparados entre sí (Szumni y col., 2010). En ese estudio los autores concluyen que el desecado por microondas es el método que más disminuye la concentración de los

compuestos volátiles, y que la combinación de ambos procesos es la mejor estrategia (Szumny y col., 2010).

Para la extracción de los aceites esenciales se han utilizado la hidrodestilación (Salehi y col., 2007) o la hidrodifusion por microondas (Bousbia y col., 2009), centradas en obtener los compuestos volátiles. En cuanto a los extractos de romero, se han utilizado para su obtención técnicas convencionales como la extracción sólido-líquido (Doolaege y col., 2007), la hidrodestilación (Almela y col., 2006) o la destilación por arrastre de vapor (Roldan-Gutierrez y col., 2008). También se han utilizado técnicas como la extracción asistida por ultrasonidos (Paniwnyk y col., 2009), el Soxhlet (Bicchi y col., 2000) o la extracción mediante procesos medioambientalmente limpios, como son el empleo de fluidos presurizados y de fluidos supercríticos (Herrero y col., 2010b, Vicente y col., 2013), con algunas variantes (Sánchez-Camargo y col., 2014; Sánchez-Camargo y col., 2016). En estos trabajos se demuestra que tanto la técnica como el disolvente empleados afectan de manera muy importante al rendimiento de la extracción y al tipo de compuestos obtenidos. Así, la extracción con solventes orgánicos como el pentano o el hexano disminuye enormemente el rendimiento de la extracción de fenoles, y aumenta la aparición de sus productos oxidados, como el carnosol y el rosmanol (Bellumori y col., 2015). En otro estudio se determinó que, tanto en la destilación como en la extracción con acetona/hexano, y en la extracción con fluidos supercríticos, el borneol, acetato de bornilo, canfor, β-cariofileno y verbenona eran los compuestos volátiles más abundantes en el aceite esencial de romero (Scollard y col., 2014). También se ha demostrado que la extracción con fluidos supercríticos es la técnica que permite una mayor recuperación de ácido carnósico, y el uso de bajas temperaturas evita la oxidación del ácido carnósico a carnosol, una reacción muy rápida en presencia de oxígeno (Peng y col., 2007). Además, algunas modificaciones en esta técnica como la extracción por etapas, ha permitido enriquecer los extractos en ácido

carnósico y carnosol, los dos compuestos fenólicos mayoritarios en esta planta (Sánchez-Camargo y col., 2014).

1.3.2 Actividad biológica de romero

Las técnicas modernas de análisis han permitido la identificación y cuantificación de los compuestos principales de romero, y han permitido estudiar sus efectos sobre la salud. Como ya se ha mencionado, hay dos grupos de compuestos que son los responsables principales de la actividad biológica del romero, los compuestos volátiles y los compuestos fenólicos. Aun así, ciertos estudios han demostrado que los compuestos minoritarios pueden ser muy importantes ya que pueden producir efectos sinérgicos con los demás compuestos (Ojeda-Sana y col., 2013). A continuación, se describen las propiedades más importantes atribuidas al romero y en particular a sus constituyentes fenólicos que serán los compuestos objeto de esta Tesis doctoral.

1.3.2.1 Actividad antioxidante

Las propiedades antioxidantes del romero se conocen desde comienzos de los años 50, cuando se descubrió que era una de las especias que mayor actividad antioxidante poseía, siendo por ello muy estudiada desde entonces (Rac y Ostric-Matijasevic, 1955). Estudios posteriores demostraron que el componente responsable de esta actividad era un polifenol, el ácido carnósico (Wu y col., 1982). Posteriormente se ha atribuido esta actividad a los dos polifenoles mayoritarios, el ácido carnósico y el carnosol, que pueden representar el 5% en peso seco de la hoja de romero (Aruoma y col., 1992). Ambos compuestos tienen la capacidad de secuestrar las especies reactivas del oxígeno, por lo que

protegen frente a la peroxidación lipídica y, por tanto, frente al daño producido en las membranas celulares. Además del ácido carnósico y del carnosol, otros compuestos del romero como el ácido rosmarínico, han demostrado tener un alto poder antioxidante (Kontogianni y col, 2013). Por otro lado, algunos de los compuestos minoritarios o de degradación como el rosmanol, el carnosato de metilo, la luteolina, el ácido betulínico y la genkwanina podrían tener efectos sinérgicos en la capacidad antioxidante total del extracto de romero (Peng y col., 2007).

Debido a su capacidad antioxidante, tanto el aceite esencial, como el extracto de romero han sido reconocidos como compuestos GRAS (del inglés *Generally Recognized As Safe*) para su uso en alimentación, acorde a la sección 408 de la FDA (del inglés *Food and Drug Administration*) de los Estados Unidos y a la Directiva 2010/67/EU de la Comisión Europea. Además, se ha demostrado que los extractos de romero tienen mayor actividad antioxidante que algunos compuestos sintéticos utilizados en alimentación, como el butilhidroxitianosol, el ácido ascórbico o el α-tocoferol (Babovic y col., 2010; Peng y col., 2007; Romano y col., 2009). Por ello, se ha investigado su uso como aditivo alimentario, adicionado directamente al alimento o incorporado durante el envasado, actuando como agente antimicrobiano y antioxidante.

1.3.2.2 Actividad antimicrobiana

La actividad antimicrobiana del romero se conoce desde la antigüedad, por lo que también ha sido estudiada en profundidad (Mangena y Muyima, 1999). Varios trabajos han demostrado que el romero, y en concreto su aceite esencial, es efectivo frente a un gran número de bacterias como, por ejemplo, *Staphylococcus aureus*, *Bacillus cereus*, *Bacillus subtilis*, *Bacillus pumilis*, *Pseudomonas aeruginosa*, *Salmonella poona*, *Escherichia coli*,

Listeria innoca, *Bacillus thermosphacta*, *Listeria innocua*, *Listeria monocytogenes* y *Staphylococcus putrefaciens* (Hussain y col., 2010, Teixeira y col., 2013); y hongos de las especies *Aspergillus flavus* y *Aspergillus niger* (Souza y col., 2013). En estos trabajos, la actividad se atribuye a los compuestos volátiles 1,8-cineol, canfor, eugenol y α-pineno. Se ha demostrado que el aceite esencial de romero tiene una actividad antimicrobiana mayor que el 1,8-cineol, el compuesto mayoritario, indicando que su efecto puede deberse a una sinergia entre este compuesto y los compuestos minoritarios (Hussain y col., 2010). Este efecto también se ha encontrado en extractos polifenólicos de romero, atribuyendo el efecto al ácido carnósico (Rožman y Jersek, 2009).

1.3.2.3 Actividad antiinflamatoria

Diversos estudios han demostrado que el romero, y en concreto el ácido carnósico, el carnosol y algunos compuestos flavonoideos como la luteína, tienen efectos antiinflamatorios (Peng y col., 2007; Bai y col., 2010). El estudio llevado a cabo por el grupo de Peng y col. en macrófagos murinos RAW 264.7 demuestra que un extracto de romero obtenido con CO_2 supercrítico posee actividad antiinflamatoria, ya que disminuye la producción de óxido nítrico (Peng y col., 2007). En estas mismas células, un extracto metanólico de romero (constituido principalmente por ácido carnósico y carnosol), también ha demostrado reducir la inflamación mediante la disminución del óxido nítrico (Yu y col., 2013). Los autores de este trabajo relacionan la disminución del óxido nítirico con la inhibición de las enzimas óxido nítrico sintasa y ciclooxigenasa 2 tras el tratamiento con el extracto de romero. Además, otro estudio ha demostrado que la luteína también es responsable de la disminución del óxido nítrico en estas células (Bai y col., 2010). Por otro lado, la actividad antiinflamatoria de la fracción basolateral de monocapas de células Caco-

2 expuestas a un extracto de romero supercrítico también ha sido evaluada recientemente (Arranz y col., 2015). Los resultados indican que la fracción recuperada tras la absorción del extracto mediante células Caco-2 disminuye la excreción de citoquinas inflamatorias en macrófagos humanos THP-1.

1.3.2.4 Actividad anticancerígena

Según datos extraídos del informe World Cancer Report de 2014 elaborado por la Organización Mundial de la Salud, en el año 2012 se diagnosticaron aproximadamente 14 millones de nuevos casos de cáncer y alrededor de 8.2 millones de muertes a nivel mundial (Stewart y Wild, 2014). Además, se espera que el número de nuevos casos se incremente en un 70% en las próximas dos décadas, llegando a 22 millones de casos.

El cáncer es un término genérico usado para definir un conjunto de enfermedades relacionadas entre sí y que pueden afectar a casi cualquier parte del organismo (WHO, 2015). La transformación de una célula normal en una célula tumoral comienza a partir de una lesión precancerosa que finalmente desencadena en la formación de un tumor maligno. En una situación normal, las células humanas crecen y se dividen para formar células nuevas que reemplacen las células viejas o dañadas que el organismo no necesita. Sin embargo, cuando se desarrolla el cáncer, este proceso se interrumpe. A medida que las células se vuelven anormales, las células viejas o dañadas sobreviven cuando deberían morir. Estas células pueden continuar dividiéndose sin control y acumularse formando nódulos o tumores. En el caso de que los tumores se desarrollen en tejidos se consideran “tumores sólidos”, pero si se desarrollan en la sangre, como la leucemia, se denominan “tumores líquidos”.

Una diferencia importante entre las células de cáncer y las células normales es que las células de cáncer están menos especializadas que las células normales. Mientras que las células normales maduran en distintos tipos celulares con funciones específicas, las células de cáncer no lo hacen, y continúan multiplicándose sin control. Además, las células de cáncer escapan al control de la apoptosis, un proceso de muerte celular programada que se activa cuando las células están dañadas.

El cáncer es considerado una enfermedad genética, causada por cambios en genes que controlan la función de las células, especialmente en la forma en la que crecen e invaden. El 5-10% de los cambios genéticos que causan el cáncer pueden ser heredados, pero la gran mayoría (90-95%) surgen como resultado de errores que se producen cuando las células se dividen, o debido a daños en el DNA causado por ciertos factores ambientales (Anand y col., 2008). Algunos de los principales factores de riesgo de cáncer son el tabaco, la dieta, las infecciones o los contaminantes medioambientales. También se ha demostrado que el consumo de alcohol aumenta el riesgo de padecer cáncer de boca, faringe o hígado. De entre estos factores, la dieta es el principal factor de riesgo de cáncer, siendo la causa del 30-35% de los casos diagnosticados. En cuanto a las distintas dietas, se ha demostrado una gran asociación entre las dietas basadas en carnes rojas y procesadas y el cáncer de colon (Sinha y col., 1999). Sin embargo, las dietas basadas en alimentos vegetales (frutas y verduras), como el caso de la dieta mediterránea, se ha asociado con un menor riesgo de padecer cáncer (Gerber y Hoffman, 2015).

En general, el desarrollo del cáncer consiste en varias etapas: la iniciación, la promoción y la progresión. Un agente anticancerígeno es aquel compuesto capaz de bloquear eficientemente una o varias de estas etapas. En este sentido, la actividad anticancerígena del extracto de romero y la actividad de sus polifenoles mayoritarios (ácido carnósico y carnosol) ha sido muy estudiada en los últimos años (Ibáñez y col., 2012). Estos

estudios se han llevado a cabo en modelos *in vitro*, utilizando distintas líneas celulares de cáncer de mama (Cheung y Tai, 2007), leucemia (Ishida y col., 2014), hígado (Xiang y col., 2015), pulmón (Yesil-Celiktas y col., 2010), próstata (Petiwala y col., 2013), colon (Ibáñez y col., 2012) u ovario (Tai y col., 2012), aunque también se han utilizado modelos celulares no tumorales (López-Jiménez y col., 2013) y modelos *in vivo* (Petiwala y col., 2014; Yan y col., 2015). La actividad anticancerígena del romero puede dividirse en función de su capacidad para proteger frente a la iniciación (o actividad quimioprotectora), en su capacidad para inhibir la promoción (o actividad antiproliferativa), y en su capacidad para detener la progresión del cáncer (o actividad antiinvasiva o antimetastásica).

La actividad quimioprotectora del romero y de sus compuestos mayoritarios se ha relacionado con sus propiedades antioxidantes, y en particular con su capacidad para secuestrar radicales libres, lo que podría proteger frente al daño oxidativo de lípidos, proteínas y DNA (Slamenova y col., 2002; Xiang y col., 2013). Estos compuestos también podrían tener una capacidad protectora indirecta mediante la inducción de la respuesta frente al estrés oxidativo modulada por el factor de transcripción nuclear eritroide 2 (NRF2, *Nuclear Factor (Erythroid-Derived 2)-like 2*) (Satoh y col., 2008). El factor de transcripción NRF2 regula la expresión de numerosos genes involucrados en la respuesta antioxidante, en la detoxificación, o en la generación de NADPH (del inglés *Nicotinamide Adenine Dinucleotide Phosphate*), entre otros. En una situación normal, NRF2 se encuentra en el citoplasma unido a la proteína KEAP1 (*Kelch-Like ECH-Associated Protein 1*). La unión de la proteína KEAP1 al factor de transcripción NRF2 permite la ubiquitinación de NRF2, y su posterior degradación por el proteasoma. En un estudio llevado a cabo por el grupo de Satoh y col., se ha demostrado que la forma quinona del ácido carnósico tiene la capacidad de reaccionar con la proteína KEAP1, desestabilizando el sistema KEAP1/NRF2 (Satoh y col., 2008). La desestabilización de KEAP1/NRF2 evita la degradación de NRF2,

permitiendo que NRF2 sea translocado desde el citoplasma al núcleo. Una vez en el núcleo, NRF2 se une a las secuencias promotoras ARE (del inglés *Antioxidant Response Elements*), regulando la expresión de los genes que están bajo su control. Por otro lado, el carnosol también tiene la capacidad de activar el factor de transcripción NRF2 en células tumorales de hígado (Chen y col., 2011). Los autores de este trabajo demuestran que la activación de NRF2 induce la expresión de los genes que controlan la síntesis de glutatión, contribuyendo así a mejorar la capacidad antioxidante endógena de la célula.

Además de los efectos protectores derivados de la respuesta frente al estrés oxidativo, también hay estudios que sugieren que los polifenoles derivados de las plantas presentan actividad antiproliferativa. Un estudio llevado a cabo en células de cáncer de hígado HepG2 demuestra que la actividad antiproliferativa del ácido carnósico se debe a su capacidad para desestabilizar la membrana mitocondrial y la consiguiente liberación de proteínas pro-apoptóticas al citoplasma (Xiang y col., 2015). Una vez en el citoplasma, estas proteínas son capaces de activar otras proteínas (como por ejemplo la caspasa 3), que activan a su vez la muerte celular programada. El trabajo del grupo de Xiang y col. demuestra que el ácido carnósico activa la inducción de la caspasa 3 y la hidrólisis de PARP1 (*Poly (ADP-ribose) polymerase 1*) de manera dependiente del tiempo y la concentración. Además, el ácido carnósico también reduce la fosforilación de la proteína con actividad quinasa AKT, perteneciente a la ruta de señalización PI3K/AKT (una ruta constitutivamente activa en las células de cáncer, Crowell y col., 2007). Esta ruta de señalización está involucrada en la proliferación, el crecimiento y la supervivencia de las células cancerígenas, y su inactivación podría desencadenar la muerte celular por apoptosis. La inhibición de la fosforilación de Akt por el ácido carnósico también ha sido demostrada por el grupo de Gao y col. utilizando la misma línea celular HepG2 (Gao y col., 2015). Además de inhibir la fosforilación de AKT, el ácido carnósico inhibe la fosforilación de

mTOR (*Mammalian Target of Rapamycin*), una proteína con actividad quinasa reguladora de autofagia, que está controlada por la ruta PI3K/AKT. La inhibición de la fosforilación de AKT/mTOR unida a la inducción de la formación de vacuolas autofágicas, indica que el ácido carnósico podría reducir la proliferación de las células HepG2 mediante la activación de autofagia. En un estudio en células de cáncer de próstata PC3, Johnson y col. (2008) observaron que el carnosol detiene las células en la fase G2/M del ciclo celular e induce la muerte celular por apoptosis. Los autores sugieren que el efecto antiproliferativo del carnosol se debe a la inhibición de la fosforilación de mTOR mediante la activación de la proteína TSC2 (*Tuberous Sclerosis Complex 2*), un regulador negativo de la actividad de mTOR. En otro estudio llevado a cabo por el grupo de González-Vallinas y col. (2015b), los autores demuestran que el efecto antiproliferativo de los extractos de romero en células de cáncer de colon y de páncreas es mayor cuanto mayor es su contenido en ácido carnósico. En el mismo trabajo, los autores sugieren que la actividad antiproliferativa del extracto de romero podría estar relacionada con la inducción del supresor tumoral GCNT3 (*N-acetil-glucosaminil transferase-3*) (Huang y col., 2006), un gen involucrado en la adhesión, movilidad e invasividad de las células de cáncer de colon. En otro estudio, Park y col. (2014b) observaron que el carnosol reduce la proliferación de las células de cáncer de colon HCT-116 en función del tiempo y de la concentración, además de aumentar los niveles de caspasa 9, caspasa 3, y de PARP1 hidrolizado, indicativos de apoptosis. Además, la apoptosis inducida por el carnosol también está relacionada con la inactivación del factor de transcripción STAT3 (*Signal Transducer and Activator of Transcription-3*). El factor de transcripción STAT3 regula la expresión de genes de supervivencia, y su expresión está inducida en células de cáncer de colon, por lo que su inactivación podría estar asociada con la muerte celular por apoptosis. El carnosol también induce efectos pro-apoptóticos en células de leucemia (Ishida y col., 2014). El análisis proteómico mediante electroforesis

diferencial en gel y espectrometría de masas demuestra que el tratamiento con 40 μM de carnosol induce la traducción de proteínas relacionadas con la producción de NADPH (NAD(P)H-flavina oxidorreductasa, biliverdina reductasa y tiorredoxina reductasa). La inducción de estas proteínas unida a la disminución de los niveles de glutatión implica cambios en los niveles de las especies reactivas del oxígeno de la célula que podrían ser responsables de la muerte celular por apoptosis.

Por último, la actividad antimetastásica del romero y de sus compuestos mayoritarios también ha sido estudiada en profundidad. La metástasis es el proceso por el cual las células de cáncer son capaces de desplazarse del lugar original del tumor y formar tumores en otros tejidos. En el caso de las células epiteliales, el proceso de invasión de otros órganos está regulado a través de la activación del programa celular denominado transición epitelio-mesénquima (EMT, *Epithelial–Mesenchymal Transition*). La activación del programa EMT en las células epiteliales implica cambios en el citoesqueleto que favorecen la invasividad y la movilidad celular, así como la pérdida de la polaridad celular y del contacto célula-célula. Durante el proceso de invasión, las células epiteliales tienen que atravesar la membrana basal y desorganizar la matriz extracelular, por lo que las células expresan proteasas capaces de degradar o procesar los componentes de la matriz extracelular. Algunas de las proteínas responsables de esta actividad son las metaloproteinasas de matriz (MMP-2, *Matrix Metalloproteinase-2* y MMP-9, *Matrix Metalloproteinase-9*) y el activador de plasminógeno tipo uroquinasa (uPA, *Urokinase-type Plasminogen Activator*), por lo que se han utilizado como marcadores de la actividad metastásica. En relación a esto, el grupo de Barni y col. (2012) ha demostrado que el ácido carnósico es capaz de reducir la capacidad invasiva en el modelo celular de cáncer de colon Caco-2 mediante la reducción de MMP-2, MMP-9 y uPA. La capacidad del ácido carnósico para inhibir la migración celular también se ha demostrado en un modelo celular de

melanoma de ratón (Park y col., 2014a). Este estudio revela que el ácido carnósico, además de disminuir de los niveles de MMP-9 y de uPA, induce la expresión del inhibidor de metaloproteinasas (TIMP-2, *Metallopeptidase Inhibitor-2*). Otra serie de estudios indican que el carnosol también puede inhibir la adhesión celular en distintas líneas tumorales y no tumorales. Por ejemplo, el estudio de Vergara y col. (2014) demuestra que el carnosol es capaz de inhibir la adhesión de distintas líneas de cáncer de colon, ovario y mama, y que este efecto es dependiente de la concentración de carnosol. En otro trabajo, tanto el ácido carnósico como el carnosol han demostrado inhibir la migración celular de dos líneas celulares no tumorales (López-Jiménez y col., 2013). Además, este último estudio también revela que el ácido carnósico, y en menor medida el carnosol, son capaces de inhibir la angiogénesis *in vivo*. La angiogénesis, o la formación de nuevos vasos sanguíneos a partir de los ya existentes, tiene un papel fundamental en el crecimiento y la diseminación del cáncer, por lo que la inhibición de este proceso es esencial para combatir esta enfermedad.

Los estudios mencionados anteriormente han demostrado que el romero y sus polifenoles mayoritarios (ácido carnósico y carnosol) tienen efectos anticancerígenos muy diversos y que dependen tanto del tipo celular como de las condiciones experimentales. En la mayoría de estos trabajos, la determinación de la actividad anticancerígena de los polifenoles del romero se ha llevado a cabo mediante metodologías analíticas dirigidas al estudio de un grupo reducido de marcadores moleculares. Como alternativa, la aplicación de una aproximación Alimentómica mediante el uso combinado de varias tecnologías ómicas y herramientas bioinformáticas avanzadas permite abordar el estudio del efecto anticancerígeno de los componentes de la dieta desde un punto de vista holístico. El empleo de esta estrategia puede, por tanto, proporcionar un mayor conocimiento de los efectos de los polifenoles a nivel molecular, tanto en las rutas de transducción de señales, como en los procesos metabólicos. Esto, a su vez, permite establecer los mecanismos de acción de estos

compuestos y además identificar posibles biomarcadores de la actividad anticancerígena de los mismos.

1.4 Leucemia

Según las estimaciones del proyecto GLOBOCAN, la leucemia ocupa el duodécimo tipo de cáncer con más incidencia en el mundo (Ferlay y col., 2013). En el año 2012 hubo 352.000 nuevos casos de leucemia en el mundo, siendo su incidencia mayor en las regiones menos desarrolladas (211.000 casos nuevos), frente a las regiones más desarrolladas (141.000). En Europa, la leucemia ocupa el decimotercer lugar en la lista de cánceres, diagnosticándose más de 90.000 casos nuevos en 2012. En España se estima que en 2014 se diagnosticaron un total de 6.248 nuevos casos de leucemia, siendo 3.633 en hombres y 2.615 en mujeres. El informe del proyecto GLOBOCAN no proporciona información concreta sobre el número de casos diagnosticados de leucemia mieloide crónica, pero en España se estima que la leucemia mieloide crónica supone el 15% de todas las leucemias, con una incidencia de 1-2 casos por cada 100.000 habitantes/año (Jemal y col., 2010).

La leucemia es un cáncer que se origina en las células productoras de sangre de la médula ósea (Linet y col., 1996). Cuando una de estas células presenta lesiones que la convierten en cancerosa, no madura normalmente, sino que se divide más rápido de lo normal para formar nuevas células. Además, las células leucémicas no mueren cuando deberían hacerlo, sino que se acumulan en la médula ósea desplazando a las células normales. En un determinado momento, las células de leucemia pueden salir de la médula ósea y entrar en el torrente sanguíneo, causando un aumento en el número de glóbulos blancos en la sangre. Una vez en la sangre, las células leucémicas pueden propagarse a otros órganos, impidiendo así su funcionamiento normal.

La leucemia mieloide crónica es un tipo de leucemia en la que se produce un cambio genético en las células mieloides inmaduras (células que producen glóbulos rojos, plaquetas, y la mayoría de los glóbulos blancos). Los principales factores de riesgo para

que se produzca esta alteración genética son la exposición a dosis altas de radiaciones ionizantes y la edad (IARC, 2000), siendo la edad media de diagnóstico de 66 años, y con un mayor predominio en hombres que en mujeres. El cambio genético producido en las células de leucemia mieloide crónica da lugar a un gen anormal llamado BCR-ABL (*Breakpoint Cluster Region/Abelson Tyrosine-Protein Kinase*), y las células mieloides que poseen este gen se caracterizan por aumentar la producción de granulocitos en todas las etapas de la diferenciación celular (Clarkson y Strife, 1993).

El proceso por el que se desencadena la leucemia mieloide crónica ha sido muy bien caracterizado. La mayoría de los casos de leucemia mieloide crónica comienzan con una translocación de DNA entre los cromosomas 9 y 22 durante la división celular. Parte del cromosoma 9 pasa al cromosoma 22 y parte del cromosoma 22 pasa al 9, dando como resultado un cromosoma 22 más corto de lo normal. Este nuevo cromosoma anormal se conoce como el cromosoma Filadelfia, y está presente en un 95% de los pacientes con leucemia mieloide crónica (Groffen y col., 1984). El intercambio de DNA entre los cromosomas ocasiona la formación de un nuevo gen (un oncogén) en el cromosoma 22, el gen BCR-ABL. Este gen produce una proteína quimérica de 210 kDa, denominada $p210^{BCR-ABL}$, que tiene su actividad tirosina quinasa constitutivamente activa (Ren, 2002). La expresión de la proteína $p210^{BCR-ABL}$ desencadena varias rutas de supervivencia que confieren ventajas proliferativas y resistencia a la apoptosis (Faderl y col., 1999; Evans y col., 1993). Debido a su papel en la transformación maligna, la proteína $p210^{BCR-ABL}$ se ha utilizado como diana terapéutica en el tratamiento de la leucemia mieloide crónica. Estas terapias están basadas en el uso de fármacos que inhiben la actividad tirosina quinasa (TKI, *Tyrosine Kinase Inhibitor*) de la proteína $p210^{BCR-ABL}$. La actividad tirosina quinasa de la proteína $p210^{BCR-ABL}$ requiere ATP (*Adenosine 5'-Triphosphate*), por lo que los TKIs se han diseñado para reconocer y unirse a los sitios de unión de ATP de la proteína (Druker y

Lydon, 2000). Esta unión evita la fosforilación de los sustratos y bloquea las señales que causan el crecimiento de las células de leucemia mieloide crónica. El fármaco TKI más utilizado frente a la leucemia mieloide crónica es el Imatinib (Gleevec®). No obstante, y a pesar de que el Imatinib ha demostrado ser efectivo en el control de la leucemia mieloide crónica durante al menos diez años, eventualmente se pueden producir mecanismos de resistencia (Quintas-Cardama y col., 2009). La resistencia frente a los fármacos es uno de los factores más importantes en el fracaso de esta terapia (Persidis y col., 1999). Se han descrito varios mecanismos de resistencia frente a los TKIs, como las mutaciones en el gen BCR-ABL que evitan que los fármacos puedan actuar, el aumento de la expresión de la proteína $p210^{BCR-ABL}$, la activación de rutas alternativas de señalización de la actividad quinasa, o la inducción de genes involucrados en la excreción de fármacos de las células. Para evitar la resistencia de estas células frente al Imatinib, se han desarrollado otros TKIs más efectivos, como el Dasatinib (Sprycel®) y el Nilotinib (Tasigna®) (Santos y Ravandi, 2009). Sin embargo, las células de leucemia mieloide crónica también podrían desarrollar resistencias frente a los nuevos TKIs, por lo que las investigaciones actuales se han centrado en la búsqueda de nuevos compuestos que puedan revertir la resistencia frente a estos fármacos y por tanto mejorar su efectividad. Debido a los efectos anticancerígenos que han demostrado los polifenoles derivados de las plantas en las células de leucemia mieloide crónica (Nakazato y col., 2005; Khlifi y col., 2013; Han y col., 2013b; Mahbub y col., 2013), estos compuestos han sido muy estudiados como posibles complementos al tratamiento con los TKIs (Iwasaki y col., 2009; Chaabane y col., 2014; Can y col., 2012).

1.5 Cáncer de colon

En 2012, según las estimaciones del proyecto GLOBOCAN, hubo 1.360.000 casos nuevos de cáncer de colon o cáncer colorrectal en todo el mundo, representando casi un 10% del total de cánceres y siendo el tercer cáncer más común en todo el mundo (Ferlay y col., 2013). En cuanto a la distribución por sexo, se diagnosticaron 746.000 casos en hombres y 614.000 en mujeres. En Europa, el cáncer de colon es el segundo cáncer con mayor incidencia, diagnosticándose 447.000 nuevos casos y alcanzando 215.000 muertes en 2012. En ese mismo año se estimó que hubo 694.000 muertes por cáncer de colon en todo el mundo, siendo la cuarta causa más común de muertes asociadas al cáncer. En España, el cáncer de colon ocupa la primera posición, y se ha estimado que el número de nuevos casos en 2014 fue de 39.500, diagnosticándose 23.500 en hombres y 16.000 en mujeres.

El cáncer de colon se origina en el colon o el recto y en un 95% de los casos comienza como un crecimiento en el revestimiento interno del colon o del recto llamado pólipo (Watson y Collins, 2011). Algunos tipos de pólipos pueden convertirse en cáncer con el paso del tiempo. La probabilidad de transformarse en un cáncer depende del tipo de pólipo. Los dos tipos principales de pólipos son los adenomatosos (adenomas precancersosos o adenocarcinomas) y los inflamatorios (no precancerosos).

Los adenocarcinomas se originan en las células glandulares que producen mucosidad para lubricar el interior del colon y del recto. Otros tipos de tumores menos comunes también pueden comenzar en el colon y en el recto. Entre estos se incluyen el tumor estromal gastrointestinal (Lamba y col., 2012), el tumor carcinoide gastrointestinal (Sun y Jung, 2004), el linfoma gastrointestinal (Solidoro y col., 1981) o el melanoma gastrointestinal (Khalid y col., 2011).

Se han encontrado varios factores de riesgo que pueden aumentar las probabilidades de que una persona presente pólipos adenomatosos o cáncer de colon, clasificándose en factores de riesgo modificables o no modificables. Dentro de los factores de riesgo no modificables, la edad es el principal factor de riesgo del cáncer de colon. Más del 90% de casos son diagnosticados en personas mayores de 50 años. Sin embargo, existen antecedentes personales que pueden aumentar el riesgo de sufrir cáncer de colon, como haber tenido previamente pólipos adenomatosos, o padecer enfermedades como la enfermedad inflamatoria del intestino (colitis ulcerosa o enfermedad de Crohn) o el síndrome del intestino o colon irritable (Freeman y col., 2008). También existen antecedentes familiares que pueden aumentar el riesgo de padecer esta enfermedad, como tener familiares que hayan tenido pólipos adenomatosos, o presentar síndromes heredados como la poliposis adenomatosa familiar, el síndrome de Lynch, u otros síndromes menos comunes, como el síndrome de Turcot o el síndrome de Peutz-Jeghers (Jasperson y col., 2010). La mayoría de estos síndromes están producidos por mutaciones genéticas que se transmiten de una generación a otra. En el caso de la poliposis adenomatosa familiar, la principal mutación ocurre en el gen APC (*Adenomatous Polyposis Coli*) (Morin y col., 1997). El gen APC es un supresor tumoral que al mutarse se desactiva, favoreciendo la formación de cientos de pólipos en el colon. Con el tiempo, el cáncer se desarrolla a partir de uno o más de estos pólipos debido a nuevas mutaciones genéticas en otros genes. El 80% de los adenomas que se producen tempranamente en el desarrollo del cáncer de colon contienen una mutación en el gen APC (Goss y Groden, 2000). En el caso del síndrome de Lynch, las mutaciones se producen en los genes que reparan el DNA dañado, pudiendo afectar a genes reguladores del crecimiento (Rustgi, 2007). En el caso del síndrome Peutz-Jeghers, estas mutaciones afectan principalmente al supresor tumoral STK11 (Gammon y col., 2009).

En el caso de los factores de riesgo modificables, se ha demostrado que los factores relacionados con el estilo de vida (la alimentación, el peso y la actividad física) están muy asociados con el riesgo de sufrir cáncer de colon (Boutron-Ruault y col., 2001). Por ejemplo, un índice de masa corporal alto está asociado con un mayor riesgo de padecer cáncer de colon, así como la distribución de la grasa, siendo la obesidad abdominal la más relacionada con la incidencia del cáncer de colon (Bardou y col., 2013). Por otro lado, la actividad física actúa como protector frente a este cáncer, y diversos estudios poblacionales han demostrado que las personas que realizan actividad física regular tienen entre un 40% y un 50% menor riesgo de padecer cáncer de colon (Wolin y col., 2011). Sin embargo, uno de los factores de riesgo modificables más importantes es la dieta. El consumo de carne roja, o de carne cocinada en contacto directo con el fuego (favorece la formación de compuestos cancerígenos como, por ejemplo, los hidrocarburos aromáticos policíclicos) ha sido relacionada con un aumento en el riesgo de sufrir cáncer de colon (Sinha y col., 1999). Además, en los últimos años también se ha evidenciado el papel del alcohol como factor de riesgo en consumos superiores a 100 gramos a la semana (Fedirko y col., 2011). Por el contrario, la dieta mediterránea ha demostrado ser protectora frente a este tipo de cáncer (Hadziabdić y col., 2012).

A pesar de que el cáncer de colon se puede curar en más del 90% si se detecta precozmente, se estima que un 80% de los cánceres de colon son evitables sólo con medidas nutricionales (Ahmed, 2004). Debido a ello, en las últimas décadas se ha estudiado el efecto de varios grupos de ingredientes alimentarios en el desarrollo del cáncer de colon, y existe un número creciente de estudios relativos al potencial efecto quimioprotector de compuestos como los polifenoles (Rudolf y col., 2007; Sant y col., 2007; Araujo y col., 2011; Bobe y col., 2012), las isoflavonas (Bennink, 2001), los fitoesteroles (Rao y Janezic, 1992), los ácidos grasos (Williams y col., 2010; Cai y col., 2012; Gerber, 2012; Key y col.,

2012; Wu y col., 2012), la fibra (Hansen y col., 2012), las proteínas (Williams y col., 2010), los carbohidratos (Aune y col., 2012), los carotenoides (Wang y col., 2012), las vitaminas (Gorham y col., 2005; Key y col., 2012; Tavani y col., 2012) y los minerales (Chen y col., 2012; Key y col., 2012; Wang y col., 2012; Wark y col., 2012), entre otros. Muchos de estos trabajos se han llevado a cabo utilizando modelos *in vitro*, que, aunque son una simplificación de la realidad, son herramientas muy valiosas para analizar los efectos que los compuestos de la dieta pueden tener sobre el cáncer de colon a nivel molecular.

2. OBJETIVOS Y PLAN DE TRABAJO

2. OBJETIVOS Y PLAN DE TRABAJO

OBJETIVOS

El cáncer está considerado una enfermedad genética causada por alteraciones en genes que controlan las funciones celulares. Diversos estudios han demostrado que la dieta es el principal factor de riesgo y que está involucrada en el 30% de los casos de cáncer diagnosticados, llegando al 80% en el caso del cáncer de colon. En cuanto a la leucemia mieloide crónica, y a pesar de que la alimentación no está implicada en su aparición, diversos estudios han demostrado que algunos compuestos de la dieta pueden ayudar a disminuir la aparición de resistencias frente a los fármacos más utilizados. Por otro lado, numerosos estudios epidemiológicos indican una menor incidencia de enfermedades como el cáncer en poblaciones que siguen preferentemente una "Dieta Mediterránea". Las propiedades saludables de esta dieta se han atribuido principalmente al consumo de alimentos vegetales debido a su alto contenido en compuestos bioactivos como los polifenoles. Dentro de los alimentos vegetales que componen la "Dieta Mediterránea" se encuentra el romero, una planta rica en polifenoles que ha demostrado tener propiedades anticancerígenas.

Tradicionalmente, la actividad antiproliferativa del romero se ha determinado mediante metodologías analíticas dirigidas al estudio de un grupo reducido de marcadores moleculares. Sin embargo, la aplicación de una estrategia que permita abordar el estudio del efecto antiproliferativo del romero desde un punto de vista molecular global no ha sido llevada a cabo hasta la fecha.

De acuerdo con estas consideraciones, el objetivo principal de la presente Tesis doctoral es el estudio del efecto antiproliferativo de polifenoles de origen alimentario

siguiendo una aproximación alimentómica. Para ello se propone el uso combinado de tecnologías ómicas y herramientas bioinformáticas avanzadas que permitan la interpretación y la integración de la información procedente de los distintos niveles de expresión (transcriptoma, proteoma y metaboloma).

Para conseguir este objetivo general, se han planteado los siguientes objetivos parciales:

1. Evaluar los efectos de un extracto de romero con actividad antiproliferativa en el transcriptoma y el metaboloma de dos líneas celulares de leucemia mieloide crónica con distinto fenotipo de resistencia a fármacos.
2. Evaluar los efectos de un extracto de romero con actividad antiproliferativa en el transcriptoma de dos líneas celulares de cáncer de colon con distinto perfil mutacional.
3. Estudiar la contribución de los compuestos fenólicos mayoritarios del extracto de romero al efecto antiproliferativo del mismo en las células de cáncer de colon, y evaluar el efecto de los compuestos más activos en el transcriptoma y el metaboloma.
4. Investigar la relación entre los cambios tempranos en el transcriptoma y el metaboloma de las células de cáncer de colon y los efectos antiproliferativos del extracto de romero y sus compuestos más activos.
5. Evaluar los efectos en el tiempo del extracto de romero y sus compuestos más activos en el proteoma de las células de cáncer de colon.
6. Identificar los posibles mecanismos moleculares del efecto antiproliferativo de los polifenoles de romero en células de cáncer de colon a partir de los datos transcriptómicos, metabolómicos y proteómicos.

PLAN DE TRABAJO

Considerando los antecedentes expuestos anteriormente, y para alcanzar los objetivos planteados, la presente Tesis doctoral se ha estructurado en dos secciones:

En la primera parte de esta Tesis doctoral (sección 3.1), se ha estudiado la actividad antiproliferativa de varios extractos de romero en dos líneas celulares de leucemia mieloide crónica; la elucidación de su efecto a nivel molecular se obtiene tras aplicar una aproximación alimentómica.

A continuación, se detalla el plan de trabajo seguido para el desarrollo del trabajo de esta primera sección:

1. Determinación del efecto antiproliferativo de varios extractos de romero enriquecidos en compuestos fenólicos en las líneas de leucemia K562 y K562/R mediante el método colorimétrico MTT (*3-(4,5-Dimethylthiazol-2-yl)-2,5-Diphenyltetrazolium Bromide*).
2. Determinación del efecto de los extractos de romero en el ciclo celular de las dos líneas de leucemia mediante citometría de flujo.
3. Selección del extracto de romero con mayor actividad antiproliferativa para llevar a cabo los posteriores estudios alimentómicos.
4. Análisis global de los cambios en la expresión génica en respuesta al tratamiento con el extracto de romero en las líneas celulares de leucemia. El plan de trabajo consistió en las siguientes etapas:
   4.1. Extracción de la fracción de RNA total de las células control y las tratadas con el extracto.
   4.2. Preparación de las muestras e hibridación en microarrays.
   4.3. Obtención de los datos crudos del análisis con microarrays de expresión génica y procesado de datos.

4.4. Análisis estadístico de los datos e identificación de los genes expresados diferencialmente en los grupos de muestras tratadas con polifenoles con respecto al grupo control.

4.5. Selección de genes para su posterior validación mediante RT-qPCR (*quantitative reverse transcription PCR*).

4.6. Diseño y optimización de los sistemas de amplificación por RT-qPCR.

4.7. Validación de los genes seleccionados mediante los métodos optimizados de RT-qPCR.

4.8. Análisis de enriquecimiento funcional de la lista de genes expresados diferencialmente en respuesta al tratamiento con el extracto empleando herramientas bioinformáticas.

5. Análisis global de los cambios producidos en el metaboloma en respuesta al tratamiento con el extracto de romero en las líneas celulares de leucemia. El plan de trabajo consistió en las siguientes etapas.

5.1. Extracción de los metabolitos de las células control y las tratadas con el extracto.

5.2. Análisis de los extractos de metabolitos mediante CE-MS y LC-MS.

5.3. Obtención de los datos crudos del análisis y procesado de los datos mediante herramientas bioinformáticas específicas.

5.4. Análisis estadístico de las señales con el fin de determinar los cambios estadísticamente significativos en los grupos de muestras tratadas con el extracto con respecto al grupo control.

5.5. Identificación tentativa de metabolitos empleando distintas bases de datos.

5.6. Confirmación de la identidad de algunos metabolitos mediante el empleo de compuestos estándar.

5.7. Mapeo de los metabolitos en rutas metabólicas mediante la herramienta informática IPA y la base de datos KEGG.

En la segunda parte de esta Tesis doctoral (sección 3.2), se ha investigado la actividad antiproliferativa de varios extractos de romero y de sus polifenoles mayoritarios en dos líneas celulares de cáncer de colon; la elucidación de su efecto a nivel molecular se obtiene tras aplicar una aproximación alimentómica.

A continuación, se detalla el plan de trabajo seguido para el desarrollo del trabajo de esta segunda sección:

1. Determinación del efecto antiproliferativo de varios extractos de romero enriquecidos en compuestos fenólicos en las líneas de cáncer de colon HT-29 y SW480 mediante el método colorimétrico MTT.
2. Determinación del efecto de los extractos de romero en el ciclo celular de las dos líneas de cáncer de colon mediante citometría de flujo.
3. Selección del extracto de romero con mayor actividad antiproliferativa para llevar a cabo los posteriores estudios alimentómicos.
4. Análisis global de los cambios en la expresión génica en respuesta al tratamiento con el extracto de romero en las líneas celulares de cáncer de colon. Para el desarrollo de estos análisis se siguieron los mismos procedimientos de análisis transcriptómico que los descritos en los puntos 4.1-4.7 del plan de trabajo planteado para los estudios en células de leucemia
5. Determinación de la actividad antiproliferativa, así como de los posibles efectos sinérgicos, antagónicos y aditivos de los compuestos fenólicos mayoritarios (ácido carnósico y carnosol) del extracto de romero en la línea celular HT-29.

6. Análisis global de los cambios en la expresión génica y el metaboloma en respuesta al tratamiento con el ácido carnósico en la línea celular HT-29. Para el desarrollo de estos análisis se siguieron los mismos procedimientos de análisis transcriptómico y metabolómico que los descritos en los puntos 4.1-4.8 y 5.1-5.7 del plan de trabajo planteado para los estudios en células de leucemia.
7. Análisis dirigido de los cambios temporales de los metabolitos que potencialmente guarden relación con el efecto antiproliferativo del extracto de romero y el ácido carnósico en células HT-29 mediante GC-MS.
8. Análisis global de los cambios tempranos en la expresión génica en respuesta al tratamiento con el extracto de romero y el ácido carnósico en células HT-29. Para el desarrollo de estos análisis, se siguió el mismo procedimiento que el descrito en los puntos 4.1-4.8.
9. Análisis de los patrones temporales de expresión de genes involucrados en respuestas frente al estrés oxidativo y proteotóxico, relacionadas con el efecto antiproliferativo del extracto de romero y el ácido carnósico en células HT-29 mediante RT-qPCR.
10. Análisis de los cambios en los niveles de las especies reactivas del oxígeno intracelulares en respuesta al extracto de romero, el ácido carnósico y el carnosol en células HT-29 mediante citometría de flujo.
11. Estudio de posibles fenómenos de autooxidación de los polifenoles de romero en el medio de cultivo.
12. Análisis global de los cambios en la expresión de proteínas en respuesta al tratamiento con el extracto de romero, ácido carnósico y carnosol en la línea celular HT-29.
    12.1. Extracción de las proteínas de las células tratadas con polifenoles de romero empleando el detergente n-octyl-β-D-glucopyranoside.
    12.2. Determinación de contenido total de proteínas y digestión.

12.3. Marcaje químico de los digeridos utilizando formaldehido normal (muestras del grupo control) o formaldehido deuterado (muestras tratadas con polifenoles), y mezcla de las muestras en proporción 1:1.

12.4. Análisis proteómico de las mezclas mediante nano-LC-Orbitrap MS/MS.

12.5. Obtención de los datos crudos, y posterior procesado para la identificación y cuantificación relativa de las proteínas.

12.6. Análisis estadístico de las proteínas identificadas y cuantificadas con el fin de determinar aquellas proteínas cuyos niveles estén alterados significativamente en los grupos de muestras tratadas con polifenoles con respecto al grupo control.

12.7. Análisis bioinformático de los conjuntos de datos con el fin de identificar posibles alteraciones en las rutas de transducción de señales y metabólicas, así como en la actividad de los factores de transcripción que guardan relación con la proliferación y otros procesos celulares relevantes en las células de cáncer.

13. Determinación del efecto del extracto de romero en la formación de agresomas en la línea celular de cáncer de colon HT-29.

14. Determinación del efecto inhibitorio *in vitro* del ácido carnósico y del carnosol sobre el proteasoma.

3. RESULTADOS Y DISCUSIÓN

3. RESULTADOS Y DISCUSIÓN

3.1 Una aproximación Alimentómica para el estudio del efecto de polifenoles de romero en leucemia

3.1.1 Prefacio

Como se ha mencionado en la Introducción de esta Memoria, la leucemia mieloide crónica es un tipo de leucemia que se produce tras la aparición del oncogén BCR-ABL. Además del uso de fármacos dirigidos a reducir la actividad de este gen, también se han utilizado otros fármacos quimioterapéuticos generales como, por ejemplo, las antraciclinas. Las antraciclinas son antibióticos que dificultan la actividad de las enzimas involucradas en la replicación del DNA. La daunomicina pertenece a este grupo de fármacos e interacciona con el DNA a través del surco menor, evitando la progresión de la enzima topoisomerasa II y deteniendo el proceso de división celular. No obstante, y al igual que ocurre con los fármacos dirigidos a reducir la actividad de una proteína, eventualmente las células también pueden desarrollar resistencias frente a este tipo de fármacos, que reducen la efectividad de la terapia.

Algunos polifenoles de origen vegetal han demostrado tener propiedades anticancerígenas y ser efectivos frente a células resistentes de leucemia mieloide crónica (Iwasaki y col., 2009). Dado el elevado contenido de polifenoles en las hojas de romero, en esta Tesis doctoral, se seleccionó esta planta para estudiar su efecto antiproliferativo en dos líneas celulares de leucemia mieloide crónica con distinto fenotipo de resistencia a daunomicina. Los resultados de este estudio están recogidos en la sección 3.1.2, correspondiente al trabajo titulado “Effect of dietary polyphenols on K562 leukemia cells: A Foodomics approach” de A. Valdés y col., y publicado en *Electrophoresis* 2012, *33*, 2314-2327. Como paso previo, se llevó a cabo la determinación del efecto antiproliferativo

de una serie de extractos de romero enriquecidos en compuestos fenólicos en las dos líneas de leucemia. Los extractos de romero utilizados se obtuvieron mediante extracción con fluidos supercríticos (SFE, *Supercritical Fluid Extraction*) y extracción con líquidos presurizados (PLE, *Pressurized Liquid Extraction*), y se caracterizaron químicamente en el laboratorio de Alimentómica del CIAL. A continuación, se efectuó el estudio del ciclo celular que permitió establecer que los extractos más activos poseen efecto citostático mediante citometría celular. Finalmente, se seleccionó el extracto más activo para llevar a cabo una evaluación Alimentómica del efecto antiproliferativo del extracto en las dos líneas celulares. Esta estrategia analítica consistió en estudiar los cambios en el transcriptoma y el metaboloma de las dos líneas de leucemia en respuesta al tratamiento con el extracto durante 48 h. Para el estudio transcriptómico, se llevó a cabo un análisis con microarrays de expresión génica de Affymetrix que permitió identificar los genes expresados diferencialmente en respuesta al tratamiento con el extracto de romero. Algunos de los genes expresados diferencialmente se seleccionaron y se validaron mediante RT-qPCR, para lo que se diseñaron y optimizaron sistemas específicos de amplificación. Posteriormente, la lista de genes expresados diferencialmente se analizó mediante la herramienta bioinformática IPA para determinar las funciones y procesos biológicos alterados tras el tratamiento con el extracto de romero. Para estudiar los efectos del extracto de romero en el metaboloma de las células de leucemia mieloide crónica, los metabolitos extraídos tras el tratamiento se analizaron utilizando dos plataformas complementarias, electroforesis capilar acoplada a un analizador de tiempo de vuelo (CE-TOF MS) y cromatografía de líquidos de ultra alta resolución en fase inversa acoplada a un analizador de tiempo de vuelo (RP/UHPLC-TOF MS). Los datos obtenidos por estas plataformas se procesaron y analizaron estadísticamente con el objetivo de identificar los metabolitos alterados diferencialmente. Posteriormente, estos metabolitos se identificaron

tentativamente empleando distintas bases de datos, y la identidad de algunos de ellos se confirmó mediante el empleo de compuestos estándar. Los metabolitos identificados se mapearon mediante la herramienta bioinformática IPA para determinar las rutas metabólicas en las que están involucrados. La herramienta bioinformática IPA también se utilizó para integrar los cambios transcriptómicos y metabolómicos observados en respuesta al tratamiento con el extracto de romero. Para ello, los datos transcriptómicos se mapearon en las rutas metabólicas significativamente alteradas obtenidas del análisis metabolómico, y los datos metabolómicos se mapearon en los procesos y funciones biológicas significativamente alteradas obtenidas del análisis transcriptómico.

3.1.2 Effect of dietary polyphenols on K562 leukemia cells: A Foodomics approach

Valdés, A., Simó, C., Ibáñez, C., Rocamora-Reverte, L., Ferragut, J. A., *García-Cañas, V., Cifuentes, A. *Electrophoresis* 2012, *33*, 2314 - 2327.

DOI: http://dx.doi.org/doi:10.1002/elps.201200133

Alberto Valdés[1]
Carolina Simó[1]
Clara Ibáñez[1]
Lourdes Rocamora-Reverte[2]
José Antonio Ferragut[2]
Virginia García-Cañas[1]
Alejandro Cifuentes[1]

[1]Laboratory of Foodomics, CIAL (CSIC), Madrid, Spain
[2]Institute of Molecular and Cellular Biology, Miguel Hernández University, Elche, Alicante, Spain

Received February 29, 2012
Revised March 27, 2012
Accepted March 27, 2012

Research Article

Effect of dietary polyphenols on K562 leukemia cells: A Foodomics approach

In this work, a global Foodomics strategy has been applied to study the antiproliferative effect of dietary polyphenols from rosemary on two human leukemia lines, one showing a drug-sensitive phenotype (K562), and another exhibiting a drug-resistant phenotype (K562/R). To this aim, whole-transcriptome microarray together with an MS-based non-targeted analytical approach (via CE-TOF MS and UPLC-TOF MS) have been employed to carry out transcriptomics and metabolomics analyses, respectively. Functional enrichment analysis was done using ingenuity pathway analysis (IPA) software as a previous step for a reliable interpretation of transcriptomic and metabolomic profiles. Rosemary polyphenols altered the expression of approximately 1% of the genes covered by the whole transcriptome microarray in both leukemia cell lines. Overall, differences in the transcriptional induction of a number of genes encoding phase II detoxifying and antioxidant genes, as well as differences in the metabolic profiles observed in the two leukemia cell lines suggest that rosemary polyphenols may exert a differential chemopreventive effect in leukemia cells with different phenotypes. IPA predictions on transcription factor analysis highlighted inhibition of Myc transcription factor function by rosemary polyphenols, which may explain the observed antiproliferative effect of rosemary extract in the leukemia cells. Metabolomics analysis suggested that rosemary polyphenols affected differently the intracellular levels of some metabolites in two leukemia cell sublines. Integration of data obtained from transcriptomics and metabolomics platforms was attempted by overlaying datasets on canonical (defined) metabolic pathways using IPA software. This strategy enabled the identification of several differentially expressed genes in the metabolic pathways modulated by rosemary polyphenols providing more evidences on the effect of these compounds.

Keywords:
Dietary polyphenols / Foodomics / Leukemia cells / Metabolomics / Transcriptomics
DOI 10.1002/elps.201200133

1 Introduction

Chronic myelogenous leukemia (CML) is a myeloproliferative syndrome linked to a hematopoietic stem cell disorder, characterized by increased production of granulocytes at all stages of differentiation [1]. Up to 95 % of CML patients consistently carry the Philadelphia chromosome, a result of a cytogenetic translocation [2]. This translocation is responsible for the expression of a 210 kDa chimeric fusion protein, p210 BCR-ABL that is a constitutively active tyrosine kinase [3]. BCR-ABL triggers several downstream survival pathways, including that collectively provide proliferative advantages and resistance to apoptosis [4, 5]. Based on its role in malignant transformation, BCR-ABL has served as a target for therapeutic intervention in CML. However, despite significant hematologic and cytogenetic responses to different drugs, resistance may occur. Such multidrug resistance (MDR) can be a major factor in the failure of many forms of chemotherapy [6,7]. Several mechanisms of resistance have been reported for CML including mutations in the BCR/ABL gene, BCR/ABL gene amplification, increased BCR/ABL protein expression, the switch to alternative kinase signaling pathways, and mechanisms related to pharmacokinetic factors of drug deliver, such as overexpression of *ABC* transporter genes.

Correspondence: Dr. Virginia García-Cañas, Laboratory of Foodomics, CIAL (CSIC), Nicolas Cabrera 9, 28049 Madrid, Spain.
E-mail: virginia.garcia@csic.es
Fax: +34-910-017-900

Abbreviations: CML, Chronic myelogenous leukemia; **DEG**, differentially expressed gene; **DNM**, daunomycin; **FDR**, false discovery rate; **GSH**, reduced glutathione; **GSSG**, oxidized glutathione; **IPA**, ingenuity pathway analysis; **MDR**, multidrug resistance

*__Colour Online:__ See the article online to view Fig. 3 in colour.

Dietary polyphenols have been reported to be of potential therapeutic benefit in the treatment and/or prevention of several degenerative diseases including cancers and cardiovascular diseases [8–13]. A number of studies demonstrate that certain dietary polyphenols may overcome MDR in many multidrug resistant cells [14]. The biological activities of rosemary (*Rosmarinus officinalis*) polyphenols have been investigated by several research groups [15, 16]. Carnosic acid, one of the main polyphenols in rosemary, has proven anti-inflammatory properties in neurons [17], antiproliferative activity in colon cancer cells [18], and potential to promote differentiation of leukemia cells [19]. Carnosol, another rosemary diterpene, poses strong antioxidant and chemopreventive activities. This diterpene has demonstrated anti-inflammatory and anti-cancer activities on for example prostate, skin, or breast cancer [20].

At present, the emerging Foodomics field and its omics tools [21, 22] are expected to play a crucial role in the investigation of the interactions between nutrients or bioactive food compounds and genes [23]. High-density microarrays are widely used for comprehensive gene expression studies in part due to their great transcriptome coverage. After microarray data preprocessing, statistical tests are usually carried out in order to detect significant changes in the expression of every gene between repeated measurements in two or more conditions (groups) [24]. Metabolite analysis is especially useful for identifying pathways modified in a given biological system after certain pathology, perturbation, or treatment. Metabolomics discipline is particularly complex since low-molecular-weight metabolites represent a diverse range of chemicals in a wide dynamic range of concentrations in biological samples. To this aim, NMR- and MS-based analytical platforms are typically used. In this context, the use of high-resolution mass analyzers is particularly useful to obtain accurate masses for the determination of elemental compositions of metabolites and to carry out tentative identification based on metabolite databases. Since metabolomics generates large amounts of data, the implementation of advanced software to accomplish preprocessing (noise reduction, spectrum deconvolution, electropherogram/chromatogram alignment, and peak integration, among others) and statistical analysis is a must.

Biological interpretation of omic data is very challenging. Over the last years, the use of biological knowledge accumulated in public databases by means of bioinformatics allows to systematically analyze large gene, protein, and/or metabolite lists in an attempt to assemble a summary of the most enriched and significant biological aspects [25]. Thus, a variety of bioinformatics platforms are currently available for the analysis of omic data, such as Ingenuity® Pathway Analysis (IPA, Ingenuity Systems) and MetaCore (GeneGo, Thomson and Reuters). These bioinformatics resources systematically map the list of interesting (differentially expressed) entities (gene, protein, or metabolite) to the associated annotation terms of dedicated databases and then statistically examine the enrichment of the data for each of the terms by comparing them to a reference dataset.

The aim of this work was to conduct genome-wide transcriptomics and metabolomics analysis to investigate the effect of rosemary extracts rich in polyphenols in two human erythroleukemia lines, one showing a drug-sensitive phenotype (K562), and another exhibiting a drug-resistant phenotype (K562/R). IPA was used for functional enrichment analysis as a previous step for a reliable data interpretation obtained from transcriptomics and metabolomics, and for cross-platform data integration.

2 Materials and methods

2.1 Chemicals

All chemicals were of analytical reagent grade and used as received. Reagents and solvents employed in the preparation of LC mobile phases, CE electrolytes, sheath liquid, and standard solutions were of MS grade: formic acid and 2-propanol were from Riedel-de Haën (Seelze, Germany), ACN and water were from Labscan (Gliwice, Poland). A PBS containing 138 mM sodium chloride, 2.7 mM potassium chloride, and 10 mM sodium hydrogen phosphate at pH 7.4, was purchased from Sigma-Aldrich. Composition of homogenization buffer was next: 10 mM Tris-HCl, 5 mM EDTA, 120 mM NaCl, at pH 7.4, all of them from Sigma-Aldrich. A protease inhibitor cocktail containing 4-(2-aminoethyl) benzenesulfonyl fluoride, pepstatin A, E-64, bestatin, leupeptin, and aprotinin, was also purchased from Sigma-Aldrich. The primers for RT-qPCR were purchased from Fisher Scientific (Alcobendas, Spain).

2.2 Preparation of rosemary extracts

Five rosemary extracts marked as rom1 to rom5 were obtained from dried rosemary leaves using either supercritical fluid extraction (SFE) or pressurized liquid extraction (PLE) as reported by Herrero and coworkers [16]. The extracts obtained by PLE with a 100 bar pressure for 20 min under the following conditions of solvent and temperature were: rom1, using water at 100°C; rom2, using ethanol at 150°C; and rom3, using water at 200°C. On the other side, the extracts obtained by SFE at 40°C for 30 min were: rom4, using supercritical CO2 and 7% ethanol at 150 bar; and rom5, using supercritical CO2 at 400 bar. Previous chemical characterization studies provided information on the major phenolic constituents in each extract [16]. A major phenolic compound in rom1, rom2, and rom3 extracts was rosmarinic acid with concentrations of 14.19, 16.78, and 8.59 μg/mg extract. Rom4 and rom5 were reported to contain high concentrations of carnosol (226.39 and 224.65 μg/mg extract, respectively) and carnosic acid (151.55 and 106.46 μg/mg extract, respectively), being rosmarinic acid undetected. Carnosol and carnosic acid were also present in rom2 extract at concentrations of 104.26 and 66.23 μg/mg extract, respectively. Rom1 and rom3 contained similar concentration of carnosol (~45 μg/mg extract), and

carnosic acid was present at concentrations of 0.01, 66.23, and 5.78 μg/mg in rom1, rom2, and rom3, respectively. The extracts have also been reported to show antioxidant activity (EC50) ranging from 5.3 to 10.5 μg/mL [16]. Extracts were diluted at the indicated concentrations using ethanol and their content in polyphenols determined as gallic acid equivalents (GAE), expressed as mg gallic acid/g extract [26]. Total concentrations of polyphenols (given as μM) in the extracts were then calculated using the molecular weight of gallic acid as average value.

2.3 Cells and cell culture

Human erythroleukemia K562 cell line obtained from ATCC (American Type Culture Collection, LGC Promochem, UK) and a daunomycin (DNM)-resistant K562/R cell subline derived from K562 cells by stepwise increments of the drug, were grown in logarithmic phase in RPMI 1640 medium supplemented with 10% heat-inactivated fetal calf serum, 2 mM L-glutamine, 50 U/mL penicillin G, and 50 μg/mL streptomycin, at 37°C in humidified atmosphere and 5% CO_2. IC_{50} values for DNM were 1.1 μM and 398.7 μM on K562 and K562/R, respectively. Therefore, K562/R cells exhibit approximately 350-fold increased tolerance to DNM.

2.4 Cell viability assays

Control and cell viability in the presence of the rosemary extracts was measured by counting total and nonviable cells with ADAM Cell Counter (Digital-Bio, Korea) technology which is based on a fluorescent microscopy technique with a sensitive CCD camera. Harvested cells were washed and diluted in PBS to a final concentration of 5×10^4–4×10^6 cells/mL. These cells were stained with T solution (total cells) containing PBS-Triton 0.5% with propidium iodide (25×10^{-3} μg/mL), and N solution (nonviable cells), which is composed of the fluorescent dye and PBS (both stain solutions were provided by the manufacturer). Then, the cells were counted separately by measuring the fluorescence at 617 nm.

2.5 Cell cycle study

Cell cycle analysis was performed by flow cytometry in an Epics XL instrument (Beckman Coulter, Miami, FL, USA) as follows: cells were centrifuged and washed with cold 10 mM phosphate buffer pH7.4, supplemented with 2.7 mM KCl and 137 mM NaCl (PBS), and centrifuged again. The pelleted cells were resuspended in 75% cold ethanol, fixed for 1 h at −20°C, centrifuged, and resuspended in 0.5 mL of PBS supplemented with 0.5% Triton X-100 and 0.05% RNase A. Then, cells were incubated for 30 min at room temperature, stained with propidium iodide, and the distribution of cellular DNA content was analyzed. From the cellular distribution pattern of DNA, the apoptosis induced by treatment of the cells with the phenolic extracts was measured by determining the amount of apoptotic cells in the sub-G1 peak by flow cytometry. Flow cytometry data analysis was made upon gating the cells to eliminate dead cells and debris. A total of 10^5 cells were measured during each sample analysis.

2.6 Transcriptomics analysis

Triplicate samples for each leukemia cell line incubated with 5 μM total polyphenols solutions from rosemary extract rom4 for 48 h, and their respective untreated controls were collected for gene expression microarray analyses. Total RNA was isolated from cells using RNeasy Mini Kit (Qiagen, Spain) according to manufacturer protocol. The quality of the isolated RNA was determined with a NanoDrop ND1000 (Thermo, Spain) and a Bioanalyzer 2100 (Agilent, Spain). Only those samples with A260/A280 ratio between 1.8 and 2.1 and a 28S/18S ratio within 1.5–2 were further processed. Sample preparation and microarray hybridization onto Human Gene 1.0ST chips (Affymetrix) was performed by Servicio de Genómica (Parque Científico de Madrid, Spain). Generated CEL files were subjected to quality assessment using Expression Console™ (Affymetrix). Raw data were processed using the Robust Multi-Array (RMA) normalization in the BioConductor package affy for R [27, 28]. Significance analysis and multiple testing correction [29] were performed using the BioConductor package limma (Linear Models for Microarray Data; [30]) in order to control or estimate the false discovery rate (FDR) in the datasets. To identify the statistically most significant changes in gene expression, microarray data was subjected to gene filtering based on a combination of M-value cutoff, which represents a log2-fold change between the two experimental conditions (treatment with polyphenols versus control), and the statistical significance (FDR applied on moderated *t*-statistics). In this study, differentially expressed genes (DEGs) were identified based on 0.6 as *M*-value cutoff that corresponds to expression ratios (fold-change) ≥ 1.5 for upregulated and ≤ 0.6 for downregulated genes; and the statistical filter was established at 5% FDR (adjusted *p*-value <0.05).

Reverse transcription quantitative PCR (RT-qPCR) was used to confirm relative changes in mRNA levels of selected genes from microarray datasets. The selection of genes was based on their biological function. Starting amounts of 1 μg of total RNA isolated from cells were reverse transcribed in a volume of 20 μL using Transcriptor First Strand cDNA Synthesis kit with oligo(dT) primers (Roche Diagnostics, Barcelona, Spain). Each real-time quantitative PCR reaction was performed on 1 μL aliquots of diluted (1:20) cDNA solutions using LightCycler® 480 Real-Time PCR (Roche Diagnostics) and LightCycler® 480 Probes Master kit. Human Universal Probe Library probes and target-specific PCR primers were selected using the Probe Finder assay design software (Roche Diagnostics, http://www.roche-applied-science.com/sis/rtpcr/upl/index.jsp). Primers were designed to span exon-exon junctions and to have melting temperature values close to 60°C. The

Table 1. Primer sequences and LNA probes used to perform RT-qPCR analyses

Gene symbol (accession number)	Sequence (5′-3′)	LNA probe number
MYC (AY214166)	For: GCTGCTTAGACGCTGGATTT Rev: CGAGGTCATAGTTCCTGTTGG	66
CCNE1 (AF518727)	For: GAAGGAGCGGGACACCAT Rev: CGTCCTGTCGATTTTGGC	1
OSGIN1 (AY258066)	For: CTTCTACGCCCAGACACAGAC Rev: GGATCACCATGGAGCCTTC	12
NQO1 (BC007659)	For: CTTTGAAGAAGAAAGGATGGGA Rev: ACAGACTCGGCAGGATACTGA	22
ABL1 (DQ145721)	For: TGCCCAGAGAAGGTCTATGAA Rev: GGATTTCAGCAAAGGAGGG	86
GUSB (BC014142)	For: AACGCCCTGCCTATCTGTATT Rev: GATGAGGAACTGGCTCTTGG	57
B2M (AB021288)	For: CTATCCAGCGTACTCCAAAGATT Rev: TGGATGAAACCCAGACACATAG	42

designed primers were then checked with Oligo Analyzer 3.1 software (Integrated DNA Technologies, http://eu.idtdna.com/analyzer/Applications/OligoAnalyzer) to predict possible secondary structures, heterodimers, and homodimers, and to redesign the primers if needed (see Table 1 for the primer sequences and LNA probes used to perform RT-qPCR analyses).

Two technical replicates were performed for each sample in a 96-well format plate. On each plate, three endogenous control genes (*GUSB*, *B2M*, and *ABL1*) and no-template-controls were also performed in duplicate. Cycle threshold (Ct) values were calculated using second derivative maximum method [31] and the amplification efficiency (E) of each system was calculated by the following formula: $E = 10-1/\text{slope}$. All primers utilized displayed PCR efficiencies higher than 90%. Using the Relative Expression Software Tool (REST, [32]), the relative expression of selected genes, calculated using efficiency correction option, in treated cells was compared to that of control cells. The randomization test method, as a part of the REST software, was used to assess statistical significance of up or downregulation of target genes after normalization to the three reference genes.

2.7 Functional enrichment and transcription factor analysis

In this work, Ingenuity® Pathway Analysis (IPA, Ingenuity Systems, USA) was used for functional enrichment analysis as a previous step for a reliable data interpretation obtained from microarray analysis. This bioinformatics tool was used in order to interpret the gene expression data in the context of biological processes and pathways. To this aim, the Core Analysis function included in IPA was applied to analyze the lists of DEGs identified in microarray analysis. Based on the list of up and downregulated genes, IPA performs functional enrichment analysis in order to identify the biological processes and functions over-represented in a given list of genes. Significance of the enriched categories was tested by the Fisher Exact test *p*-value. In addition to this, based on information stored in the Ingenuity® Knowledge Base, transcription factor analysis was performed using IPA software. The analysis is based on the examination of the known targets of each transcription regulator in the list of DEGs and compares their direction of change to what is expected from the literature. The prediction algorithm calculates a z-score, and it is designed to reduce the chance that random data would generate significant predictions.

2.8 Metabolomics analysis

Metabolite extraction was performed as follows: treated and control cells were washed with PBS solution and centrifuged. The pellets were suspended with homogenization buffer and protease inhibitor cocktail. Next, cells were disrupted with a Polytron homogenizer and centrifuged (14 min at 14 000 × *g* and 4°C). Collected supernatants were centrifuged again for 1 h at 100 000 × *g* and 4°C (cytoplasmic fraction). The obtained supernatants were subjected to an ultrafiltration procedure using an Amicon Ultra 3 kDa centrifugal device from Millipore (Bedford, MA, USA). For this purpose, 400 μL of cytoplasmic fraction samples were ultrafiltrated at 14 000 × *g* and 20°C for 40 min. Fractions with molecular weight lower than 3 kDa were aliquoted and stored at −80°C until CE-MS or UPLC-MS analysis (by quintuplicate). Samples were analyzed using two advanced MS-based methodologies: CE-MS and UPLC-MS.

Analyses with CE-MS were carried out in a P/ACE 5500 CE apparatus from Beckman Instruments (Fullerton, CA, USA) coupled to a TOF MS instrument (model micrOTOF) from Bruker Daltonics (Bremen, Germany) through an orthogonal electrospray ionization (ESI) interface model G1607A from Agilent Technologies (Palo Alto, CA, USA). Electrical contact at the electrospray needle tip was established via a sheath liquid delivered by a 74900-00-05 Cole Palmer syringe pump (Vernon Hills, IL, USA). CE instrument was controlled by a PC running the System Gold software from Beckman, and TOF MS instrument was controlled by a PC running the micrOTOF control software from Bruker Daltonics. All CE separations were performed on uncoated fused-silica capillaries (50 μm internal diameter and 80 cm total length) from Composite Metal Services (Worcester, England). Prior to first use, capillaries were conditioned by rinsing with 1 M NaOH for 10 min, followed by 20 min with water. After each run, the capillary was conditioned with water during 2 min, followed by separation buffer during 4 min. Injections were made at the anodic end by hydrodynamic injection mode (60 s at 0.5 psi). Separations were performed at 25°C with an applied voltage of +25 kV in a BGE composed of 1M formic acid. Electrical contact at the electrospray needle tip was established via a sheath liquid based on isopropanol water (50:50, v/v)

and delivered at a flow rate of 0.24 mL/min. Analysis was performed under positive-ion ESI MS mode. The nebulizer and drying gas conditions were 0.4 bar N2 and 4 L/min N2, respectively, maintaining the ESI chamber temperature at 250°C. MS data were recorded in the 50–600 *m/z* range every 90 ms. Accurate mass data of the molecular ions were processed using the DataAnalysis 4.0 software from Bruker Daltonics. External and internal calibration of the TOF MS instrument was performed by introducing a 10 mM sodium formate solution through the separation capillary. The ions used for the calibration of the TOF MS instrument were next: 90.9766, 158.9641, 226.9515, 294.9389, 362.9263, 430.9138, 498.9012, and 566.8886 *m/z*. CE-MS data was processed using the XCMS open-source package [33] written in the platform-independent programming language R (www.r-project.com). Peak detection method used in XCMS was the CentWave algorithm [34] that finds a region of interest based on the mass accuracy and expected chromatographic/electrophoretic peak width. Nonlinear retention time correction was carried out using the OBI-Warp algorithm (Ordered Bijective Interpolated Warping) [35]. Detected peaks from CE-MS analysis were reported in the form of "features", which are defined as a unique *m/z* value at a unique time point. Redundant responses from the same ion (isotopes, adducts, fragment ions, etc.) were detected using the R-software package AStream [36]. Thus, a multidimensional data matrix of time-aligned detected features with their corresponding migration time, *m/z*, and peak area was obtained for each sample.

The LC-MS analysis were performed on ultra-high performance liquid chromatography (UHPLC) system Agilent 1290 (Agilent Technologies, Santa Clara, CA, USA) connected to a quadruple-time-of-flight mass spectrometer Agilent 6540 Q/TOF (Agilent Technologies) equipped with an orthogonal electrospray interface (Agilent Jet Stream, AJS) with Jet Stream thermal gradient focusing technology and operating in positive ion mode. The instrument was controlled by a PC running the Mass Hunter Workstation software from Agilent. Reversed phase chromatographic separation was performed on an Agilent ZORBAX C18, Rapid Resolution HT (2.1 × 50 mm, 1.8 μm) column maintained at 40°C. Metabolites were eluted from the LC column using the following linear gradient: 0–6 min: 2–20% B; 6–10 min: 20–100% B; 10–12 min: 100% B; 12–17 min 2% B for re-equilibration. Solvent A was water and solvent B was ACN, both solvents containing 0.1% formic acid. TOF MS operation parameters were the following: capillary voltage, −4000 V; nebulizer pressure, 40 psi; drying gas flow rate, 10 L/min; gas temperature, 300°C; skimmer voltage, 45 V; fragmentor voltage was 125 V in positive mode. TOF MS accurate mass spectra were recorded across the range of 50–1000 *m/z* every 200 ms. Internal mass calibration of the instrument was carried out using an AJS ESI electrospray source with an automated calibrant delivery system. External calibration of the TOF MS was carried out using a commercial calibrant mixture from Agilent with next *m/z* values: 118.086255, 322.048121, 622.028960, 922.009798, 1221.990637, and 1521.971475 *m/z*. The reference compound solution for internal mass calibration of the Q/TOF mass spectrometer containing 5 μM of purine ([C5H5N4]+ at 121.050873 *m/z*) and 2.5 μM HP-0921, hexakis (1H,1H,3H-tetrafluoropropoxy) phosphazine ([C18H19O6N3P3F24]+ at 922.009798 *m/z*) in ACN water (95:5, v/v) was also from Agilent. UPLC-MS data was processed using the MassHunter 4.0 (MH) and Mass Profiler Professional 2.2 (MPP) software, both from Agilent. MH program uses a proprietary peak detection algorithm (molecular feature extraction) to find compounds and filter adducts, isotopes, dimers from the same molecule. Detected peaks were then exported to MPP software for retention time correction, area normalization, statistics, and visualization of results. Metabolite tentative identification was performed by matching the obtained accurate *m/z* values and theoretical *m/z* values contained in different free available databases, namely: Human Metabolome Database [37], METLIN [38], KEGG compound [39], and PubChem [40] with a mass accuracy window of 7 ppm. Generate-Molecular Formula Editor within Data Analysis 4.0 (Bruker) and Molecular Formula Generator algorithm within MassHunter software were used to support the agreement, in terms of mass error (ppm) and in comparison to the theoretical isotopic pattern. When available, standards were used to confirm metabolite identification. When isomers exist for a given formula, metabolite identification was sorted giving preference to metabolites from central metabolic pathways in KEGG and number of databases containing each metabolite. Both CE-MS and UPLC-MS data processing were carried out using a standard HP computer Z400 (2.8 GHz, 4 GB memory) running Windows 7. A two-way parametric student's *t*-test was applied to compare the significance of changes in measured metabolite responses after polyphenol treatment relative to the control. Differences with a critical probability value $p < 0.05$ were considered statistically significant.

Once identified, the significant altered metabolite levels in each cell line after treatment with rosemary extract, metabolomics datasets were uploaded in IPA software for pathway analysis. For mapping purposes, KEGG metabolite identifiers and the corresponding fold change values of the significant metabolites were included in the datasets. Each metabolite identifier was mapped to its corresponding metabolite object in the Ingenuity Pathway Knowledge Base prior to metabolomic analysis with IPA. This analysis allows the identification of canonical metabolic pathways affected by the treatment.

In order to link the observed changes between transcriptomic and metabolomic platforms, we applied an integrative approach based on the capabilities of IPA software for mapping different levels of expression in the same pathway. Thus, in order to discover associations across both platforms, transcriptomic data were overlaid on top-scored canonical pathways obtained from metabolomic analysis, and vice versa.

3 Results and discussion

3.1 Effects of rosemary extracts on cell viability and cell cycle of leukemia cells

Two human erythroleukemia cell lines, one showing a daunomycin (DNM)-sensitive phenotype (K562, also called wild-type or K562wt) and another exhibiting a DNM-resistant phenotype (K562/R), were selected in this study to investigate the effects of rosemary polyphenols on cell viability, cell cycle, and gene expression. K562/R cells display the main molecular characteristic associated to the MDR phenotype that is the overexpression of the multidrug transporter P-glycoprotein codified by the *ABCB1* gene [41], responsible for the active drug efflux of many antineoplastic drugs [42, 43].

To determine the effective concentration range, dose effect of rosemary polyphenols on cell viability in K562 and K562/R cell lines was evaluated after exposure of the cells to different concentrations of each extract. Rosemary extracts showing concentrations of 5 and 10 μM of polyphenols did not exert significant effect on leukemia cell viability after 24-h incubation with any of the tested extracts (data not shown). Incubation of the cells for longer time (48 h) with a 5 μM polyphenols solution from rom4 extract, reduced cell viability in K562 cells (46%), and K562/R cells (74%), while the rest of tested extracts did not exert appreciable effect (Fig. 1). It seems clear that DNM-resistant K562/R cells display significant resistance against the cytotoxicity promoted by the rom4 extract. Incubation with a higher concentration (10 μM polyphenols), reduced cell viability in both cell lines after treatment for 48 h with rom4 and rom5 rosemary extracts. Thus, the percentage of living cells decreased in a dose-dependent manner. It is worth noting that the cytotoxic effect induced by rom4 was significantly stronger than that induced by rom5 both compared at 10 μM of polyphenols (42% with rom4 versus 70% with rom5 of viable K562 cells and 38% with rom4 versus 84% with rom5 of K562/R cells).

Next, the distribution of cellular DNA of the cells upon incubation with the extracts and further staining with propidium iodide was analyzed by flow cytometry. The purpose of the experiments was to provide more insight on the mechanism of action behind the antiproliferative effect of the rosemary extracts. Figure 2 shows that incubations with 5 μM polyphenols solution from rom4 and rom5 extracts for 48 h induce an apoptotic effect indicated by the appearance of sub-G1 cell population (19.5% of cells ± 0.7 and 19.8% ± 8.0 in rom4 and 5 treated versus 2.1% ± 1.2 in control K562 cells). A common finding observed in Fig. 2 is the G2/M arrest (increases from 20.0% ± 5.9 to 24.0% ± 5.7 and from 19.8 ± 5.6 to 24.8% ± 6.1 in sensitive and resistant cells, respectively), concomitant to a decrease on G1 in both cell lines treated with rom4 extract (from 52.7 ± 9.0 to 37.5% ± 5.1 and from 53.1% ± 8.5 to 44.4% ± 2.2 in sensitive and resistant cells, respectively), indicating coexistence of cytostatic and cytotoxic effects induced by the treatment with rosemary polyphenols.

In good agreement with our results, it was found in literature that concentrations of rosmarinic acid ranging from 6.25 to 50 μg/mL (139 μM) showed proliferative effects rather than cytotoxic activity [44]. Also, the same polyphenol induced little effect on the viability of human monocytic leukemia U937 cells [45]. To the opposite, studies with carnosic acid and carnosol indicated that these polyphenols reduce viability of different types of tumor cells [18, 44, 46–48]. Particularly, Yesil-Celiktas and coworkers reported that concentrations of 19 μM of carnosic acid reduced cell viability to 19% in K562 cells [44]. Similar effects have been reported for this rosemary polyphenol on viability of human myeloid leukemia cells (HL60). In consonance with the reported study, rosemary extracts assayed in our work showed different antiproliferative activity on leukemia cells. More precisely, carnosol and carnosic acid-enriched extracts, rom4, and rom5 showed the strongest effect on the proliferation of both cell lines, whereas the rosmarinic acid-enriched extracts (rom1, rom2, or rom3) exerted lower antiproliferative activity. Based on the results obtained from cell viability

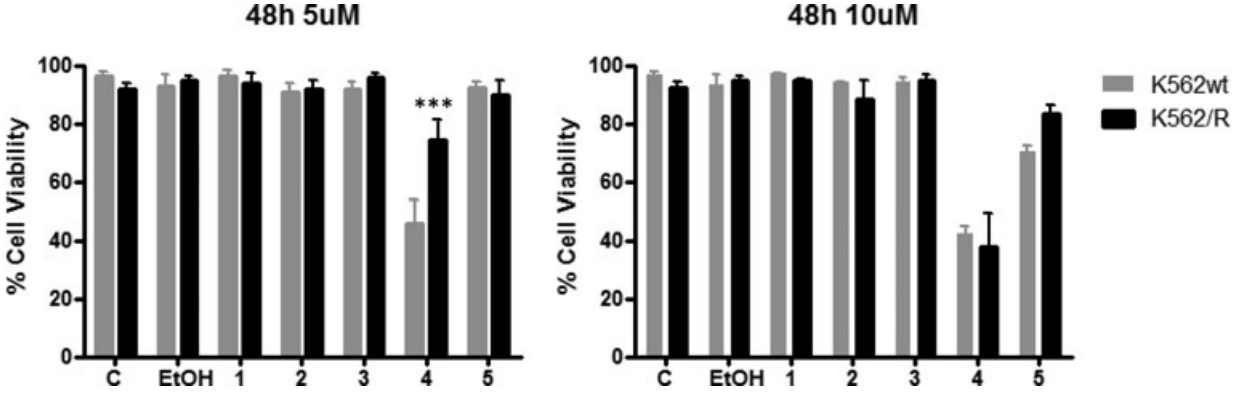

Figure 1. Cell viability in K562 and K562/R cells upon treatment for 48 h with solutions containing 5 or 10 μM of polyphenols from five different rosemary extracts (indicated by numbers 1 to 5). EtOH refers to incubation of both cell lines with ethanol used as solvent of rosemary extracts. C refers to untreated cells. $^{***}p < 0.0001$ between K562 and K562/R (*t*-test). Error bars are given as SD ($n = 4$).

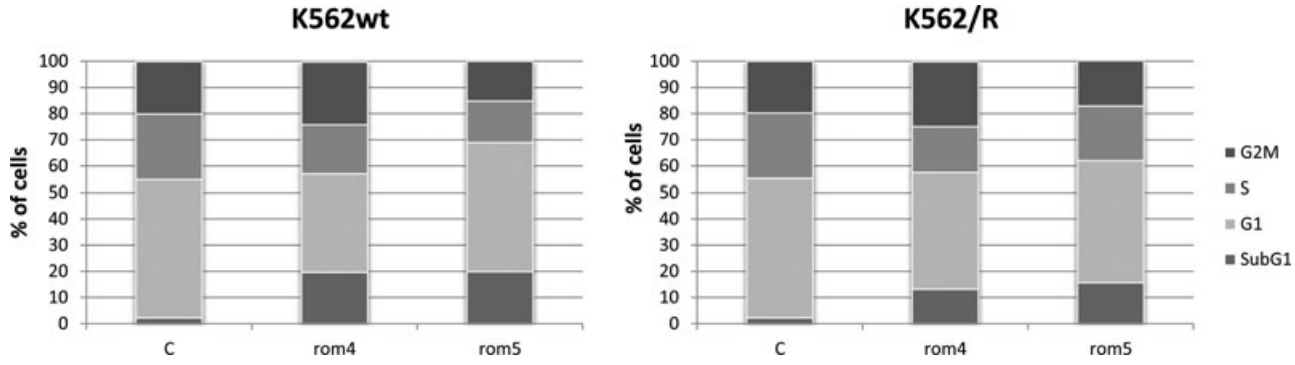

Figure 2. Cell cycle distribution of K562 and K562/R cells upon incubation with a 5 μM solution of polyphenols from rosemary extracts 4 (rom4) and 5 (rom5) for 48 h determined by flow cytometry. C: Control, untreated cells.

and cell cycle studies, rom4 extract was selected for further investigations.

3.2 Transcriptomic profiling and functional enrichment analysis

3.2.1 K562 versus K562/R cells

Comparative transcriptomic analysis was initially performed between K562 and resistant K562/R cells. Examination of the transcriptome profiles showed 227 genes that exhibited a significant differential expression in K562/R compared to K562 cells (data not shown). As expected, strong induction of *ABCB1* (also *MDR1*) was detected in K562/R cells (*M*-value of 7.5, corresponding to 181-fold change). As mentioned above, the protein encoded by this *ABCB1* gene is P-glycoprotein (Pgp), an energy-dependent drug efflux pump responsible for decreased drug accumulation in multidrug-resistant cells [49,50]. It seems possible that overexpression of Pgp could be involved in the removal of cytotoxic components, contributing to the greater tolerance exhibited by the K562/R cells with respect to the K562 cells against the rosemary polyphenols (Fig. 1).

3.2.2 Effect of rosemary polyphenols on leukemia cells

Gene expression microarray analyses were carried out in order to study at transcriptome level the effect of rosemary polyphenols from rom4 extract on K562 and K562/R leukemia cells. After microarray data processing, predefined *M*-value ($M = 0.6$) and false discovery ratio (FDR) of 5% (adjusted *p*-value <0.05) were applied to identify DEGs in response to the rosemary polyphenols treatment. According to these criteria, within the full list of 28 132 genes represented in the microarray, 289 and 387 genes were found in K562 and K562/R, respectively, to be differentially expressed in response to the treatment (see Supporting Information Table S1A and B). Among these DEGs, the expression of 129 genes (~33–44% of DEGs) was commonly altered in both cell lines with the same direction of change.

A set of genes induced in both lines and associated with biological functions of interest were selected for RT-qPCR validation. Based on this criterion, *MYC*, *CCNE1*, *OSGIN1*, and *NQO1* genes were selected for validation. In this study, three reference genes (*GUSB*, *ABL1*, and *B2M*), that have been reported to provide good normalization of RT-qPCR data in leukemia were used [51–53]. As shown in Table 2, changes in the expression ratio of all selected genes,

Table 2. Comparison of gene expression ratios in response to rom4 treatment as determined by microarray analysis and RT-qPCR in leukemia cell lines K562 and K562/R

Gene symbol	K562				K562/R			
	Microarray		RT-qPCR		Microarray		RT-qPCR	
	FC[a)]	*p*-value[b)]	FC[a)]	*p*-value[c)]	FC[a)]	*p*-value[b)]	FC[a)]	*p*-value[c)]
MYC	0.72	0.049	0.32	0.037	0.56	0.006	0.30	<0.001
CCNE1	0.84	0.271	0.53	0.037	0.64	0.013	0.42	<0.001
OSGIN1	2.09	0.009	3.85	0.033	2.39	0.004	4.80	0.036
NQO1	2.42	0.002	3.66	0.033	1.67	0.024	2.57	<0.001

a) For comparison purposes, *M*-values (log2 ratio) obtained from microarray analysis were converted to Fold Change (FC) values.
b) Adjusted *p*-value (FDR).
c) Statistical significance calculated by REST.

were provided by REST with high statistical significance (p-value <0.05). In general, gene expression ratios obtained with RT-qPCR confirm the results obtained by microarray. As an exception, the change in the expression of *CCNE1* gene was not statistically significant in the microarray analysis of K562 cells while it was found significantly repressed by RT-qPCR, showing a similar pattern in treated K562/R cells.

In order to identify the biological processes that might be altered in response to rosemary polyphenols, functional enrichment analysis on microarray datasets using IPA software was first performed. Lists of identified DEGs obtained from microarray analyses were imported into IPA software. In these analyses, 375 and 279 genes from K562/R and K562 microarray data, respectively, were eligible for biological function and pathway analysis. Functional analysis identified significant (Fisher Exact test p-value < 0.05) over-represented molecular and cellular functions that were common in the imported datasets (see Table 3). Some of these functions were associated to cell-to-cell signaling interaction, free radical scavenging, cellular movement, and cell death. Further enrichment analysis on defined (canonical) pathways of IPA Knowledge Base provided significant over-represented pathways across the entire list of DEGs. In K562/R enrichment analysis, *NRF2-mediated oxidative stress response* was identified as the top canonical pathway (Fig. 3). Furthermore, two other pathways related with the transcription of genes encoding phase I and II metabolizing enzymes and antioxidant proteins were over-represented, namely, *LPS/IL-1-mediated inhibition of RXR function* and *Aryl hydrocarbon receptor signaling*. In K562/R analysis, examination of the three related pathways evidenced transcriptional induction of a number of genes encoding phase II detoxifying and antioxidant genes, namely, *NQO1* (NADPH quinone oxidoreductase), *GST* (glutathione S-transferase), and *SULT* (sulfotransferase). These enzymes exert efficient cytoprotection against toxicants through a variety of reactions, promoting elimination or inactivation of toxic reactive species (including potential carcinogens) before they cause damage to the cell [54–58]. To the contrary, genes encoding phase I metabolizing enzymes, namely, *CAT* (catalase), *EPHX1* (epoxide hydrolase), and several members of *ALDH* gene family, were downregulated in response to the treatment in the same cell line. The effect of rosemary polyphenols on the modulation of genes associated with xenobiotic metabolism and response to oxidative stress observed was less evident in treated K562 cells than in the K562/R cells. The expression of the antioxidant and tumor suppressor gene *OSGIN1* (oxidative stress-induced growth inhibitor 1) was also induced in both cell lines. Although IPA did not include this gene in NRF2-mediated response to oxidative stress, the expression of *OSGIN1* is regulated via NRF2 nuclear transcription factor pathway in response to oxidative signals [59]. In general, the observed transcriptional response of the leukemia cells to rosemary polyphenols is in agreement with reported data in the literature regarding catechol-type electrophilic compounds. Accumulating evidence from in vitro studies with neuronal cells and dietary polyphenols suggests that this type of compound, such as carnosic acid and carnosol, initiates S-alkylation of cysteine thiol of the KEAP1 protein [17, 60]. This event may induce protective effects dependent of the cell type by promoting the translocation of NRF2 from the cytoplasm to the nucleus, where it heterodimerizes with small MAF proteins, and binds to AREs (antioxidant or electrophile response elements). AREs are found in the 5′ upstream promoter region of many of the phase II/antioxidant genes involved in xenobiotic metabolism and oxidative stress response. Induction of ARE-gene expression in an NRF2-dependent manner by carnosic acid and carnosol has shown to inhibit adipocyte differentiation in mouse [61] and to regulate expression of nerve growth factor mediated by NRF2 activation, conferring protection in glioblastoma cells [62]. A wide variety of dietary compounds, namely, sulforaphane, curcumin, and caffeic acid phenethyl has been also described to act as potent inducers of ARE-regulated gene expression providing a chemopreventive effect to cultured cells [63].

Next, transcription factor analysis was performed using IPA software. The purpose of these analyses was to obtain predictions of transcriptional regulators that may be potentially responsible for gene expression changes observed in the lists of DEGs. Using this bioinformatics tool, three transcription regulators, namely, *GATA1*, *PPARD*, and *HIF1A*, were predicted to be inhibited in treated K562 cells (Table 4). Interestingly, mRNA levels of *GATA1*, an erythroid-cell-specific gene with a pivotal role in erythroid differentiation, remained unaltered. However, according to IPA,

Table 3. Molecular and cellular functions obtained from the functional analysis for the K562 and K562/R datasets using IPA

Cell line	Molecular and cellular functions	p-values[a)]	Number of genes
K562	Cellular movement	8.2×10^{-7}–2.5×10^{-2}	55
	Cell-to-cell signaling and interaction	1.6×10^{-6}–2.4×10^{-2}	47
	Free radical scavenging	4.2×10^{-5}–1.3×10^{-2}	18
	Cell death	1.8×10^{-4}–2.4×10^{-2}	44
	Protein synthesis	2.9×10^{-4}–2.1×10^{-2}	14
	Antigen presentation	4.7×10^{-4}–1.8×10^{-2}	14
	Cellular function and maintenance	4.7×10^{-4}–2.3×10^{-2}	41
K562/R	Cell-to-cell signaling and interaction	1.8×10^{-6}–9.7×10^{-3}	63
	Antigen presentation	2.1×10^{-6}–9.0×10^{-3}	15
	Free radical scavenging	2.6×10^{-6}–4.6×10^{-3}	26
	Cell morphology	3.0×10^{-6}–8.7×10^{-3}	30
	Cellular growth and proliferation	3.8×10^{-6}–9.5×10^{-3}	108
	Cellular movement	4.5×10^{-6}–9.6×10^{-3}	68
	Cell death	9.2×10^{-6}–9.7×10^{-3}	87

a) Significance value calculated with the right-tailed Fisher's exact test.

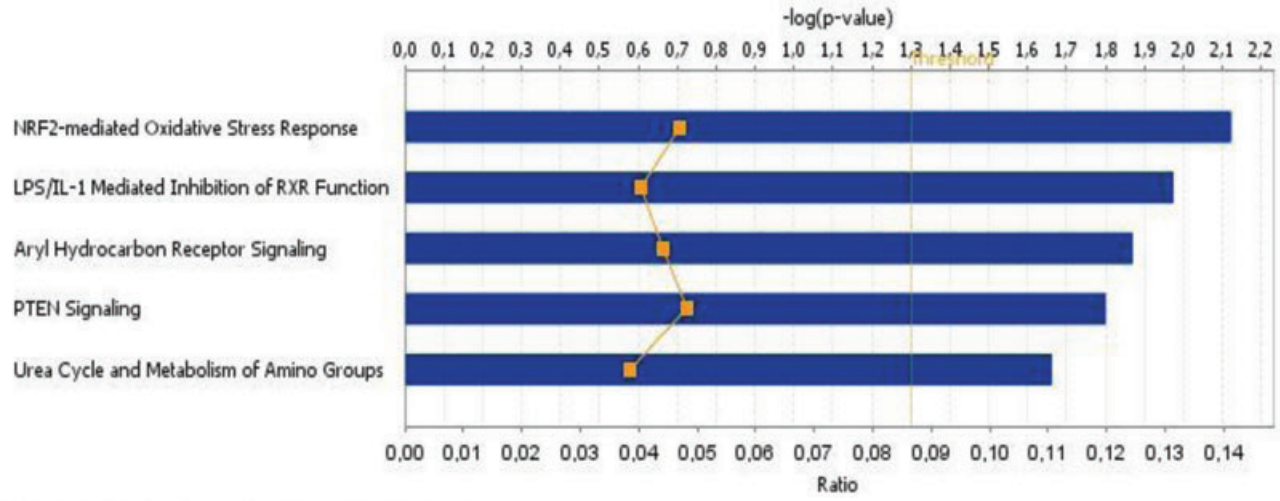

Figure 3. Canonical pathways significantly modulated by rosemary polyphenols in treated K562/R cell line. Fisher's exact test was used to calculate a *p*-value determining the probability that the association between the genes in the dataset and the canonical pathway is explained by chance. Histogram displays–log (*p*-value) calculated for each canonical pathway and yellow trace indicates the corresponding ratio (genes in a given pathway that meet cutoff criteria in our dataset, divided by total number of genes that make up that pathway).

Table 4. Transcription regulator analysis for K562/R and K562 cells

Cell line	Transcription regulator	Predicted activation state	Z-score	Target molecules in dataset[a)]
K562/R	*MYC*	Inhibited	−3.230	↑ANXA4, ↑CASP8, ↓CCNE1, ↑CLU, ↑CTSB, ↑CTSD, ↑ERAP1, ↑GCSH, ↑GM2A, ↑ICAM1, ↑IFI35, ↑ITGAX, ↓KIAA0664, ↓PKLR, ↑PLAUR, ↓PPID, ↓RPL13
	PPARGC1A	Inhibited	−2.707	↓CAT, ↓CD36, ↑CD68, ↓SREBF1, ↓TFAM
	PPARG	Inhibited	−2.108	↓CA2, ↓CAT, ↓CD36, ↑EPHX1, ↓SREBF1, ↑TBXA2R, ↑TBXAS1
	RB1	Activated	2.001	↑CASP8, ↓CCNE1, ↓HIST1H2AB, ↓MYC
K562	*HIF1A*	Inhibited	−2.372	↓EGLN3, ↓EREG, ↓FAM162A, ↓HIST1H2AG, ↑LIFR
	GATA1	Inhibited	−2.308	↓ABCB10, ↓AHSP, ↓CD36, ↓HBB, ↑ITGAX, ↓SPTB, ↓TUBB1
	PPARD	Inhibited	−2.050	↑CD68, ↓PKLR, ↓SORD

a) The arrows indicate an increase (↑) or decrease (↓) in the transcript levels.

inhibition of this transcription factor is predicted by the expression pattern of seven different genes (see Table 4). Among these genes, the strong downregulation (−2.72) observed for the gene encoding for α-hemoglobin stabilizing protein (*AHSP*) is noteworthy. Reduction of *AHSP* gene product in hemin-induced K562 cells has been related with increased cell death [64]. On the other hand, predictions for treated K562/R cells pointed out activation of *RB1* and inactivation of *MYC*, *PPARGC1A*, and *PPARG*. Microarray analysis also indicated downregulation of mRNA levels (−0.83, i.e calculated fold change of 0.56) for *MYC* gene in K562/R in response to the treatment with polyphenols. In the analysis of treated K562 cells, the expression of *MYC* gene changed significantly but the extent of the downregulation was borderline (−0.48; ca. fold change of 0.72). *MYC* is an oncogene that encodes a transcription factor that dimerizes with Max, a ubiquitously expressed protein, and the Myc-Max dimers bind to E-boxes in regulatory regions to transactivate genes including a number of positive regulators of cell cycle progression as CDK4, cyclin E, and cyclin D while it represses the CDK inhibitors p21 and p27. Moreover, *MYC* elicits a variety of biological responses related to cell cycle progression, apoptosis, immortalization, genomic instability, and control of cell differentiation among others [65]. *MYC* gene is overexpressed in most cancer cells and its inhibition has been widely studied for potential cancer therapy [66]. Several evidences suggest that downregulation of *MYC* gene may be of importance for the antiproliferative activity of certain phenolic compounds in cancerous cells [67–70]. For instance, in vivo treatment of mice with epigallocatechin gallate (EGCG) caused apoptosis in Sarcoma180 cells through alteration in G2/M phase of the cell cycle by downregulation of *MYC* and *bcl-2* [68]. Similar transcriptional effect has been observed upon butein treatment of leukemia cancer cells [69]. In this work, a Myc target related with cell cycle progression, such as cyclin E (*CCNE1*), was also downregulated in resistant leukemia cells by rosemary polyphenols, which is consistent with the cell cycle arrest observed in the cells after the treatment [71]. Also,

in the same cell line, mRNA levels of *CRYAB* and *PPID* genes were decreased, suggesting a pro-apoptotic effect [72, 73]. In addition to these effects, a number of repressible Myc targets were found overexpressed, including genes with apoptotic effects on leukemia cells (i.e. *CTSD* and *CASP8*) among other functions [74, 75]. Interestingly, two genes involved in transcriptional repression of *MYC* gene were identified as differentially expressed, namely, *MIRLET7A1* [76] and *HTATIP2* [77]. Apart from the upregulation of these transcriptional repressors of *MYC* gene, upregulation of *MXD1* gene, considered a biological antagonist of Myc protein, was detected in both cell lines after the treatment suggesting a potential inhibition of Myc function [78]. Single-gene level analysis of microarray data from treated K562/R cells also provided interesting information such as for example, the significant induction of *TNFSF10* gene, which encodes the tumor necrosis factor-related apoptosis inducing ligand (TRAIL protein). The overexpression of this gene product has been associated with pro-apoptotic effects in K562 leukemia cells [79]. Although the change in the expression of this pro-apoptotic gene was not significant in the analysis of K562 cells, the expression of other genes, such as *TGM2*, *DUSP1*, and *HIPK2*, linked to pro-apoptotic processes [80–82], was found to be modulated in this cell line by the treatment with rosemary polyphenols.

3.3 Metabolomic analysis

Regarding the metabolomic study, a combination of different analytical methodologies provided wide metabolic information and coverage due to its complementary nature. In Fig. 4A and D, metabolic profiles from K562 line obtained with CE-TOF MS and RP/UPLC-TOF MS are represented. Differences observed in metabolic profiles from both analytical platforms were due to their different separation mechanisms. CE-MS is mainly focused on the analysis of ionic, weakly ionic, and/or highly polar metabolites, which comprises a high proportion of the already known metabolites. Separation mechanism in UPLC (using a C18 column) is dominated by hydrophobic interactions providing different selectivity than CE-MS. Compared to UPLC-MS, higher drift in migration times was obtained in CE-MS caused by run-to-run variations of the electroosmotic flow. Deviations in migration/retention time are shown in Fig. 4B and E. Higher drifts in migration times obtained by CE-MS resulted in higher complex data processing. In this sense, alignment of CE-MS electropherograms was performed using a higher tolerance value for migration time. As a result, visual examination to minimize false positives in both analytical platforms (particularly in CE-MS) was mandatory. After data processing of CE-MS analysis, 68 and 70 compounds were found to change ($p < 0.05$) into the human K562 and K562/R cells, respectively,

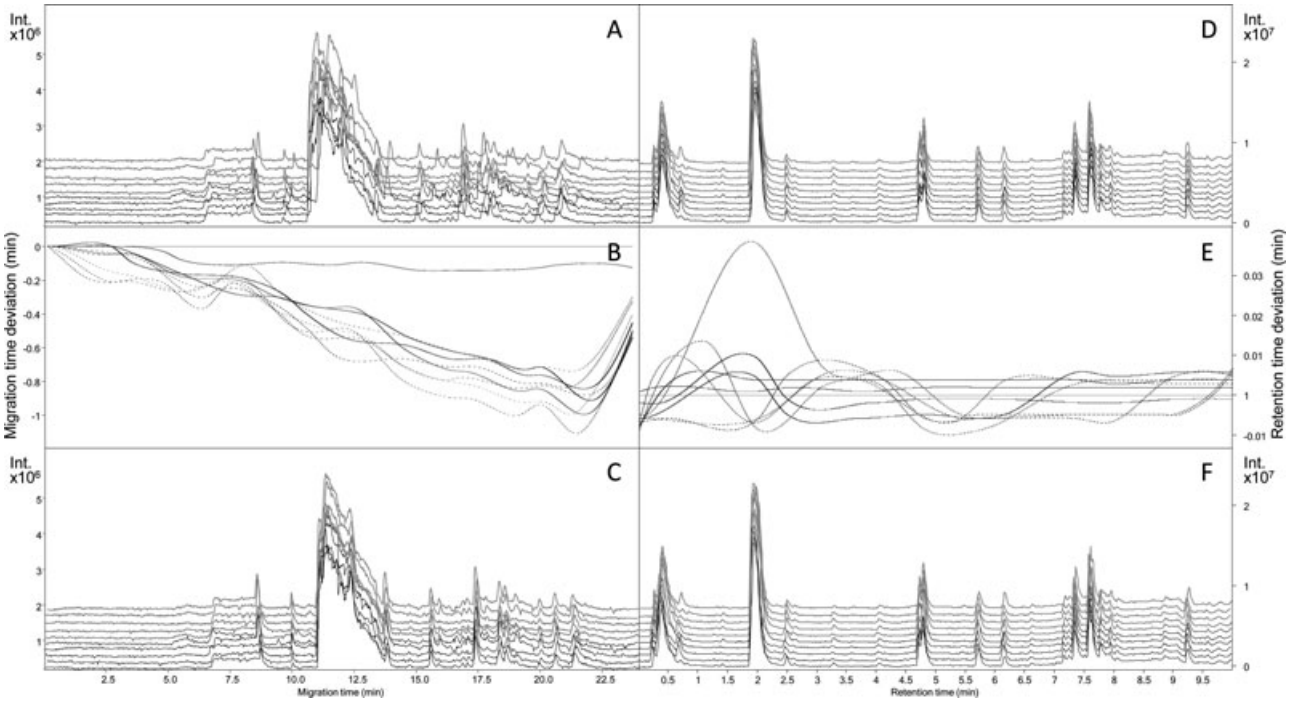

Figure 4. (A) CE-TOF MS total ion electropherograms from control and treated K562 cells (five replicates each). (B) Migration time deviation between CE-TOF MS analysis. (C) CE-TOF MS total ion electropherograms from control and treated K562 cells (five replicates each) after migration time correction. (D) UPLC-TOF MS total ion chromatograms from control and treated K562 cells (five replicates each). (E) Retention time deviation between UPLC-TOF MS analysis. (F) UPLC-TOF MS total ion chromatograms from control and treated K562 cells (five replicates each) after retention time correction. Color code: gray line, polyphenol-treated cells; black line, nontreated cells.

as a response to the treatment with rosemary polyphenols. Among these compounds, 27 could be tentatively identified (see Supporting Information Tables S2 and S3). On the other hand, 121 and 105 compounds were observed to be differently expressed ($p < 0.05$) when using RP/UPLC-MS in K562 and K562/R cell lines after polyphenols treatment. In this case, 38 metabolites were tentatively identified (see Supporting Information Tables S2 and S3). As can be deduced from the limited number of compounds identified, metabolite identification is still one of the major challenges in metabolomics since databases are still growing.

Datasets of tentatively identified metabolites and their statistically significant variations were analyzed using metabolomic function of IPA software. This analysis identified significant canonical metabolic pathways for each cell line. Table 5 summarizes top-scored metabolic pathways obtained for both K562/R and K562 cell lines. Owing to the numerous amino acids in the datasets, *aminoacyl-tRNA biosynthesis* was the most significant pathway in both leukemia cell lines (Table 5). In addition, a common feature for both cell lines was the ubiquitous presence of glutamate in most of the top-scored pathways. This amino acid participates in the mentioned *aminoacyl-tRNA biosynthesis* as well as in the metabolism of glutathione, arginine, proline, nitrogen, glutamate, amino groups, and urea cycle. Also, glutamate is an intermediate of glutamine utilization in mitochondria providing carbon to the tricarboxylic acid cycle. Thus, increased mitochondrial processing of glutamine is associated with an increase in the oxidative stress response [83]. This metabolic process has been established along with glucose utilization as a hallmark of tumor metabolism [84]. Moreover, glutamate may act as a precursor in reduced glutathione (GSH) synthesis [85]. In this regard, it was observed that rosemary polyphenols increased reduced (GSH) and oxidized (GSSG) glutathione in both K562 and K562/R cells. However, the calculated GSH/GSSG ratios for K562 and K562/R were 0.4 and 1.2, respectively, after exposure to the rosemary extract. The change in the intracellular levels of glutathione is essential for the maintenance of the cellular functions in mammalian cells, since it has a central role in the maintenance of the thiol-disulfide redox state. Glutathione metabolism participates in both, cancer prevention and progression. For example, under stress conditions, GSH scavenges harmful molecules such as electrophiles (by GSH conjugation) and reactive oxide species, preventing tumor initiation [86]. It has been reported that GSH depletion is a common feature of apoptotic cell death triggered by a wide variety of stimuli including activation of death receptors, stress, environmental agents, and cytotoxic drugs [85]. Thus, modulation of intracellular GSH content has been largely studied for potential anticancer therapies. The moderately increased GSH/GSSG ratio observed in treated K562/R cells is in agreement with the reported chemopreventive activity of catechol-type electrophilic compounds such as carnosol and carnosic acid in neuronal cells [17, 60]. Conversely, the oxidized glutathione levels were elevated relative to GSH levels in the treated K562 cell line suggesting a weaker chemopreventive and antioxidant response of this cell line to the treatment compared to the resistant subline. This differential ability of leukemia lines to accumulate intracellular GSH may partially explain

Table 5. List of metabolites and genes mapped on top significant metabolic pathways obtained by IPA analysis of metabolomics datasets of leukemia cells

	K562/R			K562		
Pathway	*p*-value[a)]	Metabolites[b,c)]	Genes[b)]	*p*-value[a)]	Metabolites[b,c)]	Genes[b)]
Aminoacyl-tRNA biosynthesis	2.3×10^{-6}	↑Met, ↑Leu, ↑Glu, ↑Tyr, ↓Lys, ↓Phe	↑VARS	1.4×10^{-8}	↑Met, ↑Leu, ↑Glu, ↑Tyr, ↓Lys, ↓Phe, ↑Val, ↑Trp	
Glutathione metabolism	5.5×10^{-4}	↑GSSG, ↑GSH, ↑glutamate	↑GSTM2			
Arginine and proline metabolism	2.0×10^{-3}	↑Glu, ↑spermidine, ↓adenine, ↓Gbn	↑P4HA2 ↓CKMT1A ↑ALDH1A1	3.3×10^{-5}	↑Glu, ↓Orn, ↑spermidine, ↑spermine, ↓Gbn, ↑creatine	↑P4HA2 ↓CKMT1A ↑CPS1
Nitrogen metabolism	2.4×10^{-3}	↑Tyr, ↓Phe, ↑Glu	↓GCSM ↓CA2	2.6×10^{-4}	↑Tyr, ↓Phe, ↑Glu, ↑Trp	↑CPS1 ↓THM2
Glutamate metabolism	3.0×10^{-3}	↑GSSG, ↑GSH, ↑Glu	↑NAGK			
Urea cycle and metabolism of amino groups				1.6×10^{-5}	↓Orn, ↑spermine, ↑spermidine, ↑Glu, ↑creatine	↑CPS1 ↓CKMT1

a) Significance value calculated with the right-tailed Fisher's exact test.
b) The arrows indicate an increase (↑) or decrease (↓) in the transcript levels.
c) Met (methionine), Leu (leucine), Glu (glutamate), Tyr (tyrosine), Lys (lysine), Phe (phenylalanine), Val (valine), Trp (tryptophan), Orn (ornithine), Gbn (4-guanidinobutanoate).

the higher proportion of apoptotic K562 cells (20%) after incubation with rom4 extract compared to the values obtained for K562/R (13%).

Apart from the aforementioned metabolites, in this work decreased levels of hypoxanthine were detected in K562/R cells after the treatment with rosemary polyphenols. This metabolite has been related to the generation of reactive oxygen species by the action of xanthine oxidase. Recently, low levels of hypoxanthine have been associated with the chemopreventive effect of the polyphenol resveratrol in metabolomics studies with rat tissues [87]. Moreover, treatment with rosemary polyphenols induced a significant decrease of N1-acetylspermidine, the excretable form of spermidine, whereas spermidine levels showed only a modest increase in K562/R cells. A similar polyamine profile was observed in the analysis of K562 line, showing marked decreased levels of acetylated spermidine, slight increased levels of spermidine and spermine, but in this case, ornithine, a precursor of polyamine synthesis, was strongly decreased in treated K562 cells.

Although cancer cell lines are well-established models to study specific cellular mechanisms characteristic for different types of cancer, it is not a trivial matter to connect transcriptome to metabolome results, since a given metabolite pattern can reflect several transcriptomic changes. In this study, IPA software was used overlaying transcriptomic datasets on canonical pathways obtained from metabolomics analysis and vice versa. This strategy enabled several DEGs to be identified in top-significant metabolic pathways modulated by polyphenol treatment. Table 5 summarizes the findings obtained using this strategy. As an example, the increased expression in K562/R of *GSTM2* gene, coding for an isoform of glutathione transferase, was found to participate in the *glutathione metabolism* pathway, where the GSH levels were also elevated. However, the establishment of direct associations between genes and metabolites was not always straightforward. This was the case for the molecules mapped on *Arginine and proline metabolism*. Although similar metabolic and transcriptional profiles were observed for this pathway in both leukemia cell lines (see Table 5), most of the mapped molecules were unconnected from the rest of molecules. Conversely, a direct association was found by overlaying metabolomic data on the *urea cycle and metabolism of amino groups* pathway obtained for K562/R with transcriptomic data (data not shown). In this case, accumulation of glutamate by approximately two-fold in treated cells compared to the untreated control cells could potentially be linked to the decreased mRNA levels of *ALDH18A1* gene, which encodes for the glutamate 5-kinase, an enzyme that transforms glutamate into glutamyl phosphate.

4 Concluding remarks

Our results revealed that rosemary polyphenols pose cytotoxic and, to a lesser extent, cytostatic activity against K562 and K562/R leukemia cell lines. In this regard, our observations indicate that the cytotoxic effect was concomitant with apoptosis induced in the cells by rosemary polyphenols. K562/R cells were less sensitive to the cytotoxic effect of rosemary polyphenols. This greater resistance could be explained, at least in part, by the overexpression of the *ABCB1* gene product, responsible for the active (drug) efflux of many antineoplastic drugs and xenobiotics. Also, rosemary polyphenols induced a chemopreventive effect via transcriptionally activated genes that encode antioxidant and phase II detoxifying enzymes (*NQO1*, *GST*, *SULT*, and *OSGIN1*) in the leukemia cell lines, especially in K562/R cells, what can explain the higher resistance of these cells to polyphenols. These findings are consistent with the reported NRF2 activating effect of carnosic acid and carnosol, two of the major phenolic compounds in the rosemary extract under study. IPA helped on providing information on transcription regulators that might be activated or inhibited. In this regard, inhibition of *MYC* transcription factor was highlighted, providing new data about the transcriptional response of leukemia cells potentially linked to the antiproliferative effect of rosemary polyphenols. Metabolomics analysis showed that rosemary polyphenols induced metabolic changes on leukemia cells under the conditions assayed in this work. In particular, the treatment with rosemary polyphenols affected differently the intracellular levels of glutathione in leukemia cell sublines. Elevated levels of GSH and decreased levels of hypoxanthine provided additional evidences to transcriptomic results regarding the stronger chemopreventive and antioxidant response of leukemia K562/R cells to rosemary polyphenols in comparison with the observed response in K562 cell line. The integrative Foodomics strategy enabled the identification of various differentially expressed genes in the metabolic pathways modulated by rosemary polyphenols and vice versa, providing stronger evidences on the molecular mechanisms that can explain the effect of the compounds tested in this work. However, direct associations between the changes observed at transcriptome and metabolome level could be established only in few cases.

This work was supported by AGL2008-05108-C03-01, AGL2008-05108-C03-02, and AGL2011-29857-C03-01 projects (Ministerio de Ciencia e Innovación, Spain), and CSD2007-00063 FUN-C-FOOD (Programa CONSOLIDER, Ministerio de Educacion y Ciencia, Spain). Authors thank Agilent Technologies for its support. C.I. thanks the Ministerio de Ciencia e Innovación for her FPI pre-doctoral fellowship. A.V. thanks the Fundación Universidad Autónoma de Madrid for his pre-doctoral fellowship.

The authors have declared no conflict of interest.

5 References

[1] Clarkson, B., Strife, A., *Leukemia* 1993, *7*, 1683–1721.

[2] Groffen, J., Stephenson, J. R., Heisterkamp, N., de Klein, A., Bartram, C. R., Grosveld, G., *Cell* 1984, *36*, 93–99.

[3] Ren, R., *Oncogene* 2002, *21*, 8629–8642.

[4] Faderl, S., Talpaz, M., Estrov, Z., O'Brien, S., Kurzrock, R., Kantarjian, H. M., *New Engl. J. Med.* 1999, *341*, 164–172.

[5] Evans, C., Owen-Lynch, P., Whetton, A. D., Dive, C., *Cancer Res.* 1993, *53*, 1735–1738.

[6] Persidis, A., *Nat. Biotechnol.* 1999, *17*, 94–95.

[7] Tan, B., Piwnica-Worms, D., Ratner, L., *Curr. Opin. Oncol.* 2000, *12*, 450–458.

[8] Johnson, I. T., *P. Nutr. Soc.* 2007, *66*, 207–215.

[9] Ramos, S., *J. Nutr. Biochem.* 2007, *18*, 427–442.

[10] Pierini, R., Gee, J. M., Belshaw, N. J., Johnson, I. T., *Brit. J. Nutr.* 2008, *99*, ES53–ES59.

[11] Ramos, S., *Mol. Nutr. Food. Res.* 2008, *52*, 507–526.

[12] Fresco, P., Borges, F., Marques, M. P. M., Diniz, C., *Curr. Pharm. Design.* 2010, *16*, 114–134.

[13] Araújo, J. R., Gonçalves, P., Martel, F., *Nutr. Res.* 2011, *31*, 77–87.

[14] Chen, C., Zhou, J., Ji, C., *Life Sci.* 2010, *87*, 333–338.

[15] Ngo, S. T., Williams, D. B., Head, R. J., *Crit. Rev. Food Sci.* 2011, *51*, 946–954.

[16] Herrero, M., Plaza, M., Cifuentes, A., Ibáñez, E., *J. Chromatogr. A* 2010, *1217*, 2512–2520.

[17] Satoh, T., Izumi, M., Inukai, Y., Tsutsumi, Y., Nakayama, N., Kosaka, K., Shimojo, Y., Kitajima, C., Itoh, K., Yokoi, T., Shirasawa, T., *Neurosci. Lett.* 2008a, *434*, 260–265.

[18] Visanji, J. M., Thompson, D. G., Padfield, P. J., *Cancer Lett.* 2006, *237*, 130–136.

[19] Danilenko, M., Wang, X., Studzinski, G. P., *J. Natl. Cancer I.* 2001, *93*, 1224–1233.

[20] Johnson, J. J., *Cancer Lett.* 2011, *305*, 1–7.

[21] Herrero, M., García-Cañas, V., Simó, C., Cifuentes, A., *Electrophoresis* 2010, *31*, 205–228.

[22] Herrero, M., Simó, C., García-Cañas, V., Ibáñez, E., Cifuentes, A., *Mass Spectrom. Rev.* 2012, *31*, 49–69.

[23] García-Cañas, V., Simó, C., León, C., Cifuentes, A., *J. Pharmaceut. Biomed.* 2010, *51*, 290–304.

[24] Smyth, G. K., *Stat. Appl. Genet. Mol. Biol.* 2004, *3*, 3.

[25] Waagmeester, A. S., Kelder, T., Evelo, C., *Genes Nutr.* 2008, *3*, 139–142.

[26] Kosar, M., Dorman, H. J. D., Hiltunen, R., *Food Chem.* 2005, *91*, 525–533.

[27] Gentleman, R., Carey, V. J., Bates, D. M., Bolstad, B., Dettling, M., Dudoit, S., Ellis, B., Gautier, L., Ge, Y., Gentry, J., Hornik, K., Hothorn, T., Huber, W., Iacus, S., Irizarry, R., Leisch, F., Li, C., Maechler, M., Rossini, A. J., Sawitzki, G., Smith, C., Smyth, G., Tierney, L., Yang, J., Zhang, J., *Genome Biol.* 2004, *5*, R80.

[28] Gautier, L., Cope, L., Bolstad, B. M., Irizarry, R. A., *Bioinformatics* 2004, *20*, 307–315.

[29] Benjamini, Y., Hochberg, Y., *J. Roy. Stat. Soc. B.* 1995, *57*, 289–300.

[30] Smyth, G. K., in: Gentleman, R., Carey, V., Dudoit, S., Irizarry, R., Huber, W. (Eds), *Bioinformatics and Computational Biology Solutions using R and Bioconductor*, Springer, New York, 2005, pp. 397–420.

[31] Pfaffl, M. W., in: Dorak, M. T. (Ed), *Real-time PCR*, Taylor & Francis Group, Newcastle, 2006, pp. 63–82.

[32] Pfaffl, M. W., Horgan, G. W., Dempfle, L., *Nucleic Acids Res.* 2002, *30*, e36.

[33] Smith, C. A., Want, E. J., Tong, G. C., Abagyan, R., Siuzdak, G., *Anal. Chem.* 2006, *78*, 779–787.

[34] Tautenhahn, R., Böttcher, C., Neumann, S., *BMC Bioinformatics* 2008, *9*, 504–519.

[35] Prince, J. T., Marcotte, E. M., *Anal. Chem.* 2006, *78*, 6140–6152.

[36] Alonso, A., Julià, A., Beltran, A., Vinaixa, M., Díaz, M., Ibañez, L., Correig, X., Marsal, S., *Bioinformatics* 2011, *27*, 1339–1340.

[37] Wishart, D. S., Knox, C., Guo, A.C., Eisner, R., Young, N., Gautam, B., Hau, D.D., Psychogios, N., Dong, E., Bouatra, S., Mandal, R., Sinelnikov, I., Xia, J., Jia, L. Cruz, J. A., Lim, E., Sobsey, C. A., Shrivastava, S., Huang, P., Liu, P., Fang, L., Peng, J., Fradette, R., Cheng, D., Tzur, D., Clements, M., Lewis, A., De Souza, A., Zuniga, A., Dawe, M., Xiong, Y., Clive, D., Greiner, R., Nazyrova, A., Shaykhutdinov, R., Li, L., Vogel, H. J., Forsythe, I., *Nucleic Acids Res.* 2009, *37*, D603–D610.

[38] Smith, C. A., O'Maille, G., Want, E. J., Qin, C., Trauger, S. A., Brandon, T. R., Custodio, D. E., Abagyan, R., Siuzdak, G., *Ther. Drug. Monit.* 2005, *27*, 747–751.

[39] Kanehisa, M., Goto, S., *Nucleic Acids Res.* 2000, *28*, 27–30.

[40] Bolton, E. E., Wang, Y., Thiessen, P. A., Bryant, S. H., *Ann. Rep. Comput. Chem.* 2008, *4*, 217–241.

[41] Rocamora-Reverte, L., Carrasco-García, E., Ceballos-Torres, J., Prashar, S., Kaluderovic, G. N., Ferragut, J. A., Gómez-Ruiz, S., *Chem. Med. Chem.* 2012, *7*, 301–310.

[42] Borst, P., Oude Elferink, R., *Annu. Rev. Biochem.* 2002, *71*, 537–592.

[43] Gottesman, M. M., Fojo, T., Bates, S. E., *Nat. Rev. Cancer* 2002, *2*, 48–58.

[44] Yesil-Celiktas, O., Sevimli, C., Bedir, E., Vardar-Sukan, F., *Plant Food Hum. Nutr.* 2010, *65*, 158–163.

[45] Moon, D. O., Kim, M. O., Lee, J. D., Choi, Y. H., Kim, G. Y., *Cancer Lett.* 2010, *288*, 183–191.

[46] Gigante, B., Santos, C., Silva, A. M., Curto, M. J. M., Nascimento, M. S. J., Pinto, E., Pedro, M., Cerqueira, F., Pinto, M. M., Duarte, M. P., Laires, A., Rueff, J., Gonçalves, J., Pegado, M. I., Valdeira, L., *Bioorgan. Med. Chem.* 2003, *11*, 1631–1638.

[47] Guerrero, I. C., Andrés, L. S., León, L. G., Machín, R. P., Padrón, J. M., Luis, J. G., Delgadillo, J., *J. Nat. Prod.* 2006, *69*, 1803–1805.

[48] Johnson, J. J., Syed, D. N., Heren, C. R., Suh, Y., Adhami, V. M., Mukhtar, H., *Pharm. Res.* 2008, *25*, 2125–2134.

[49] Gottesman, M. M., Pastan, I., *Annu. Rev. Biochem.* 1993, *62*, 385–422.

[50] Mahon, F., Belloc, F., Lagarde, V., Chollet, C., Moreau-Gaundry, F., Reiffers, J., Goldman, J. M., Melo, J. V., *Blood* 2003, *101*, 2368–2373.

[51] Lupberger, J., Kreuzer, K. -A., Baskaynak, G., Peters, U. R., Coutre, P., Schmidt, C. A., *Mol. Cell. Probe.* 2002, *16*, 25–30.

[52] Beillard, E., Pallisgaard, N., van der Velden, V. H. J., Bi, W., Dee, R., van der Schoot, E., Delabesse, E., Macintyre, E., Gottardi, E., Saglio, G., Watzinger, F., Lion, T., van

Dongen, J. J. M., Hokland, P., Gabert, J., *Leukemia* 2003, *17*, 2474–2486.

[53] Wang, Y. L., Lee, J. W., Cesarman, E., Jin D. K., Csernus, B., *J. Mol. Diagn.* 2006, *8*, 231–239.

[54] Aruoma, O. I., Halliwell, B., Aeschback, R., Lolingers, J., *Xenobiotica* 1992, *22*, 257–268.

[55] Jeong, W. S., Jun, M., Kong, A. N. T., *Antioxid. Redox. Sign.* 2006, *8*, 99–106.

[56] Martin, D., Rojo, A. I., Salinas, M., Diaz, R., Gallardo, G., Alam, J., Ruiz de Galarreta, C. M., Cuadrado, A., *J. Biol. Chem.* 2004, *279*, 8919–8929.

[57] Rau, O., Wurglics, M., Paulke, A., Zitzkowski, J., Meindl, N., Bock, A., Dingermann, T., Abdel-Tawab, M., Schubert-Zsilavecz, M., *Planta Med.* 2006, *72*, 881–887.

[58] Kaspar, J. W., Niture, S. K., Jaiswal, A. K., *Free Radical Bio. Med.* 2009, *47*, 1304–1309.

[59] Li, R., Chen, W., Yanes, R., Lee, S., Berliner, J. A., *J. Lipid Res.* 2007, *48*, 709–715.

[60] Satoh, T., Kosaka, K., Itoh, K., Kobayashi, A., Yamamoto, M., Shimojo, Y., Kitajima, C., Cui, J., Kamins, J., Okamoto, S., Izumi, M., Shirasawa, T., Lipton, S. A., *J. Neurochem.* 2008b, *104*, 1116–1131.

[61] Takahashi, T., Tabuchi, T., Tamaki, Y., Kosaka, K., Takikawa, Y., Satoh, T., *Biochem. Bioph. Res. Co.* 2009, *382*, 549–554.

[62] Mimura, J., Kosaka, K., Maruyana, A., Satoh, T., Harada, N., Yoshida, H., Satoh, K., Yamamoto, M., Itoh, K., *J. Biochem.* 2011, *150*, 209–217.

[63] Lee, J. S., Surh, Y. J., *Cancer Lett.* 2005, *224*, 171–184.

[64] Oliveira Pinho, F., Martins de Albuquerque, D., Olalla Saad, S. T., Ferreira Costa, F., *Exp. Hematol.* 2008, *36*, 265–272.

[65] Acosta, J. C., Ferrándiz, N., Bretones, G., Torrano, V., Blanco, R., Richard, C., O'connell, B., Sevidy, J., Delgado, M. D., León, J., *Mol. Cell. Biol.* 2008, *28*, 7286–7295.

[66] Soucek, L., Whitfield, J., Martins, C. P., Finch, A. J., Murphy, D. J., Sodir, N. M., Karnezis, A. N., Swigart, L. B., Nasi, S., Evan, G. I., *Nature* 2008, *455*, 679–83.

[67] Thatte, U., Bagadey, S., Dahanukar, S., *Cell. Mol. Biol.* 2000, *46*, 199–214.

[68] Manna, S., Banerjee, S., Mukherjee, S., Das, S., Panda, C. Kr., *Apoptosis* 2006, *11*, 2267–2276.

[69] Moon, D.-O., Kim, M. -O., Lee, J. –D., Choi, Y. H., Kim, G. –Y., *Cancer Lett.* 2009, *286*, 172–179.

[70] Manna, S., Mukherjee, S., Roy, A., Das, S., Panda, C. Kr., *J. Nutr. Biochem.* 2009, *20*, 337–349.

[71] García, P., Frampton, J., Ballester, A., Calés, C., *Oncogene* 2000, *19*, 1820–1833.

[72] Kamradt, M. C., Chen, F., Cryns, V. L., *J. Biol. Chem.* 2001, *276*, 16059–16063.

[73] Schubert, A., Grimm, S., *Cancer Res.* 2004, *64*, 85–93.

[74] Carew, J. S., Nawrocki, S. T., Kahue, C. N., Zhang, H., Yang, C., Chung, L., Houghton, J. A., Huang, P., Giles, F. J., Cleveland, J. L., *Blood* 2007, *110*, 313–322.

[75] Secchiero, P., Gonelli, A., Mirandola, P., Melloni, E., Zamai, L., Celeghini, C., Milani, D., Zauli, G., *Blood* 2002, *100*, 2421–2429.

[76] Davis, B. N., Hata, A., *Cell Commun. Signal.* 2009, *7*, 18.

[77] Jiang, C., Ito, M., Piening, V., Bruck, K., Roeder, R. G., Xiao, H., *J. Biol. Chem.* 2004, *279*, 27781–27789.

[78] Leon, J., Ferrandiz, N., Acosta, J. C., Delgado, M. D., *Cell cyle* 2009, *8*, 1148–1157.

[79] Di Pietro, R., Zauli, G., *J. Cell Physiol.* 2004, *201*, 331–340.

[80] Li, Z., Xu, X., Bai, L., Chen, W., Lin, Y., *J. Biol. Chem.* 2011, *286*, 21164–21172.

[81] Wang, Z., Cao, N., Nantajit, D., Fan, M., Liu, Y., Li, J. J., *J. Biol. Chem.* 2008, *283*, 21011–21023.

[82] Stefano, V. D., Blandino, G., Sacchi, A., Soddu, S., D'Orazi, G., *Oncogene* 2004, *23*, 5185–5192.

[83] Medina, M. A., *J. Nutr.* 2001, *131*, 2539S–2542S.

[84] Yang, C., Sudderth, J., Dang, T., Bachoo, R.M., McDonald, J. G., DeBerardinis, R. J., *Cancer Res.* 2009, *69*, 7986–7993.

[85] Franco, R., Cidlowski, J. A., *Cell Death Differ.* 2009, *16*, 1303–1314.

[86] Forman, H. J., Zhang, H., Rinna, A., *Mol. Aspects Med.* 2008, *30*, 1–12.

[87] Li, H., Yan, Z., Zhu, J., Yang, J., He, J., *Neuropharmacology* 2011, *60*, 252–258.

3.2 Una aproximación Alimentómica para el estudio del efecto de polifenoles de romero en cáncer de colon

3.2.1 Prefacio

La dieta es el factor de riesgo modificable más relacionado con la aparición del cáncer colorrectal, por lo que en las últimas décadas se ha investigado el efecto de varios compuestos de origen alimentario en el desarrollo de esta enfermedad. Entre los compuestos de la dieta más estudiados se encuentran los polifenoles (Scalbert y col., 2005). Diversos trabajos en modelos celulares *in vitro* han demostrado la capacidad de esta clase de compuestos para evitar la iniciación, inhibir la promoción y detener la progresión del cáncer (Surh, 2003). Como se ha comentado en la Introducción de esta Memoria, el romero es un alimento que posee una gran cantidad de polifenoles y se le han atribuido, entre otras propiedades, la capacidad para inhibir la proliferación de células de cáncer. En las siguientes secciones se presentan los resultados obtenidos en varios estudios del efecto antiproliferativo de polifenoles de romero en células de cáncer de colon desde un punto de vista alimentómico.

A continuación, la sección 3.2.2 incluye los resultados del trabajo titulado "Effect of rosemary polyphenols on human colon cancer cells: transcriptomic profiling and functional enrichment analysis" de A. Valdés y col., publicado en la revista *Genes and Nutrition* 2013, *8*, 43-60. En esta publicación, inicialmente se llevó a cabo la determinación del efecto antiproliferativo de una serie de extractos de romero enriquecidos en compuestos fenólicos en dos líneas celulares de cáncer de colon con perfiles mutaciones distintos, SW-480 y HT-29. Al igual que en el estudio anterior en células de leucemia, los extractos de romero utilizados se obtuvieron mediante los métodos SFE y PLE y se caracterizaron en el laboratorio de Alimentómica del CIAL. Tras determinar su actividad antiproliferativa, se

efectuó el estudio del ciclo celular que permitió establecer que los extractos más activos poseen efecto citostático mediante citometría celular. Posteriormente, se seleccionó el extracto más activo para llevar a cabo una evaluación Alimentómica del efecto antiproliferativo del extracto en las dos líneas celulares. Para ello, se estudiaron los cambios en el transcriptoma de las líneas celulares SW-480 y HT-29 en respuesta al tratamiento con el extracto de romero durante 24 y 72 horas, respectivamente. En este trabajo, se emplearon microarrays de expresión génica de Affymetrix y el análisis permitió identificar los genes expresados diferencialmente en las dos líneas celulares en respuesta al tratamiento con el extracto. Algunos de los genes expresados diferencialmente se seleccionaron y se validaron mediante RT-qPCR, para lo que se diseñaron y optimizaron sistemas específicos de amplificación. Finalmente, se llevó a cabo el análisis exploratorio de las listas de genes mediante herramientas bioinformáticas, con el fin de determinar las funciones y procesos biológicos alterados tras el tratamiento con el extracto de romero.

Teniendo en cuenta que el ácido carnósico y el carnosol son los polifenoles mayoritarios del extracto de romero que presentó una actividad antiproliferativa mayor, la siguiente etapa del trabajo consistió en determinar si estos dos diterpenos eran los responsables de la actividad antiproliferativa del extracto. Para llevar a cabo esta parte del estudio, se seleccionó la línea celular de cáncer de colon HT-29. Este estudio se presenta en la sección 3.2.3, y corresponde al trabajo titulado "Comprehensive foodomics study on the mechanisms operating at various molecular levels in cancer cells in response to individual rosemary polyphenols" de A. Valdés y col., publicado en *Analytical Chemistry* 2014, *86*, 9807-9815. Inicialmente, se llevó a cabo un estudio comparativo de la actividad antiproliferativa del ácido carnósico, del carnosol y del extracto de romero a distintos tiempos de incubación. Este estudio permitió determinar la concentración inhibitoria del 50% del crecimiento (GI50, *50% Growth inhibition*), la concentración inhibitoria del 100%

del crecimiento (TGI, *Total Growth Inhibition*) y la concentración letal del 50% de las células (LC50, *50% Lethal Concentration*). En este estudio se identificó el ácido carnósico como el principal responsable de los efectos antiproliferativos del extracto de romero. A continuación, se investigó el posible efecto aditivo, sinérgico o antagónico de ambos diterpenos en la actividad antiproliferativa. También se llevó a cabo una evaluación Alimentómica con el fin de determinar los cambios en la expresión génica y en el metabolismo en las células HT-29 en respuesta al ácido carnósico. Para ello, se incubaron las células con una concentración citostática de ácido carnósico durante 48 horas. El estudio del efecto en el transcriptoma se llevó a cabo mediante microarrays de expresión génica de Affymetrix y permitió identificar los genes expresados diferencialmente en respuesta al tratamiento con el ácido carnósico. Los resultados obtenidos del análisis con microarrays se validaron mediante la técnica RT-qPCR. Además, con el fin de determinar las funciones y procesos biológicos alterados tras el tratamiento con el ácido carnósico, los genes expresados diferencialmente se analizaron mediante la herramienta bioinformática IPA. Para estudiar los efectos en el metabolismo, los metabolitos extraídos de las células control y tratadas con ácido carnósico se analizaron utilizando las plataformas complementarias CE-TOF MS y UHPLC-TOF MS. Tras el procesado de los datos obtenidos por ambas técnicas de análisis, se llevó a cabo el tratamiento estadístico de los datos para determinar los metabolitos alterados diferencialmente. Posteriormente, estos metabolitos se identificaron tentativamente empleando distintas bases de datos, y la identidad de algunos de ellos se confirmó mediante el empleo de compuestos estándar. Finalmente, estos metabolitos se mapearon mediante la herramienta bioinformática IPA para determinar las rutas metabólicas en las que están involucrados.

Los resultados obtenidos en los estudios transcriptómicos anteriores (secciones 3.2.2 y 3.2.3) indicaron que tanto el ácido carnósico como el extracto de romero alteran la

expresión de varios genes que codifican para proteínas (HMGCS1, HMGCR, IDI2, FDPS) con un papel fundamental en la síntesis y el metabolismo del colesterol en las células HT-29. Teniendo en cuenta que la alteración del metabolismo de lípidos es una característica frecuente durante los procesos de reprogramación metabólica en células de cáncer, y un requisito para mantener la tasa de proliferación elevada, resultó interesante profundizar en el efecto de los polifenoles de romero en el metabolismo del colesterol, e investigar la posible relación entre los cambios a nivel metabólico y transcriptómico con su actividad antiproliferativa. Este trabajo se presenta en la sección 3.2.4 e incluye el artículo titulado "Rosemary polyphenols induce unfolded protein response and changes in cholesterol metabolism in colon cancer cells" de A. Valdés y col., publicado en *Journal of Functional Foods* 2015, *15*, 429-439. En este estudio, se llevó a cabo el análisis mediante GC-MS de los niveles de colesterol total y colesterol libre en células tratadas con concentraciones citostáticas de polifenoles de romero (extracto enriquecido y ácido carnósico) a lo largo de 72 horas. El análisis indicó que el tratamiento con polifenoles de romero, especialmente con el extracto de romero, induce la acumulación de colesterol a partir de las 24 horas de incubación. A continuación, se efectuó un estudio transcriptómico con el fin de determinar si los cambios en los niveles de colesterol observados a 24 h en las células tratadas con polifenoles de romero se pueden atribuir a los cambios transcripcionales en los genes que controlan el metabolismo y la absorción del colesterol, y si además se producen otros cambios transcripcionales que pudieran explicar el efecto antiproliferativo de los tratamientos. Este estudio permitió identificar cambios en el transcriptoma que permitieron explicar la acumulación de colesterol observada en las células tratadas y, además, el análisis de enriquecimiento funcional de los datos transcriptómicos permitió identificar la activación de la *Respuesta a Proteínas Desplegadas* y la *Respuesta al Estrés Oxidativo*, como dos de los efectos más significativos de los tratamientos con el extracto y el ácido

carnósico. Además, se llevó a cabo el análisis de los patrones temporales de expresión de algunos genes clave en la absorción, síntesis, y degradación de colesterol, y de algunos genes efectores de la *Respuesta al Estrés Oxidativo* y la *Respuesta a Proteínas Desplegadas*, mediante la técnica RT-qPCR. Dada la estrecha relación entre la *Respuesta a Proteínas Desplegadas* y la *Respuesta al Estrés Oxidativo* con la generación intracelular de las especies reactivas del oxígeno, en esta parte del estudio también se analizaron los niveles de las especies reactivas del oxígeno mediante citometría de flujo. Los datos obtenidos demuestran que tanto el extracto de romero como el ácido carnósico, inducen la generación las especies reactivas del oxígeno tras 6 horas de tratamiento, siendo este efecto más evidente en el tratamiento con el extracto de romero.

Aunque un número importante de polifenoles inducen efectos antioxidantes *in vitro*, algunos trabajos han atribuido la actividad antiproliferativa de algunos compuestos fenólicos a su actividad prooxidante (Saeidnia y Abdollahi, 2013). Por otro lado, varios trabajos científicos han demostrado que en algunos casos la actividad antiproliferativa de algunos polifenoles de plantas (como por ejemplo el ácido gálico o el resveratrol) podría ser un resultado artefactual de los modelos *in vitro*, ya que cuando se autooxidan en el medio de cultivo generan niveles de especies del oxígeno reactivas que pueden llegar a ser tóxicos (Long y col., 2010; Forester y Lambert, 2011).

Con el objetivo de investigar este fenómeno en nuestros modelos *in vitro* con los polifenoles de romero, se llevó a cabo un estudio de la autooxidación *in vitro* del ácido carnósico, del carnosol y del extracto de romero, y su relación con la actividad antiproliferativa en las células de cáncer de colon HT-29 (sección 3.2.5). Los resultados de este trabajo están recogidos en "Foodomics study on the effects of extracellular production of hydrogen peroxide by rosemary polyphenols on the anti-proliferative activity of rosemary polyphenols against HT-29 cells" de A. Valdés y col., publicado en

Electrophoresis 2016, *00*, 1-10. En este estudio, se estudió la capacidad del ácido carnósico, el carnosol y el extracto de romero para generar peróxido de hidrógeno en el medio de cultivo. Además, se estudió la relación entre la producción de peróxido de hidrógeno en el medio extracelular y la generación intracelular de las especies reactivas del oxígeno, los niveles de glutatión intracelular, los cambios en el ciclo celular y en la expresión de determinados marcadores de estrés.

Con el objetivo de profundizar en los mecanismos de acción de los polifenoles de romero (extracto de romero, ácido carnósico y carnosol) en la línea celular HT-29, se decidió llevar a cabo una serie de estudios proteómicos que permitieran confirmar algunos de los resultados obtenidos en los estudios transcriptómicos y obtener información de otro nivel molecular. Los resultados de estos estudios están recogidos en la sección 3.2.6, "Comprehensive proteomic study of the antiproliferative activity of a polyphenol-enriched rosemary extract on colon cancer cells using nano-liquid chromatography-orbitrap MS/MS" (aceptado para su publicación en *Journal of Proteome Research*) y en la sección 3.2.7, "Nano-liquid chromatography-orbitrap MS-based quantitative proteomics reveals differences between the mechanisms of action of carnosic acid and carnosol in colon cancer cells" (enviado para su publicación en la revista *Molecular and Cellular Proteomics)*. Para el desarrollo de estos trabajos se optó por emplear una estrategia Proteómica de tipo "shotgun" basada en la cuantificación relativa de proteínas mediante el marcaje isotópico diferencial y su posterior análisis mediante nanocromatografía y espectrometría de masas de alta resolución (nano-LC-Orbitrap MS/MS). El diseño experimental consistió en el tratamiento de la línea HT-29 con distintas concentraciones citostáticas y citotóxicas del extracto enriquecido, ácido carnósico o carnosol durante 2, 6 y 24 horas.

La aproximación "shotgun" consistió en la extracción de las proteínas de las células y su digestión utilizando una mezcla de enzimas proteolíticas (tripsina/Lys-C) y su

posterior marcaje químico con DML previo al análisis cromatográfico. El procesado de los datos mediante la herramienta bioinformática MaxQuant permitió la identificación y cuantificación de las proteínas, y la herramienta bioinformática Perseus se utilizó para realizar un análisis estadístico con el que determinar las proteínas alteradas diferencialmente. Una vez determinadas las listas de proteínas alteradas significativamente se analizaron mediante la herramienta bioinformática IPA, con el objetivo de determinar los procesos biológicos más alterados tras el tratamiento con polifenoles de romero. Finalmente, para confirmar algunas de las hipótesis generadas a partir de los datos proteómicos, se analizó el efecto del extracto de romero en la formación de agresomas, y se evaluó el efecto inhibitorio *in vitro* del ácido carnósico y del carnosol sobre el proteasoma.

3.2.2 Effect of rosemary polyphenols on human colon cancer cells: transcriptomic profiling and functional enrichment analysis

Valdés, A., *García-Cañas, V., Rocamora-Reverte, L., Gómez-Martínez, A., Ferragut, J. A., Cifuentes, A. *Genes Nutr*. 2013, *8*, 43 - 60.

DOI: http://dx.doi.org/doi:10.1007/s12263-012-0311-9

Genes Nutr (2013) 8:43–60
DOI 10.1007/s12263-012-0311-9

RESEARCH PAPER

Effect of rosemary polyphenols on human colon cancer cells: transcriptomic profiling and functional enrichment analysis

Alberto Valdés · Virginia García-Cañas · Lourdes Rocamora-Reverte · Ángeles Gómez-Martínez · José Antonio Ferragut · Alejandro Cifuentes

Received: 17 January 2012 / Accepted: 2 August 2012 / Published online: 25 August 2012

Abstract In this work, the effect of rosemary extracts rich on polyphenols obtained using pressurized fluids was investigated on the gene expression of human SW480 and HT29 colon cancer cells. The application of transcriptomic profiling and functional enrichment analysis was done via two computational approaches, Ingenuity Pathway Analysis and Gene Set Enrichment Analysis. These two approaches were used for functional enrichment analysis as a previous step for a reliable interpretation of the data obtained from microarray analysis. Reverse transcription quantitative-PCR was used to confirm relative changes in mRNA levels of selected genes from microarrays. The selection of genes was based on their expression change, adjusted p value, and known biological function. According to genome-wide transcriptomics analysis, rosemary polyphenols altered the expression of ~4 % of the genes covered by the Affymetrix Human Gene 1.0ST chip in both colon cancer cells. However, only ~18 % of the differentially expressed genes were common to both cell lines, indicating markedly different expression profiles in response to the treatment. Differences in induction of G2/M arrest observed by rosemary polyphenols in the two colon adenocarcinoma cell lines suggest that the extract may be differentially effective against tumors with specific mutational pattern. From our results, it is also concluded that rosemary polyphenols induced a low degree of apoptosis indicating that other multiple signaling pathways may contribute to colon cancer cell death.

Keywords Colon cancer · Dietary polyphenols · Microarray · Nutrigenomics · Transcriptomics

Introduction

Dietary polyphenols are currently receiving considerable attention for their presumed role in the prevention of various degenerative diseases such as cancers and cardiovascular diseases (Araújo et al. 2011). The biological activities of rosemary (*Rosmarinus officinalis*) polyphenols have been investigated by several research groups (Herrero et al. 2010). Carnosol, one of the main polyphenols in rosemary, poses strong antioxidant and chemopreventive activities. This diterpene has demonstrated anti-inflammatory and anticancer activities on prostate, skin, breast, leukemia, and colon cancer (Johnson 2011). Another rosemary diterpene, carnosic acid, has proven antiproliferative activity in colon cancer cells (Visanji et al. 2006), anti-inflammatory properties in neurons (Satoh et al. 2008), and potential to promote differentiation of leukemia cells (Danilenko et al. 2001).

During the last years, owing to the extensive optimization and standardization, gene expression microarray has become a leading analytical technology in Nutrigenomics research and is expected to play also a crucial role in the

Special section: "Foodomics"; Guest Editors Dr. A. Bordoni and F. Capozzi.

Electronic supplementary material The online version of this article (doi:10.1007/s12263-012-0311-9) contains supplementary material, which is available to authorized users.

A. Valdés · V. García-Cañas (✉) · A. Cifuentes
Laboratory of Foodomics, CIAL (CSIC),
Nicolas Cabrera 9, 28049 Madrid, Spain
e-mail: virginia.garcia@csic.es

L. Rocamora-Reverte · Á. Gómez-Martínez · J. A. Ferragut
Institute of Molecular and Cellular Biology,
Miguel Hernandez University, Avda. Universidad s/n,
03202 Elche, Alicante, Spain

emerging Foodomics field (Herrero et al. 2012) for the investigation of the interactions between nutrients and other bioactive food compounds and genes (García-Cañas et al. 2010). High-density microarrays are widely used for comprehensive gene expression studies in part due to their great transcriptome coverage. After microarray data preprocessing, statistical test is usually carried out in order to detect significant changes in the expression of every gene between repeated measurements in two or more conditions (groups). This multiple testing procedure leads to an increased probability of observing false positives, which grows with the number of statistical tests performed. To alleviate the multiple testing problems, methods for correcting the significance level of individual tests should be applied.

The biological interpretation of microarray data is very challenging. In the conventional approach for analysis of microarray data, only the top few individual genes that are differentially expressed between two conditions (groups) are reviewed. Although such individual genes may demonstrate to be relevant in a given biological context, it is increasingly questioned whether large fold changes in individual genes will have more biological relevance than smaller but coordinated fold changes in a set of genes encoding proteins involved in a particular pathway. Over the last years, the use of biological knowledge accumulated in public databases by means of bioinformatics allows to systematically analyze large gene lists in an attempt to assemble a summary of the most enriched and significant biological aspects (Waagmeester et al. 2008). The principle behind enrichment analysis is that if a certain biological process is occurring in a given study, the co-functioning genes involved should have a higher (enriched) potential to be selected as a relevant group by high-throughput screening technologies. This approach increases the probability for researchers to identify the correct biological processes most pertinent to the biological mechanism under study (Huang et al. 2009). Thus, a variety of high-throughput enrichment tools (e.g., DAVID, IPA, MetaCore, Onto-Express, FatiGO, GOminer, EASE, ProfCom, etc.) have been developed in the last years to assist microarray end user to understand the biological mechanisms behind the large set of regulated genes. Many of these bioinformatics resources systematically map the list of interesting (differentially expressed) genes to the associated biological annotation terms of the Gene Ontology (GO) database (www.geneontology.org) and then statistically examine the enrichment of gene members for each of the terms by comparing them to a reference gene set (whole genome or genes included in the chip). This allows identification of the main biological processes associated with the list of differentially expressed genes (DEGs) obtained from microarray analysis. It is obvious that the application of different cutoff thresholds or criteria for the identification of DEGs will alter the gene profile of the resulting list, which in turn, might affect the results obtained from further enrichment analysis. On the other hand, gene set enrichment analysis (GSEA) approach performs enrichment analysis considering all genomic information available from a microarray analysis rather than focusing on individual genes passing a certain significance threshold.

The aim of this work was to conduct genome-wide transcriptomics analysis to investigate the effect of rosemary extracts enriched in polyphenols in two colon cancer cell lines. Two computational approaches, Ingenuity Pathway Analysis (IPA) and GSEA, were used for functional enrichment analysis as a previous step for a reliable data interpretation obtained from microarray analysis.

Materials and methods

Preparation of rosemary extracts

Five rosemary extracts marked as rom1 to rom5 were obtained from dried rosemary leaves using either supercritical fluid extraction (SFE) or pressurized liquid extraction (PLE) as reported by Herrero et al. (2010). The extracts obtained by PLE with a 100 bar pressure for 20 min under the following conditions of solvent and temperature were as follows: rom1, using water at 100 °C; rom2, using ethanol at 150 °C; and rom3, using water at 200 °C. On the other side, the extracts obtained by SFE at 40 °C for 30 min were as follows: rom4, using supercritical CO_2 and 7 % ethanol at 150 bar; rom5, using supercritical CO_2 at 400 bar. Previous chemical characterization studies provided information on the major phenolic constituents in each extract (Herrero et al. 2010). A major phenolic compound in rom1, rom2, and rom3 extracts was rosmarinic acid with concentrations of 14.19, 16.78, and 8.59 μg/mg extract. Rom4 and rom5 were reported to contain high concentrations of carnosol (226.39 and 224.65 μg/mg extract, respectively) and carnosic acid (151.55 and 106.46 μg/mg extract, respectively), being rosmarinic acid undetected. Carnosol and carnosic acid were also present in rom2 extract at concentrations of 104.26 and 66.23 μg/mg extract, respectively. Rom1 and rom3 contained similar concentration of carnosol (~45 μg/mg extract), and carnosic acid was present at concentrations of 0.01, 66.23, and 5.78 μg/mg in rom1, rom2, and rom3, respectively. The extracts have also been reported to show antioxidant activity (EC_{50}) ranging from 5.3 to 10.5 μg/mL (Herrero et al. 2010). Extracts were diluted at the indicated concentrations using ethanol and their content in polyphenols determined as gallic acid equivalents (GAE), expressed as mg gallic acid/g extract.

Total concentrations of polyphenols (given as μM) in the extracts were then calculated using the molecular weight of gallic acid as average value.

Cells and cell culture

Colon adenocarcinoma HT29 and SW480 cells obtained from IMIM (Institut Municipal d'Investigació Médica, Barcelona, Spain) and ATCC (American Type Culture Collection, LGC Promochem, UK), respectively, were grown in DMEM supplemented with 5 % heat-inactivated fetal calf serum, 2 mM L-glutamine, 50 U/mL penicillin G, and 50 μg/mL streptomycin, at 37 °C in humidified atmosphere and 5 % CO_2. Cells were plated at a density of 10,000 cells/cm^2 in 60-mm-diameter culture plates and permitted to adhere overnight at 37 °C. When cells reach 80 % confluence, they were trypsinized (1 mL/25 cm^2), neutralized with culture medium at 1:5 ratio (trypsin/medium) and pelleted for further analysis.

Antiproliferative activity assays

To study the effect of rosemary extracts on the proliferation of HT29 and SW480 lines, cells were seeded onto 60-mm-diameter culture plates at 10,000 cells/cm^2, permitted to adhere overnight at 37 °C, and exposed to different rosemary extracts containing 0–10 μM total polyphenols for 0–72 h depending on the experiment. After incubation with the rosemary extracts for the indicated time in each case, cell proliferation was estimated by the MTT assay as follows: the MTT reagent was added and incubated for 3 h at 37 °C in humidified 5 % CO_2/air atmosphere. After the incubation, the media were aspirated and 200 μL of DMSO was added to each well to dissolve the formazan product by shaking for 30 min. Then, the absorbance at 570 nm was measured in a microplate reader (Anthos 2001 Labtec Instruments GmbH, Wals, Austria).

Cell cycle study

Cell cycle analysis was carried out essentially as previously described (Carrasco-García et al. 2011). Briefly, for cell cycle distribution of DNA content, control and cells treated with the different phenolics were trypsinized, washed with PBS, and fixed with 75 % cold ethanol at −20 °C for at least 1 h. Then, cells were incubated with 0.5 Triton X-100 and 25 μg/mL RNase A in PBS, stained with 25 ng/mL propidium iodide, incubated for 30 min in the dark, and analyzed using an Epics XL flow cytometer equipped with a 0.75 W argon laser set at 488 nm (Beckman Coulter Co., Miami, FL). From the cellular distribution pattern of DNA, the apoptosis induced by treatment of the cells with the phenolic extracts was measured by determining the amount of apoptotic cells in the sub-G1 peak by flow cytometry. Flow cytometry data analysis was made upon gating the cells to eliminate dead cells and debris. A total of 105 cells were measured during each sample analysis.

Microarray analysis

Triplicate samples for each colon cancer cell type, treatment condition, and their respective controls were collected for gene expression microarray analyses. Total RNA was isolated from cells using RNeasy Mini Kit (Qiagen, Spain) according to manufacturer protocol. The quality of the isolated RNA was determined with a NanoDrop ND1000 (Thermo, Spain) and a Bioanalyzer 2100 (Agilent, Spain). Only those samples with A260/A280 ratio between 1.8 and 2.1 and a 28S/18S ratio within 1.5–2 were further processed. Each triplicate RNA sample was prepared and hybridized onto a separate microarray (Servicio de Genómica, Parque Científico de Madrid, Spain). A starting amount of 200 ng of total RNA was used for double-stranded cDNA synthesis and generation of biotin-labeled cRNA, following the manufacturer protocol (Affymetrix, UK) prior to hybridization onto Human Gene 1.0ST chips (Affymetrix). Generated CEL files were subjected to quality assessment using Expression Console™ (Affymetrix). In this process, summary statistics was computed for each array and then compared across the arrays. Then, CEL files were processed using the Robust Multi-Array (RMA) normalization in the BioConductor package affy for R (Gentleman et al. 2004). Significance analysis was performed using the BioConductor package limma (Linear Models for Microarray Data; Smyth 2005). Limma provides a number of summary statistics useful to select DEGs. Moderated *t* statistics was used for significance analysis of each probe set and each contrast. Then, Benjamini and Hochberg's (1995) method was applied for multiple testing correction. This procedure allows the control or estimation of the false discovery rate (FDR) in a particular data set. To identify the statistically most significant changes in gene expression, microarray data were subjected to gene filtering based on a combination of *M* value cutoff, which represents a $\log_2$-fold change between the two experimental conditions (treatment with polyphenols vs. control), and the statistical significance (FDR applied on moderated *t* statistics). In this study, DEGs were identified based on 0.7 as *M* value cutoff that corresponds to expression ratios (fold change) $\geq$1.6 for up-regulated and $\leq$0.6 for down-regulated genes; and the statistical filter was established at 5 % FDR (adjusted *p* value <0.05).

Reverse transcription quantitative-PCR (RT-qPCR) validation of gene expression

RT-qPCR was used to confirm relative changes in mRNA levels of selected genes from microarray data sets. The selection of genes was based on their degree of expression change, adjusted p value, and/or known biological function. Starting amounts of 0.5 μg of total RNA isolated from cells were reverse transcribed in a volume of 20 μL using Transcriptor First Strand cDNA Synthesis kit with oligo(dT) primers (Roche Diagnostics, Barcelona, Spain). Each real-time quantitative PCR was performed on 0.5 μL aliquots of diluted (1:10) cDNA solutions using LightCycler® 480 Real-Time PCR (Roche Diagnostics) and LightCycler® 480 Probes Master kit. Human Universal Probe Library probes and target-specific PCR primers were selected using the Probe Finder assay design software (Roche Diagnostics, http://www.roche-applied-science.com/sis/rtpcr/upl/index.jsp). Primers were designed to span exon–exon junctions and to have melting temperature values close to 60 °C. The designed primers were then checked with Oligo Analyzer 3.1 software (Integrated DNA Technologies, http://eu.idtdna.com/analyzer/Applications/OligoAnalyzer) to predict possible secondary structures, heterodimers and homodimers, and to redesign the primers if needed. The primers were purchased from Fisher Scientific (Alcobendas, Spain). Supplementary Table S1 summarizes the primers and probes used in this study. Two technical replicates were performed for each sample in a 96-well format plate. On each plate, four endogenous control genes (*GAPDH*, *B2M*, *IPO8*, and *PPIA*) and no-template-controls (NTC) were also performed in duplicate. Cycle-threshold (Ct) values were calculated using second derivative maximum method, and the amplification efficiency (E) of each system was calculated by the following formula: $E = 10^{-1}/\text{slope}$. All primers utilized displayed PCR efficiencies higher than 90 %. Using the Relative Expression Software Tool (REST, Pfaffl et al. 2002), the relative expression of selected genes, calculated using efficiency correction option, in treated cells was compared to that of control cells. The randomization test method, as a part of the REST software, was used to assess statistical significance of up- or down-regulation of target genes after normalization to the four reference genes. Spearman's rho test was used to perform correlation analysis between the microarray and qPCR results for the selected gene set.

Functional enrichment and pathway analysis

In this work, two computational tools were used for functional enrichment analysis as a previous step for a reliable data interpretation obtained from microarray analysis. The bioinformatics tool Ingenuity Pathway Analysis (IPA, Ingenuity Systems, USA) was used in order to interpret the gene expression data in the context of biological processes and pathways. To this aim, the *Core Analysis* function included in IPA was applied to analyze the lists of DEGs identified in microarray analysis. Up- and down-regulated identifiers were defined as value parameters for the analysis. Based on the list of identifiers, IPA performs functional enrichment analysis in order to identify the biological processes and functions over-represented in a given list of genes. Significance of the molecular and cellular functions, as well as the signaling pathways was tested by the Fisher's exact test p value.

As an alternative approach to identify biological processes and functions that are modulated upon exposure to rosemary polyphenols, exploratory functional analysis was also performed with Gene Set Enrichment Analysis (GSEA, Subramanian et al. 2005). In order to implement the GSEA algorithm, RMA-normalized microarray data were uploaded into GSEA v2.0 software (http://www.broadinstitute.org/gsea/index.jsp). Then, for the analysis of each cell line, the GSEA algorithm ranked all microarray genes according to their expression under each experimental condition (treated and untreated). The resulting ranked score values are therefore a function of the correlation between a gene signal intensity, the experimental conditions in question, that is, treatment or control and all other genes in the data set. This enrichment strategy uses a priori defined gene sets to determine whether the members of a given gene set are randomly distributed throughout the ranking, or to the contrary, are primarily found at the top (induced gene expression) or bottom (repressed gene expression) of the rank list of genes. To do this, enrichment scores (ES) are calculated in order to determine the extent to which individual genes from a gene set are represented at the extremes of the ranked gene list. A null distribution of ES is subsequently generated by permutation filtering to evaluate the statistical significance of the observed ES values. After this procedure has been repeated for each gene set, the ES are normalized (NES) to account for differences in gene set size. Then, the false discovery rate (FDR %) is calculated relative to the NES values to determine the false-positive rate. In this work, significant p values and FDR were defined as <0.05 and 25 %, respectively. GSEA analyses were conducted to compare treated versus control cells, for both colon cancer cell lines, SW480 and HT29, using the C5.BP catalog of gene sets from Molecular Signatures Database v3.0 (MSigDB, http://www.broadinstitute.org/gsea/msigdb/index.jsp) containing 850 gene sets consisting of genes annotated by the Gene Ontology (http://www.geneontology.org) biological process terms. Based on the aforementioned cutoff values, leading-edge analyses were

performed on the list of over-represented gene sets (GO terms) to identify leading-edge subsets of genes, defined as the core of a gene set that accounts for the enrichment signal.

Results

Colorectal cancer is known to be strongly linked to dietary factors. Two colon carcinoma cell lines were selected in this study to investigate the effects of rosemary polyphenols on cell viability, cell cycle, and gene expression. SW480 and HT29 cell lines were chosen because they represent different genetic abnormalities of human colon cancer. Both lines contain truncated or mutant adenomatous polyposis coli (*APC*) gene, but differ in mutated *P53* and *RAS* gene, namely, HT29 cells have a mutated *P53* gene (Arg to His-273) but a wild-type *RAS* gene, whereas SW480 cells contain mutated *P53* (Arg to His-273 and Pro to Ser-309) and mutated *RAS* (Val to Glu-12) genes.

Effects of rosemary extracts on cell proliferation

To determine the effective concentration range, dose effect of rosemary polyphenols on cell proliferation in HT29 and SW480 cell lines was evaluated after exposure of the cells to different concentrations of each extract by MTT assay. Rosemary extracts concentrations of 0.1 and 1 μM of polyphenols did not exert significant effect on colon cancer cell proliferation after 72-h incubation with any of the tested extracts (data not shown). Incubation with higher concentrations (10 μM polyphenols) reduced cell proliferation in HT29 and SW480 cells after treatment for 48 h with rom2, rom4, and rom5 rosemary extracts, while rom1 and rom3 extracts did not exert appreciable effect. In general, SW480 cell line was notably more sensitive to the antiproliferative effect of rosemary extracts, especially to rom4 and rom5 extracts, which reduced cell viability to 0 and 18.47 %, respectively, after incubation for 48 h. Therefore, 10 μM total polyphenols solutions from rosemary extracts rom2, rom4, and rom5 were selected for the subsequent experiments.

Cell cycle analysis

To determine whether the antiproliferative effect of rosemary extracts on SW480 and HT29 cells was accompanied by cytotoxicity, distribution of cellular DNA of the cells upon incubation with the extracts and further staining with propidium iodide was analyzed by flow cytometry (FCM). Because HT29 cells were more refractory than SW480 cells to the antiproliferative activity of rosemary extracts, distribution of cellular DNA in the former was done at larger incubation times (72 h) than in the case of SW480 cells (24 and 48 h). Cell cycle analysis showed that rom2, rom4, and rom5 tend to induce a modest apoptotic effect indicated by the small sub-G1 cell population with respect to control cells (data not shown). G2/M arrest was concomitant to a decrease on G1 in SW480 cells treated with rom4 and rom5 extracts, as well as in HT29 incubated with rom4. This effect was especially apparent in the case of SW480 cells incubated with rom4 for 48 h, indicating that the G2/M arrest was sustained in time. Therefore, rom4 extract was selected and its antiproliferative effect against colon cancer cells investigated via transcriptomic analysis.

Microarray analysis and validation of selected targets by RT-qPCR

Gene expression microarray analyses were carried out in order to investigate at transcriptomic level the effect of rom4 extract on both colon cancer cell lines. For this analysis, total RNA was isolated from triplicate cultures of cells incubated with rom4 extract for 24 h (SW480 cells) and 72 h (HT29 cells), together with their respective untreated controls. After microarray data preprocessing, empirical Bayes linear models for statistical analysis (Limma) were implemented in the microarray analysis pipeline to identify DEGs in response to the treatment. Predefined M value ($M = 0.7$) and FDR of 5 % (adjusted p value <0.05) were applied to identify DEGs in response to the treatment with rom4 extract. According to these criteria, within the full list of 28,132 genes represented in the microarray, 1,250 and 1,308 genes were found in SW480 and HT29, respectively, to be differentially expressed in response to the treatment with rom4 extract (Supplementary material, Table S2 and S3). Among these DEGs, the expression of 234 genes ($\sim$18 % of DEGs) was commonly altered in both cell lines, while the expression of 23 genes ($\sim$2 % of DEGs) was altered in both cell lines but with opposite direction of change (up-regulated vs. down-regulated).

Among the lists of DEGs, we selected for RT-qPCR validation a set of genes induced in both lines with remarkable significance levels and expression ratios. Based on this criterion, *HMOX1*, *OSGIN1*, *DUSP1,* and *ARRDC3* genes were selected for validation. We included an additional gene, *MUC1*, that showed different expression pattern in both cell lines and whose expression is associated with poor prognosis in colon cancer (Finn et al. 2011). In this study, *GAPDH* gene and other three reference genes (*IPO8*, *PPIA,* and *B2M*), that have been reported to provide good normalization of RT-qPCR data in colon cancer studies (Sorby et al. 2010), were used for data normalization of selected genes. As shown in Table 1, changes in the expression ratio of all selected genes, except *MUC1* in

Table 1 Comparison of gene expression ratios in response to rom4 treatment as determined by microarray analysis and RT-qPCR in colon cancer cell lines SW480 and HT29

Gene symbol	SW480				HT29			
	Microarray		qPCR		Microarray		qPCR	
	FC[a]	*p* value[b]	FC[a]	*p* value[c]	FC[a]	*p* value[b]	FC[a]	*p* value[c]
HMOX1	24.6	0.0000001	141.6	0.030	3.0	0.0003202	4.0	<0.001
OSGIN1	3.6	0.0003437	13.3	0.035	3.1	0.0014385	5.6	<0.001
DUSP1	11.4	0.0000004	39.5	0.035	2.5	0.0006308	3.0	<0.001
ARRDC3	7.7	0.0000013	15.2	<0.001	5.0	0.0000195	4.6	<0.001
MUC1	1.0	0.7230161	0.7	0.624	0.4	0.0035951	0.3	<0.001

[a] Fold change (expression ratio)

[b] Adjusted *p* value (FDR)

[c] Statistical significance calculated by REST

SW480, were provided by REST with high statistical significance (p value <0.05). The change in the gene expression of *MUC1* was not statistically significant in the microarray analysis of SW480. Therefore, gene expression ratios obtained with RT-qPCR confirm the results obtained by microarray. Significant correlation of 0.964 was observed between data sets obtained by both technologies (Spearman's rho, $p < 0.0000007$).

Functional enrichment analysis and pathway analysis using IPA

In order to identify the biological processes that might be altered in response to rosemary polyphenols, functional enrichment analysis was performed on microarray data sets using different bioinformatics approaches. Enrichment analysis using IPA software was first performed. Lists of identified DEGs obtained from microarray analyses were imported into IPA software. In these analyses, 1,103 and 1,045 genes from SW480 and HT29 microarray data, respectively, were eligible for biological function and pathway analysis. Functional analysis identified significant (Fisher's exact test p value <0.05) over-represented molecular and cellular functions in the imported data sets that were associated to *cell death*, *cellular development*, *cellular growth and proliferation*, and *cell cycle*. Further enrichment analysis on defined (canonical) pathways of IPA Knowledge Base provided significant over-represented pathways across the entire lists of DEGs (Fig. 1). Retinoid X receptor α (*RXRα*) function was identified in three closely related canonical pathways, namely, *LPS/IL-1-mediated inhibition of RXR function*, *xenobiotic metabolism signaling*, and *PXR/RXR activation* in the analysis of treated HT29 cells, and also, in *VDR/RXR activation* pathway identified in the analysis of treated SW480 cells. IPA revealed altered expression of a remarkable number of genes associated to xenobiotic metabolism function as one of the main effects derived from the treatment of HT29 with rom4 extract. In this cell type, examination of *LPS/IL-1-mediated inhibition of RXR function* signaling pathway evidenced strong transcriptional down-regulation of a number of genes targeted by several nuclear receptors, including, *RXRα*, pregnane X receptor (*PXR*), constitutive androstane receptor (*CAR*), and peroxisome proliferator–activated receptor (*PPAR*) (see Fig. 2). Genes encoding phase I metabolizing enzymes, namely, *FMO*, *SOD3*, *CYP3A7*, *CYP2B6*, *CAT,* and several members of *ALDH* gene family, were down-regulated in treated HT29 cells. Also, mRNA levels of the phase II metabolizing enzymes *PAPSS2* and *SULT*, and lipid metabolism–related genes such as cytosolic and mitochondrial *HMGCS* genes were decreased suggesting modulation of xenobiotic and lipid metabolism. On the other side, induction of phase III transporters, *MRP2* and *ABCB9*, was observed. In this canonical signaling pathway, over-expression of two members of IL-1 receptor (*IL1RAP* and *IL1RAPL1*) was coincident with induction of pro-inflammatory cytokine *IL-1β* and *TGFB2*. Coincident with this, IL-1 receptor antagonist (*IL1RN*) was notably over-expressed, whereas TNF receptor (*TNFRSF11B*) and *TLR4* mRNA levels were decreased. In treated SW480 cells, some differences were found in the expression pattern of genes involved in this pathway, namely, the expression of cytokine *IL-1α* was induced, while the mRNA level of *TGFB2* was remarkably decreased. Also, no significant expression changes were detected in the mRNA levels of genes involved in cytochrome P450-mediated phase I metabolism of xenobiotics in this cell line (data not shown). On the other hand, similar to the results obtained in treated HT29 cells, expression of phase III transporters (MRP2 and MDR1) was induced, and it was coincident with down-regulation of gene expression associated with fatty acid and lipid metabolism (*FABP*, *FATP,* and *ACS*). Further examination of *Xenobiotic metabolism* signaling pathway obtained from enrichment

analysis of HT29 transcriptomics data allowed identification of aryl hydrocarbon receptor (*AHR*)-mediated transcriptional induction of phase I metabolizing genes, *CYP1A1* and *CYP1B1*.

In addition to the aforementioned *AHR*/*RXR*/*CAR*/*PXR*-regulated phase I and II enzymes, xenobiotic metabolism signaling may also be regulated by nuclear factor (erythroid-derived 2)-like 2 (*NRF2*). The analysis of *Xenobiotic metabolism* signaling pathway indicated over-expression of phase II detoxifying and antioxidant genes, *GCLC* and *HMOX1* and down-regulation of *UGT* in treated HT29 cells (data not shown). Interestingly, analysis of SW480 suggested that rosemary extract also exerted enhanced antioxidant and xenobiotic detoxifying effects in this cell type through the modulation of *NRF2* function, as it is observed in the enriched canonical pathway *NRF2-mediated oxidative stress response* identified with IPA (Fig. 3). Examination of the downstream target genes of *NRF2* suggested transcriptional *NRF2*-mediated induction of several phase II detoxifying and antioxidant genes, including *HMOX1* (heme oxygenase-1), *TXNRD1* (cytoplasmic thioredoxin reductase-1), and *GCLM* (glutamate-cysteine ligase, modifier subunit) in both colon cancer cell lines. The expression of the antioxidant and tumor suppressor gene *OSGIN1* was also induced in both cell lines. Although IPA did not include this gene in *NRF2*-mediated response to oxidative stress, the expression of *OSGIN1* is known to be regulated via *NRF2* pathway and to follow similar expression pattern to that of *HMOX1* and *GCLM* in response to oxidative signals. In addition to these genes, *FTH1* (ferritin heavy chain) and *SOD2* (mitochondrial superoxide dismutase) genes were induced in SW480,

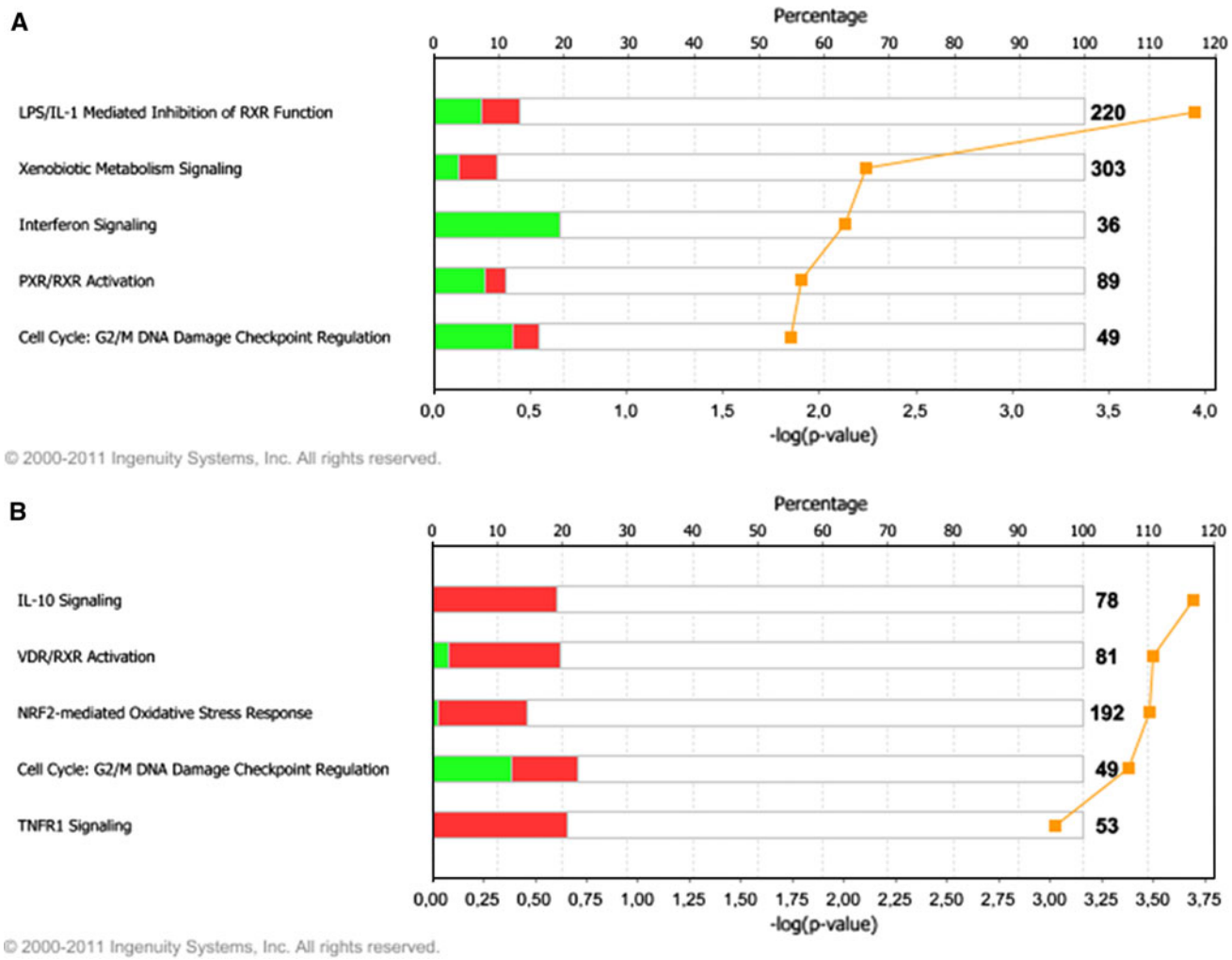

Fig. 1 Canonical pathways significantly modulated by rosemary polyphenols. SW480 (**a**) and HT29 (**b**) colon cancer cells treated for 24 and 72 h, respectively, with rom4 extract. Fisher's exact test was used to calculate a *p* value determining the probability that the association between the genes in the data set and the canonical pathway is explained by chance. Stacked histogram displays % of up- and down-regulated genes in a given pathway. *Light* (*green*) *bars* represent the fraction of down-regulated genes. *Dark* (*red*) *bars* represent the fraction of up-regulated genes. Values at the *right* side indicate the number of genes involved in a particular pathway (color figure online)

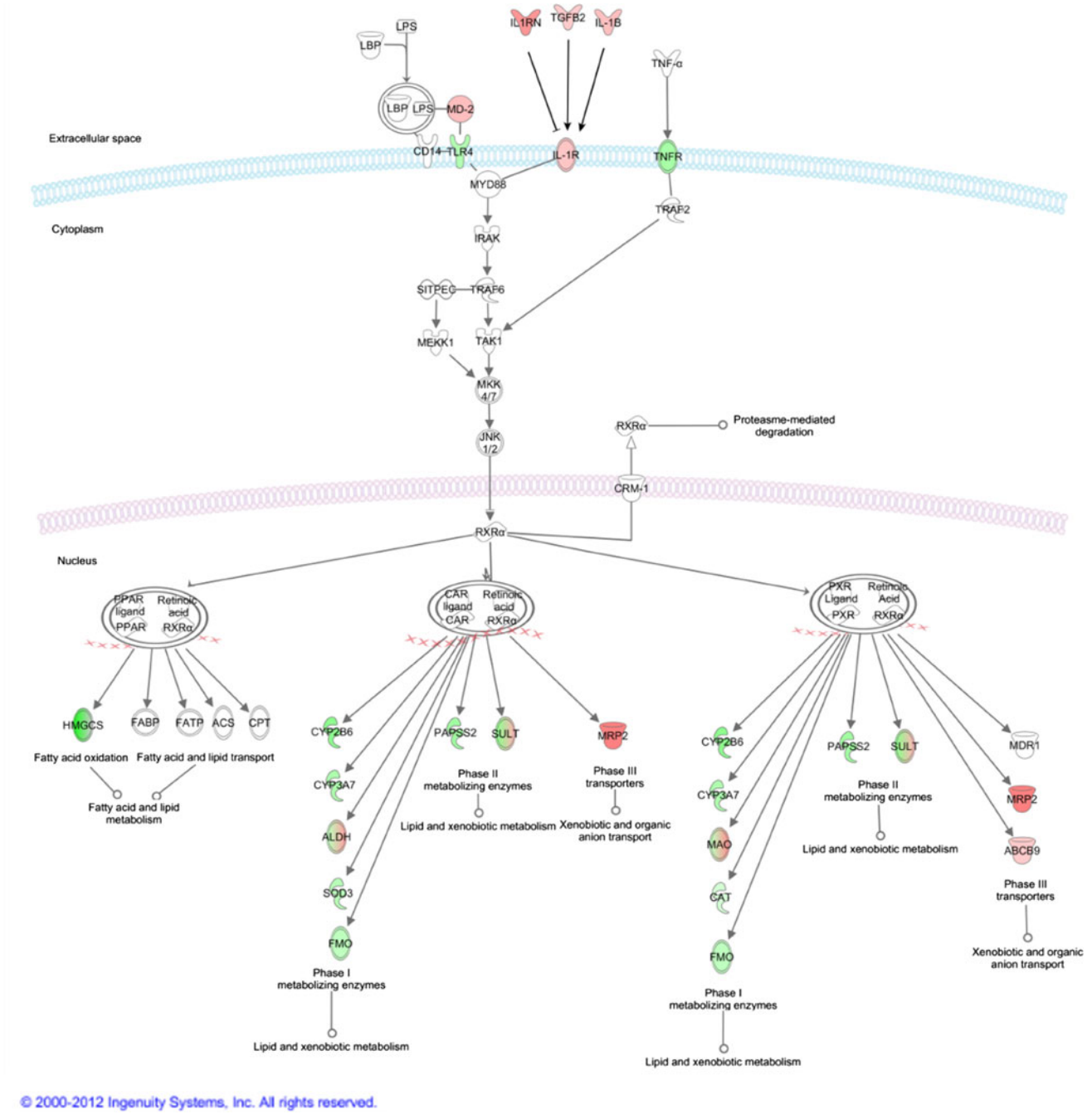

Fig. 2 Canonical pathway representing LPS/IL-1-mediated inhibition of RXR function obtained by IPA from the analysis of HT29 data set. Up- and down-regulated genes are in *red* and *green,* respectively (color figure online)

whereas *GCLC* (glutamate–cysteine ligase, catalytic subunit) and *EPHX1* (epoxide hydrolase 1) genes were up-regulated in HT29. Also, associated with this pathway, the transcript levels of the phase III transporter *ABCC2* were increased in both cell types upon treatment. Observation of transcript levels of upstream signaling molecules of *NRF2* function in SW480 analysis indicated strong induction of genes encoding for protein members of adaptor protein-1 (AP-1), precisely, *C-FOS*, *C-JUN,* and *JUNB*, as well as moderate induction of genes encoding mitogen-activated protein kinases (*MEK1/2*), protein kinase C (*PKC*), and eukaryotic translation initiation factor 2-alpha kinase 3 (*EIF2AK3*), also known as *PERK*. This transmembrane protein kinase has been defined as the central regulator of translational control during unfolded protein response and also represents a linking node between *NRF2* function and endoplasmic reticulum (ER) stress. To expand on our observations in this aspect, we sought to identify up and

downstream molecules mediating ER stress signaling in the transcriptomics data sets using IPA software. As can be observed in Fig. 4, mRNA levels of transcription factors with a known role in ER stress, *XBP1* and *ATF4*, remained unaltered. However, significant induction on the expression of their respective regulated genes was observed. These include the expression of *PPP1R15A* (GADD34) and other ER chaperones (*DNAJB9* and *DNAJB2*). It is worth noting that DNA-damage inducible transcript gene (*DDIT3*) gene expression was notably high in both cell types. Interestingly, the expression of *TRIB3* gene, a stress inducible gene by *DDIT3* and *ATF4*, that recently has been associated with ER stress–dependent apoptosis, was also over-expressed in treated cells. Consistent with the transcriptional activity of *DDIT3*-encoded protein (CHOP, GADD153), its over-expression in SW480 cells was associated with a concomitant increase in the mRNA levels of its inducible pro-apoptotic target genes, *BAK1 (BAK)* and *BCL2L11 (BIM)*. ER resident caspase 4 (*CASP4*) as well as downstream caspase genes, *CASP3*, *CASP7* and *CASP9*, were moderately over-expressed in treated SW480. Other strongly up-regulated genes associated to ER stress transcriptional activation were *DDIT4* gene, an inhibitor of the mTOR survival pathway, and growth differentiation factor 15 (GDF15), whose up-regulation is associated with growth arrest in colon cancer cells. In HT29, the levels of death receptor 5 gene (DR5, *TNFRSF10B*) mRNA were up-regulated by treatment with rosemary extract (data not shown).

According to IPA results, *Cell cycle: G2/M DNA damage checkpoint regulation* pathway was found significant in both cell lines. However, examination of genes regulating this pathway indicated different transcriptomic profiles between cell lines. Despite rosemary extract was able to up-regulate the expression of the *CDKN1A* (p21) and *14-3-3σ* (stratifin) gene and down-regulate *CCNB2* (cyclin B) and *TOPO2* genes in these cells, the expression of other important regulatory genes of G2/M DNA damage checkpoint, such as *CHK1* and *CDC25C,* was selectively down-regulated in HT29. On the other hand, the induction of *GADD45A, GADD45B,* and *GADD45G* was detected in SW480, whereas the mRNA levels of *PRKDC*, *ATM* and *WEE1* genes were decreased in the same line. In SW480 analysis, *Vitamin D receptor (VDR)/RXR activation* signaling pathway was also significant. Examination of this pathway revealed transcriptional activation of *VDR/RXR* heterodimer. Accordingly, the expression of several genes including *KLK6*, *CDKN1A* (p21), *MAD*, *GADD45A*, *OPN*, *CALB1*, *CD14,* and *KLF4* was induced.

Complementary to IPA, GSEA was used to identify groups of genes that shared common biological functions in our microarray data sets. For each group of gene sets (GO annotations), GSEA calculated an ES and evaluated statistical significance in the ES. The normalized enrichment score reflected the degree to which a gene set is over-represented in a given data set. GSEA analysis identified 23 down-regulated gene sets that were significant at 25 % FDR in treated HT29 cells with rom4 extract (Table 2), whereas only 8 down-regulated gene sets fulfill the criteria for significant enrichment in the analysis of treated SW480 cells with the same extract. Among the highest scored functional annotations, a number of down-regulated gene sets common to both cell lines were identified. Most of the gene sets shared by both lines were represented with genes involved in different stages of mitosis, including chromosome segregation and cytokinesis. An example of gene enrichment analysis is shown in Fig. 5a for *Sister chromatid segregation* gene set. The heatmap representation of this subset of genes (Fig. 5b) revealed that most of the genes in this GO term were down-regulated after treatment with the rosemary extract. Leading-edge analysis was subsequently applied in order to identify those gene subsets that account for the enrichment signal in each GO term. Table 3 summarizes the statistically significant enriched gene sets grouped on the basis of the leading-edge gene subsets that they share. Leading-edge subset groupings revealed that 4 and 3 GO terms, related with chromosome segregation, shared 10 and 8 genes in HT29 and SW480, respectively. Also, leading-edge analysis showed that a subset of 8 and 9 down-regulated genes was common to cytokinesis annotations in HT29 and SW480, respectively. On the other hand, two wider subsets consisting of 22 down-regulated genes were part of several GO annotations related with M phase of mitotic cell cycle in the treated HT29 and SW480 transcriptomes, respectively. With regard to other down-regulated functions in HT29, leading-edge analysis revealed other categories related to *DNA repair* and *RNA processing*. Within the leading-edge subsets, we focused on those genes exhibiting enough statistical significance (adjusted p value <0.05) obtained from microarray analyses (bold names in Table 3). Examination of significant genes revealed several common features in the transcriptional response of both cell lines to rom4 treatment. More precisely, important G2/M transition genes such as polo-like kinase 1 (*PLK1*) and its activator aurora A (*AURKA*) were identified as down-regulated in both cell lines. Accompanied with down-regulation of G2/M transition and mitotic entry genes, down-regulation of important genes encoding proteins involved in mitotic checkpoint signaling, such as *BUB1,* was detected in both lines. This down-regulation of mitotic checkpoint function was more prominent in treated HT29 cells, showing decreased transcript levels of other important genes for spindle checkpoint control, namely, *MAD2L1*, *ZWINT,* and *NDC80* (*HEC1*). In both cell lines, genes *ESPL1* (separase) and *CENPE*, associated with sister chromatid separation and chromosome segregation, were

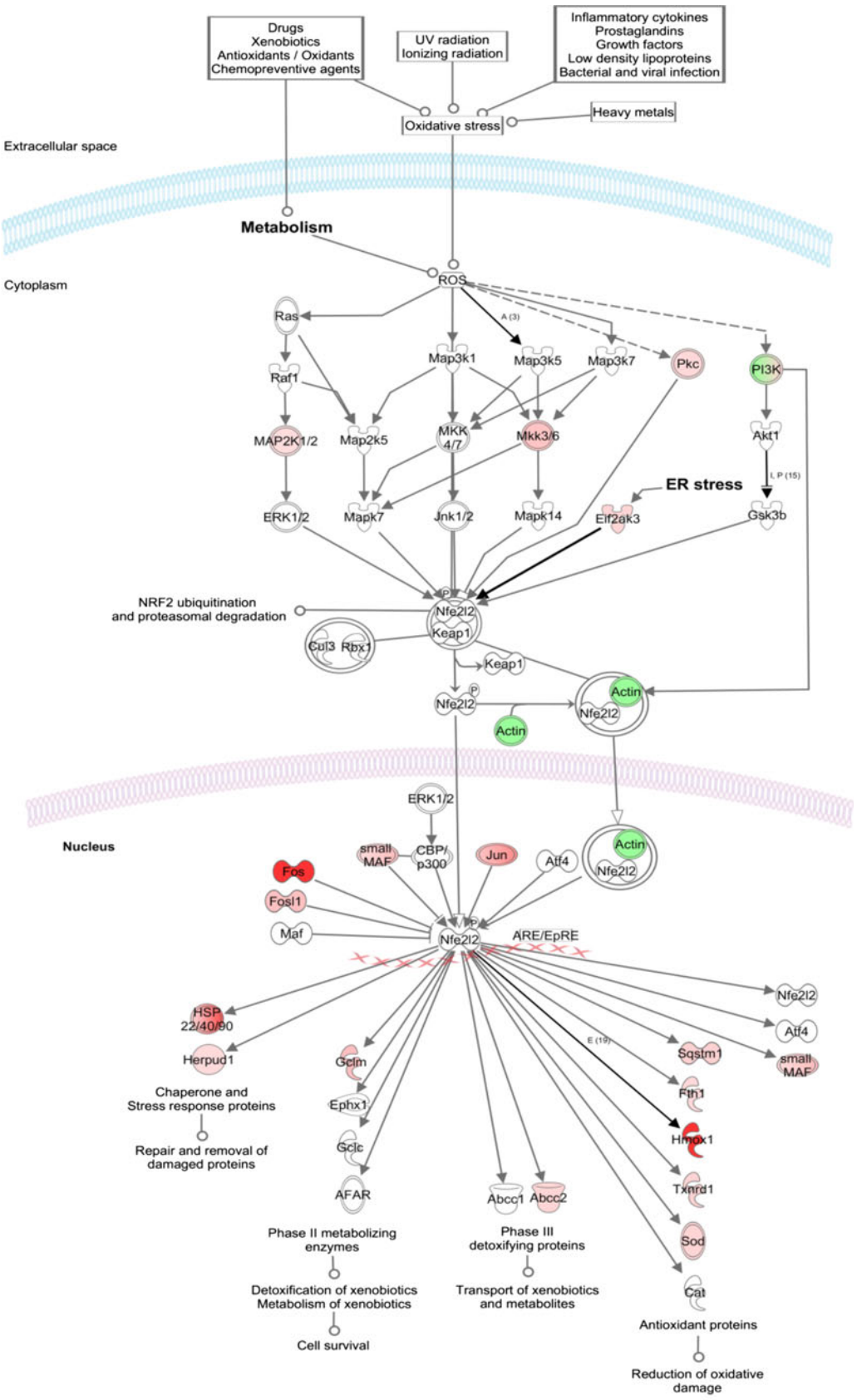

◄ **Fig. 3** Canonical pathway representing NRF2-mediated oxidative stress response obtained by IPA from the analysis of SW480 data set. Up- and down-regulated genes are in *red* and *green,* respectively (color figure online)

down-regulated. The expression of cytokinesis genes, *PCR1* and *RACGAP1,* was also decreased in both treated cell lines.

Discussion

Rosemary constituents have demonstrated different in vitro cytotoxicity effects depending on the cell type, concentration, and time of exposition. For instance, studies with carnosic acid showed that concentrations of 6.25 μg/mL reduced between 13 and 30 % the viability of different types of tumor cells (Yesil-Celiktas et al. 2010). Similar effects have been reported for carnosic acid on viability of five human cancer cell lines (Gigante et al. 2003). To the opposite, concentrations of rosmarinic acid ranging from 6.25 to 50 μg/mL (139 μM) showed proliferative effects rather than cytotoxic activity (Yesil-Celiktas et al. 2010). Carnosol exhibited growth inhibition 50 % (GI_{50}) values ranging from 3.6 to 26 μM in five tumor cells (Guerrero et al. 2006). Also, Visanji et al. (2006) reported IC50 values of 23 μM of carnosol for Caco-2 cells, a value close to the observed (34 μM) in prostate cancer cells after 72 h of treatment (Johnson 2011). In our study, rosemary extracts showed different antiproliferative activity on colon cancer cells. More precisely, carnosol-enriched extracts, rom4 and rom5, showed the strongest effect on the proliferation of both cell lines.

In general, rosmarinic acid–enriched extracts (rom1-3) exerted lower antiproliferative activity. Among these extracts, the highest antiproliferative effect was observed in rom2, the extract containing high concentration of carnosol (104.26 μg/mg) and carnosic acid (66.23 μg/mg). On the other hand, rom1, the extract containing traces (0.01 μg/mg) of carnosic acid and 46.11 μg carnosol/mg, exhibited negligible antiproliferative activity. Our data also indicated that rom4 and rom5 extracts inhibited colon cancer cell growth by inducing G2/M cell cycle arrest after 24 and 72 h of exposition in SW480 and HT29, respectively, the effect being maintained for 48 h in SW480 cells with rom4. A low level of apoptosis was observed indicating coexistence of cytostatic and cytotoxic effects induced by treatment with rom4 and rom5 extracts. Induction of G2/M cell cycle arrest by carnosol-enriched extracts (rom4 and rom5) is in consonance with the observations found in the

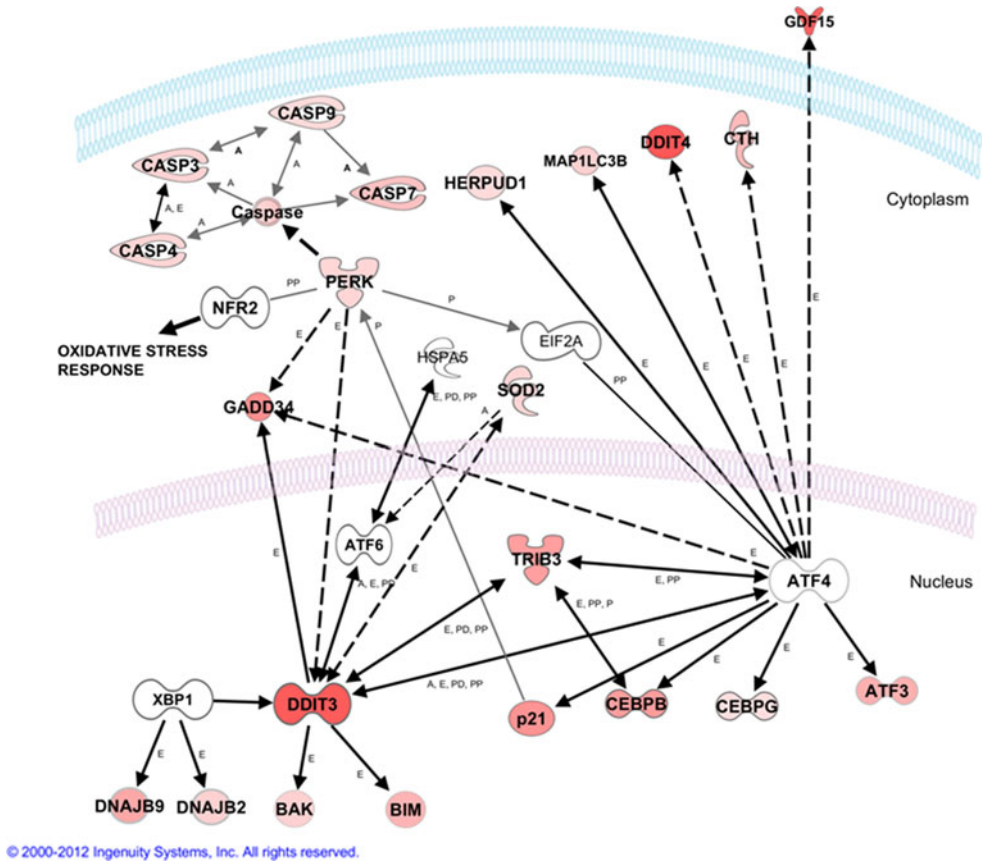

Fig. 4 Gene network obtained from IPA Knowledge Base illustrating direct (*solid line*) and indirect (*dashed line*) interactions between transcriptional regulators and their target inducible genes involved in ER stress modulated by rosemary polyphenols in SW480 cells. The type of interaction is indicated between *brackets*: *E* expression; *A* activation; *P* phosphorylation; *PP* protein–protein interaction; *PD* protein–DNA interaction. Expression type interactions are highlighted by *black arrows*

Table 2 Over-represented down-regulated gene sets microarray transcriptomics data obtained from treatment of colon cancer cells with rom4 extract

Cell line	Name	Size	NES[a]	NOM p val[b]	FDR q val[c]
HT29	Sister chromatid segregation	16	−1.97	0.000	0.044
	Mitotic sister chromatid segregation	15	−2.00	0.000	0.064
	Cell cycle process	176	−1.89	0.000	0.075
	Chromosome segregation	30	−1.84	0.002	0.079
	Cytokinesis	18	−1.85	0.000	0.088
	Mitotic cell cycle	140	−1.78	0.000	0.090
	Cell cycle phase	158	−1.79	0.000	0.092
	Mitosis	75	−1.75	0.000	0.094
	M phase	103	−1.74	0.003	0.096
	M phase of mitotic cell cycle	77	−1.80	0.000	0.097
	Chromosome organization and biogenesis	110	−1.76	0.000	0.098
	DNA repair	107	−1.72	0.000	0.109
	Cell cycle	286	−1.70	0.000	0.120
	Regulation of membrane potential	15	−1.66	0.027	0.138
	mRNA processing	66	−1.67	0.005	0.140
	RNA splicing	76	−1.65	0.000	0.142
	Positive regulation of secretion	17	−1.63	0.014	0.157
	Double strand break repair	20	−1.60	0.022	0.165
	Cell cycle checkpoint	43	−1.61	0.017	0.167
	DNA recombination	41	−1.60	0.020	0.169
	Microtubule cytoskeleton organization and biogenesis	33	−1.58	0.033	0.185
	Response to DNA damage stimulus	138	−1.56	0.006	0.207
	Cell division	20	−1.55	0.043	0.207
SW480	Sister chromatid segregation	16	−1.87	0.003	0.081
	Cell division	20	−1.91	0.005	0.108
	Mitotic sister chromatid segregation	15	−1.81	0.000	0.109
	Cytokinesis	18	−1.77	0.005	0.121
	Chromosome segregation	30	−1.66	0.003	0.199
	Extracellular structure organization and biogenesis	29	−1.62	0.017	0.202
	M phase of mitotic cell cycle	77	−1.62	0.000	0.219
	Mitosis	75	−1.62	0.005	0.244

[a] Normalized enrichment score

[b] Nominal p value

[c] False discovery rate (q value)

literature with carnosol and carnosic acid (Visanji et al. 2006). According to genome-wide transcriptomics analysis, rom4 extract altered the expression of ~4 % of the genes covered by the Affymetrix Human Gene 1.0ST chip in both colon cancer cells. However, only ~18 % of DEGs were common to both cell lines, indicating a markedly different expression profile in one line in comparison with the other in response to the treatment.

Based on IPA results, a noteworthy number of differentially expressed genes were associated with *cellular development*, *cell death*, *cellular growth and proliferation* and *cell cycle*, in both cell lines indicating a clear alteration of similar important biological functions in response to the treatment with rosemary polyphenols. Studies of dietary ingredients, principally phytochemicals, have demonstrated their anticarcinogenic effects as blocking agents. Certain phytochemicals prevent genotoxic carcinogens from forming adducts with DNA, either by inhibiting their activation from pro-carcinogens or by promoting their detoxification and excretion. These actions are mainly controlled by the balance between phase I enzyme activity and phase II detoxifying enzyme activity. Phase I metabolism involves the oxidation, reduction, and hydrolysis of xenobiotics, including drugs, toxins, and carcinogens, mainly by the cytochrome P450 (CYP) enzymes. A common mode for xenobiotic metabolism enzyme regulation is

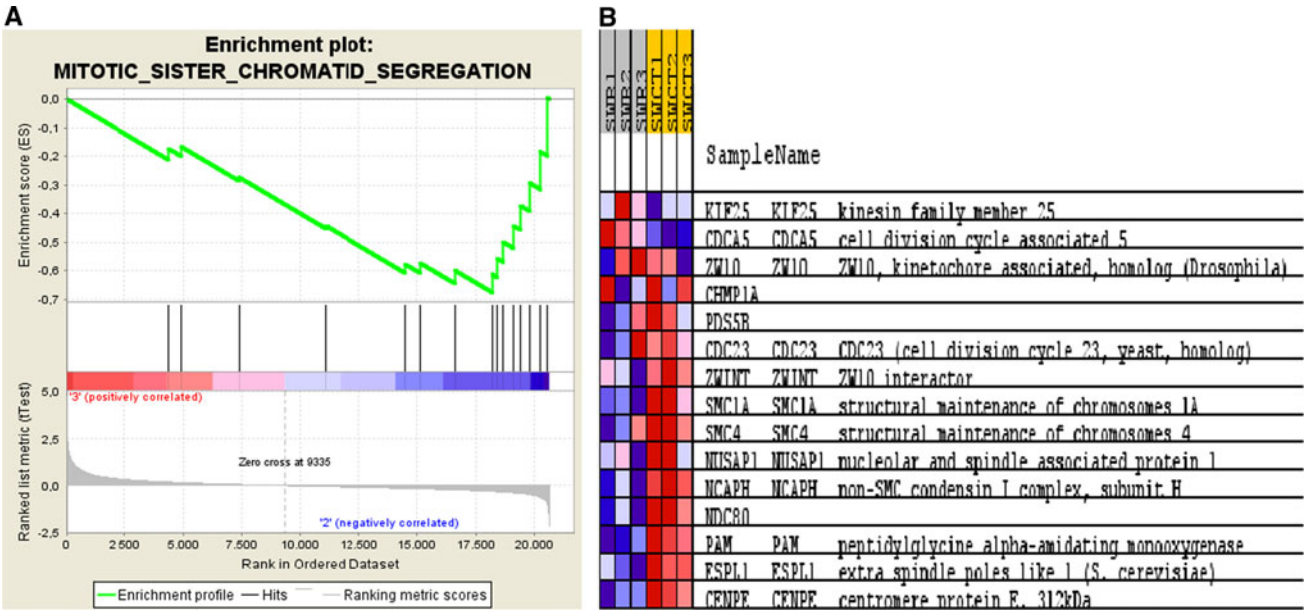

Fig. 5 Example of GSEA enrichment plot for *Mitotic Sister Chromatid Segregation* in SW480. **a** The *x* axis lists all microarray genes ranked based on their association with the comparison treated SW480 versus control. The *black vertical bars* indicate candidate genes in the target gene set. The ES profile (*green* trace) records the cumulative score of the gene ranks from the target gene set. Here, a majority of gene ranks from the candidate gene set are low (i.e., toward the down-regulated genes of the ranking) compared to the rest of genes, and the cumulative ranking score (ES profile) will have a negative peak, suggesting a significant enrichment of this gene set. The significant genes are determined by the position of the peak of the profile. There are 8 candidate genes up to this peak position that are claimed as significant (leading-edge subset). They are plotted in the heatmap shown in **b** (*red* means high expression level, and *blue* means low expression level) (color figure online)

transcriptional control by receptors. Several receptors including *RXR*, *PXR, CAR*, *AHR*, *VDR*, retinoic acid receptor (*RAR*), and glucocorticoid receptor (*GR*) are implicated in xenobiotic metabolism enzymes regulation. According to our transcriptomics data, xenobiotic heterodimer receptors *RXRα/CAR*, *RXRα/PXR,* and *RXRα/PPAR* did not induce transcriptional up-regulation of most of their target genes in treated HT29. To the contrary, a global down-regulated expression of *RXRα*-inducible genes was revealed by IPA analysis. Transcriptional activity of *RXRα* can be decreased by pro-inflammatory cytokine, which induce increased nuclear export of *RXRα*, leading to reduced nuclear *RXRα* levels and decreased nuclear DNA binding. Interestingly, over-expression of members of IL-1 receptor as well as pro-inflammatory cytokine IL1 in both cell types might be responsible for the observed transcriptional inactivation of *RXRα* functions, particularly those affecting phase I metabolizing enzymes and lipid metabolism. However, this effect may be partially counteracted by the up-regulation of the IL-1 receptor antagonist that acts blocking the IL-1 receptor. Activation of the AHR nuclear factor was deduced by the modest over-expression of *CYP1A1* and *CYP1B1* genes observed in treated HT29 cells. The activation of AHR signaling by naturally occurring dietary chemicals including carotenoids, phenolics, and flavonoids has been reported in the literature (Rodeiro et al. 2008). Also, induction of expression of the efflux transporter *MRP2* in both cell lines may be related to a cellular defense response aimed at increasing the excretion of the xenobiotic or their metabolites.

One of the main similarities found on the effect of rom4 extract in both cell lines was associated with the transcriptional activation of typical nuclear factor *NRF2* target genes such as *HMOX1*, *TXNRD1*, *GCLM,* and *OSGIN1* in both colon cancer cell lines; *FTH1* and *SOD2* in SW480; and *GCLC* and *EPHX1* in HT29. These enzymes exert efficient cytoprotection against toxicants through a variety of reactions, promoting elimination or inactivation of toxic reactive species (including potential carcinogens) before they cause damage to critical cellular macromolecules (Martin et al. 2004). In our transcriptomics data sets, the expression level of *HMOX1* gene was remarkably high, especially in treated SW480. RT-qPCR confirmed that *HMOX1* and *OSGIN1* were significantly up-regulated in both cells by rom4. *HMOX1* gene encodes heme oxygenase-1 isozyme that catalyzes the degradation of heme into three products, namely, carbon monoxide (CO), biliverdin, and free iron. Biliverdin is converted to bilirubin by the action of biliverdin reductase, whose expression was also induced in treated SW480. Many reports have demonstrated the potent antioxidant activity of the heme-derived metabolites generated by heme oxygenase-1 catalysis (biliverdin and

Table 3 Leading-edge subsets of genes found in down-regulated GO terms obtained in functional enrichment analysis of microarray data using GSEA

Functional group	HT29		SW480	
	Gene set (GO term)	Leading-edge subsets of genes[a]	Gene set (GO term)	Leading-edge subsets of genes[a]
Cytokinesis	Cell division, cytokinesis	SEPT4, SEPT6, SEPT7, **BRCA2**, **PRC1**, **RACGAP1**, **ANLN**, **NUSAP1**	Cell division, cytokinesis	**INCENP**, **PRC1**, DIAPH2, BRCA2, **RACGAP1**, SEPT6, **MYH10**, BIRC5, NUSAP1
Chromosome segregation	Sister chromatid segregation, Mitotic sister chromatid segregation, chromosome segregation, chromosome organization and biologenesis	**NUSAP1**, CDC23, PDS5B, **ZWINT**, **ESPL1**, **NDC80**, NCAPH, **PAM**, **CENPE**, **SMC4**	Sister chromatid segregation, Mitotic sister chromatid segregation, chromosome segregation	**PAM**, NCAPH, **CENPE**, **ESPL1**, NDC80, SMC4, **SMC1A**, NUSAP1
M phase of mitotic cell cycle	Cell cycle process, cell cycle phase, mitotic cell cycle, mitosis, M phase of mitotic cell, M phase, cell cycle	**TTK**, **KIF2C**, **KIF11**, **CCNA2**, **PML**, **MAD2L1**, **BUB1**, **KNTC1**, **AURKA**, NEK2, **TPX2**, **CIT**, **PLK1**, **KIF15**, **NUSAP1**, **ZWINT**, **ESPL1**, **NDC80**, NCAPH, **PAM**, **CENPE**, **SMC4**	Mitosis, M phase of mitotic cell	**PAM**, NCAPH, **CENPE**, **ESPL1**, NDC80, SMC4, **SMC1A**, BIRC5, **KNTC1**, **TTK**, **AURKA**, **KIF2C**, **BUB1**, **PBRM1**, CCNA2, **KIF11**, **KIF15**, **TPX2**, **SMC3**, MAD2L1, **PLK1**, **CIT**
RNA processing	RNA processing, RNA splicing	PPARGC1A, SFRS6, NONO, SFRS7, SFRS1, SFRS2, SFRS11, CWC15, PRPF31, SRPK2, SF3B3, USP39, SFPQ, TXNL4A, SNRPD1, SMNDC1, EFTUD2, SLU7, SNW1, **TRA2A**, SFRS2IP		
DNA repair	Double strand DNA repair, DNA repair, response to DNA damage stimulus	MRE11A, RAD54B, RAD51, **RAD21**, POLA1		

[a] Bold: genes with adjusted p value <0.05

bilirubin) and the cytoprotective actions of CO on vascular endothelium and nerve cells. Hence, it is now widely accepted that induction of *HMOX1* expression represents an adaptive response that increases cell resistance to oxidative injury. The signaling mechanisms used to activate transcription of *HMOX1* are dependent of the cell type and the inducing agent. For instance, carnosol, a major phenolic compound in rom4 extract, seems to rapidly induce *HMOX1* gene expression through *NRF2* transcription factor in conjunction with the survival signaling pathway represented by phosphatidylinositol 3-kinase (PI3 K)/AKT in mouse PC12 cells (Martin et al. 2004).

Induction of phase II detoxifying and antioxidant enzymes is mediated primarily by the antioxidant or electrophile response elements (ARE/EpRE), which are found in the 5′ upstream promoter region of many of the phase II/antioxidant genes involved in xenobiotic metabolism and oxidative stress response. *NRF2* nuclear transcription factor plays an essential role in ARE-gene expression. In absence of stimuli, *NRF2* element is sequestered in the cytoplasm by binding to *KEAP1* gene product, an actin-binding protein. Under oxidative stress or in the presence of electrophiles, *KEAP1* protein is inactivated by oxidative modification of its cysteine residues, allowing for *NRF2* receptor translocation into the nucleus, where it heterodimerizes with small *MAF* proteins, and binds to AREs. A wide variety of dietary compounds, namely, sulforaphane, curcumin, and caffeic acid phenetyl, that act as potent inducers of ARE-regulated gene expression, have been reported to provide chemopreventive effects (Lee and Surh 2005). Accumulating evidence from in vitro studies with neuronal cells and dietary polyphenols suggests that catechol-type electrophilic compounds such as carnosic acid and carnosol initiate S-alkylation of cysteine thiol of the *KEAP1* protein–inducing protective effects dependent of the cell type by promoting the translocation of *NRF2* from the cytoplasm to the nucleus (Satoh et al. 2008). Induction of ARE-gene expression in a *NRF2*-dependent manner by carnosic acid and carnosol has shown to inhibit adipocyte differentiation in mouse (Takahashi et al. 2009) and to regulate expression of nerve growth factor mediated by *NRF2* activation, conferring protection in glioblastoma cells (Mimura et al. 2011).

It is also interesting to note the observed increase in mRNA levels of *PERK* gene in treated SW480 cells. *PERK*

represents a link node between unfolded protein signaling, in response to ER stress, and *NRF2* function. It has been suggested that *NRF2* activation through *PERK* contributes to the maintenance of glutathione levels, which functions as a buffer against the accumulation of reactive oxygen species during the unfolded protein response caused by ER stress (Cullinan et al. 2003). Treatment of colon cancer cells with rom4 extract was found to induce a number of signature ER stress markers including (*PPP1R15A*, *DDIT3,* and *TRIB3*) suggesting the induction of ER stress. Furthermore, the increased expression of the transcriptional regulator *DDIT3* is often associated with RE stress–induced apoptosis (Rao et al. 2004). This transcription factor is known to regulate the expression of a set of genes including pro-apoptotic genes, including *BAK* and *BIM*, to originate mitochondrial cell death. *TRIB3* protein is an inducible target of *DDIT3* acts as a sensor for ER stress–induced apoptosis. It has been proposed that during mild ER stress, *TRIB3* down-regulates *DDIT3* expression via negative feedback mechanism, allowing the cell to adapt to ER stress. In contrast, induction of *TRIB3* would be more robust during severe or persistent ER stress, promoting apoptosis through inhibition (dephosphorylation) of Akt (Ohoka et al. 2005). This feedback mechanism could facilitate ER stress–mediated apoptosis in severely ER stressed cells that have successfully reached pro-apoptotic threshold levels of *DDIT3* (Zou et al. 2009). Rom4 extract seems to initiate the *DDIT3* pro-apoptotic transcription activity since the expression of its immediate inducible target genes, *BAK* and *BIM,* was also over-expressed in SW480. In this cell line, the increase in the expression of these pro-apoptotic genes was concomitant with the increase in mRNA levels of *CASP4*, which activation has been associated to ER stress (Hitomi et al. 2004). Recent evidences suggest that ER stress may be of importance for the cytotoxic activity of certain phenolic compounds. For instance, treatment with curcumin caused DNA damage in the form of single-strand breaks in HCT116 colon cancer cell and induced oxidative stress. This effect was accompanied by the induction of *DDIT3* gene expression and subsequent apoptosis (Scott and Loo 2004). Huang et al. (2011) have recently reported the pro-apoptotic effects of a phloroglucinol derivative in various human colon cancer cells. The observed effects were mediated by ER stress response through the induction of *DDIT3* and *HSPA5* genes as well as the activation of GSK3α/B, caspases 3, 7, and 9. Similarly, resveratrol has been demonstrated to increase the expression of *DDIT3* and *HSPA5* genes in colon cancer cells (Um et al. 2010). Polyisoprenylated benzophenones inhibited growth of human colon cancer cells by the activation of *DDIT3*, *ATF4,* and *XBP1* genes and inhibition of mTOR cell survival pathway through over-expression of *DDIT4* gene (Protiva et al. 2008). In a recent report, *DDIT3* induction has been also associated with up-regulation of *DR5* and subsequent apoptosis in human colon carcinoma HT29 cells following treatment with the polyphenol rottlerin (Lim et al. 2009). Transcriptomics data suggest that rom4 extract may induce RE stress–dependent apoptosis in colon cancer cells, especially in SW480 cell type. However, this pro-apoptotic effect may be counteracted by other mechanism in light to the low degree of apoptosis observed in vitro. Further investigations are required to elucidate the nature and the underling mechanisms of the cellular stress induced by the extract.

Data revealed strong transcriptional induction of AP-1 members, *C-JUN*, *JUNB,* and *C-FOS* in response to rom4 treatment in SW480 cells. Several works on dietary agents such as sulforaphan, allyl isothiocyanate (AITC), curcumin, (−)-epigallocatechin-3-gallate (EGCG), and resveratrol, with proven chemopreventive and cell growth inhibition activities, modulate AP-1 transcription activation in a cell type- and dose-dependent manner. Excepting EGCG and AITC, most of them induce early and transient transcriptional activation at low-range concentrations (1–50 μM) that is decreased at higher doses (75–100 μM) in colon cancer cellular models (Jeong et al. 2004). AP-1 activity is involved in many diverse cellular processes including apoptosis, proliferation, transformation, and differentiation. Moreover, its activation is often associated with a positive role in cell proliferation. The reasons for the discrepant observation of AP-1 induction and effects observed in vitro after exposure to the mentioned dietary factors are not clear yet.

Vitamin D receptor (VDR)/Retinoid X receptor (RXR) activation pathway was also significant in the treatment of SW480. *VDR* is a member of the nuclear receptor family of transcription factors and exists as a heterodimer with *RXR*. Vitamin D3-bound *VDR-RXR*, along with other co-activator proteins, mediates the transcriptional regulation of a number of genes involved in immune function, tumor suppression, growth regulation, and regulation/metabolism of calcium. Carnosic acid has shown to act synergistically with 1α,25-dihydroxyvitamin D3 by increasing the transcriptional *VDR* levels in HL60 leukemia cells (Danilenko et al. 2001). This effect was directly associated with enhanced differentiation of leukemia cells, suggesting that carnosic acid may also increase binding of VDR/RXRα heterodimers to vitamin D response elements in promoters of VDR-targeted genes. The same effects on cell differentiation have been observed to a certain extent with other antioxidant compounds (i.e., curcumin, silibinin, lycopene, b-carotene). Therefore, it has been suggested that these effects are not dependent on any particular structural similarity, indicating that the antioxidant properties of each molecule may be the common mechanism. Carnosic acid has demonstrated to be capable of protecting cells against

oxidative stress by decreasing the intracellular levels of reactive oxygen species (ROS) concomitant with an increase in total glutathione content. Furthermore, these changes have been suggested to serve as sensing signals of the cellular redox status for the regulation of early response transcription factors, such as AP-1, that may exhibit increased binding capacity to its cognate DNA element in the promoter region of *VDR* gene (Danilenko and Studzinski 2004). In our study, SW480 cells treated with rosemary polyphenols exhibited increased levels of AP-1 and *VDR* transcript. Also, VDR-inducible genes, including *CDKN1A* and *KLK6* (involved in cell differentiation), *MAD* and *GADD45A* (related to growth regulation), and *KLF4* (regulation of cell cycle progression), were over-expressed, whereas *TGFB2* (associated to grown inhibition) was down-regulated. To the contrary, HT29 analysis revealed the transcriptional induction of *VDR*-repressor *NCOR2* coincident with decreased mRNA levels of its repressible target, *IP-10* gene. In this cell line, rom4 also up-regulated the *VDR*-inducible genes *KLF4*, *CDKN1A*, as well as the mediator of tumor suppression *SEMA3B* and *PPARD* (growth regulation).

IPA results provided evidences of alteration of G2/M checkpoint control function by modulation of the expression of important genes, including *CDKN1A* and *14-3-3σ* in both cell lines. Interestingly, rom4 induced the expression of stress-response family of *GADD45* genes in SW480. Recently, induction of *GADD45* gene expression by a secoiridoid-rich phenolic extract form olive oil has been associated with activation of G2/M checkpoint control in breast cancer cells (Oliveras-Ferraros et al. 2011). In addition to IPA results, GSEA provided complementary information regarding the cell cycle progression functions altered in colon cancer cells in response to the rosemary extract treatment. The main benefits of GSEA approach are the reduction in the arbitrary factors in the typical gene selection step that could impact the traditional enrichment analysis; and the use of all the information obtained from microarray analysis by allowing the minimally changing genes, which cannot pass the selection thresholds, to contribute to the enrichment analysis (Huang et al. 2009). GSEA showed that rom4 extract induces changes in a range of cell cycle processes. A significant number of moderately down-regulated genes related with M phase, chromosome segregation and cytokinesis, enriched data sets obtained in gene expression microarray analysis. In our study, *AURKA*, the main activator of *PLK1* protein, was also down-regulated in the treated colon cancer cells in relation to their respective untreated controls, probably affecting centrosome maturation and microtubule dynamics during G2/M transition (Macürek et al. 2008). In recent years, *PLK1* has emerged as an important regulator in cell cycle progression (Barr et al. 2004). *PLK1* is known to play a pivotal role in the regulation of mitotic entry, chromosome segregation, and cytokinesis (Lowery et al. 2005). Owing to the strong association of this kinase with cell proliferation and elevated expression in a variety of tumors, including colon tumors, inhibition of *PLK1* function has been suggested as a potential alternative for cancer therapy (Chopra et al. 2010). Moreover, depletion of *PLK1* is associated with the decrease in cell viability and induction of apoptosis in various cancerous cells (Liu and Erikson 2003). Cancer cells with depleted *PLK1* activity show inability to completely separate the sister chromatids during mitosis. It has been shown that *PLK1*-depleted cancer cells eventually undergo induction of G2/M arrest and apoptosis (Liu and Erikson 2003). Coincident with down-regulation of *PLK1*, several members involved in the mitotic checkpoint function remained also down-regulated in treated cells. Partial loss of checkpoint control by such genes has often been associated to abnormal mitosis (Jeganathan et al. 2007). Among the down-regulated mitotic checkpoint gene members detected in this work, it is noteworthy the down-regulation of *HEC1* gene. Interestingly, *HEC1* has been suggested as a potential target for therapeutic intervention in cancer and hyper-proliferative diseases since its depletion in HeLa cells by siRNA technique has shown to result in mitotic catastrophe, whereas normal checkpoint-proficient cells arrest transiently in response to *HEC1* inhibition (Martin-Lluesma et al. 2002). Dysregulation of sister chromatid and chromosome segregation functions in colon cancer cells after treatment with rom4 extract was evidenced by the altered expression of important genes (*ESPL1* (separase) and *CENPE*). Consistent with the observation that rom4 extract accumulate the colon cancer cells in G2/M phase under assayed conditions in this work, a delay in mitosis entry (arrest in G2/M) and mitosis failure by the coordinated decrease in expression of key genes for mitosis entry and mitotic cell cycle may be expected. Although the support for this hypothesis is derived from the collective down-regulation of several genes involved in G2/M transition, mitosis, and cytokinesis, further investigation is needed in order to elucidate the exact mechanisms underlying the G2/M arrest observed after addition of rosemary extract. Differences in induction of G2/M arrest observed by rom4 in the two colon adenocarcinoma cell lines suggest that the extract may be differentially effective against tumors with specific mutational pattern.

Conclusions

Taken together, our results revealed that rosemary polyphenols markedly affected the viability of the assayed colon cancer cell types through multiple pathways. Thus,

rosemary polyphenols induced chemopreventive effects through transcriptionally activated genes that encode antioxidant phase II enzymes in the colon cancer cell lines. These findings are consistent with the reported *NRF2*-activating effect of carnosic acid and carnosol, two of the major phenolic compounds in the rosemary extract under study. Our data highlight other plausible mechanism by which rosemary polyphenols may also trigger the *NRF2*-mediated induction of detoxification and antioxidant enzymes. This complementary signaling pathway may entail activation of gene products involved ER stress. Evidences of transcriptional activation of pro-apoptotic genes have been collected in this study; however, cell viability experiments with rosemary polyphenols showed modest accumulation of apoptotic cells suggesting other multiple signaling pathways may also contribute. The two computational tools used in the study shed some light on the mechanisms underlying the observed G2/M cell cycle arrest exerted by rosemary polyphenols. IPA helped in providing information on those markedly changed gene expressions on G2/M checkpoint signaling pathway, while GSEA provided information on sets of simultaneously, but moderately altered genes, closely related in G2/M transition, mitosis, and cytokinesis in response to the treatment. Although the mRNA expression profile alone does not allow us to directly determine the role of any specific protein, especially those involved in phosphorylation/dephosphorylation signaling cascades, the microarray-based prediction herein allows to investigate novel signaling pathways to elucidate the effect of rosemary polyphenols in colon cancer cells.

Acknowledgments This work was supported by AGL2008-05108-C03-01, AGL2011-29857-C03-01 and 200970I083 projects (Ministerio de Ciencia e Innovación) and CSD2007-00063 FUN-C-FOOD program (Programa CONSOLIDER, Ministerio de Educacion y Ciencia).

Conflict of interest Authors declare no conflict of interest.

References

Araújo JR, Gonçalves P, Martel F (2011) Chemopreventive effect of dietary polyphenols in colorectal cancer cell lines. Nutr Res 31:77–87

Barr FA, Silljé HH, Nigg EA (2004) Polo-like kinases and the orchestration of cell division. Nat Rev Mol Cell Biol 5:429–440

Benjamini Y, Hochberg Y (1995) Controlling the False Discovery Rate: a practical and powerful approach to multiple testing. J R Stat Soc B 57:289–300

Carrasco-García E, Saceda M, Grasso S, Rocamora-Reverte L, Conde M, Gómez-Martínez A, García-Morales P, Ferragut JA, Martínez-Lacaci I (2011) Small tyrosine kinase inhibitors interrupt EGFR signaling by interacting with erbB3 and erbB4 in glioblastoma cell lines. Exp Cell Res 317:1476–1489

Chopra P, Sethi G, Dastidar SG, Ray A (2010) Polo-like kinase inhibitors: an emerging opportunity for cancer therapeutics. Expert Opin Inv Drug 19:27–43

Cullinan SB, Zhang D, Hannink M, Arvisais E, Kaufman RJ, Diehl JA (2003) Nfr2 is a direct PERK substrate and effector of PERK-dependent cell survival. Mol Cell Biol 23:7198–7209

Danilenko M, Studzinski GP (2004) Enhancement by other compounds of the anti-cancer activity of vitamin D3 and its analogs. Exp Cell Res 298:339–358

Danilenko M, Wang X, Studzinski GP (2001) Carnosic acid and promotion of monocytic differentiation of hl60-g cells initiated by other agents. J Natl Cancer Inst 93:1224–1233

Finn OJ, Gantt KR, Lepisto AJ, Pejawar-Gaddy S, Xue J, Beatty PL (2011) Importance of MUC1 and spontaneous mouse tumor models for understanding the immunobiology of human adenocarcinomas. Immunol Res 50:261–268

García-Cañas V, Simó C, León C, Cifuentes A (2010) Advances in Nutrigenomics research: novel and future analytical approaches to investigate the biological activity of natural compounds and food functions. J Pharm Biomed 51:290–304

Gentleman R, Carey VJ, Bates DM, Bolstad B, Dettling M, Dudoit S, Ellis B, Gautier L, Ge Y, Gentry J, Hornik K, Hothorn T, Huber W, Iacus S, Irizarry R, Leisch F, Li C, Maechler M, Rossini AJ, Sawitzki G, Smith C, Smyth G, Tierney L, Yang J, Zhang J (2004) Bioconductor: open software development for computational biology and bioinformatics. Genome Biol 5:R80

Gigante B, Santos C, Silva AM, Curto MJM, Nascimento MSJ, Pinto E, Pedro M, Cerqueira F, Pinto MM, Duarte MP, Laires A, Rueff J, Gonçalves J, Pegado MI, Valdeira L (2003) Catechols from abietic acid: synthesis and evaluation as bioactive compounds. Bioorgan Med Chem 11:1631–1638

Guerrero IC, Andrés LS, León LG, Machín RP, Padrón JM, Luis JG, Delgadillo J (2006) Abietane diterpenoids from Salvia pachyphylla and S. clevelandii with cytotoxic activity against human cancer cell lines. J Nat Prod 69:1803–1805

Herrero M, Plaza M, Cifuentes A, Ibáñez E (2010) Green processes for the extraction of bioactives from Rosemary: chemical and functional characterization via ultra-performance liquid chromatography-tandem mass spectrometry and in vitro assays. J Chromatogr A 1217:2512–2520

Herrero M, Simó C, García-Cañas V, Ibáñez E, Cifuentes A (2012) Foodomics: MS-based strategies in modern Food Science and Nutrition. Mass Spectrom Rev 31:49–69

Hitomi J, Katayama T, Eguchi Y, Kudo T, Taniguchi M, Koyama Y, Manabe T, Yamagishi S, Bando Y, Imaizumi K, Tsujimoto Y, Tohyama M (2004) Involvement of caspase-4 in endoplasmic reticulum stress-induced apoptosis and AB-induced cell death. J Cell Biol 165:347–356

Huang DW, Sherman BT, Lempicki RA (2009) Bioinformatics enrichment tools: paths toward the comprehensive functional analysis of large gene lists. Nucleic Acids Res 37:1–13

Huang SM, Cheung CW, Chang CS, Tang CH, Liu JF, Lin YH, Chen JH, Ko SH, Wong KL, Lu DY (2011) Phloroglucinol derivative MCPP induces cell apoptosis in human colon cancer. J Cell Biochem 112:634–652

Jeganathan K, Malureanu L, Baker DJ, Abraham SC, Van Deursen JM (2007) Bub1 mediates cell death in response to chromosome missegregation and acts to suppress spontaneous tumorigenesis. J Cell Biol 179:255–267

Jeong WS, Kim IW, Hu R, Kong ANT (2004) Modulation of AP-1 by natural chemopreventive compounds in human colon HT-29 cancer cell line. Pharm Res 21:649–660

Johnson JJ (2011) Carnosol: a promising anti-cancer and anti-inflammatory agent. Cancer Lett 305:1–7

Lee JS, Surh YJ (2005) Nrf2 as a novel molecular target for chemoprevention. Cancer Lett 224:171–184

Lim JH, Park JW, Choi KS, Park YB, Kwon TK (2009) Rottlerin induces apoptosis via death receptor 5 (DR5) upregulation through CHOP-dependent and PKCδ-independent mechanism in human malignant tumor cells. Carcinogenesis 20:729–736

Liu X, Erikson RL (2003) Polo-like kinase (Plk)1 depletion induces apoptosis in cancer cells. Proc Natl Acad Sci USA 100:5789–5794

Lowery DM, Lim D, Yaffe MB (2005) Structure and function of Polo-like kinases. Oncogene 24:248–529

Macürek L, Lindqvist A, Lim D, Lampson MA, Klompmaker R, Freire R, Cluin C, Taylor SS, Yaffe MB, Medema RH (2008) Polo-like kinase-1 is activated by aurora A to promote checkpoint recovery. Nature 455:119–123

Martin D, Rojo AI, Salinas M, Diaz R, Gallardo G, Alam J, Ruiz de Galarreta CM, Cuadrado A (2004) Regulation of heme oxygenase-1 expression through the phosphatidylinositol 3-kinase/Akt pathway and the Nrf2 transcription factor in response to the antioxidant phytochemical carnosol. J Biol Chem 279:8919–8929

Martin-Lluesma S, Stucke VM, Nigg EA (2002) Role of Hec1 in spindle checkpoint signaling and kinetochore recruitment of Mad1/Mad2. Science 297:2267–2270

Mimura J, Kosaka K, Maruyana A, Satoh T, Harada N, Yoshida H, Satoh K, Yamamoto M, Itoh K (2011) Nrf2 regulates NGF mRNA induction by carnosic acid in T98 glioblastoma cells and normal human astrocytes. J Biochem 150:209–217

Ohoka N, Yoshii S, Hattori T, Onozaki K, Hayashi H (2005) TRB3, a novel ER stress-inducible gene, is induced via ATF4-CHOP pathway and is involved in cell death. EMBO J 24:1243–1255

Oliveras-Ferraros C, Fernández-Arroyo S, Vazquez-Martin A, Lozano-Sánchez J, Cufí S, Joven J, Micol V, Fernández-Gutiérrez A, Segura-Carretero A, Menendez JA (2011) Crude phenolic extracts from extra virgin olive oil circumvent de novo breast cáncer resistance to HER1/HER2-targeting drugs by inducing GADD45-sensed cellular stress, G2/M arrest and hyperacetylation of Histone H3. Int J Oncol 38:1533–1547

Pfaffl MW, Horgan GW, Dempfle L (2002) Relative expression software tool (REST) for group-wise comparison and statistical analysis of relative expression results in real-time PCR. Nucleic Acids Res 30:e36

Protiva P, Hopkins ME, Baggett S, Yang H, Lipkin M, Holt PR, Kennelly EJ, Bernard WI (2008) Growth inhibition of colon cancer cells by polyisoprenylated benzophenones is associated with induction of the endoplasmic reticulum response. Int J Cancer 123:687–694

Rao RV, Poksay KS, Castro-Obregon S, Schilling B, Row RH, del Rio G, Gibson BW, Ellerby HM, Bredesen DE (2004) Molecular components of a cell death pathway activated by endoplasmic reticulum stress. J Biol Chem 279:177–187

Rodeiro I, Donato MT, Lahoz A, Garrido G, Delgado R, Gómez-Lechón MJ (2008) Interactions of polyphenols with P450 system: possible implications on human therapeutics. Mini-Rev Med Chem 8:97–106

Satoh T, Izumi M, Inukai Y, Tsutsumi Y, Nakayama N, Kosaka K, Shimojo Y, Kitajima C, Itoh K, Yokoi T, Shirasawa T (2008) Carnosic acid protects neuronal HT22 Cells through activation of the antioxidant-responsive element in free carboxylic acid- and catechol hydroxyl moieties-dependent manners. Neurosci Lett 434:260–265

Scott DW, Loo G (2004) Curcumin-induced GADD153 gene up-regulation in human colon cancer cells. Carcinogenesis 25:2155–2164

Smyth GK (2005) Limma: Linear Models for Microarray Data. In: Gentleman R, Carey V, Dudoit S, Irizarry R, Huber W (eds) Bioinformatics and Computational Biology Solutions using R and Bioconductor. Springer, New York, pp 397–420

Sorby LA, Andersen SN, Bukhlom IRK, Jacobsen MB (2010) Evaluation of suitable reference genes for normalization of real-time reverse transcription PCR analysis in colon cancer. J Exp Clin Canc Res 29:144

Subramanian A, Tamayo P, Mootha VK, Mukherjee S, Ebert BL, Gillette MA, Paulovich A, Pomeroy SL, Golub TR, Lander ES, Mesirov JP (2005) Gene set enrichment analysis: a knowledge-based approach for interpreting genome-wide expression profiles. Proc Natl Acad Sci USA 102:15545–15550

Takahashi T, Tabuchi T, Tamaki Y, Kosaka K, Takikawa Y, Satoh T (2009) Carnosic acid and carnosol inhibit adipocyte differentiation in mouse 3T3-L1 cells through induction of phase 2 enzymes and activation of glutathione metabolism. Biochem Bioph Res Co 382:549–554

Um HJ, Bae JH, Park JW, Suh H, Jeong NY, Yoo YH, Kwon TK (2010) Differential effects of resveratrol and novel resveratrol derivative, HS-1793, on endoplasmic reticulum stress-mediated apoptosis and Akt inactivation. Int J Oncol 36:1007–1013

Visanji JM, Thompson DG, Padfield PJ (2006) Induction of G2/M phase cell cycle arrest by carnosol and carnosic acid is associated with alteration of cyclin A and cyclin B1 levels. Cancer Lett 237:130–136

Waagmeester AS, Kelder T, Evelo C (2008) The role of bioinformatics in pathway curation. Genes Nutr 3:139–142

Yesil-Celiktas O, Sevimli C, Bedir E, Vardar-Sukan F (2010) Inhibitory effects of rosemary extracts, carnosic acid and rosmarinic acid on the growth of various human cancer cell lines. Plant Food Hum Nutr 65:158–163

Zou CG, Cao XZ, Zhao YS, Gao SY, Li SD, Liu XY, Zhang Y, Zhang KQ (2009) The molecular mechanism of endoplasmic reticulum stress-induced apoptosis in PC-12 neuronal cells: the protective effect of insulin-like growth factor I. Endocrinology 150:277–285

3.2.3 Comprehensive foodomics study on the mechanisms operating at various molecular levels in cancer cells in response to individual rosemary polyphenols

Valdés, A., *García-Cañas, V., Simó, C., Ibáñez, C., Micol, V., Ferragut, J. A., Cifuentes, A. *Anal Chem.* 2014, *86*, 9807 - 9815.

DOI: http://dx.doi.org/doi:10.1021/ac502401j

analytical chemistry

Article

pubs.acs.org/ac

Comprehensive Foodomics Study on the Mechanisms Operating at Various Molecular Levels in Cancer Cells in Response to Individual Rosemary Polyphenols

Alberto Valdés,[†] Virginia García-Cañas,*[,†] Carolina Simó,[†] Clara Ibáñez,[†] Vicente Micol,[‡] Jose A. Ferragut,[‡] and Alejandro Cifuentes[†]

[†]Laboratory of Foodomics, Institute of Food Science Research (CIAL), CSIC, Nicolas Cabrera 9, Campus de Cantoblanco, 28049 Madrid, Spain

[‡]Institute of Molecular and Cellular Biology, Miguel Hernandez University. Avda. Universidad s/n, Elche, Alicante, Spain

Supporting Information

ABSTRACT: In this work, the contribution of carnosic acid (CA) and carnosol (CS), two major compounds present in rosemary, against colon cancer HT-29 cells proliferation is investigated using a comprehensive Foodomics approach. The Foodomics study reveals that CA induces transcriptional activation of genes that encode detoxifying enzymes and altered the expression of genes linked to transport and biosynthesis of terpenoids in the colon cancer cell line. Functional analysis highlighted the activation of the ROS metabolism and alteration of several genes involved in pathways describing oxidative degradation of relevant endogenous metabolites, providing new evidence about the transcriptional change induced by CA in HT-29 cells. Metabolomics analysis showed that the treatment with CA affected the intracellular levels of glutathione. Elevated levels of GSH provided additional evidence to transcriptomic results regarding chemopreventive response of cells to CA treatment. Moreover, the Foodomics approach was useful to establish the links between decreased levels of *N*-acetylputrescine and its degradation pathway at the gene level. The findings from this work and the predictions based on microarray data will help explore novel metabolic processes and potential signaling pathways to further elucidate the effect of CA in colon cancer cells.

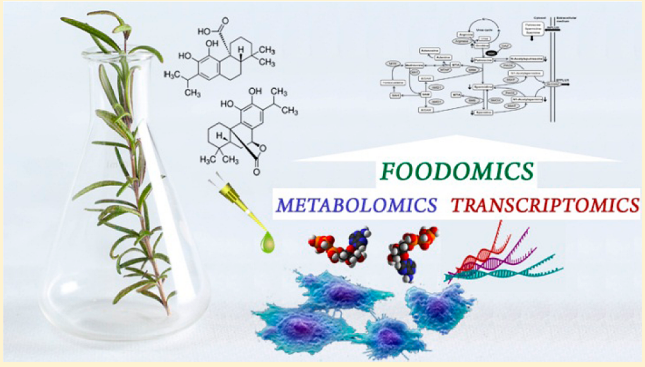

Commonly known as rosemary, *Rosmarinus officinalis* L. is a Labiatae species from Mediterranean origin. Phenolic diterpenes as carnosic acid (CA) and carnosol (CS) are abundant in rosemary leaves, representing approximately 5% of the dry weight of rosemary leaves and accounting for >90% of the antioxidant activity of rosemary extracts.[1] For many years, the potent antioxidant activity of rosemary extracts has attracted great interest for the preservation of food material, and recently the European Union (EU) has approved the use of rosemary extracts as additives for food preservation.[2] In addition to their strong antioxidant properties, rosemary extracts have been also of interest for their anti-inflammatory and anticancer activities.[3] A great body of evidence from *in vitro* and *in vivo* studies indicates that rosemary extracts exert chemoprotective effects through different mechanisms.[4,5] Such chemoprotective activity has also conferred upon rosemary extracts' cancer preventive properties.[6] Thus, the antiproliferative effect of rosemary extracts have been studied on leukemia,[7] ovarian cancer,[8] liver cancer,[9] and colon cancer[10] cells. The anticancer activities of the major rosemary diterpenes, CA and CS, have also been the object of several studies.[11−15] In addition to the antiproliferative and antiinvasive activities of CA, *in vitro* and *in vivo* neuroprotection is one of the most widely studied biological activities that have been attributed to this particular diterpene.[16,17] In general, rosemary extracts, as well as CA and CS, show differential antiproliferative activity in several human tumor cell lines.[18] One of the mechanisms underlying the antiproliferative activity of these compounds is linked to their ability for altering cell cycle progression. However, although both diterpenes are structurally related, they affect different phases of the cell cycle. Furthermore, these compounds appear to exert a different effect on cell cycle phase distribution depending on the concentration assayed and the cell type.[10,15] Apart from the possible alteration of cell cycle regulatory genes, other specific mechanisms associated with the antiproliferative activity of rosemary compounds cannot be dismissed since they seem to be differentially effective against cells with specific mutational

Received: June 30, 2014
Accepted: September 4, 2014
Published: September 4, 2014

patterns.[7] However, comprehensive studies centered on the investigation of the mechanisms operating at various molecular levels in cancer cells in response to individual rosemary polyphenols are still lacking. In this regard, a global methodology such as Foodomics, based on the combination of several omics platforms and data processing, is well suited to perform comprehensive evaluations of the health benefits of food ingredients.[19−23] In previous work, a polyphenol-enriched rosemary extract (RE) obtained in our laboratory using supercritical fluid extraction exhibited inhibitory effect on proliferation of several cancer cell models, such as K562,[7] SW480,[10] and HT-29.[24,25] Our findings suggested that the RE altered some cell cycle regulatory genes as well as various signaling pathways in colon cancer cells. However, the observed antiproliferative activity has not been correlated to any compound present in the extract yet. In order to address this question, the contribution of two major compounds, CA and CS, present in the RE, to the activity of the extract on HT-29 cell proliferation is investigated in this work. To achieve this, proliferation inhibition assays and studies of potential synergistic, additive, or antagonistic effects of both diterpenes have been conducted in this work. Then, the experiments were focused on the effects of CA on cell cycle distribution analyses in combination with a Foodomics evaluation based on genome-wide transcriptomics and metabolomics analysis to investigate the cellular and molecular changes operating in HT-29 cells in response to CA treatments. Functional enrichment analysis was applied as a previous step for a reliable data interpretation obtained from transcriptomics and metabolomics and for cross-platform data integration.

EXPERIMENTAL SECTION

Standards and Rosemary Extract Samples. CA and CS were purchased as pure standards (Sigma-Aldrich, St. Louis, MO). The rosemary extract (RE) was obtained from dried rosemary leaves using supercritical CO_2 and 7% ethanol at 150 bar as reported by Herrero et al.[26] Chemical characterization of the RE indicated that two main diterpenes, CA and CS, were found at high concentrations in the RE, namely, 256.0 and 37.1 μg/mg extract, respectively. Dry extract and standards samples were dissolved in dimethyl sulfoxide (DMSO, Sigma-Aldrich) at 30 μg/mL and 100 μM, respectively, and stored as aliquots at −80 °C until use.

Cell Culture Conditions. Colon adenocarcinoma HT-29 cells obtained from ATCC (American Type Culture Collection, LGC Promochem, U.K.) were grown in McCoy's 5A supplemented with 10% heat-inactivated fetal calf serum, 50 U/mL penicillin G, and 50 U/mL streptomycin, at 37 °C in humidified atmosphere and 5% CO_2. When cells reached ∼50% confluence, they were trypsinized, neutralized with culture medium, plated in different culture plates, and allowed to adhere overnight at 37 °C.

Antiproliferative Activity Assay. In order to study the effect of rosemary extracts on the proliferation of the HT-29 line, cells were seeded onto 96-well culture plates at 10 000 cells/cm^2, permitted to adhere overnight at 37 °C, and exposed to different treatments with different concentrations of CA, CS, or RE for 24−72 h depending on the experiment. After incubation with the bioactive compounds for the indicated time in each case, cell proliferation was estimated by the MTT assay as follows: 0.5 mg/mL of MTT reagent (Sigma-Aldrich) was added and incubated for 3 h at 37 °C in humidified 5% CO_2/air atmosphere. After the incubation, the media was aspirated and 100 μL of DMSO was added to each well to dissolve the formazan (the metabolic product of MTT). Then, the absorbance at 570 nm was measured in a microplate reader (Multiskan FC microplate photometer, Thermo Fisher Scientific, Vantaa, Finland). Results are provided as the mean ± 95% confidence interval of at least three independent experiments, each performed in triplicate. Cell viability at the beginning of the treatment (time zero) was used to calculate the percent of growth (PG) and the following parameters related to cell proliferation: GI50 (50% growth inhibition), TGI (total growth inhibition), and LC50 (50% cell death). These parameters were calculated according to the NIH definitions.[27] Combination assays were performed by treating HT-29 cells with appropriate concentrations of CA, CS, and mixtures with the same molar ratio of both. Cell proliferation inhibition was determined using the MTT assay, as previously described. In the assessment of synergism, antagonism, and additive effects, the combination index (CI) method was used according to the Chou-Talalay equation.[28] The calculations were performed using CompuSyn software from Biosoft (Cambridge, U.K.), which takes into account both the potency (Dm or IC50) and shape of the dose−effect curve. CI < 1 indicates synergism; CI = 1 indicates an additive effect; and CI > 1 indicates antagonism. Results are shown as the mean ± standard error of the mean of three independent experiments, each performed in triplicate.

Cell Cycle Study. Cells were seeded onto tissue culture dishes at 10 000 cells/cm^2, permitted to adhere overnight at 37 °C, and incubated with 12.5 μg/mL CA or 30 μg/mL RE in complete culture medium up to 72 h. Then, cell cycle distribution was measured using flow cytometry at different time points. Briefly, for cell cycle distribution of DNA content, control and treated cells were trypsinized, washed with PBS, and fixed with 70% cold ethanol at −20 °C for at least 24 h. Then, fixed cells were resuspended in 0.5 mL of PI/RNase staining buffer (BD Pharmingen, San Jose, CA), incubated for 15 min in the dark, and analyzed on a Gallios flow cytometer equipped with a 0.75 W argon laser set at 488 nm (Beckman Coulter, Miami Lakes, FL). Events were gated for peak width and area to exclude subcellular debris and aggregates. A total of 10 000 events were recorded for each sample and a frequency histogram of peak area was generated and analyzed using Cylchred (V.1.0.0.1) software (University of Wales College of Medicine, Cardiff, U.K.). Results are provided as the mean of the percentage of treated minus control samples ± SEM (standard error of the mean) of at least three independent experiments, each performed in triplicate. The results were analyzed using the analysis of variance (ANOVA) with Tukey post hoc test and differences were considered significant at $p < 0.05$.

Foodomics Evaluation. A Foodomics strategy, involving transcriptomics and metabolomics profiling, was applied to study molecular mechanisms operating in HT-29 cells after CA treatment. Comparative transcriptomic analysis was performed on HT-29 cells incubated with 9.9 μg/mL CA and their respective untreated controls. Microarray analyses and data processing were performed with triplicate samples for each experimental condition as described previously using Human Gene 1.0ST chips (Affymetrix).[10] After quality assessment using Expression Console (Affymetrix), CEL files were processed using the Robust Multi-Array (RMA) normalization in the BioConductor package affy for R (www.r-project.com).[29] Significance analysis was performed using the BioConductor

dx.doi.org/10.1021/ac502401j | Anal. Chem. 2014, 86, 9807−9815

package limma.[30] Moderated t statistics was used for significance analysis of each probe set and each contrast, and then false discovery rate was estimated using Benjamini and Hochberg's method for multiple testing correction.[31] To identify the statistically most significant changes in gene expression, microarray data were subjected to gene filtering based on the statistical significance (false discovery ratio, FDR, applied on moderated t statistics, adjusted p value < 0.05). Reverse transcription quantitative PCR (RT-qPCR) was used to confirm relative changes in mRNA levels of selected genes from microarray data sets. Further details are available in the Supporting Information (Supporting methods). In this work, computational tools were used for functional enrichment and pathway analysis as a previous step for a reliable data interpretation obtained from microarray analysis. The bioinformatic tool Ingenuity Pathway Analysis (IPA, Ingenuity Systems) was used in order to interpret the gene expression data in the context of biological processes and pathways. To this aim, the Core Analysis function included in IPA was applied to analyze the lists of differentially expressed genes (DEGs) identified in microarray analysis. In each analysis, expression parameters cut-offs were set at 0.4 as the M-value cutoff that corresponds to expression ratios (fold change) ≥ 1.3 for up-regulated and ≤ 0.8 for down-regulated genes. From the gene set, up- and down-regulated identifiers were defined as value parameters for the analysis. On the basis of the list of identifiers, IPA performs functional enrichment analysis in order to identify the biological processes and functions overrepresented in a given list of genes. The p-value, calculated with the Fischer's exact test, reflected the likelihood that the association between a set of genes in our data set and a related biological function is significant (p-value < 0.05). The biological functions that were expected to be increased or decreased according to the gene expression changes in our data set were identified using the IPA regulation z-score algorithm. A positive or negative z-score value indicates that a function is predicted to be increased or decreased in treated relative to untreated cells.

Metabolic profiles from HT-29 cells were determined using two complementary analytical platforms (capillary electrophoresis−time-of-flight mass spectrometry (CE−TOF MS) and hydrophilic interaction chromatography/ultra performance liquid chromatography (HILIC/UHPLC)−TOF MS) in order to widen the metabolic coverage. CE−TOF MS was carried out using a P/ACE 5500 CE system (Beckman Instruments, Fullerton, CA) connected to a TOF MS instrument (micrOTOF model) from Bruker Daltonics (Bremen, Germany) by an orthogonal electrospray ionization (ESI) interface G1607A from Agilent Technologies (Palo Alto, CA). Metabolites were separated in a fused silica capillary (90 cm, 50 μm i.d.) filled with 3 M formic acid as the electrolyte applying a voltage of +27 kV at 25 °C. Isopropanol−water (1:1, v/v) was delivered as the sheath liquid at 0.24 mL/min. ESI-TOF MS was performed in the positive ion mode, and the capillary voltage was set at 4 kV. The flow rate of heated dry nitrogen gas at 200 °C was maintained at 0.4 bar. Other conditions regarding external and internal calibration of the TOF-MS are given as Supporting Information. UHPLC−TOF MS was carried out using an Agilent 1290 system connected to a quadrupole-time-of-flight (Q/TOF) 6540 (Agilent Technologies) operating in the positive ion mode. HILIC was performed on a ZORBAX HILIC Plus HT (2.1 mm × 50 mm, 1.8 μm) column maintained at 30 °C. Elution was performed using phase A (water with 5 mM ammonium formate at pH 5.8) and phase B (acetonitrile with 0.1% (v/v) formic acid). The detailed HILIC stationary phase description and elution gradient are given as Supporting Information. TOF-MS operation parameters were the following: capillary voltage, −4000 V; nebulizer pressure, 40 psi; drying gas flow rate, 10 L/min; gas temperature, 200 °C; skimmer voltage, 45 V; fragmentor voltage was 125 V; 50−1000 m/z mass scan. Conditions regarding internal mass calibration and external calibration of the Q/TOF mass spectrometer are given as Supporting Information. Metabolomic data signals obtained from CE−MS and UHPLC−MS were exported to the MS exchange format mzXML using Trapper (available at http://tools.proteomecenter.org/wiki/index.php?title=Software:trapper). CE−MS data was then processed with the MZmine program (version 2.7.2).[32] Parameters applied for mass detection, peak deconvolution, and sample alignment are described elsewhere.[33] LC−MS data was processed using XCMS package written in the platform-independent programming language R.[34] The resulting sample files were then converted to peakML format to execute the mzMatch.R package.[35] Parameters for LC−MS analysis have been already summarized.[36] Finally peaks showing high variability within the same group (i.e., control and treated cells) were removed (with a value of median/average > 1.5) in both CE−MS and LC−MS data sets. The resulting output.csv data tables of high quality time-aligned detected peaks with their corresponding migration/retention time, m/z, and peak area obtained for each sample were merged into one file to perform statistical analysis using the STATISTICA program (v.7, Statsoft, Tulsa, OK, www.statsoft.com). Significant molecular features were detected applying an ANOVA with the p-value set at 0.05. Both CE−MS and LC−MS data processing and statistical analysis were carried out using a PC Intel Core i7-2600K processor (8 M Cache, up to 3.80 GHz and 64 bits) operating under Microsoft Windows 7. The metabolites showing significant differences (p < 0.05) were subjected to a tentative identification process by matching the experimental accurate m/z values and those contained in different free available databases, namely, the Human Metabolome Database,[37] METLIN,[38] and KEGG,[39] with a mass accuracy window of 10 ppm. The Generate Molecular Formula Editor within Data Analysis 4.0 software (Bruker) and the Molecular Formula Generator algorithm within the Mass Hunter software (Agilent) were used to compare the isotopic patterns between the molecular formula generated by the software and the proposed compound from a metabolite database search. When available, metabolite standards from Sigma-Aldrich were used to confirm identifications by means of sample coinjection and subsequent CE−MS and LC−MS analysis.

RESULTS AND DISCUSSION

Inhibition of HT-29 Cell Proliferation by CA and CS. In previous work, a polyphenol-enriched rosemary extract (RE) obtained in our laboratory using supercritical fluid extraction exhibited an inhibitory effect on proliferation of cancer cell models.[7,10,24,25] Chemical characterization of the extract indicated the presence of CA and CS at concentrations of 256.0 and 37.1 μg/mg extract, respectively, as well as other minor polyphenols (caffeic acid and p-coumaric acid). However, the observed antiproliferative activity of the extract has not been yet correlated to any compound present in the mixture. In order to address this point, the effect of the two

dx.doi.org/10.1021/ac502401j | Anal. Chem. 2014, 86, 9807−9815

major diterpenes (CA and CS) found in the extract, for which pure standards are commercially available, was investigated on HT-29 cells. To determine the antiproliferative effect of CA and CS in relation to the RE, HT-29 cells were incubated with increasing concentrations of RE, CA, and CS (from 0 to 33.2 μg/mL) for 24 h (Figure 1A), 48 h (Figure 1B), and 72 h

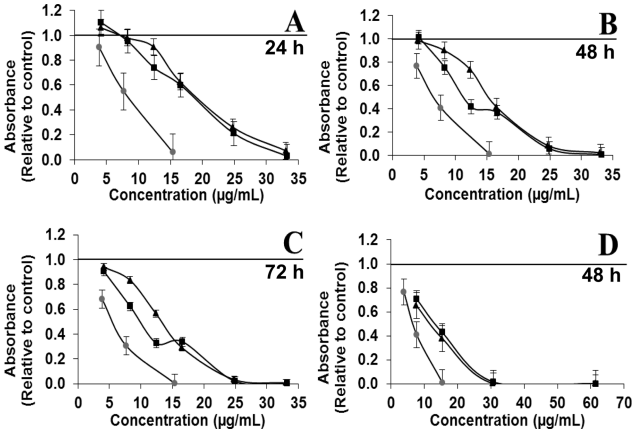

Figure 1. HT-29 cell viability upon treatment for 24 h (A), 48 h (B), and 72 h (C) with different concentrations of CA (squares), CS (triangles), and RE (gray circles); and for 48 h (D) with different concentrations of CA + CS mixture (triangle), CA (squares), and RE (gray circle). In parts A–C, the concentration data points for RE treatments are referred to the calculated CA content values in μg/mL. In part D, the concentration data points for CA + CS and RE treatments are referred to calculated CA content values in μg/mL. Error bars are given as the 95% confidence interval of three independent experiments each performed in triplicate.

(Figure 1C) and cell proliferation was analyzed by the MTT assay. As it can be observed in Figure 1, after treatment with increasing concentrations of CA, dose-dependent reduction of cell proliferation was observed starting from 8.3 μg/mL at 48 and 72 h (Figure 1B,C). Moreover, a considerable reduction (~40%) of cell proliferation is observed between 24 and 72 h after treatment with 12.5 μg/mL CA. The treatment with CS also resulted in a reduction of cell proliferation in a dose- and time-dependent manner similar to that observed for CA (Figure 1). In order to deep in the mechanisms that can explain the antiproliferative activity of these diterpenes, the response parameters, growth inhibition (GI50), total growth inhibition (TGI) as an indicator for cytostaticity, and lethal concentration (LC50) indicative of the cytotoxic level of effect were also determined for 24, 48, and 72 h incubation times (Supporting Information, Table S1). Although the inhibitory activities of both diterpenes were similar, our results indicate that CA exerted a slightly stronger effect than CS on cell proliferation provided by the lower values obtained for the parameters at the different incubation times. Moreover, the maximum inhibitory effect of CA was achieved at 48 h while CS showed its strongest inhibitory activity after 72 h. According to the literature, both diterpenes have demonstrated different *in vitro* cytotoxic and cytostatic effects depending on the cell type, concentration, and time of exposition.[10,15,18] The parameter values obtained in the present study are in the same concentration range of most of the published data for other *in vitro* cell models of cancer.[13,18,40] As an example, Gigante et al. reported GI50 values ranging from 21.6 to 47.2 μM CA (~7.2–15.7 μg/mL) for five cancer cell lines.[40]

For comparison purposes, the antiproliferative activity of the RE at the three incubation times is also depicted in Figure 1. As it can be observed, RE exerts a stronger inhibitory activity on cell proliferation than the treatments with equivalent concentrations of CA at any incubation time. More evident was the superior activity of RE compared with CS since the content of this diterpene is 6.9-fold lower than CA content in the extract. From these results, it can be deduced that none of both diterpenes are, by themselves alone, responsible for the observed antiproliferative activity of the extract. Instead, the hypothesis that the inhibitory activity of RE on cell proliferation might be due to the combined effect of both diterpenes was tested. To explore this possibility, the synergistic, additive or antagonistic effects of a combination of both compounds, CA and CS, on inhibiting cell proliferation in HT-29 cell culture was examined.

Study of Potential Synergistic, Additive, or Antagonistic Effects of CA and CS on Proliferation of HT-29 Cells. In order to investigate the inhibitory activity of CA and CS combinations, HT-29 cells were incubated and tested by MTT assay for different incubation times in the presence of a range of CA (7.7–61.4 μg/mL) and CS (1.1–8.9 μg/mL) concentrations and mixtures with the same molar ratio of CA and CS (6.9:1) that exists in the RE. The calculated potency (Dm) value for the mixture (CA + CS) at 48 h was 11.2 μg/mL. Table S2 (Supporting Information) summarizes the fractional inhibition (fa, fraction affected) of cell proliferation, combination index (CI) values, and other parameters derived from the computer-generated functions of the CI with respect to fa for the antiproliferative activity of the mixture at different concentration levels. As it can be deduced from the CI values close to 1, the CA + CS combination exhibits an additive effect at 8.8 and 17.6 μg/mL total CA + CS concentrations, which correspond to RE concentrations of 30 and 60 μg/mL, respectively. Interestingly, a synergistic effect (CI < 1) was obtained with a 35.2 μg/mL total concentration of the mixture. However, this effect was not consistent over the range assayed as it can be deduced from data obtained at higher and lower total concentrations. As it can be observed in Figure 1D, the inhibitory activity of the CA + CS mixture on cell proliferation was lower, as compared to the one exerted by RE with an equivalent CA content. According to our data, CA pure solution and CA + CS mixture account for approximately 50% and 60% of the observed effect for 30 μg/mL RE for 48 h. These results suggest that although other constituents of the extract might be also contributing to the observed antiproliferative activity of RE on HT-29 cells, most of the observed antiproliferative activity of the extract is exerted by CA and CS. Furthermore, owing to its higher content in RE and slightly superior potency, CA was the most relevant of both diterpenes regarding the antiproliferative effect. Then, the cellular and molecular mechanisms underlying the antiproliferative activity of CA in HT-29 cells were investigated. Therefore, all the subsequent experiments were focused on the study of the bioactivity of this diterpene.

Effect of CA on Cell Viability and Cell Cycle Distribution. To elucidate whether the observed effect on cell proliferation from CA was due to a potential cytotoxic or cytostatic effect, trypan blue exclusion assay was used to determine cell viability after CA treatment. Using this method, it was observed that concentrations of 12.5 μg/mL of CA did not significantly affect cell viability, compared to control cells demonstrating no cytotoxicity of CA (data not shown). Similar

dx.doi.org/10.1021/ac502401j | Anal. Chem. 2014, 86, 9807–9815

results have been recently reported on the viability of three different colon cancer cell lines upon exposure to CA.[14] Next, to investigate the possible cytostaticity exerted by CA on HT-29, cell cycle distribution was characterized by flow cytometry analysis. Incubation of exponentially growing HT-29 cells with CA at 12.5 μg/mL for 24 h resulted in a substantial inhibition of cell cycle progression, manifested by the accumulation of cells in the G1 phase (p-value = 0.014), with a concomitant decrease in the percentage of cells in the S phase (p-value = 0.025) with respect to untreated control cells (Figure 2A). No

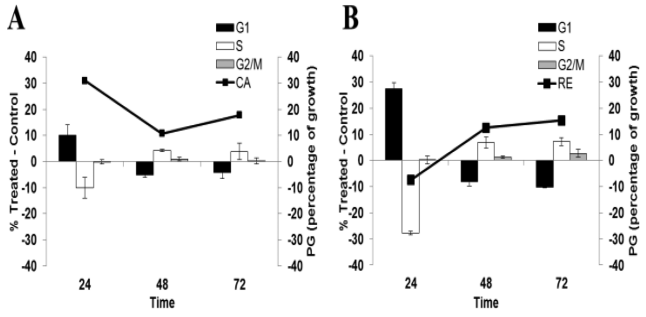

Figure 2. Cell cycle distribution patterns (bars) determined by flow cytometry and calculated percentage of growth (line) from MTT assay data of HT-29 cells exposed to 12.5 μg/mL of CA (A) and 30 μg/mL of RE, (B) for up to 72 h of incubation. Error bars are given as the standard error of the mean.

significant effect on the G2/M phase was detected. Interestingly, after longer incubation time of the exponentially growing cells with CA (48 and 72 h), a reversal of the changes in the cell cycle phase distribution was observed (see Figure 2A). Thus, at 48 h, the percentage of cells in the S phase increased significantly while decreased in the G1 phase with respect to the cell distribution at 24 h. This shift is in agreement with the partial recovery of cell proliferation observed at longer incubation times (see percentage of growth data in Figure 2A). A similar transient cell cycle block of the G1 to S phase transition at 24 h was observed when HT-29 cells were incubated with RE (Figure 2B). Interestingly, although CA concentration was higher in the assayed pure CA solution than in the RE (12.5 vs 7.7 μg/mL), such transient G1 arrest was quantitatively higher with RE than with CA treatment, suggesting that other compounds in the RE are contributing to the cell cycle arrest in the G1 phase. Moreover, the more pronounced G1 arrest obtained with RE in comparison with CA treatment correlates well with a higher and faster decrease of percentage of growth values, which reached a minimum at 24 h (Figure 2B). From these results, it can be concluded that CA and RE under the conditions assayed exert a cytostatic action, which is probably related to its ability to interfere with cell cycle progression during the initial 24 h of treatment. Although both treatments exert similar alterations on the cell cycle phases, the percentage of growth did not correlate equally in both treatments. Thus, the antiproliferative effect of CA was increasing over 48 h while with RE reached the maximum at 24 h and recovered afterward. In agreement with these results, similar effects on cell cycle and proliferation of leukemia cells have been reported with 7.5 μM (~2.5 μg/mL) of CA.[12] On the other side, the results obtained in the present study diverge, with the observations reported by Visanji et al. where 50 μM (~16.6 μg/mL) CA induced G2/M phase arrest in caco-2 cells at 24 h.[13] However, recent published data indicate that this divergence on the effect of CA on cell cycle distribution could be explained by its differential effect as a function of the assayed concentration and the cellular model selected for the study.[15]

Foodomics Study on the Effect of CA against Colon Cancer HT-29 Cells Proliferation. In order to identify potential changes at the transcriptional and metabolic levels in colon cancer HT-29 cells treated with CA, a Foodomics approach was applied. Our Foodomic platform was based on different analytical techniques and data processing for transcriptomic and metabolomic studies, allowing the determination of transcripts and metabolites that show statistically different expression in response to the CA treatment. First, gene expression microarray analyses were carried out in order to investigate the effect of CA treatment (9.9 μg/mL, 48 h) on the HT-29 cell line at the transcriptomic level. For gene expression microarray analysis, predefined FDR of 5% (p < 0.05) was applied to identify DEGs in response to the treatment. Accordingly, 341 genes, representing 1.2% of the genes covered by the whole-transcriptome microarray, were found to be differentially expressed in response to the CA exposure after 48 h. It could also be observed that most of the significantly altered genes (281 genes, i.e., 80% of the statistically significant ones) exhibited moderate (above 1.3 and below 0.8) expression ratios. In order to identify the biological processes that might be altered in treated cells compared to control cells, functional enrichment analysis on the list of identified DEGs was performed using IPA software setting an M value cutoff of 0.4, which corresponds to expression ratios (fold change) ≥ 1.3 for up-regulated and ≤0.8 for down-regulated genes (Supporting Information, Table S3). In these analyses, 213 genes from microarray data were eligible for biological function and pathway analysis. Functional analysis identified a number of significant (Fisher Exact test p-value < 0.05) over-represented canonical metabolic pathways in the imported data set that were associated with different degradation processes (see Figure 3). The examination of these results revealed altered expression of a number of

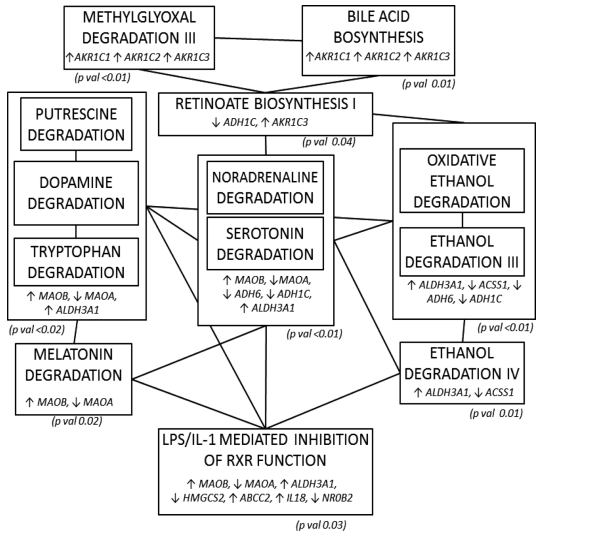

Figure 3. Overlapping of predominant canonical pathways and involved genes operating in HT-29 cells after 48 h exposure to 9.9 μg/mL CA, as inferred from IPA software. The arrows indicate an increase (↑) or decrease (↓) in the transcript levels. Significance p-values (between brackets) calculated with the right-tailed Fisher's exact test.

dx.doi.org/10.1021/ac502401j | Anal. Chem. 2014, 86, 9807−9815

enzyme-encoding genes with a reported role in interrelated pathways. For instance, MAOB and MAOA genes, whose expression was up- and down-regulated in treated cells, respectively, were involved in 7 different pathways. These genes, that encode amine oxidase enzymes with different substrate specificity, are reported to play a relevant role in the biogenic amines metabolism, and together with other amine oxidases are considered to be biological regulators, especially for cell growth and differentiation.[41] Moreover, reported evidence points to the generation of amine oxidase-mediated products (aldehydes, H_2O_2, and other reactive oxygen species (ROS)) of biogenic amines oxidation as the primary mode of action of these enzymes in cancer growth inhibition and progression.[42,43] Thus, deregulation of MAOA and MAOB genes may provide a putative link to mitochondrial dysfunction and, consequently, intensified ROS formation.[44] On the other side, CA treatment also induced the expression of genes encoding for enzymes capable of counteracting that effect by detoxifying H_2O_2 (GPX3 and GPX8 genes) and the transformation of aldehydes (ALDH3A1 gene) produced by monoamine oxidases. The latter gene, ALDH3A1, is also involved in ethanol degradation pathways, and connected with these pathways, the down-regulation of other three genes (ADH1C, ADH6, and ACSS1) was found statistically significant in treated cells (Figure 3). In addition to these genes related with detoxifying function, down-regulation of NOX1 gene, encoding for a NADPH oxidase 1, which catalyzes the production of ROS, was detected in treated cells. In Figure 3, it can be observed that LPS/IL-1 mediated inhibition of the RXR pathway is the connecting node of most of the degradation pathways provided by IPA to be altered by CA treatment. This signaling pathway involves the activity of nuclear receptors, such as Pregnane X receptor (PXR) and constitutive androstane receptor (CAR) among others that regulate the expression of MAOB and ALDH3A1 genes, respectively, suggesting modulation of xenobiotic metabolism function. Interestingly, the induction pattern of these genes was similar to the transcriptomic response of HT-29 cells treated with RE.[10] The gene expression ratios obtained by microarray were also confirmed by RT-qPCR (Supporting Information, Table S4).

The activation of NRF2-induced genes was patented by a remarkable up-regulation of several AKR1C genes (AKR1C1, AKR1C2, and AKR1C3). AKR1C genes encode for members of the aldo-keto reductase 1C superfamily, and their induction has been recently proposed as a marker for the sensitive determination of NRF2 activation.[45] These aldo-keto reductases exhibit broad substrate specificity for nonsteroidal carbonyl compounds including endogenous and xenobiotic toxic compounds; and therefore, it is not surprising to find them involved in more than one pathway (see Figure 3). For instance, these aldo-ketoreductases are suggested to be major enzymes that protect against cellular damage provoked by the cytotoxic aldehydes resulting from lipid peroxidation.[46]

In agreement with our data, a similar induction pattern of AKR1C genes together with other antioxidant response elements (ARE)-driven genes has been also observed in breast cancer cells after short exposure with 20 μg/mL CA,[15] which provides more evidence about the activity of CA as inducer of NRF2-mediated antioxidant response.[16] In addition to these studies, it is interesting to note that previous transcriptomic analyses in our laboratory have shown the prominent induction of AKR1C genes in colon cancer and leukemia cells in response to RE treatment.[7,10] *In vitro* studies have associated the induction of ARE-driven genes in a NRF2-dependent manner by CA with inhibition of adipocyte differentiation in mouse[47] and chemoprotection in glioblastoma cells.[48] Moreover, gene expression microarray analysis in studies with various *in vitro* cell models also corroborate that the induction of ARE genes, including genes that encode for phase II enzymes and enzymes involved in glutathione metabolism, is one of the main transcriptional responses in cells upon exposure to micromolar concentrations of CA.[47,49] In addition to the aforementioned analysis on the canonical pathways, IPA provided over-represented cellular and molecular functions that were predicted to be inhibited in treated cells (Table 1). According to *z*-scores obtained from IPA predictive analysis, transport of molecules, and metabolism of terpenoid functions could be significantly inhibited by the altered expression pattern of 11 and 4 genes, respectively, whereas a set of 9 genes suggested activation of the metabolism of ROS function.

Table 1. IPA Analysis of the Molecular and Cellular Functions Over-Represented in the List of Differentially Expressed Genes in HT-29 Cells after CA Treatment

annotation	*p*-val[a]	activation *z*-score	genes[b]
transport of molecules	5.10×10^{-04}	−2.379	↓CA2,↓CFTR,↓CLDN2, ↓EDN1,↓GPC3, ↓NDRG2,↓NR4A1, ↓SLC14A1,↓SLC16A7, ↓SLC5A1, ↓SLC7A2
metabolism of terpenoid	1.07×10^{-04}	−2.016	↓ADH1C,↓EDN1,↓NR4A1, ↓PRLR
metabolism of ROS	3.81×10^{-03}	+2.015	↓NR4A1,↑IL18, ↓HEPH, ↓SPRY2,↓SESN1, ↑MAOB, ↓mir-21, ↑IL8, ↑NCF1

[a]Significance value calculated with the right-tailed Fisher's exact test. [b]Arrows indicate an increase (↑) or decrease (↓) in the transcript levels.

For the metabolomic study, a combination of different analytical methodologies provided wide metabolic information and coverage due to its complementary nature. Namely, metabolic profiles from untreated and treated HT-29 cells with CA were determined using two complementary analytical platforms, CE−TOF MS and HILIC/UHPLC−TOF MS. Table 2 summarizes the 21 compounds with statistically significant (p-value < 0.05) altered levels in treated HT-29 cells with respect to the untreated cells. It is interesting to mention that only 2 out of the 21 metabolites were detected by both CE−TOF MS and UHPLC−TOF MS approaches, demonstrating the complementarity of these two metabolomic methodologies. The extracted ion electropherograms (EIEs) and extracted ion chromatograms (EICs) of some of the metabolites whose levels statistically changed by CA treatment are provided in Supporting Information (Figure S1). From the examination of the metabolite list given in Table 2, it was observed an increase of reduced glutathione (GSH) that was concomitant with a depletion of the oxidized form of glutathione (GSSG) in treated HT-29 cells. Furthermore, the calculated GSH/GSSG ratio was 6.4 in HT-29 exposed to CA while in control cells the ratio was 0.7. This elevation of GSH/GSSG ratio is in agreement with the reported chemopreventive activity of similar catechol-type electrophilic compounds as CA in other *in vitro* models.[16,47] Combined with transcriptomic data, these results may indicate higher GSH availability,

dx.doi.org/10.1021/ac502401j | *Anal. Chem.* 2014, 86, 9807−9815

Table 2. Differentially Expressed Metabolites in HT-29 Cells after CA Treatment

migration/retention time	m/z	ion	formula	error (ppm)	metabolite	standard coinjection	database identifier	expression
4.21[a]	131.118	M + H	C6H14N2O	−2.9	*N*-acetyl-putrescine	yes	HMDB02064	down
6.07[a]	104.070	M + H	C4H9NO2	−6.7	γ-aminobutyric acid	yes	HMDB00650	down
7.73[a]	298.096	M + H	C11H15N5O3S	−3.8	methyl-thio-adenosine	yes	HMDB01173	down
8.96[a]	179.049	M + H	C5H10N2O3S	4.5	cysteinyl-glycine	no	HMDB28775	up
8.32[a]	307.086	M + 2H	C20H32N6O12S2	8.5	oxidized glutathione	yes	HMDB03337	down
8.96[a]	308.092	M + H	C10H17N3O6S	1.8	reduced glutathione	yes	HMDB00125	up
7.28[a]	244.094	M + H	C9H13N3O5	5.5	cytidine	yes	HMDB00089	down
2.38[b]	456.246	M + NH_4	C14H22O3	5.0	oxo-tetradecadienoic acid	no	LMFA01060185	down
2.64[b]	306.059	M + K	C10H13N5O4	6.5	adenosine	yes	HMDB00050	down
2.70[b]	393.194	M + NH_4	C15H25N3O8	4.2	tripeptide (I/L, D, E)	no	MID20124	up
2.71[b]	161.092	M + H	C6H12N2O3	−3.7	alanyl-alanine	no	HMDB28680	down
3.21[b]	471.171	M + H	C23H26N4O5S1	−1.3	tripeptide (C, Y, W)	no	MID22112	down
3.28[b]	112.041	M + H	C5H5NO2	3.7	pyrrole-carboxylic acid	no	HMDB04230	down
3.40[b]	453.168	M + Na	C21H26N4O6	2.5	tripeptide (W, E, P)	no	MID 19517	down
3.42[b]	244.092	M + H	C9H13N3O5	3.3	cytidine	yes	HMDB00089	down
3.59[b]	455.176	M + H	C23H26N4O4S1	1.4	tripeptide (F, W, C)	no	MID18550	down
3.64[b]	327.324	M + H	C21H42O2	−6.1	dodecyl-nonanoate	no	LMFA07010453	up
5.79[b]	274.201	M + H	C14H27NO4	−0.8	heptanoyl-carnitine	no	HMDB13238	down
6.48[b]	127.123	M + H − H_2O	C7H16N2O	4.8	*N*-acetyl-cadaverine	yes	HMDB02284	down
6.81[b]	308.092	M + H	C10H17N3O6S	−0.5	reduced glutathione	yes	HMDB00125	up
7.00[b]	162.115	M + H	C7H15NO3	−1.9	carnitine	yes	HMDB00062	up

[a]Identified metabolites from CE−ESI-TOF MS analysis. [b]Identified metabolites from UHPLC−ESI-TOF MS analysis.

necessary for the activity of GPXs gene products, up-regulated by CA treatment, suggesting an enhanced detoxifying cellular capability. In the last years, accumulating evidence from *in vitro* studies suggests that the balance between amine-oxidizing enzymes and antioxidant enzymes appears to be a crucial point for cancer growth inhibition or progression.[41,44] Other data that can be potentially related to the antiproliferative activity of CA in HT-29 cells included decreased levels of *N*-acetylputrescine, *N*-acetylcadaverine, and γ-aminobutyric acid, derived from polyamine metabolism. Polyamine metabolism is involved in important cellular processes including cell proliferation and viability, and its alteration in colon cancer cells has been already linked to RE exposure.[24]

Interestingly, another potential link was found between transcriptomic and metabolomic data sets in the Putrescine degradation pathway that predicted *N*-acetylputrescine depletion. This metabolic change could be explained in silico by the up-regulation of the MAOB gene product, involved in the enzymatic transformation of *N*-acetylputrescine to 4-acetamidobutanal, that can be further transformed to 4-acetamidobutanoate by the ALDH1A3 gene product (also induced by the CA treatment). Metabolomics data also indicated a decrease in methylthioadenosine and adenosine levels. Recently, chemically induced inhibition of polyamine metabolism in HT-29 cells has been associated with unexpected changes in these methionine cycle intermediates and a decrease in the nucleoside thymidine pool, causing a cytostatic effect.[50] In the present study, a significant intracellular depletion of the nucleoside cytidine by CA treatment was corroborated by both analytical platforms. Further investigations are required to elucidate the role and the underling mechanisms of the effect of cytidine pool depletion in HT-29 cell proliferation.

CONCLUSIONS

In summary, the results of the present study reveal that CA and CS exhibit an additive antiproliferative effect on colon cancer HT-29 cells when they are combined in solution at a molar ratio of 6.9:1. With regard to CA, our observations indicate that a concentration close to the 50% growth inhibition causes a transient cell cycle block of G1 to the S phase that may explain the cytostatic activity of this diterpene in HT-29 cells. Also, CA induced transcriptional activation of genes that encode detoxifying enzymes in the colon cancer cell line. These findings are consistent with the reported NRF2 activation effect from CA. In addition, CA treatment altered the expression of genes linked to other relevant functions such as transport and biosynthesis of terpenoids. Furthermore, functional analysis highlighted the activation of the ROS metabolism and alteration of several genes involved in pathways describing oxidative degradation of relevant endogenous metabolites, providing new evidence about the transcriptional variation of HT-29 cells in response to the CA exposure. Metabolomics analysis showed that treatment with CA affected the intracellular levels of glutathione. Elevated levels of GSH provided additional evidence to transcriptomic results regarding chemopreventive response of cells to CA treatment. Moreover, the Foodomics approach was useful to establish the links between decreased levels of *N*-acetylputrescine and its degradation pathway at the gene level. The findings from this work as well as the predictions based on microarray data will allow exploring novel metabolic processes and potential signaling pathways to elucidate the effect of CA in colon cancer cells. Last but not least, this novel Foodomics strategy, combining transcriptomics, metabolomics, and bioinformatics, provides a remarkable analytical power, and it is expected to help to overcome many of the new challenges emerging in food science and nutrition, particularly in the research field of bioactive food ingredients

■ ASSOCIATED CONTENT

Supporting Information

Additional information as indicated in text. This material is available free of charge via the Internet at http://pubs.acs.org.

■ AUTHOR INFORMATION

Corresponding Author

*E-mail: virginia.garcia@csic.es.

Author Contributions

The manuscript was written through contributions of all authors. All authors have given approval to the final version of the manuscript.

Notes

The authors declare no competing financial interest.

■ ACKNOWLEDGMENTS

This work was supported by an AGL2011-29857-C03-01 project (Ministerio de Educacion y Ciencia, Spain). A.V. thanks the Ministerio de Economía y Competitividad for his FPI predoctoral fellowship.

■ REFERENCES

(1) Aruoma, O. I.; Halliwell, B.; Aeschbach, R.; Loligers, J. *Xenobiotica* **1992**, *22*, 257−268.
(2) European Food Safety Authority.. *EFSA J.* **2008**, *721*, 1−29.
(3) Yu, M. H.; Choi, H. H.; Chae, I. G.; Im, H. G.; Yang, S. A.; More, K.; Lee, I. S.; Lee, H. *Food Chem.* **2013**, *136*, 1047−1054.
(4) Singletary, K. W.; Rokused, J. T. *Plant Foods Hum. Nutr.* **1997**, *50*, 47−53.
(5) Gutierrez, R.; Alvarado, J. L.; Presno, M.; Pérez-Veyna, O.; Serrano, C. J.; Yahuaca, P. *Phytother. Res.* **2010**, *24*, 595−601.
(6) Ngo, S. N.; Williams, D. B.; Head, R. J. *Crit. Rev. Food Sci. Nutr.* **2011**, *51*, 946−954.
(7) Valdés, A.; Simó, C.; Ibáñez, C.; Rocamora-Reverte, L.; Ferragut, J. A.; García-Cañas, V.; Cifuentes, A. *Electrophoresis* **2012**, *33*, 2314−2327.
(8) Tsai, C. W.; Lin, C. Y.; Lin, H. H.; Chen, J. H. *Neurochem. Res.* **2011**, *36*, 2442−2451.
(9) Vicente, G.; Molina, S.; González-Vallinas, M.; García-Risco, M. R.; Fornari, T.; Reglero, G.; Ramírez de Molina, A. *J. Supercrit. Fluids* **2013**, *79*, 101−108.
(10) Valdés, A.; García-Cañas, V.; Rocamora-Reverte, L.; Gómez-Martínez, A.; Ferragut, J. A.; Cifuentes, A. *Genes Nutr.* **2013**, *8*, 43−60.
(11) Petiwala, S. M.; Puthenveetil, A. G.; Johnson, J. J. *Front. Pharmacol.* **2013**, *4*, 1−4 article 29.
(12) Steiner, M.; Priel, I.; Giat, J.; Levy, J.; Sharoni, Y.; Danilenko, M. *Nutr. Cancer* **2001**, *41*, 135−144.
(13) Visanji, J. M.; Thompson, D. G.; Padfield, P. J. *Cancer Lett.* **2006**, *237*, 130−136.
(14) Barni, M. V.; Carlini, M. J.; Cafferata, E. G.; Puricelli, L.; Moreno, S. *Oncol. Rep.* **2012**, *27*, 1041−1048.
(15) Einbond, L. S.; Wu, H.; Kashiwazaki, R.; He, K.; Roller, M.; Su, T.; Wang, X.; Goldsberry, S. *Fitoterapia* **2012**, *83*, 1160−1168.
(16) Satoh, T.; Kosaka, K.; Itoh, K.; Kobayahi, A.; Yamamoto, M.; Shimojo, Y.; Kitajima, C.; Cui, J.; Kamins, J.; Okamoto, S.; Izumi, M.; Shirasawa, T.; Lipton, A. S. *J. Neurochem.* **2008**, *104*, 1116−1131.
(17) Kayashima, T.; Matsubara, K. *Biosci., Biotechnol., Biochem.* **2012**, *1*, 115−119.
(18) Yesil-Celiktas, O.; Sevimli, C.; Bedir, E.; Vardar-Sukan, F. *Plant Foods Hum. Nutr.* **2010**, *65*, 158−163.
(19) Herrero, M.; Simó, C.; García-Cañas, V.; Ibáñez, E.; Cifuentes, A. *Mass Spectrom. Rev.* **2010**, *31*, 49−69.
(20) Castro-Puyana, M.; García-Cañas, V.; Simó, C.; Cifuentes, A. *Electrophoresis* **2012**, *33*, 147−167.
(21) García-Cañas, V.; Simó, C.; Herrero, M.; Ibáñez, E.; Cifuentes, A. *Anal. Chem.* **2012**, *84*, 10150−10159.
(22) Ibáñez, C.; Simó, C.; García-Cañas, V.; Cifuentes, A.; Castro-Puyana, M. *Anal. Chim. Acta* **2013**, *802*, 1−13.
(23) García-Cañas, V.; Simó, C.; Castro-Puyana, M.; Cifuentes, A. *Electrophoresis* **2014**, *35*, 147−169.
(24) Ibáñez, C.; Simó, C.; García-Cañas, V.; Gómez-Martínez, A.; Ferragut, J. A.; Cifuentes, A. *Electrophoresis* **2012**, *33*, 2328−2336.
(25) Ibáñez, C.; Valdés, A.; García-Cañas, V.; Simó, C.; Celebier, M.; Rocamora-Reverte, L.; Gómez-Martínez, A.; Herrero, M.; Castro-Puyana, M.; Segura-Carretero, A.; Ibáñez, E.; Ferragut, J. A.; Cifuentes, A. *J. Chromatogr., A* **2012**, *1248*, 139−153.
(26) Herrero, M.; Plaza, M.; Cifuentes, A.; Ibáñez, E. *J. Chromatogr., A* **2010**, *1217*, 2512−2520.
(27) Monks, A.; Scudiero, D.; Skehan, P.; Shoemaker, R.; Paull, K.; Vistica, D.; Hose, C.; Langley, J.; Cronise, P.; Vaigro-Wolff, A.; Gray-Goodrich, M.; Campbell, H.; Mayo, J.; Boyd, M. *J. Natl. Cancer Inst.* **1991**, *83*, 757−766.
(28) Chou, T. C.; Talalay, P. *Adv. Enzyme Regul.* **1984**, *22*, 27−55.
(29) Gentleman, R.; Carey, V. J.; Bates, D. M.; Bolstad, B.; Dettling, M.; Dudoit, S.; Ellis, B.; Gautier, L.; Ge, Y.; Gentry, J.; Hornik, K.; Hothorn, T.; Huber, W.; Iacus, S.; Irizarry, R.; Leisch, F.; Li, C.; Maechler, M.; Rossini, A. J.; Sawitzki, G.; Smith, C.; Smyth, G.; Tierney, L.; Yang, J.; Zhang, J. *Genome Biol.* **2004**, *5*, R80.
(30) Smyth, G. K. Limma: Linear Models for Microarray Data. In *Bioinformatics and Computational Biology Solutions using R and Bioconductor*; Gentleman, R., Carey, V., Dudoit, S., Irizarry, R., Huber, W., Eds.; Springer: New York, 2005; pp 397−420.
(31) Benjamini, Y.; Hochberg, Y. *J. R. Stat. Soc. B* **1995**, *57*, 289−300.
(32) Katajamaa, M.; Oresic, M. *BMC Bioinf.* **2005**, *6*, 179.
(33) Ibáñez, C.; Simó, C.; Martín-Álvarez, P. J.; Kivipelto, M.; Winblad, B.; Cedazo-Mínguez, A.; Cifuentes, A. *Anal. Chem.* **2012**, *84*, 8532−8540.
(34) Smith, C.; Want, E. J.; O'Maille, G.; Abagyan, T.; Siuzdak, G. *Anal. Chem.* **2006**, *78*, 779−787.
(35) Scheltema, R. A.; Jankevics, A.; Jansen, R. C.; Swertz, M. A.; Breitling, R. *Anal. Chem.* **2011**, *83*, 2786−2793.
(36) Ibáñez, C.; Simó, C.; Barupal, D. K.; Fiehn, O.; Kivipelto, M.; Cedazo-Mínguez, A.; Cifuentes, A. *J. Chromatogr., A* **2013**, *1302*, 65−71.
(37) Wishart, D. S.; Knox, C.; Guo, A. C.; Eisner, T.; Young, N.; Gautam, B.; Hau, D. D.; Psychogios, N.; Dong, E.; Bouatra, S.; Mandal, R.; Sinelnikov, I.; Xia, J.; Jia, L.; Cruz, J. A.; Lim, E.; Sobsey, C. A.; Shrivastava, S.; Huang, P.; Liu, P.; Fang, L.; Peng, J.; Fradette, R.; Cheng, D.; Tzur, D.; Clements, M.; Lewis, A.; De Souza, A.; Zuniga, A.; Dawe, M.; Xiong, Y.; Clive, D.; Greiner, R.; Nazyrova, D.; Shaykhutdinov, R.; Li, L.; Vogel, H. J.; Forsythe, I. *Nucleic Acids Res.* **2009**, *37*, D603.
(38) Smith, C. A.; O'Maille, G.; Want, E. J.; Qin, C.; Trauger, S. A.; Brandon, T. R.; Custodio, D. E.; Abagyan, R.; Siuzdak, G. *Ther. Drug Monit.* **2005**, *27*, 747−751.
(39) Kanehisa, M.; Araki, M.; Goto, S.; Hattori, M.; Hirakawa, M.; Itoh, M.; Katayama, T.; Kawashima, S.; Okuda, S.; Tokimatsu, T.; Yamanishi, Y. *Nucleic Acids Res.* **2008**, *36*, D480.
(40) Gigante, B.; Santos, C.; Silva, A. M.; Curto, M. J. M.; Nascimento, M. S. J.; Pinto, E.; Pedro, M.; Cerqueira, F.; Pinto, M. M.; Duarte, M. P.; Laires, A.; Rueff, J.; Gonçalves, J.; Pegado, M. I.; Valdeira, M. L. *Bioorg. Med. Chem.* **2003**, *11*, 1631−1638.
(41) Toninello, A.; Pietrangeli, P.; De Marchi, U.; Salvi, M.; Mondovì, B. *Biochim. Biophys. Acta* **2006**, *1765*, 1−13.
(42) Henle, K. J.; Moss, A. J.; Nagle, W. A. *Cancer Res.* **1986**, *46*, 175−182.
(43) Bachrach, U.; Ash, I.; Abu-Elheiga, L.; Hershkovitz, M.; Loyter, A. *J. Cell Physiol.* **1987**, *131*, 92−98.
(44) Agostinelli, E.; Tempera, G.; Molinari, A.; Salvi, M.; Battaglia, V.; Toninello, A.; Arancia, G. *Amino Acids* **2007**, *33*, 175−187.
(45) Jung, K. A.; Choi, B. Y.; Nam, C. W.; Song, M.; Kim, S. T.; Lee, J. Y.; Kwak, M. K. *Toxicol. Lett.* **2013**, *218*, 39−49.
(46) Burczynski, M. E.; Sridhar, G. R.; Palackal, N. T.; Penning, T. M. *J. Biol. Chem.* **2001**, *276*, 2890−2897.

(47) Takahashi, T.; Tabuchi, T.; Tamaki, Y.; Kosaka, K.; Takikawa, Y.; Satoh, T. *Biochem. Biophys. Res. Commun.* **2009**, *382*, 549−554.
(48) Kosaka, K.; Mimura, J.; Itoh, K.; Satoh, T.; Shimojo, Y.; Kitajima, C.; Maruyama, A.; Yamamoto, M.; Shirasawa, T. *J. Biochem.* **2010**, *147*, 73−81.
(49) Tamaki, Y.; Tabuchi, T.; Takahashi, T.; Kosaka, K.; Satoh, T. *Planta Med.* **2010**, *76*, 683−688.
(50) Witherspoon, M.; Chen, Q.; Kopelovich, L.; Gross, S. S.; Lipkin, S. M. *Cancer Discovery* **2013**, *3*, 1072−1081.

3.2.4 Rosemary polyphenols induce unfolded protein response and changes in cholesterol metabolism in colon cancer cells

Valdés, A., Sullini, G., Ibáñez, E., Cifuentes, A., *García-Cañas, V. *J. Funct. Foods* 2015, *15*, 429 - 439.

DOI: http://dx.doi.org/doi:10.1016/j.jff.2015.03.043

Journal of Functional Foods 15 (2015) 429–439

Available online at www.sciencedirect.com

ScienceDirect

journal homepage: www.elsevier.com/locate/jff

Rosemary polyphenols induce unfolded protein response and changes in cholesterol metabolism in colon cancer cells

Alberto Valdés, Giuseppe Sullini, Elena Ibáñez, Alejandro Cifuentes, Virginia García-Cañas *

Laboratory of Foodomics, Institute of Food Science Research (CIAL, CSIC), Calle Nicolás Cabrera 9, Madrid 28049, Spain

ARTICLE INFO

Article history:
Received 20 February 2015
Received in revised form 18 March 2015
Accepted 19 March 2015
Available online 17 April 2015

Keywords:
Carnosic acid
Colon cancer
Foodomics
Rosemary
Transcriptomics
Unfolded protein response

ABSTRACT

Several studies have demonstrated that rosemary polyphenols exert changes in the lipid metabolism in adipose and hepatic cells. In this work, the effects of a polyphenol-enriched supercritical rosemary extract (SC-RE) and carnosic acid (CA) on the transcriptome and cholesterol metabolism in HT-29 colon cancer cells were examined using a Foodomics approach. Targeted metabolomics analysis indicated that the SC-RE treatment induced cholesterol accumulation after 24 h. Transcriptomic analysis suggested that most of the changes induced by the SC-RE and CA were orchestrated by unfolded protein response (UPR) and triggered by endoplasmic reticulum stress. Results suggested up-regulation of VLDLR gene as the principal contributor to the observed cholesterol accumulation in SC-RE-treated cells. In addition, the SC-RE attenuated the activity of *E2F* transcription factor, down-regulating several genes involved in G1–S transition of the cell cycle.

1. Introduction

Rosemary (*Rosmarinus officinalis L.*) polyphenols possess numerous desirable characteristics, including antioxidant, anti-inflammatory and chemoprotective activities for the prevention or treatment of diseases (Ben Jemia et al., 2013; Johnson, 2011; Xiang et al., 2013). In the last few years, many reports have demonstrated the *in vitro* antiproliferative activity of rosemary polyphenols in several cancer cell models (Petiwala, Puthenveetil, & Johnson, 2013; Tsai, Lin, Lin, & Chen, 2011; Valdés et al., 2012). Regarding colon cancer, despite investigations on rosemary polyphenols in the last years, most *in vitro* studies use targeted traditional biological approaches (biochemical analysis of specific compounds) trying to understand the molecular mechanisms of their antiproliferative activities.

* *Corresponding author*. Laboratory of Foodomics, Institute of Food Science Research (CIAL, CSIC), Calle Nicolás Cabrera 9, 28049 Madrid, Spain. Tel.: +34 910 017 950; fax: +34 910 017 905.
E-mail address: virginia.garcia@csic.es (V. García-Cañas).

Abbreviations: CA, carnosic acid; DCF-DA, 2′,7′-dichlorofluorescin diacetate acetyl ester; DEGs, differentially expressed genes; ER, endoplasmic reticulum; ERAD, ER-associated degradation; FC, free cholesterol; FDR, false discovery ratio; IPA, ingenuity pathway analysis; ROS, reactive oxygen species; SC-RE, supercritical rosemary extract; SIM, selected ion monitoring; TC, total cholesterol; UPR, unfolded protein response; UR, upstream regulator

http://dx.doi.org/10.1016/j.jff.2015.03.043
1756-4646/

Following this common strategy, a broad range of cellular and molecular effects of these compounds have been described in the literature (Barni, Carlini, Cafferata, Puricelli, & Moreno, 2012; Yana, Lia, Petiwala, Householter, & Johnson, 2015). In addition, the application of novel Foodomics approaches (García-Cañas, Simó, Herrero, Ibáñez, & Cifuentes, 2012) for the comprehensive analysis of different *in vitro* cancer cell models have demonstrated that rosemary polyphenols exert substantial modulation of the transcriptome and metabolome (Ibáñez, Simó et al., 2012; Ibáñez, Valdés et al., 2012). This general conclusion in all these studies supports the idea that the underlying mechanisms of action of rosemary extracts are diverse and complex, not only because of the reported pleiotropic cellular and molecular effects of some of the major constituents, but also for the presence of other compounds with unknown bioactivities.

Recently, novel bioactivities of rosemary extracts and the two major phenolic diterpenes present in rosemary, i.e., carnosic acid (CA) and carnosol, have been linked to glucose and lipid metabolism. In this regard, studies on different animal models indicate that rosemary polyphenols limit lipid absorption *in vivo* through their inhibitory activity against lipase (Ibarra et al., 2011), and protect against steatosis by reducing fasting plasma triacylglycerol and cholesterol levels (Wang et al., 2011). Different studies, although reporting contrasting results, suggest that rosemary extracts and some of their major compounds regulate the activity of different master transcriptional regulators of cell metabolism such as *PPARγ*, *C/ebpα*, and *C/ebpβ* (Gaya et al., 2013; Ibarra et al., 2011). Despite recent *in vivo* and *in vitro* studies that have provided significant insight into the mechanisms underlying the antiadipogenic effect of rosemary compounds in adipose and hepatic cells, very limited information is available about the effect of these compounds on lipid metabolism in cancer cells. Altered lipid metabolism has long been recognized as an important feature of cancer cell metabolic reprogramming and a prerequisite for the rapid proliferation rates (Santos & Schulze, 2012). Indeed, inhibition of cholesterol and fatty acid biosynthesis pathways constitute an important strategy to block cancer cell growth (Abramson, 2011). Previous results obtained in our laboratory, using gene expression microarrays, have shown that rosemary polyphenols alter expression of various genes involved in cholesterol biosynthesis, trafficking and metabolism in colon cancer cells (data not shown). Thus, it is tempting to speculate (based on these observations) that some rosemary polyphenols may also exert modulating effects on cholesterol metabolism in colon cancer cells. In order to explore this aspect and its potential connection with the antiproliferative activity of rosemary compounds, in this work, colon cancer cells were treated with CA and a SC-RE enriched in CA and their effect on cholesterol metabolism and transcriptome was investigated. The relations between the observed metabolic changes and the transcriptional responses in colon cancer cells after the mentioned treatments can provide crucial information on the molecular mechanisms behind the observed changes in metabolism and cell proliferation. To attain this, a Foodomics approach, based on targeted metabolomics, transcriptomics and bioinformatics tools, is applied to analyze the different levels of information obtained from HT-29 colon cancer cells exposed to CA and the SC-RE.

2. Materials and methods

2.1. Standards and supercritical rosemary extract samples

CA and cholesterol were purchased from Sigma (St. Louis, MO, USA); ergosterol was purchased from Acros Organics (Geel, Belgium). SC-RE was obtained from dried rosemary leaves using supercritical CO_2 and 7% ethanol at 150 bar as reported in Sánchez-Camargo et al. (2014). Chemical characterization of the SC-RE indicated that two main diterpenes, CA and carnosol, were found at high concentrations in the extract, namely, 363.3 and 45.6 μg/mg extract, respectively. The chromatographic analysis of the SC-RE is shown in Supplementary Fig. S1. Dry extract and standards samples were dissolved in dimethyl sulfoxide (DMSO) at 30 mg/mL and 100 mM, respectively, and stored as aliquots at –80 °C until use.

2.2. Cell culture conditions

Colon adenocarcinoma HT-29 cells obtained from ATCC (American Type Culture Collection, LGC Promochem, Middlesex, UK) were grown in McCoy's 5A supplemented with 10% heat-inactivated fetal calf serum, 50 U/mL penicillin G, and 50 U/mL streptomycin, at 37 °C in humidified atmosphere and 5% CO_2. When cells reached ~50% confluence, they were trypsinized, neutralized with culture medium, plated in different culture plates at 10,000 cells/cm^2 and allowed to adhere overnight at 37 °C.

2.3. Cell proliferation assays and cell cycle flow cytometry analysis

Cell viability was determined using the MTT assay. Briefly, cells were treated with the vehicle, CA (12.5 μg/mL) or SC-RE (30 μg/mL) for 24–72 h followed by incubation with 0.5 mg/mL MTT solution at 37 °C for 3 h. The medium was removed, and the purple formazan crystals were dissolved in dimethyl sulfoxide. The absorbance was measured at 570 nm. For cell cycle analysis, cells were treated with the vehicle, CA (12.5 μg/mL) or SC-RE (30 μg/mL) for 24 h, and then trypsinized, washed with PBS, and fixed with 70% cold ethanol at –20 °C for at least 24 h. Fixed cells were resuspended in 0.5 mL of PI/RNase staining buffer (BD Pharmingen, San Jose, CA, USA), incubated for 15 min in the dark, and analyzed on a Gallios flow cytometer equipped with a 0.75 W argon laser set at 488 nm (Beckman Coulter, Miami, FL, USA).

2.4. Cholesterol analysis by GC–MS

Total cholesterol (TC) and free cholesterol (FC) levels were measured on HT-29 cells exposed to 30 μg/mL of SC-RE or 12.5 μg/mL of CA for 0–72 h. After incubation, cells were trypsinized and centrifuged at 300 × *g* for 5 min at 25 °C. The supernatant was discarded and cell pellets were washed with PBS and further centrifuged. To obtain cellular lipids, the pellets were treated according to Folch method (Folch, Lees, & Sloane-Stanley, 1957) using chloroform/methanol (2:1, v/v), and ergosterol was used as internal standard. Each extract was dried under N_2, dissolved

in 2 mL of $CHCl_3$ and divided equally into two aliquots. One aliquot was saponified for quantification of TC by adding 1 mL of 0.05 M KOH in ethanol for 2 hours and afterwards, 2 mL of a saturated sodium chloride solution. After saponification, sterols were extracted with 2 mL of n-hexane for three times, and then dried with anhydrous Na_2SO_4, filtered, evaporated and solubilized in 1 mL of chloroform. A total volume of 100 μL of both saponified (TC) and non-saponified (FC) aliquots were evaporated and resuspended in 50 μL of the reagent N-Methyl-N-(trimethylsilyl) trifluoroacetamide (Sigma) for derivatization. Reaction was performed at 60 °C for 30 min and the samples were transferred to vials for direct injection. Cholesterol analysis was performed using a GCMS-QP2010 Plus system (Shimadzu, Kyoto, Japan), equipped with a DB-5ms column (30 m × 0.25 mm I.D. × 0.25 μm df, Quadrex Corporation, Woodbridge, CT, USA). Column temperature was set at 100 °C, held for 1 min, and then raised to 250 °C at 20 °C/min and held for 2 min. Finally, the temperature was raised to 300 °C at 10 °C/min and held for 30 min. Split injection (2 μL) with a split ratio of 1:10 was used; injection temperature was set at 250 °C. High purity helium was used as carrier gas of 0.79 mL min^{-1}. The interface and source temperatures were 280 and 250 °C, respectively. The mass spectrometer was operated in selected ion monitoring (SIM) mode. Cholesterol was identified based on its retention time and mass patterns; ions having m/z 368.3 and 363.3 were selected as quantification ions and 329.3 and 337.3 as confirmation ions for cholesterol and ergosterol, respectively. Quantification of cholesterol was carried out using the internal standard procedure.

2.5. *Gene expression microarray analysis*

Comparative transcriptomic analysis was performed on HT-29 cells incubated with 12.5 μg/mL of CA and 30 μg/mL of SC-RE for 24 h, and their respective untreated controls. Total RNA was isolated from cells using TRIzol Plus RNA Kit (Invitrogen, Barcelona, Spain) according to manufacturer protocol. Microarray analyses and data processing were performed in triplicate using Human Gene 2.0ST chips (Affymetrix, High Wycombe, UK) as previously described (Valdés et al., 2013). To identify the statistically most significant changes in gene expression, microarray data were subjected to gene filtering based on the statistical significance (false discovery ratio, FDR, applied on moderated t statistics, adjusted p value < 0.05). Raw and normalized data of microarray analysis were submitted to the Gene Expression Omnibus database and are accessible through GEO Series accession number GSE65722 (http://www.ncbi.nlm.nih.gov/geo/query/acc.cgi?acc=GSE65722). The lists of differentially expressed genes (DEGs) identified in microarray analyses were uploaded in the bioinformatics tool Ingenuity Pathway Analysis (IPA; Qiagen, Redwood City, CA, USA) to perform Upstream Regulator (UR) analysis. In UR analysis, upstream regulators are considered as those molecules (transcription factors, ligand-dependent nuclear receptor, kinases, etc.) that can affect the expression of another gene (molecule). The activation state for each regulator was predicted based on global direction of changes in a given experimental condition (i.e., CA and SC-RE treatments vs control) for previously published targets of this regulator. Significance of the activation or deactivation of molecules predicted by UR analysis was tested by the Fisher Exact test p-value, considering only the predictions with significant p-value <0.05, and regulation z-score <–2 or >2, for deactivation and activation, respectively.

2.6. *RT-PCR analysis*

Starting amounts of 0.5 μg of total RNA isolated from cells were reverse transcribed using Transcriptor First Strand cDNA Synthesis kit with oligo(dT) primers (Roche Diagnostics, Barcelona, Spain). Each real-time quantitative PCR reaction was performed using ViiA™ 7 Real-Time PCR System (Life Technologies, Alcobendas, Spain); LightCycler® 480 Probes Master kit and Human UPL probes (Roche Diagnostics). Amplification systems are summarized in Supplementary Table S1. Two endogenous control genes (GAPDH and IPO8) were used to normalize the relative expression of target genes in treated cells compared to that of control cells. Relative Expression Software Tool (Pfaffl, Horgan, & Dempfle, 2002) with a randomization test method was applied to calculate expression ratios. Results are shown as the mean expression ratio of the target genes ± 95% C.I. of three independent experiments (see below).

2.7. *Determination of intracellular ROS*

For the measurement of intracellular ROS, cells were treated with CA or SC-RE for different times. The intracellular ROS levels were determined by flow cytometry using the oxidation-sensitive fluorescent probe 2′,7′-dichlorofluorescin diacetate acetyl ester (DCF-DA) (Sigma). Briefly, cells were loaded with 10 μM of DCF-DA dissolved in McCoy's 5A phenol red free and incubated for 30 min in the dark at 37 °C. For each analysis, 20,000 events were recorded. Results are shown as the mean of the log mean fluorescence intensity relative to control ± SEM of three independent experiments. The results were analyzed using a Student's t-test and differences were considered significant at $p < 0.05$.

3. Results

3.1. *SC-RE and CA inhibit proliferation of HT-29 cells and arrest cell cycle in G1/S*

The inhibitory effect of SC-RE and CA on HT-29 cell proliferation and cell cycle progression was confirmed by MTT assay and flow cytometry. Namely, incubation of exponentially growing HT-29 cells with SC-RE at 30 μg/mL and CA at 12.5 μg/mL resulted in inhibition of cell proliferation (Fig. 1A) and cell cycle arrest in the G1 phase at 24 h (Fig. 1B), in good agreement with our former results (Valdés et al., 2014).

3.2. *Effect of SC-RE and CA on cholesterol levels in HT-29 cells*

Because previous microarray data indicated the simultaneous differential expression in SC-RE-treated HT-29 cells of genes related with cholesterol biosynthesis, trafficking, and metabolism (data not shown), the effect of SC-RE (and CA) on

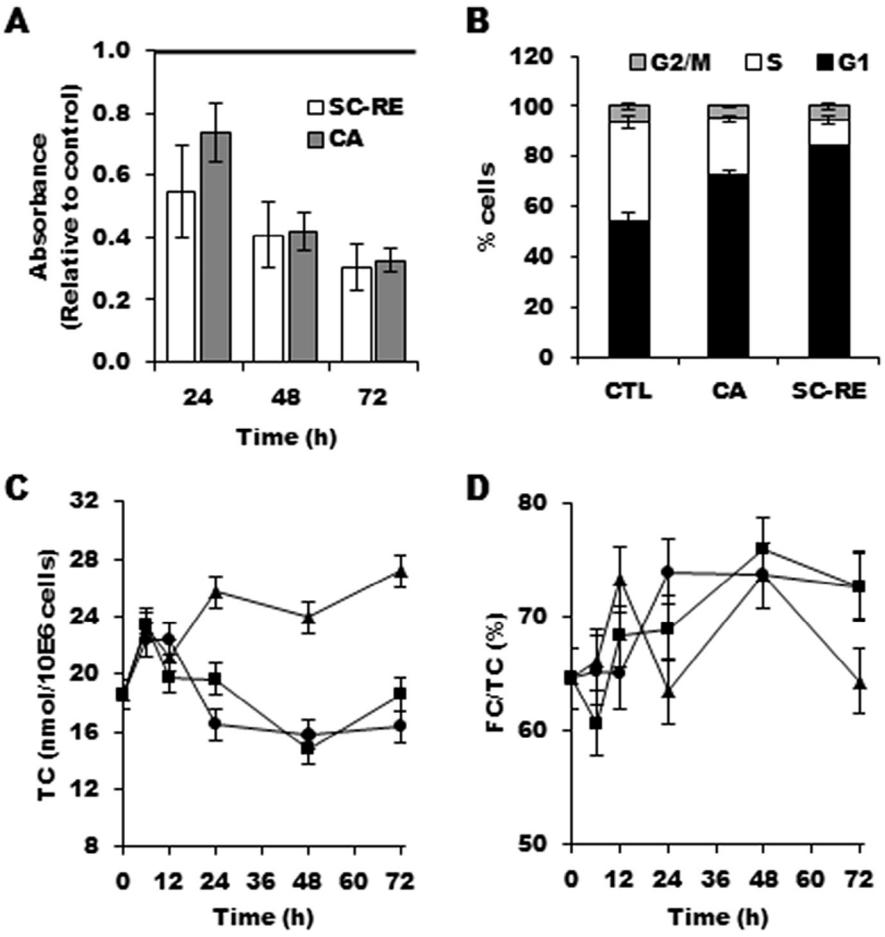

Fig. 1 – Effect of 30 μg/mL of SC-RE and 12.5 μg/mL of CA on (A) HT-29 cell proliferation at different time points; and (B) cell cycle progression at 24 h (CTL: control). (C) Time-dependent variation of total cholesterol, TC content (nmol/10^6 cells), and (D) Free cholesterol/Total cholesterol, FC/TC, (%) ratio. Untreated control cells (circles), cells exposed to 30 μg/mL of SC-RE (triangles) and 12.5 μg/mL of CA (squares). Error bars are given as the 95% CI of three independent experiments.

cholesterol metabolism in HT-29 cells was further investigated. As shown in Fig. 1C, treatment with 30 μg/mL of SC-RE significantly increased TC levels from 24 to 72 h by approximately 60%, compared to the control. By contrast, 12.5 μg/mL of CA only induced a slight but significant increase in TC levels at 24 h. The effects of SC-RE and CA treatments on the free and ester cholesterol levels were investigated. As it is shown in Fig. 1D, control and CA-treated cells showed similar trend for the calculated free cholesterol/total cholesterol, FC/TC, ratios over the time period of the experiment. On the contrary, FC/TC ratios changed significantly at different time points compared to controls when HT-29 cells were treated with SC-RE.

3.3. *SC-RE and CA induce extensive changes at mRNA level*

A gene expression microarray experiment was performed to assess the effects of rosemary polyphenols on the transcriptome of HT-29 cells following the mentioned treatments (i.e., 24 h with 30 μg/mL of SC-RE and 12.5 μg/mL of CA). To identify DEGs as a factor of treatment, pairwise comparisons were made between each treatment and control cells. Predefined FDR of 5% ($p < 0.05$) and M-value (log ratio) cutoff of 0.6, that corresponds to expression ratios ≥1.52 for up-regulated and ≤ 0.66 for down-regulated genes were applied to identify DEGs in each data set. Using these filtering criteria, 2340 and 636 annotated genes were found to be differentially expressed in response to the SC-RE and CA exposures, respectively (Supplementary Tables S2 and S3). To explore and characterize the molecular mechanisms underlying the effects of SC-RE and CA on proliferation and lipids metabolism, UR analysis was completed using IPA bioinformatics tool (Table 1). Coincident with previous studies, UR analysis predicted activation of *Nrf2* transcription factor (encoded by NFE2L2 gene) in SC-RE- and CA-treated cells (Ibáñez, Valdés et al., 2012; Satoh et al., 2008). The analysis also revealed that CA and SC-RE activated common regulators, such as XBP1 (*Xbp1*) gene related with the unfolded protein response (UPR); several key regulators of metabolism including SREBF1/SREBF2 (*Srebp1/2*), CEBPA (*C/ebpA*), and NR1I2 (*Pxr*) genes; NUPR1 and TFEB genes related with autophagy; and others with a role in modulating the cellular response to DNA damage (SP1 and P73). Major modulators of endoplasmic reticulum (ER) stress, ERN1 (encoding *Ire1*), ATF4 (*Atf4*), EIF2AK3 (*Perk*), and DDIT3 (*Chop*) genes were predicted to be only activated in response to SC-RE. Furthermore, for SC-RE treatment, bioinformatics also provided significant pre-

Table 1 – Activation or deactivation of molecules predicted by UR analysis (IPA software) in CA- and SC-RE-treated HT-29 cells.

CA treatment				SC-RE treatment			
Molecule type	Gene symbol	z-score	p-val[a]	Molecule type	Gene symbol	z-score	p-val[a]
TR	**NFE2L2**	**4.99**	**1,75E-11**	**TR**	**NUPR1**	**10.51**	**1,54E-51**
TR	**SP1**	**3.60**	**2,73E-08**	K	CDKN1A	4.82	4,54E-38
NR	**NR1I2**	**2.97**	**1,54E-06**	TR	RB1	5.32	1,50E-32
TR	**NUPR1**	**2.67**	**2,71E-06**	TR	CCND1	–5.42	4,38E-28
TLR	EIF4E	2.14	2,83E-06	TR	E2F1	–4.81	4,50E-28
TR	**CEBPA**	**2.98**	**5,84E-06**	TR	TBX2	–6.25	9,59E-27
NR	PPARG	3,49	5,43E-06	TR	MYC	–4.34	1,32E-23
NR	**PGR**	**3.36**	**1,41E-05**	TR	CDKN2A	6.06	2,44E-21
TR	**SREBF1**	**2.68**	**1,61E-05**	**GPR**	**PTGER2**	**–5.86**	**4,70E-19**
TR	**SREBF2**	**2.36**	**4,19E-05**	TR	E2F3	–3.53	7,70E-18
TR	**TP73**	**2.60**	**4,75E-05**	TR	E2F2	–3.43	7,60E-17
TR	**STAT4**	**3.68**	**1,95E-04**	K	EIF2AK3	2.02	4,20E-16
TR	**TFEB**	**2.44**	**2,88E-04**	TR	FOXM1	–4.27	1,41E-15
NR	NR1I3	2.33	2,90E-04	TR	E2F6	2.85	6,40E-15
NR	ESR2	2.58	3,31E-04	TR	KDM5B	3.88	2,83E-14
GPR	**PTGER2**	**–2.16**	**4,52E-04**	TR	ATF4	3.13	2,29E-13
TR	STAT3	2.22	6,37E-04	TR	RBL1	4.36	2,36E-13
TR	FOS	2.58	6,51E-04	**TR**	**XBP1**	**5.76**	**2,14E-12**
TR	TP63	2.45	7,49E-04	**NR**	**PGR**	**3.04**	**1,79E-09**
TR	VDR	2.41	2,36E-03	**TR**	**SP1**	**2.22**	**1,96E-08**
TR	**XBP1**	**3.43**	**5,40E-03**	TR	SMARCB1	4.17	1,32E-07
TR	USF1	2.20	7,26E-03	**TR**	**NFE2L2**	**5.47**	**3,31E-07**
TR	EGR1	2.90	8,07E-03	**TR**	**TP73**	**2.39**	**1,66E-06**
TR	**PPRC1**	**2.20**	**1,29E-02**	**TR**	**TFEB**	**3.72**	**2,08E-06**
				TR	HDAC2	2.07	6,44E-06
				TR	TCF3	3.53	6,48E-06
				TLR	EIF4G1	–2.53	8,63E-06
				TR	**CEBPA**	**2.56**	**8,68E-06**
				TR	FOXP3	2.55	1,19E-05
				TR	TOB1	2.32	6,34E-05
				TR	**SREBF1**	**2.20**	**1,39E-04**
				TR	**PPRC1**	**3.35**	**1,15E-04**
				TR	KDM5A	2.63	1,40E-04
				TR	**SREBF2**	**2.08**	**5,32E-04**
				NR	**NR1I2**	**2.65**	**6,98E-04**
				TR	**STAT4**	**3.31**	**1,77E-03**
				K	ERN1	2.74	2,27E-03
				TR	ELF4	2.94	7,48E-03
				TR	DDIT3	3.07	2,45E-02

TR: transcription regulator; NR: ligand-dependent nuclear receptor; TLR: translation regulator; GPR: G-protein coupled receptor; K: kinase. **Bold letters** indicate common findings for CA and SC-RE treatments.
[a] Significance value calculated with the Fisher's exact test.

dictions for a set of genes (E2F1, E2F3, E2F3, MYC, RB1, TOB1, and CDKN1A) that are tightly linked with cell proliferation.

3.4. *SC-RE induces more intense and sustained UPR signaling in HT-29 cells than CA*

To further investigate the similarities and differences between treatments on the gene induction pattern of UPR in HT-29 cells, the gene patterns that support the activity of the predicted UPR regulators were examined (Supplementary Table S4). Data indicated that endoplasmic reticulum chaperone genes were mostly up-regulated by *Ire1*/*Xbp1* activity. As it is outlined in Fig. 2, the expression of genes associated with metabolism and autophagosome function was driven by the activation of *Atf4*, a key regulator within the *Perk* branch of UPR. Downstream targets of *Chop*, a relevant multifunctional transcription factor in ER stress response, were mainly related with cell death, response to cellular stress and other functions. Activated *Perk* also has the potential to phosphorylate and activate *Nrf2*, whose status, according to UR analysis, was significantly activated in treated cells. CA treatment also induced *Xbp1* activation; however, compared to the effect of SC-RE treatment, this polyphenol altered the expression of fewer genes at 24 h (underlined gene symbols in Table S4) and the expression ratios were lower than those observed for SC-RE treatment, most of them falling below the fold change threshold established for UR analysis. Considering the fact that the gene expression profiling analysis was performed after 24 h treatment, and therefore, some early gene induction may have been missed for CA treatment, the expression profile of several UPR markers was

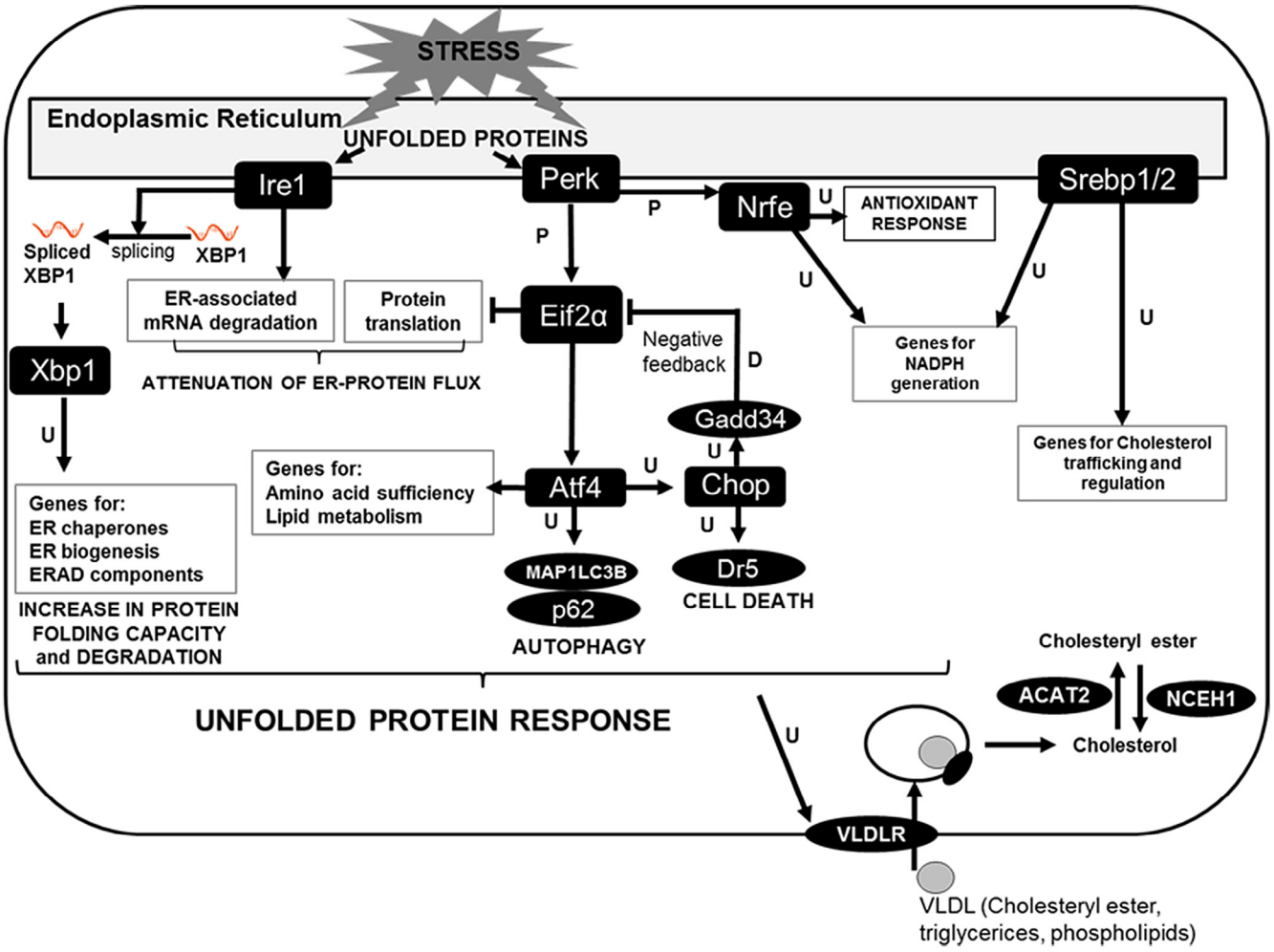

Fig. 2 – Schematic representation of results. UR analysis predicted activation of the UPR pathway signaling and alteration of the transcriptional activity of several factors and genes involved in cholesterol metabolism in HT-29 cells treated with SC-RE for 24 h. Under conditions of ER stress, unfolded proteins accumulate causing activation of *Perk* and *Ire1*. Activated *Ire1* produces active form of *Xbp1* that induces genes involved in protein folding and degradation. Activated *Perk* inactivates *eIF2α*, which suppresses global mRNA translation, but activates *ATF4* translation. *ATF4* induces the transcription of *Chop* and genes for amino acid and lipid metabolism. *Perk* also activates *Nrfe*, which induces antioxidant genes. Activation of *Srebp1/2* is consistent with up-regulation of genes involved in cholesterol transport. Black squares, predicted transcriptional regulators; oval shapes, downstream targets; P, phosphorylation, D, dephosphorylation; U, up-regulation.

investigated at earlier incubation times by RT-PCR analysis. As it is shown in Fig. 3A, differences in the magnitude and temporal induction pattern of DDIT3 (*Chop*) and PPP1R15A (*Gadd34*) genes between treatments indicate that transcription of downstream targets of the *Perk*/*Atf4* arm is lower and declined faster in CA- than in SC-RE-treated cells. Regarding ERN1 (*Ire1*) and spliced XBP1 transcripts, maximum levels were reached at 12 h with both treatments; however, the expression ratio at the maximum induction time point was significantly higher in cells treated with extract compared with those observed in CA-treated cells (Fig. 3B). Fig. 3C shows that HMOX1, a prototypic antioxidant response element-driven gene, typically controlled by *Nrf2*, followed a similar induction pattern as the one observed in genes modulated by *Perk*/*Atf4* axis in each treatment (Fig. 3A), showing a strong induction at 6 hours after initial exposure to both treatments, but to a much greater extent in SC-RE-treated cells.

3.5. *SC-RE and CA exerted transcriptional changes linked to lipid metabolism in HT-29 cells*

To examine potential associations between gene expression and the observed changes in cholesterol metabolism induced by SC-RE treatment, transcriptionally active regulators involved in lipid metabolism predicted by IPA were studied (Supplementary Table S5). Interestingly, activation of *Srebp1/2* was characterized by the significant induction of genes involved in cholesterol trafficking, regulation and NADPH generation. Three genes involved in cholesterol biosynthesis under *Srebp1/2* transcriptional control were up-regulated; however, such induction was low (Supplementary Table S2). Furthermore, the expression of HMGCR gene, which encodes the rate-limiting enzyme in cholesterol biosynthesis (*Hmgcr*), remained unaltered. In addition, *LDL receptor* encoding gene (LDLR), also controlled by *Srbp1/2* and relevant for cholesterol

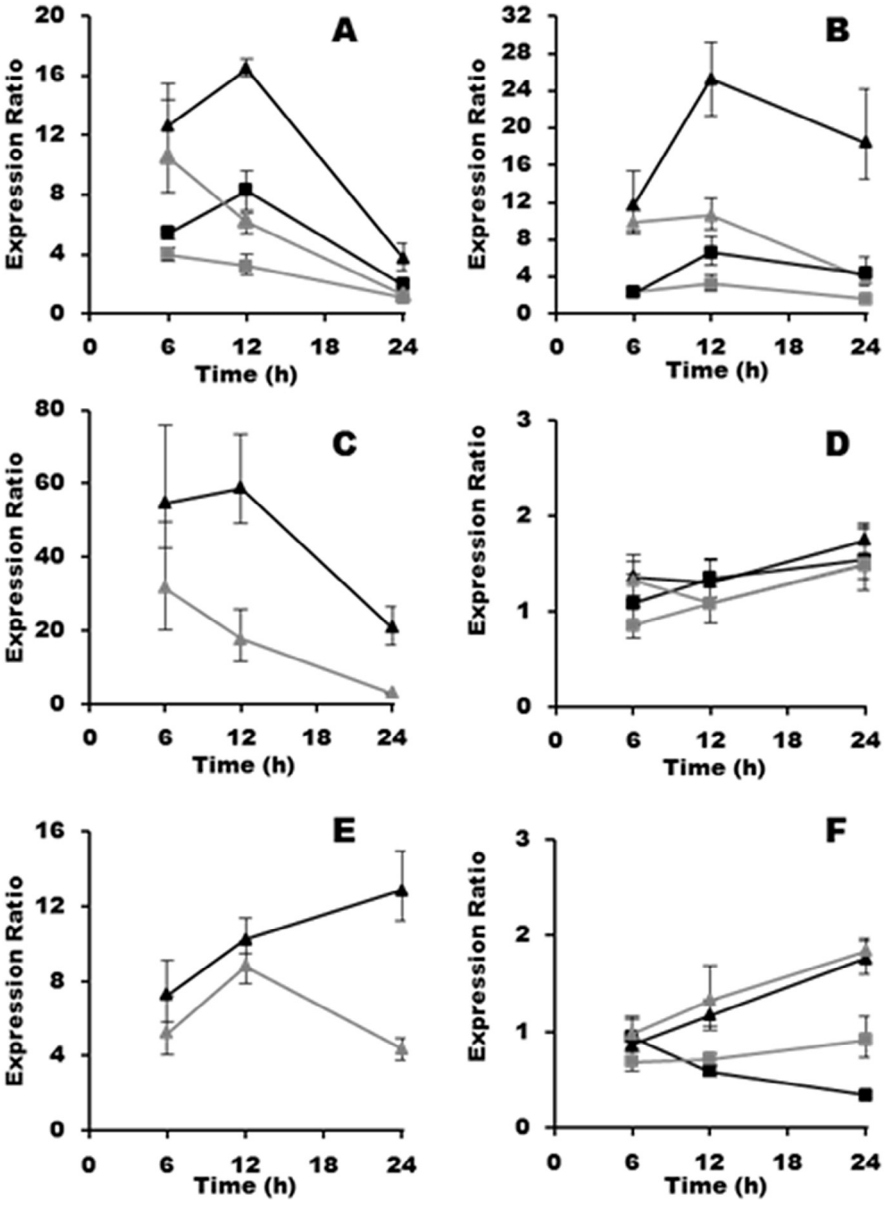

Fig. 3 – Expression ratios (relative to control) of (A) PPP1R15A (square) and DDIT3 (triangle); (B) ERN1 (square) and XBP1 (triangle); (C) HMOX1; (D) HMGCR (square) and LDLR (triangle); (E) VLDLR; (F) ACAT2 (square) and NCEH1 (triangle) in HT-29 cells exposed to 30 μg/mL of SC-RE (black lines) or 12.5 μg/mL of CA (gray lines) for 6, 12 and 24 hours. Error bars are given as the 95% CI of three independent experiments.

uptake, was not considered for IPA analysis because its expression ratio fell slightly below the threshold established in this study. To obtain more insight into the potential role of *Srebp1/2* activation in the observed cholesterol accumulation induced by SC-RE, the gene expression kinetics of HMGCR and LDLR genes were analyzed. Fig. 3D shows that both genes exhibited low expression ratios (<1.5) that in only few cases were statistically significant. Expression pattern analysis of *Srebp1/2*-unrelated genes involved in cholesterol metabolism, such as VLDLR, NCEH1, and ACAT2, shows that CA and SC-RE-treated cells overexpressed VLDLR in both treatments (Fig. 3E). However, while up-regulated VLDLR transcripts steadily increased over the time period of the experiment in SC-RE-treated cells, it reached a maximum at 12 h followed by a decline in CA-treated cells. On the other hand, results in Fig. 3F show that mRNA levels of ACAT2 gene (encoding acetyl-CoA acetyltransferase) remained unaltered in CA-treated cells, but decreased in SC-RE-treated cells relative to controls after 12 hours of incubation. NCEH1 (encoding neutral cholesterol ester hydrolase 1) gene expression, by contrast, followed slight but progressive up-regulation over time in both SC-RE- and CA-treated cells.

3.6. *SC-RE induces G1 arrest by attenuating E2F transcriptional activity*

To identify how the SC-RE extract impairs HT-29 colon cancer cell proliferation, the transcriptional activity of master regulators of cell cycle control predicted by UR analysis was studied. Thus,

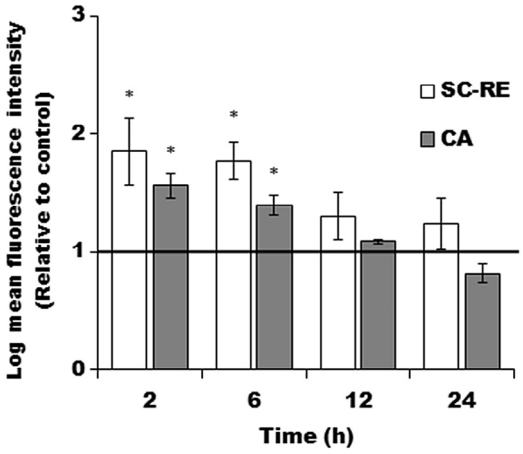

Fig. 4 – Time-dependent production of ROS (relative to control) in HT-29 cells treated with 30 μg/mL of SC-RE and 12.5 μg/mL of CA. Error bars are given as the SEM of three independent experiments. *Indicates a significant difference from the untreated control cells at each time as determined by t-test ($p < 0.05$).

52 genes were found to be down-regulated substantiating deactivation of *E2F1* (Supplementary Table S6). Repressed targets were mainly related with different functions and events that *E2F1* coordinates during DNA replication and repair. *E2F* activity is controlled by different mechanisms, and one of the most studied is the regulation by retinoblastoma (*Rb*, RB1 gene), a major negative regulator of the cell cycle whose activation was indeed predicted by UR analysis (Table 1).

3.7. *SC-RE and CA induce early changes in the intracellular redox state of HT-29 cells*

It is generally accepted that intracellular redox conditions control UPR. Besides, extracts from rosemary and particularly CA, are known to be potent inducers of *Nrf2* transcriptional activity and capable to trigger an antioxidant response and improve intracellular redox status (Satoh et al., 2008). To further examine whether the reported transcriptional induction exerted by rosemary polyphenols accounted for changes in the redox status in HT-29 cells, intracellular ROS generation was assessed in treated and control cells at different time points. Data revealed that both treatments induced detectable ROS accumulation at the earliest time assayed (2 h) in HT-29 cells (Fig. 4). ROS levels induced by CA and SC-RE remained significantly higher than the control levels at 6 h time point but declined in the time window from 12 to 24 hours to levels similar to those detected in untreated control HT-29 cells. ROS induction was higher in SC-RE-treated cells than in CA-treated cells.

4. Discussion

Different conditions interfere with endoplasmic reticulum function and can affect its homeostasis inducing the accumulation of unfolded proteins in the lumen of this organelle, a condition referred to as ER stress (Lafleur, Stevens, & Lawrence, 2013). ER stress activates a signal transduction system known as UPR that augments the protein folding capacity in ER. Upon the perturbation of protein folding, activation of specific ER sensors triggers three major downstream signaling cascades (*Perk/Atf4*, *Ire1/Xbp1* and *Atf6*), which collectively act to restore homeostasis and normal ER function (Urra, Dufey, Lisbona, Rojas-Rivera, & Hetz, 2013). Our results demonstrate that 30 μg/mL of SC-RE and 12.5 μg/mL of CA were sufficient for activation of *Ire1/Xbp1* and *Perk/Atf4*, two major signaling axes of UPR triggered by ER stress, in HT-29 cells. Activation of *Perk* pathway is experimentally supported by the induction of genes related with attenuation of translation, and by gene expression patterns that predict the activation of relevant *Perk* downstream targets, namely, *Atf4* and *Nrf2*. In agreement with our observations on the effect of SC-RE and CA on cell cycle progression, one frequently reported consequence of UPR signaling is a transient G1 phase arrest due to the rapid decline in *cyclin D1* protein (Hamanaka, Bennett, Cullinan, & Diehl, 2005). Besides the immediate effect of ER stress on cell cycle, cell fate determination under ER stress is controlled by different mechanisms that are interrelated among the UPR signaling pathways and rely on the accepted notion that UPR may be governed by a timer; if ER stress has not been mitigated at a certain point, UPR signaling turns off and directs cell to cell death (Hetz, 2012). Although the three arms of UPR enhance survival under stress conditions, all converge on the induction of *Chop*, a transcription factor that plays a pivotal role on cell fate since it may promote either cell cycle arrest, programmed cell death or adaptation (Todd, Lee, & Glimcher, 2008). *Perk*-mediated signaling is considered the predominant pathway for *Chop* induction. *Chop* controls a major negative feedback mechanism for turning off UPR by up-regulating DNA damage-inducible protein 34 (*Gadd34*) that enables restoration of general protein translation and normal functioning (Ma & Hendershot, 2003). In the event of prolonged ER-stress or failure to repair the damage, *Chop* can promote cell death, through (i) the transcriptional control of genes encoding for pro- and anti-apoptotic proteins (Merksamer & Papa, 2010) and (ii) up-regulation of TNFRSF10B gene, which encodes for death receptor 5 (*Dr5*), sensitizing cells to apoptotic stimulation by a variety of conditions that cause ER stress (Sano & Reed, 2013). In either case, adaptation to or recovery from ER stress, is accompanied by rapid degradation of *Chop* mRNA and protein (Rutkowski et al., 2008). In addition to these effects, several lines of evidence support new links between ER stress and other cellular mechanisms such as autophagy (B'chir et al., 2013). Altogether, our data indicate that SC-RE and CA treatments exerted ER stress on HT-29 cells that triggered UPR at early exposure times. However, considering the notion that UPR stress sensors can integrate the intensity of the stimulus and reflect this in the signals that they transduce, our findings suggest that SC-RE induces more severe and sustained ER stress than CA in HT-29 cells under the assayed conditions, accounted for a broader and stronger induction of UPR signaling and the up-regulation of adaptive, cell death and autophagy markers, which suggest that ER stress is still unresolved after 24 h of exposure to SC-RE.

Generation of ROS has been linked to ER stress and the UPR (Eletto, Chevet, Argon, & Appenzeller-Herzog, 2014). Studies suggest that altered redox homeostasis in the ER is sufficient to cause ER stress (Cao & Kaufman, 2014). Although CA is a

recognized antioxidant agent, several reports have recently demonstrated that this polyphenol induces intracellular ROS generation under certain experimental conditions (Tsai et al., 2011). Min, Jung, and Kwon (2014) reported that CA induced ROS production as well as the expression of *Atf4* and *Chop* in human renal carcinoma cells; and the interference to such effects partially abolished apoptosis. It is well-accepted that UPR in turn induces the production of ROS in the ER due to increased protein folding function, and it also triggers *Nrf2*-mediated antioxidant response to restore cellular redox homeostasis (Cao & Kaufman, 2014). In line with this, our results indicate two interesting findings: (i) SC-RE and CA induced ROS production at early times of exposure; and (ii) the expression patterns of the *Nrf2*-mediated antioxidant responsive gene HMOX1 appeared to follow the same kinetics as those genes regulated by *Perk/Atf4* signaling, suggesting that UPR could improve ROS scavenging capacity in HT-29 by enhancing *Nrf2* activation. This mechanism for *Nrf2* activation may enhance the one already demonstrated by Satoh et al. (2008), which involves direct interaction of rosemary diterpenes with *Keap1* protein.

One of our goals was to investigate whether CA and SC-RE treatments affect cholesterol metabolism in HT-29 cells. Our proposed Foodomics approach revealed that SC-RE induces changes in the metabolism of cholesterol at different levels. An interesting finding was that SC-RE induces cholesterol accumulation in HT-29 cells after 24 h of exposure. Several articles have reported that unbalanced cholesterol metabolism can result in ER stress (Harding et al., 2005). However, in the present study, cholesterol accumulation occurs after the onset of UPR, which discards this metabolic alteration as the cause of ER stress. By contrast, it is now recognized that ER stress plays a critical role in dysregulation of lipid metabolism in hepatic and adipocyte cell models (Basseri & Austin, 2012). Although the increased expression of the cholesterogenic and other lipogenic genes in response to ER stress has been reported in a variety of experimental settings, this expression can be also down-regulated or remain unaffected under certain ER stress conditions (Rutkowski et al., 2008). Recent reports have demonstrated that *Chop* plays a relevant role influencing changes in cell metabolism by altering the expression and transcriptional activity of key master regulators of lipid metabolism such as *Cebp/α*, which controls *Pparα*, a regulator of fatty acid oxidation; and *Srebp1* and *Srebp2*, regulators of lipogenesis and cholesterogenesis, respectively. Our data show that, in response to SC-RE and CA treatments, HT-29 cells activate the transcriptional activity of regulators with a key role in lipids metabolism. In the case of *Srebps*, their activation suggests regulation of relevant functions on cholesterol trafficking and homeostasis as well as generation of the required NADPH for lipid synthesis (Horton, Goldstein, & Brown, 2002). However, NADPH is the major reducing resource to scavenge oxidative stress, and the induction of the genes (G6PD, ME1, and PGD) involved in its production has also been associated with *Nrf2* activation. Indeed, it has been proposed that *Nrf2* factor can repress genes involved in lipid synthesis, increasing the availability of NADPH for reducing oxidative stress, instead of using it for lipid biosynthesis (Wu, Cui, & Klaassen, 2011). Changes detected in the expression of genes encoding *Hmgcr* and *LDL-receptor* over 24 h of treatment with SC-RE and CA were not relevant. In contrast, induction of the gene encoding *very low density lipoprotein (VLDL) receptor* was strikingly high and it showed a differential expression pattern during each treatment. Taken together, these results suggest that *Srebps* are not major contributors to the observed cholesterol accumulation in HT-29, whereas it seems plausible that such accumulation occurs by increased receptor-mediated uptake of *VLDL* present in the serum of culture media. Consistent with these observations, Röhrl et al. have recently reported that ER stress impairs cholesterol synthesis despite *Srebp2* activation in hepatic cells (Röhrl et al., 2014). Moreover, recent evidence has demonstrated that ER stress stimulates lipid accumulation by inducing the expression of VLDLR gene in hepatocytes, adipose tissue and liver; however, the mechanisms accounting for these observations appear to be dependent on the cell type and ER stressor (Wang et al., 2014). In the present study, SC-RE treatment induced early changes in the FC/TC ratio that could be attributed to either (or both) increased hydrolytic activity of cholesteryl esters or decreased esterification of free cholesterol molecules. However, neither NCEH1 nor ACAT2 genes were altered transcriptionally at early time points. In previous reports, changes in FC/TC ratio in HT-29 cells have been correlated to GSH depletion (Madesh, Benard, & Balasubramanian, 1998). In our study, ROS generated in HT-29 cells at the beginning of the treatments may potentially originate a temporal depletion of intracellular GSH levels. Such GSH depletion would likely affect CA- and SC-RE-treated cells, mobilizing cholesteryl ester into free cholesterol at the initial stages of the incubation. However, this effect was only observed in SC-RE-treated cells suggesting that other factors may also influence the changes in intracellular cholesterol distribution under the assayed conditions.

The family of *E2F* transcription factors and retinoblastoma *Rb* family tumor suppressor proteins play a pivotal role in control of cell proliferation (Wong, Dong, Nevins, Mathey-Prevot, & You, 2011). The *Rb/E2F* pathway is critical in regulating the initiation of DNA replication, and disruption of the pathway is common in virtually all human cancers (Nevins, 2001). It is now clear that the tumor suppressor property of *Rb* is to constrain *E2F* activity. Although *E2F* is involved in a variety of cellular activities, the best understood function of *E2F* is to regulate transcription of genes involved in the transition from G1 to S phase, regulators of S phase entry and components of the DNA replication machinery. Here, we show that SC-RE treatment down-regulated many *E2F* targets involved in nucleotide biosynthetic activities, various DNA repair and replication activities, checkpoint control, and also components of the entire apparatus of initiation factors that assemble a pre-replication complex at origins of replication. These results provide a new hypothesis that suggests that the inhibitory effect of SC-RE on HT-29 cell proliferation is mediated by down-regulation of *E2F* transcriptional activity. In conclusion, SC-RE treatment induced relevant metabolic and transcriptional changes headed by ROS generation and coordinated UPR signaling in HT-29 cells. Transcriptional data suggested that the increased receptor-mediated uptake of *VLDL* is a major contributor to the observed effect of the SC-RE on cholesterol accumulation. In addition, cell cycle progression was readily affected by SC-RE treatment, in accordance to canonical UPR activation, but our transcriptional data also suggest that this effect is also mediated by attenuation of *E2F* activity.

Acknowledgment

This work was supported by an AGL2011-29857-C03-01 project (Ministerio de Educacion y Ciencia, Spain) and S2013/ABI-2728 (Comunidad de Madrid). A.V. thanks the Ministerio de Economía y Competitividad for his FPI pre-doctoral fellowship (BES-2012-057014).

Appendix: Supplementary material

Supplementary data to this article can be found online at doi:10.1016/j.jff.2015.03.043.

REFERENCES

Abramson, H. N. (2011). The lipogenesis pathway as a cancer target. *Journal of Medicinal Chemistry*, 54, 5615–5638.

Barni, M. V., Carlini, M. J., Cafferata, E. G., Puricelli, L., & Moreno, S. (2012). Carnosic acid inhibits the proliferation and migration capacity of human colorectal cancer cells. *Oncology Reports*, 27, 1041 –1048.

Basseri, S., & Austin, R. C. (2012). Endoplasmic reticulum stress and lipid metabolism: Mechanisms and therapeutic potential. *Biochemistry Research International*, 2012, 1–13.

B'chir, W., Maurin, A. C., Carraro, V., Averous, J., Jousse, C., Muranishi, Y., Parry, L., Stepien, G., Fafournoux, P., & Bruhat, A. (2013). The eIF2α/ATF4 pathway is essential for stress-induced autophagy gene expression. *Nucleic Acids Research*, 41, 7683–7699.

Ben Jemia, M., Tundis, R., Maggio, A., Rosselli, S., Senatore, F., Menichini, F., Bruno, M., Kchouk, M. E., & Lizzo, M. R. (2013). NMR-based quantification of rosmarinic and carnosic acids, GC-MS profile and bioactivity relevant to neurodegenerative disorders of Rosmarinus officinalis L. extracts. *Journal of Functional Foods*, 5, 1873–1882.

Cao, S. S., & Kaufman, R. J. (2014). Endoplasmic reticulum stress and oxidative stress in cell fate decision and human disease. *Antioxidants & Redox Signaling*, 21, 396–413.

Eletto, D., Chevet, E., Argon, Y., & Appenzeller-Herzog, C. (2014). Redox controls UPR to control redox. *Journal of Cell Science*, 127, 3649–3658.

Folch, J., Lees, M., & Sloane-Stanley, G. H. (1957). A simple method for the isolation and purification of total lipides from animal tissues. *The Journal of Biological Chemistry*, 226, 497–509.

García-Cañas, V., Simó, C., Herrero, M., Ibáñez, E., & Cifuentes, A. (2012). Present and future challenges in food analysis: Foodomics. *Analytical Chemistry*, 84, 10150–10159.

Gaya, M., Repetto, V., Toneatto, J., Anesini, C., Piwien-Pilipuk, G., & Moreno, S. (2013). Antiadipogenic effect of carnosic acid, a natural compound present in Rosmarinus officinalis, is exerted through the C/EBPs and PPARγ pathways at the onset of the differentiation program. *Biochimica et Biophysica Acta*, 1830, 3796–3806.

Hamanaka, R. B., Bennett, B. S., Cullinan, S. B., & Diehl, J. A. (2005). PERK and GCN2 contribute to eIF2alpha phosphorylation and cell cycle arrest after activation of the unfolded protein response pathway. *Molecular Biology of the Cell*, 16, 5493–5501.

Harding, H. P., Zhang, Y., Khersonsky, S., Marciniak, S., Scheuner, D., Kaufman, R. J., Javitt, N., Chang, Y. T., & Ron, D. (2005). Bioactive small molecules reveal antagonism between the integrated stress response and sterol-regulated gene expression. *Cell Metabolism*, 2, 361–371.

Hetz, C. (2012). The unfolded protein response: Controlling cell fate decisions under ER stress and beyond. *Nature Reviews. Molecular Cell Biology*, 13, 89–102.

Horton, J. D., Goldstein, J. L., & Brown, M. S. (2002). SREBPs: Activators of the complete program of cholesterol and fatty acid synthesis in the liver. *The Journal of Clinical Investigation*, 109, 1125–1131.

Ibáñez, C., Simó, C., García-Cañas, V., Gómez-Martínez, A., Ferragut, J. A., & Cifuentes, A. (2012). CE/LC-MS multiplatform for broad metabolomic analysis of dietary polyphenols effect on colon cancer cells proliferation. *Electrophoresis*, 33, 2328–2336.

Ibáñez, C., Valdés, A., García-Cañas, V., Simó, C., Celebier, M., Rocamora-Reverte, L., Gómez-Martínez, A., Herrero, M., Castro-Puyana, M., Segura-Carretero, A., Ibáñez, E., Ferragut, J. A., & Cifuentes, A. (2012). Global Foodomics strategy to investigate the health benefits of dietary constituents. *Journal of Chromatography. A*, 1248, 139–153.

Ibarra, A., Cases, J., Roller, M., Chiralt-Boix, A., Coussaert, A., & Ripoll, C. (2011). Carnosic acid-rich rosemary (Rosmarinus officinalis L.) leaf extract limits weight gain and improves cholesterol levels and glycaemia in mice on a high-fat diet. *British Journal of Nutrition*, 106, 1182–1189.

Johnson, J. J. (2011). Carnosol: A promising anti-cancer and anti-inflammatory agent. *Cancer Letters*, 305, 1–7.

Lafleur, M. A., Stevens, J. L., & Lawrence, J. W. (2013). Xenobiotic perturbation of ER stress and the unfolded protein response. *Toxicologic Pathology*, 41, 235–262.

Ma, Y., & Hendershot, L. M. (2003). The stressful road to antibody secretion. *Nature Reviews. Immunology*, 4, 310–311.

Madesh, M., Benard, O., & Balasubramanian, K. (1998). Glutathione modulates lipid composition of human colon derived HT-29 cells. *The International Journal of Biochemistry & Cell Biology*, 30, 1345–1352.

Merksamer, P. I., & Papa, F. R. (2010). The UPR and cell fate at a glance. *Journal of Cell Science*, 123, 1003–1006.

Min, K., Jung, K., & Kwon, T. K. (2014). Carnosic acid induces apoptosis through reactive oxygen species-mediated endoplasmic reticulum stress induction in human renal carcinoma caki cells. *European Journal of Cancer Prevention*, 19, 170–178.

Nevins, J. R. (2001). The Rb/E2F pathway and cancer. *Human Molecular Genetics*, 10, 699–703.

Petiwala, S. M., Puthenveetil, A. G., & Johnson, J. J. (2013). Polyphenols from the Mediterranean herb rosemary (Rosmarinus officinalis) for prostate cancer. *Frontiers in Pharmacology*, 4, article 29.

Pfaffl, M. W., Horgan, G. W., & Dempfle, L. (2002). Relative expression software tool (REST) for group-wise comparison and statistical analysis of relative expression results in real-time PCR. *Nucleic Acids Research*, 30, article e36.

Röhrl, C., Eigner, K., Winter, K., Korbelius, M., Obrowsky, S., Kratky, D., Kovacs, W. J., & Stangl, H. (2014). Endoplasmic reticulum stress impairs cholesterol efflux and synthesis in hepatic cells. *The Journal of Lipid Research*, 55, 94–103.

Rutkowski, D. T., Wu, J., Back, S. H., Callaghan, M. U., Ferris, S. P., Iqbal, J., Clark, R., Miao, H., Hassler, J. R., Fornek, J., Katze, M. G., Hussain, M. M., Song, B., Swathirajan, J., Wang, J., Yau, G. D., & Kaufman, R. J. (2008). UPR pathways combine to prevent hepatic steatosis caused by ER stress-mediated suppression of transcriptional master regulators. *Developmental Cell*, 15, 829–840.

Sánchez-Camargo, A. P., Valdés, A., Sullini, G., García-Cañas, V., Cifuentes, A., Ibáñez, E., & Herrero, M. (2014). Two-step sequential supercritical fluid extracts from rosemary with

enhanced anti-proliferative activity. *Journal of Functional Foods*, *11*, 293–303.
Sano, R., & Reed, J. C. (2013). ER stress-induced cell death mechanisms. *Biochimica et Biophysica Acta*, *1833*, 3460–3470.
Santos, C. R., & Schulze, A. (2012). Lipid metabolism in cancer. *FEBS Journal*, *279*, 2610–2623.
Satoh, T., Kosaka, K., Itoh, K., Kobayashi, A., Yamamoto, M., Shimojo, Y., Kitajima, C., Cui, J., Kamins, J., Okamoto, S., Izumi, M., Shirasawa, T., & Lipton, S. A. (2008). Carnosic acid, a catechol-type electrophilic compound, protects neurons both in vitro and in vivo through activation of the Keap1/Nrf2 pathway via S-alkylation of targeted cysteines on Keap1. *Journal of Neurochemistry*, *104*, 1116–1131.
Todd, D. J., Lee, A. H., & Glimcher, L. H. (2008). The endoplasmic reticulum stress response in immunity and autoimmunity. *Nature Reviews. Immunology*, *8*, 663–674.
Tsai, C. W., Lin, C. Y., Lin, H. H., & Chen, J. H. (2011). Carnosic acid, a rosemary phenolic compound, induces apoptosis through reactive oxygen species-mediated p38 activation in human neuroblastoma IMR-32 cells. *Neurochemical Research*, *36*, 2442–2451.
Urra, H., Dufey, E., Lisbona, F., Rojas-Rivera, D., & Hetz, C. (2013). When ER stress reaches a dead end. *Biochimica et Biophysica Acta*, *1833*, 3507–3517.
Valdés, A., García-Cañas, V., Rocamora-Reverte, L., Gómez-Martínez, A., Ferragut, J. A., & Cifuentes, A. (2013). Effect of rosemary polyphenols on human colon cancer cells: Transcriptomic profiling and functional enrichment analysis. *Genes & Nutrition*, *8*, 43–60.
Valdés, A., García-Cañas, V., Simó, C., Ibáñez, C., Micol, V., Ferragut, J. A., & Cifuentes, A. (2014). Comprehensive Foodomics study on the mechanisms operating at various molecular levels in cancer cells in response to individual rosemary polyphenols. *Analytical Chemistry*, *86*, 9807–9815.
Valdés, A., Simó, C., Ibáñez, C., Rocamora-Reverte, L., Ferragut, J. A., García-Cañas, V., & Cifuentes, A. (2012). Effect of dietary polyphenols on K562 leukemia cells: A Foodomics approach. *Electrophoresis*, *33*, 2314–2327.
Wang, T., Takikawa, Y., Satoh, T., Yoshioka, Y., Kosaka, K., Tatemichi, Y., & Suzuki, K. (2011). Carnosic acid prevents obesity and hepatic steatosis in ob/ob mice. *Hepatology Research*, *41*, 87–92.
Wang, Z., Dou, X., Li, S., Zhang, X., Sun, X., Zhou, Z., & Song, Z. (2014). Nuclear factor (erythroid-derived 2)-like 2 activation-induced hepatic very-low-density lipoprotein receptor overexpression in response to oxidative stress contributes to alcoholic liver disease in mice. *Hepatology (Baltimore, Md.)*, *59*, 1381–1392.
Wong, J. V., Dong, P., Nevins, J. R., Mathey-Prevot, B., & You, L. (2011). Network calisthenics: Control of E2F dynamics in cell cycle entry. *Cell Cycle (Georgetown, Tex.)*, *10*, 3086–3094.
Wu, K. C., Cui, J. Y., & Klaassen, C. D. (2011). Beneficial role of Nrf2 in regulating NADPH generation and consumption. *Toxicological Sciences*, *123*, 590–600.
Xiang, Q., Wang, Y., Wu, W., Meng, X., Qiao, Y., Xu, L., & Liu, X. (2013). Carnosic acid protects against ROS/RNS-induced protein damage and upregulates HO-1 expression in RAW264.7 macrophages. *Journal of Functional Foods*, *5*, 362–369.
Yana, M., Lia, G., Petiwala, S. M., Householter, E., & Johnson, J. J. (2015). Standardized rosemary (*Rosmarinus officinalis*) extract induces Nrf2/sestrin-2 pathway in colon cancer cells. *Journal of Functional Foods*, *13*, 137–147.

3.2.5 Foodomics study on the effects of extracellular production of hydrogen peroxide by rosemary polyphenols on the anti-proliferative activity of rosemary polyphenols against HT-29 cells

Valdés, A., *García-Cañas, V., Kocak, E., Simó, C., Cifuentes, A. *Electrophoresis* 2016, *0*, 1 - 10.

DOI: http://dx.doi.org/doi:10.1002/elps.201600014

Alberto Valdés
Virginia García-Cañas
Engin Koçak
Carolina Simó
Alejandro Cifuentes

Laboratory of Foodomics, Institute of Food Science Research (CIAL, CSIC), Madrid, Spain

Received January 11, 2016
Revised January 21, 2016
Accepted January 27, 2016

Research Article

Foodomics study on the effects of extracellular production of hydrogen peroxide by rosemary polyphenols on the anti-proliferative activity of rosemary polyphenols against HT-29 cells

A number of studies have demonstrated a strong association between the antioxidant properties of rosemary polyphenols and their chemoprotective activity. However, the prooxidant effects of rosemary polyphenols have been rarely reported. In this work, a foodomics study is performed to investigate the in vitro autooxidation of carnosic acid (CA), carnosol (CS) and a polyphenol-enriched rosemary extract (SC-RE) in cell culture conditions. The results revealed that rosemary polyphenols autooxidation in culture medium generated H_2O_2 at different rates. Generated H_2O_2 levels by SC-RE and CA, but not CS, were correlated with intracellular reactive oxygen species (ROS) generation in HT-29 cells, and were partially involved in their anti-proliferative effect in this cell line. These compounds also induced different effects on glutathione metabolism. Results also indicated that high extracellular H_2O_2 concentrations, resulting of using high (45 μg/mL) SC-RE concentration in culture media, exerted some artifactual effects related with cell cycle, but they did not influence the expression of relevant molecular biomarkers of stress.

Keywords:
Antioxidant / Colon cancer / Glutathione / Prooxidant / Reactive oxygen species
DOI 10.1002/elps.201600014

1 Introduction

Carnosic acid (CA) and carnosol (CS) are the most abundant phenolic diterpenes in rosemary leaves and account for >90% of the antioxidant activity of rosemary extracts [1]. The antioxidant activity of these compounds has been extensively investigated in cell-free systems. For instance, Masuda et al. [2] proposed that CA participates in oxidation cascades that, under certain conditions, provide other antioxidant products. Further work by the same group suggested that CA and CS have the ability to recover their antioxidant activity even after oxidation [3]. A number of reports have demonstrated a strong association between the antioxidant properties, particularly the radical scavenging effects of these compounds, and their in vitro and in vivo chemoprotective activity through different mechanisms that result in protection against oxidative damage of lipids, proteins and DNA [4, 5]. Besides the free radical scavenging effect, rosemary diterpenes and extracts also indirectly exert their protective activity by modulating the *Nrf2*-mediated oxidative stress response, increasing endogenous cellular antioxidant defenses and enhancing xenobiotic detoxification capability of the cells [6]. Accumulated research evidences collected from in vitro studies suggests that low (≤10 μM) concentrations of these compounds are generally enough to protect normal cells against a variety of stressors through several mechanisms [7]. However, it is worth noting that rosemary polyphenols can also have opposite effects. As stated above, they improve cell survival and protect against cytotoxicity, but also they induce apoptosis and inhibit cell proliferation in certain cancer cell lines. In this regard, CA, CS and rosemary extracts have been shown to exert antitumor activities, mainly involving anti-proliferative and pro-apoptotic effects, at higher concentrations than those that typically promote cytoprotection [8], suggesting that the effects of these compounds are cell type- and dose-dependent. This dual property, also shared by other polyphenols such as resveratrol, has been related to the capability of polyphenols to modulate the altered redox environment of cancer cell [9]. Although

Correspondence: Dr. V. García-Cañas, Laboratory of Foodomics, Institute of Food Science Research (CIAL, CSIC), Nicolas Cabrera 9, 28049, Madrid, Spain
E-mail: virginia.garcia@csic.es
Fax: +34 910-017-905

Abbreviations: **BSO**, buthionine-(S,R)-sulfoximine; **CA**, carnosic acid; **CAT**, catalase; **CHOP**, C/EBP homologous protein; **CI**, confidence interval; **CS**, carnosol; **DCFH-DA**, dichlorofluorescin diacetate; **ER**, endoplasmic reticulum; **GSH**, reduced glutathione; **GSSG**, oxidized glutathione; **HO-1**, heme oxygenase protein; **MTT**, 3-(4,5-Dimethyl-2-thiazolyl)-2,5-diphenyl-2H-tetrazolium bromide; **ROS**, reactive oxygen species; **RT-qPCR**, quantitative reverse transcription PCR; **SC-RE**, polyphenol-enriched rosemary extract; **SOD**, superoxide dismutase

several in vitro studies reveal that *Nrf2*-mediated oxidative stress response is also modulated in cancer cell models by rosemary diterpenes, other specific molecular events have been linked to the antitumor activity of these polyphenols [10,11]. In the same line of evidence, recent literature suggests that the antioxidant activity of some phenolic compounds may not fully account for their observed anti-proliferative effects [12]. With regard to the pro-apoptotic effects of rosemary diterpenes, they seem to be exerted through different mechanisms associated with intracellular redox imbalance, such as mitochondrial dysfunction [13], endoplasmic reticulum (ER) stress promotion [14], glutathione depletion [15], reactive oxygen species (ROS) generation and ER stress-mediated ATF4 and CHOP expression [16]. In a previous study in our laboratory, cytostatic concentrations of rosemary polyphenols induced changes in intracellular ROS levels and transcriptional changes orchestrated by unfolded protein response in HT-29 colon cancer cells [17]. Although all these reports collectively demonstrate that bioactive concentrations of rosemary polyphenols against cancer cell proliferation and viability may modulate intracellular redox status in different cell types, the mechanisms underlying these molecular changes are still unknown.

Despite many phenolic compounds are commonly recognized as antioxidants, they are also able to act as prooxidants [18]. A growing body of evidence suggests that the prooxidant activities of certain phenolic compounds such as catechol, caffeic acid, epigallocatechin, gallic acid and resveratrol play important roles in their antitumor effects [19]. Some of the prooxidant effects of these compounds are induced in the presence of transition metals [12]. However, many published reports have demonstrated that the prooxidant effects of several polyphenols are attributed to an artifact derived from in vitro cell cultures [20]. Regarding rosemary polyphenols, in contrast to their widely investigated antioxidant activity, the prooxidant properties of these compounds have been scarcely reported. For instance, Aruoma et al. [1] suggested that both diterpenes accelerate bleomycin-induced DNA damage. In addition, CA was observed to generate H_2O_2 in PBS solutions; and medium to high concentrations (>10 μM) of the same diterpene were found to enhance the Cu^{2+}/H_2O_2-induced oxidation of human serum albumin in cell-free systems [5]. Furthermore, in a study by Slameňová et al. [4] on the protective effect of rosemary extracts on DNA oxidation, high concentrations (>15 μg/mL) of rosemary extracts, in contrast to lower concentrations, induced very high DNA damage and other cytotoxic effects after 24 h incubation. These findings suggest that certain rosemary polyphenols, as other reported polyphenols [21], may exhibit antioxidant or prooxidant effects depending on the assayed conditions, being the selected polyphenol concentration a determinant factor. In this work, in vitro autooxidation of CA, CS and a polyphenol-enriched rosemary extract (SC-RE) in cell culture conditions was investigated. The dependency on rosemary polyphenols autooxidation of their inhibitory effect on cell proliferation and their effects on intracellular redox status were also evaluated in HT-29 cell line. In addition, the contribution of polyphenols autooxidation to the induction of molecular markers of stress and alteration of cell cycle were also investigated.

2 Materials and methods

2.1 Standard polyphenols (CA, CS) and supercritical rosemary extract (SC-RE) sample

CA and CS were purchased from Sigma (St. Louis, MO). SC-RE was obtained from dried rosemary leaves using supercritical CO_2 and 7% (v/v) ethanol at 150 bar as reported elsewhere [22]. Chemical characterization of the SC-RE indicated that two main diterpenes, CA and CS, were found at high concentrations in the extract, namely, 363.3 and 45.6 μg/mg extract, respectively. Dry extract and standard polyphenols were dissolved in DMSO at 30 mg/mL and 100 mM, respectively, and stored as aliquots at –80°C until use.

2.2 Cell culture conditions

Colon adenocarcinoma HT-29 cells obtained from ATCC (American Type Culture Collection, LGC Promochem, UK) were grown in McCoy's 5A supplemented with 10% (v/v) heat-inactivated fetal calf serum, 50 U/mL penicillin G, and 50 U/mL streptomycin, at 37°C in humidified atmosphere and 5% CO_2. When cells reached ~50% confluence, they were trypsinized, neutralized with culture medium, plated in different culture plates at 10 000 cells/cm^2 and allowed to adhere overnight at 37°C.

2.3 Measurement of hydrogen peroxide in cell culture media

H_2O_2 was determined in the culture medium with different concentration of rosemary polyphenols, with and without cells over different incubation times by ferrous ion oxidation-xylenol orange assay using OxiSelect™ Hydrogen Peroxide Assay Kit (Cell Biolabs, Inc., San Diego, CA, USA) following manufacturer instructions. Catalase (CAT), superoxide dismutase (SOD) and buthionine-(S,R)-sulfoximine (BSO) were purchased from Sigma.

2.4 Cell proliferation assays

Cell viability was determined using the MTT (3-(4,5-Dimethyl-2-thiazolyl)-2,5-diphenyl-2H-tetrazolium bromide) assay. Briefly, cells were treated with the vehicle, different concentrations of CA (8.3–16.6 μg/mL), CS (8.3–16.5 μg/mL) or SC-RE (30–60 μg/mL), with and without CAT (30 U/mL) for 24 h, depending on the experiment, followed by incubation with 0.5 mg/mL MTT solution at 37°C for 3 h. The medium was removed, and the purple formazan crystals were dissolved in DMSO. The absorbance was measured at

570 nm. Results are provided as the mean of the percentage of treated minus control samples ± SEM of at least three independent experiments, each performed in triplicate.

2.5 Determination of intracellular ROS

For the measurement of intracellular ROS, cells were treated with CA, CS or SC-RE for 6 h. The intracellular ROS levels were determined by flow cytometry using the oxidation-sensitive fluorescent probe 2′,7′-dichlorofluorescin diacetate, acetyl ester (DCFH-DA) (Sigma, St. Louis, MO). Briefly, cells were loaded with 10 μM of DCF-DA dissolved in McCoy's 5A phenol red free and incubated for 30 min in the dark at 37ºC. For each analysis, 20 000 events were recorded. Results are shown as the mean of the log mean fluorescence intensity relative to control ± SEM. of three independent experiments. The results were analyzed using a Student's *t*-test and differences were considered significant at $p < 0.05$.

2.6 Determination of intracellular reduced and oxidized glutathione

For the measurement of intracellular reduced and oxidized glutathione, cells were treated with CA (12.5 μg/mL), CS (12.5 μg/mL) or SC-RE (45 μg/mL) for different times in 78 cm^2 cell culture dishes. After treatments, cells were trypsinized, washed with PBS solution and lysed with extraction buffer (20 mM HCl, 5 mM diethylene triamine pentaacetic acid, 10 mM ascorbic acid and 5% (v/v) trichloroacetic acid). The lysates were incubated on ice for 5 min, and cell debris was removed by centrifugation at 13 000 x *g* for 2 min. The content of intracellular reduced (GSH) and oxidized glutathione (GSSG) in supernatants was estimated in parallel with *o*-phthalaldehyde by the method of Senft et al. [23]. The levels of intracellular GSH and GSSG were quantified using GSH and GSSG standard solutions, respectively. GSH and GSSG values (nmol/μL) were normalized to the cell number in the PBS solution, determined prior to the cell lysis.

2.7 Cell cycle flow cytometry analysis

For cell cycle analysis, cells were treated with the vehicle, CA (12.5 μg/mL) or SC-RE (30 and 45 μg/mL) for 24 h, and then trypsinized, washed with PBS, and fixed with 70% (v/v) cold ethanol at –20°C for at least 24 h. Fixed cells were resuspended in 0.5 mL of PI/RNase staining buffer (BD Pharmingen, San Jose, CA), incubated for 15 min in the dark, and analyzed on a Gallios flow cytometer equipped with a 0.75 W argon laser set at 488 nm (Beckman Coulter, FL, USA). A total of 10 000 events were recorded for each sample and a frequency histogram of peak area was generated and analyzed using Cylchred (V.1.0.0.1) software (University of Wales College of Medicine, Cardiff, UK). Results are provided as the mean of the percentage of treated minus control samples ± SEM of at least three independent experiments, each performed in triplicate. The results were examined by ANOVA with Tukey post hoc test and differences were considered significant at $p < 0.05$.

2.8 Western blotting

Cells were lysed on ice in RIPA buffer (50 mM Tris titrated by HCl to pH 7.4, 1% (v/v) NP-40, 0.5% (w/v) sodium deoxycholate, 0.1% (w/v) SDS, 150 mM sodium chloride, 2 mM EDTA, 50 mM sodium fluoride) with a protease inhibitor mixture. Total protein concentration of lysates was determined by Bio-rad DC™ assay (Bio-Rad, Hercules, CA, USA). Aliquots of 50 μg for HMOX1 (heme oxygenase protein, HO-1) detection or 80 μg for C/EBP homologous protein (CHOP) detection were applied to 10% SDS-PAGE and electrophoretically transferred to a PVDF membrane (Sigma). The membrane was blocked for 1 h at room temperature with 6% (v/v) non-fat dry milk in TBST (50 mM Tris, 150 mM sodium chloride and 0.05% (v/v) Tween 20). Incubation with specific primary antibodies β-actin (1:20 000) from Sigma, and HO-1 (1:1000) and CHOP (1:1000), both from Cell Signaling (Danvers, MA, USA), was performed in blocking buffer overnight at 4°C. Horseradish peroxidase-conjugated anti-IgG (Sigma) was used as secondary antibody. The specific proteins were detected using an enhanced chemiluminescence (ECL) kit (GE Healthcase) according to the manufacturer's instructions.

2.9 Quantitative reverse transcription PCR (RT-qPCR) analysis

Starting amounts of 0.5 μg of total RNA isolated from cells were reverse transcribed using Transcriptor First Strand cDNA Synthesis kit with oligo(dT) primers (Roche Diagnostics, Spain). Each real-time quantitative PCR reaction was performed using ViiA™ 7 Real-Time PCR System (Life Technologies, Spain); LightCycler® 480 Probes Master kit and Human UPL probes (Roche Diagnostics). Amplifications of DDIT3, GADD34, ERN1, HMOX1, XBP1 and spliced XBP1 genes were performed as in previous work using GAPDH and IPO8 genes as endogenous controls [17]. Results are shown as the mean expression ratio of the target genes ± 95% confidence interval (CI) of three independent experiments (*vide infra*).

3 Results

3.1 Detection of H_2O_2 in culture medium with rosemary polyphenols

As mentioned above, recent data suggest that ROS participate in the anticancer activity of certain rosemary diterpenes and

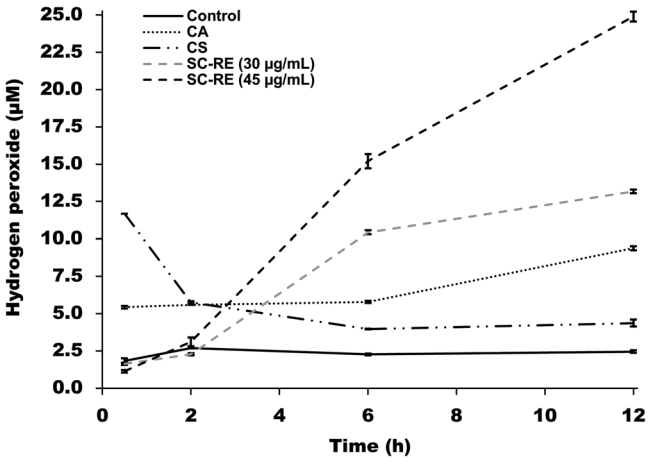

Figure 1. Quantification of H_2O_2 by the FOX assay in culture medium with phenolic compounds: CA (12.5 µg/mL), CS (12.5 µg/mL) or SC-RE (30 and 45 µg/mL). Control contained vehicle (0.2% (v/v) DMSO). Medium samples were incubated for 0–12 h at 37°C in humidified atmosphere and 5% CO_2. Error bars are given as the SEM of three replicates.

Table 1. H_2O_2 concentration (µM) in cell culture medium after 6 h incubation with rosemary polyphenols and extract. Results are expressed as the mean ± standard error of three replicates

Treatment	[Polyphenol] (µg/mL)	[H_2O_2] in cell-free culture medium	[H_2O_2] in cell-free culture medium incubated with: CAT[b]	SOD[c]	[H_2O_2] in culture medium with cells
Control[a]	0.0	2.26 ± 0.07	–[d]	–	1.04 ± 0.03
CA	4.2	3.02 ± 0.02	–	–	1.59 ± 0.05
	8.3	4.14 ± 0.14	–	–	2.06 ± 0.03
	12.5	5.79 ± 0.07	n.d.[e]	1.16 ± 0.09	2.91 ± 0.12
	16.6	7.12 ± 0.21	–	–	3.22 ± 0.04
CS	4.2	2.88 ± 0.02	–	–	2.32 ± 0.06
	8.3	3.36 ± 0.07	–	–	3.07 ± 0.03
	12.5	3.98 ± 0.02	–	–	3.39 ± 0.08
	16.6	4.88 ± 0.07	–	–	3.60 ± 0.08
SC-RE	15.0	4.60 ± 0.02	–	–	2.49 ± 0.13
	30.0	10.43 ± 0.14	n.d.	1.29 ± 0.06	4.85 ± 0.19
	45.0	15.20 ± 0.48	n.d.	1.63 ± 0.06	10.44 ± 0.44
	60.0	20.06 ± 0.14	–	–	14.45 ± 0.35

a) DMSO at a concentration of 0.2% (v/v) in cell culture medium.
b) Medium incubated with 30 Units of CAT/mL.
c) Medium incubated with 5 Units SOD/mL.
d) Not analyzed.
e) n.d., not detectable: < 1 µM H_2O_2 (limit of detection).

extracts. However, the mechanism involved in the intracellular ROS generation upon exposure to these compounds is not known yet. Some phenolic compounds autooxidize in the growth medium leading to H_2O_2 production and induction of antitumor effects [18]. In order to explore this possibility for rosemary polyphenols, the concentration of H_2O_2 was analyzed in complete culture medium (McCoy's 5A + 10% (v/v) fetal calf serum) incubated with different concentrations of CA, CS or SC-RE. The generation of H_2O_2 in culture medium containing CA, CS and SC-RE was concentration- and time-dependent (see Fig. 1 and Table 1). As it is shown in Fig. 1, detectable H_2O_2 levels were generated at the earliest incubation time tested (30 min) with CA and CS. The H_2O_2-generating potency of the different polyphenols showed different time-dependent trends in culture medium. The incubation of CA and SC-RE in culture medium caused a slow increase of H_2O_2 and reached the maximum levels after 12 h, whereas incubation with CS showed a sharp increase of H_2O_2 concentration at 30 min, followed by a rapid decrease at longer incubation times (Fig. 1). Comparatively, SC-RE produced higher concentrations of H_2O_2 than individual polyphenols. For instance, incubation of medium with 45 µg/mL SC-RE (containing equivalent concentrations of 16.4 µg/mL CA and 2.0 µg/mL CS) for 6 h provided a H_2O_2 value of 15.2 µM, whereas the incubation with similar concentrations of individual CA and CS provided H_2O_2 values lower than 7.1 and 3.0 µM, respectively (see Table 1). Supplementing cell culture medium with CAT

(30 U/mL) resulted in complete decomposition of polyphenol-generated H_2O_2 (Table 1). To elucidate the contribution of superoxide radical anions in polyphenol-mediated H_2O_2 formation, we used SOD (catalyzing the dismutation of two superoxide radical anions to H_2O_2 and O_2) instead of CAT. With 5 U/mL of SOD, a decrease of H_2O_2 could be observed for all the treatments (Table 1), suggesting that superoxide radical anion might be involved in the reaction. These results give evidence that addition of either CAT or SOD to cell culture medium efficiently lessen H_2O_2 levels in culture medium. The presence of HT-29 cells partially decreased the levels of H_2O_2 in culture media (see Table 1) suggesting that the cells' antioxidant enzymes (i.e. CAT, glutathione peroxidase and peroxiredoxins) excreted to the medium are capable of partially removing H_2O_2 generated by the phenolic compounds. However, extracellular defenses were unable to totally detoxify H_2O_2 generated in the extracellular medium by concentrations of SC-RE within 30–60 μg/mL range, decreasing H_2O_2 levels down to 4.9–14.5 μM after incubations for 6 h. Collectively, these findings suggest that a ranking according to the H_2O_2-generating potency of the rosemary polyphenols can be established as follows: SC-RE > CA > CS. In addition, cells were able to counteract mild prooxidant effects of the rosemary diterpenes, but failed on detoxifying the total H_2O_2 amounts generated by SC-RE.

3.2 Contribution of H_2O_2 production to the anti-proliferative effects of rosemary polyphenols

Previous studies have shown that rosemary polyphenols can act either as cytostatic or cytotoxic agents depending on the cell type and concentrations used [24]. Since H_2O_2 is considered a prooxidant agent that can induce cell death and cell cycle arrest [25], the potential contribution of extracellular H_2O_2 produced by rosemary polyphenols on the observed anti-proliferative effect in HT-29 cells was next investigated. Thus, the inhibitory effect of rosemary polyphenols on HT-29 cell proliferation was confirmed by MTT assay (see Fig. 2). Namely, incubation of exponentially growing HT-29 cells with different concentrations of CA, CS and SC-RE decreased cell density, which was in good agreement with our former results [11]. Then, to evaluate the contribution of generated H_2O_2 to the overall anti-proliferative activity of rosemary polyphenols, HT-29 cells were co-incubated with different concentrations of CA, CS and SC-RE and 30 U/mL CAT. As it is shown in Fig. 2, the inhibitory effect of SC-RE and CA on cell proliferation was lower in cells co-incubated with CAT. Interestingly, the mitigating effect exerted by CAT on CA inhibitory activity was concentration-dependent, alleviating by 44% the anti-proliferative effect of CA at an assayed concentration of 12.5 μg/mL. On the other hand, co-treatment with CAT increased cell proliferation by 24–27% at any of the SC-RE concentrations assayed, mitigating by 40% the anti-proliferative effect exerted by 45 μg/mL of the extract. As expected by the low H_2O_2-producing potency of

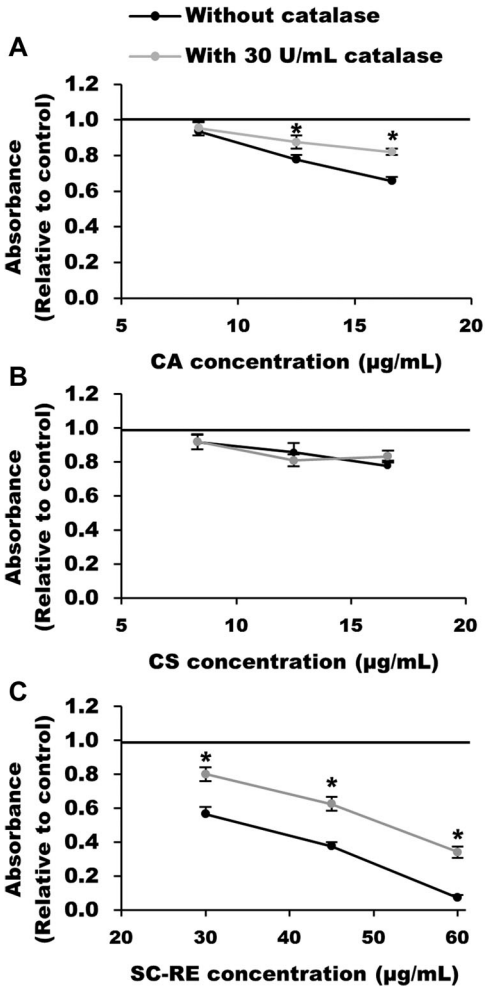

Figure 2. Effect of catalase in the anti-proliferative activity of rosemary polyphenols on HT-29 cells: (A) CA (8.3–16.6 μg/mL), (B) CS (8.3–16.5 μg/mL), and (C) SC-RE (30–60 μg/mL). Cells were incubated with 0.2% (v/v) DMSO (control) and different concentrations of polyphenols with and without catalase (30 U/mL) for 24 h. Error bars are given as the SEM of three independent experiments each performed in triplicate. * Indicates significant differences between polyphenol treatment with and without catalase, as determined by *t*-test ($p < 0.05$).

CS, CAT co-incubation had no significant inhibitory effect on CS anti-proliferative activity. Taken together, these results suggest that H_2O_2 may be at least partially involved in the anti-proliferative effect of SC-CE and CA in HT-29 cells.

3.3 Prooxidant effects of rosemary polyphenols on HT-29 cells

To evaluate the impact of rosemary polyphenols on the cellular redox status, the intracellular level of ROS was analyzed in CA-, CS- and SC-RE-treated cells. Intracellular ROS was detected in HT-29 cells using DCFH-DA which is oxidized by ROS to the highly fluorescent DCF. As it is shown in Fig. 3A, exposure of cells to CA and SC-RE for 6 h caused

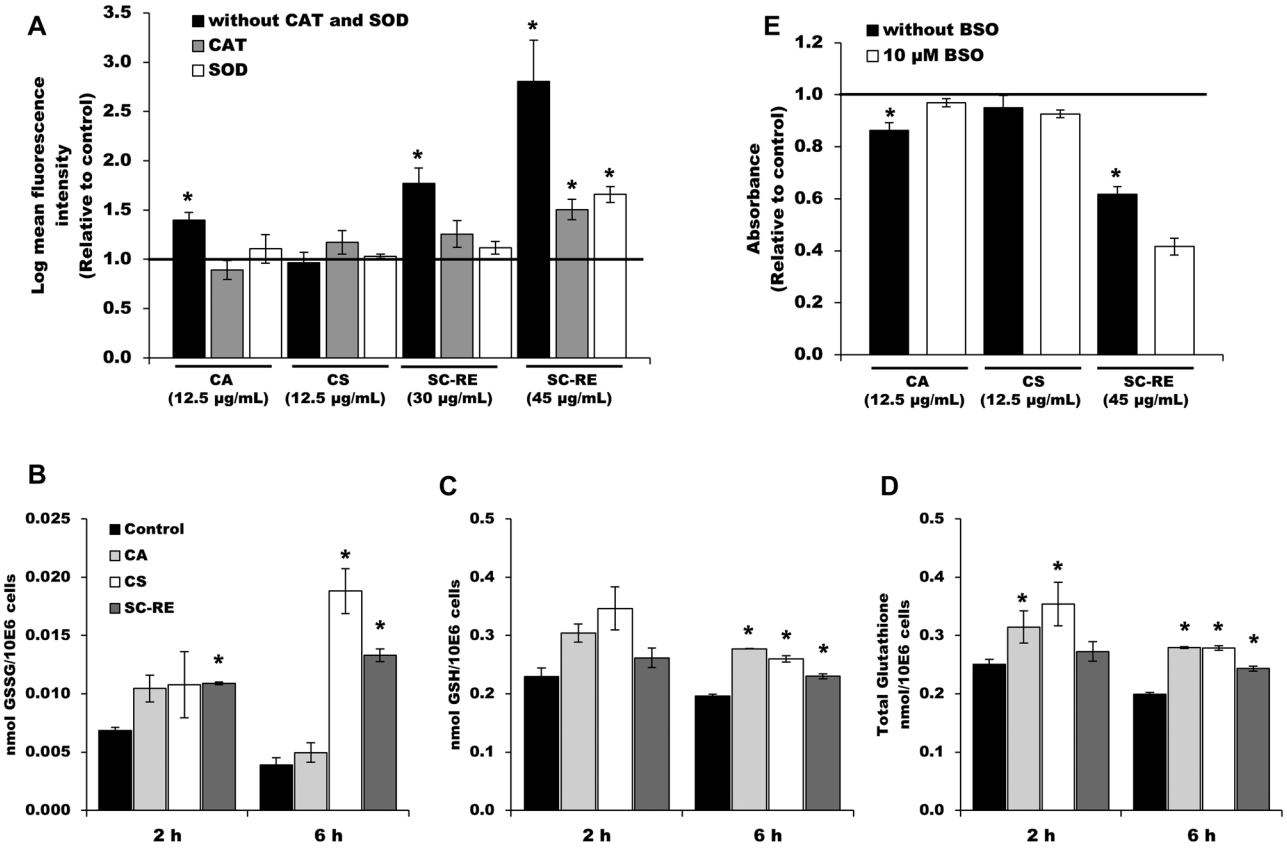

Figure 3. (A) Intracellular ROS levels in HT-29 cells treated for 6 h with 12.5 µg/mL of CA, 12.5 µg/mL of CS, and 30 or 45 µg/mL of SC-RE, with or without 30 U/mL of CAT or 5 U/mL of SOD. (B–D) Effect of rosemary polyphenols on intracellular glutathione levels. Cells, treated for 2 and 6 h with 12.5 µg/mL of CA, 12.5 µg/mL of CS, and 45 µg/mL of SC-RE, were harvested and GSSG (B) and GSH (C) levels were determined as described in Section 2.6. Total glutathione (D) was calculated as GSSG+GSH. (E) Effect of BSO pre-treatment in the anti-proliferative activity of rosemary polyphenols on HT-29 cells, as determined by the MTT assay. Error bars are given as the SEM of three independent experiments. * Indicates significant differences between each polyphenol treatment and the respective time control (0.2% (v/v) DMSO) as determined by *t*-test ($p < 0.05$).

significant (p-value < 0.05) increases of intracellular ROS levels as reflected by increased fluorescence intensity of the treated cells as compared to control cells. In addition, intracellular ROS levels detected upon SC-RE exposures were found to be concentration-dependent. As it was expected owing to the low capacity of CS to produce H_2O_2 under culture conditions, the assayed concentration of CS did not induce ROS generation in HT-29 cells at the assayed time. To assess the contribution of polyphenol-mediated H_2O_2 generation in the medium to the intracellular ROS production, cells were co-incubated with polyphenols in presence of CAT or SOD. As it is shown in Fig. 3A, ROS levels were significantly decreased with all of the assayed polyphenol concentrations with CAT and SOD. Altogether, these results suggest that the generation of H_2O_2 by autoxidation of CA and SC-RE in culture medium is correlated with intracellular ROS generation in HT-29 cells.

In order to evaluate the effects of rosemary polyphenols on the antioxidant capacity of HT-29 cells after short-term exposures (2 and 6 h), the levels of glutathione, the most abundant endogenous antioxidant in cells, were evaluated by analyzing intracellular GSH and GSSG. As deduced by the increased GSSG levels shown in Fig. 3B, exposure of cells to CS and SC-RE significantly induced glutathione oxidation over the time. On the other hand, results in Fig. 3C show the increase in GSH levels observed in CA- and CS-treated cells were comparatively higher with respect to the levels detected in SC-RE treated cells. As a general trend, exposure to rosemary polyphenols induced glutathione synthesis in HT-29 cells, indicated by the increased total glutathione levels with respect to the levels found in untreated controls (see Fig. 3D). However, stimulation of glutathione synthesis was faster and significant in CA- and CS-treated cells, whereas it appeared to be delayed and only modestly induced in SC-RE-treated cells.

BSO is a known inhibitor of γ-glutamylcysteine synthetase, an essential enzyme for the synthesis of GSH. Aiming to investigate the role of GSH in rosemary polyphenol effects, HT-29 cells were incubated with a non-toxic dose (10 µM) of BSO for 24 h and then treated with CA, CS and SC-RE for 24 h. After incubation, the effect of treatments on cell viability was measured by MTT assay. When cells were

treated with BSO alone for 24 h, a reduction of 75% was observed in GSH levels, but it did not have any significant effect on cell growth (data not shown) corroborating its activity as GSH depleter in HT-29 cells [26]. Results in Fig. 3E indicate that BSO pre-treatment sensitized cells against SC-RE (45 μg/mL) exposure, whereas BSO addition to the cell culture was unable to sensitize cells against subsequent CA or CS treatment.

3.4 Influence of rosemary polyphenols autooxidation on cell cycle and stress markers

As stated above, a number of recent studies have shown that ROS have a role as signaling molecules that can regulate various cellular processes, including proliferation [27] and cell cycle [28]. In regard to rosemary polyphenols, the SC-RE extract and CA used in this study have reported cytostatic effects by affecting cell cycle distribution in HT-29 cells [11]. In order to investigate the potential contribution of H_2O_2 produced by SC-RE and CA to the effect exerted by this polyphenols on cell cycle progression, cell cycle analysis by flow cytometry was performed on HT-29 cells incubated for 24 in the presence of 12.5 μg/mL CA and two concentrations of SC-RE (30 and 45 μg/mL). As it is shown in Fig. 4A, incubation of HT-29 cells with 12.5 μg/mL CA and 30 μg/mL SC-RE for 24 h resulted in a substantial inhibition of cell cycle progression, manifested by the accumulation of cells in the G1 phase (p-value < 0.05) with respect to untreated control cells, confirming our previous results. By contrast, 45 μg/mL of SC-RE induced a significant (p-value $= 0.0002$) increase in the percentage of cells (36%) arrested in G2/M with respect to control cells. The results of co-incubating rosemary polyphenols with CAT suggested that the presence of CAT in culture medium was able to reverse part of the effects exerted by 45 μg/mL of SC-RE, alleviating by 52% the G2/M phase arrest induced by SC-RE (i.e., from 36 to 15% G2/M arrested cells).

Previously reported effects of SC-RE on the transcriptional response of HT-29 cells have shown important variations in the genes linked to the expression of two protein biomarkers, HO-1 and CHOP, typically involved in the antioxidant and the unfold protein responses, respectively [17]. To corroborate these results, which could also give some additional light to the activity of rosemary polyphenols, their effect was analyzed at different time points. Western blot data indicated that SC-RE induced the expression of both protein biomarkers HO-1 and CHOP following slightly different kinetics (see Fig. 4B). The study was also extended to evaluate the SC-RE effects on the expression of a panel of genes involved in the mentioned stress responses by RT-qPCR. Similar to Western-blot results, all the chosen gene biomarkers of the antioxidant (HMOX1) and the unfolded protein (DDIT3, GADD34, ERN1, and spliced XBP1) responses were up-regulated by SC-RE (Fig. 4C). To examine potential contribution of the polyphenol-mediated H_2O_2 generation to the transcriptional changes induced by rosemary extract, the expression of the selected biomarkers was analyzed in cells incubated with SC-RE in presence of CAT. Results in Fig. 4B and C show that protein and mRNA levels remained unaltered in cells co-treated with SC-RE and CAT. Altogether, our data indicate that H_2O_2 generated by SC-RE in culture medium does not appear to play a relevant role, either by interfering or potentiating, in the effect of the extract on the induction of the *Nrf2*-mediated antioxidant and unfolded protein responses.

4 Discussion

Proliferation is an intrinsic property of cells that is tightly linked to the metabolic state of cells and also the environmental conditions. Internal and external conditions often result in the generation of both endogenous and exogenous free radicals in the form of ROS. Elevated levels of ROS are difficult to control and can lead to cellular mutations, being a demonstrated causative factor in tumorigenesis [29]. Cells have evolved mechanisms of sensing and signaling to respond to and even to adapt to ROS [25]. In addition, it is generally accepted that ROS act as second messengers in signal transduction pathways that govern and determine cellular proliferation, among other processes [27]. When ROS reach toxic levels can potentially induce cancer cell death, cell cycle arrest and inhibit cancer progression [25]. This apparent contradiction between the negative role of ROS as cellular toxicants and their positive role as cellular signaling elements seems to be highly dependent on the homeostatic control of their intracellular concentration [30]. In recent years, a growing body of evidence suggests that cancer cells maintain elevated ROS production as a result of their increased metabolic activity, required for keeping growth and proliferation at high levels [18]. As an adaptive mechanism, cancer cells exhibit an activated status of antioxidant response signaling to maintain ROS at levels below the threshold for lethal effects, but high enough to serve as signaling molecules [31]. In line with this, the modulation of ROS levels to treat cancer is increasingly gaining importance [32]. Recently, it has been suggested that proliferation of cancer cells is dependent on basal constitutive ROS levels and that cancer cells with higher basal ROS are more sensitive to treatments with ROS scavengers [30]. Alternatively, the alteration of redox homeostasis by prooxidant agents is also emerging as an attractive anticancer strategy [33]. The elevation of ROS levels, either by increasing ROS generation or by modulation of specific cellular targets involved in redox homeostasis, could be a strategy to selectively kill or arrest cancer cells. In this regard, H_2O_2 appears to have a key role in oxidative stress-induced cancer cell death. Flavonoids and many other phenolic compounds are unstable in the commonly used cell culture media, undergoing rapid oxidation to produce H_2O_2 and often other ROS such as superoxide [34]. In some cases, this phenomenon accounts for many of the observed in vitro effects exerted by polyphenols in cells, originating artifactual results. This work focused on the investigation of the potential occurrence of rosemary polyphenols autooxidation in culture medium and its

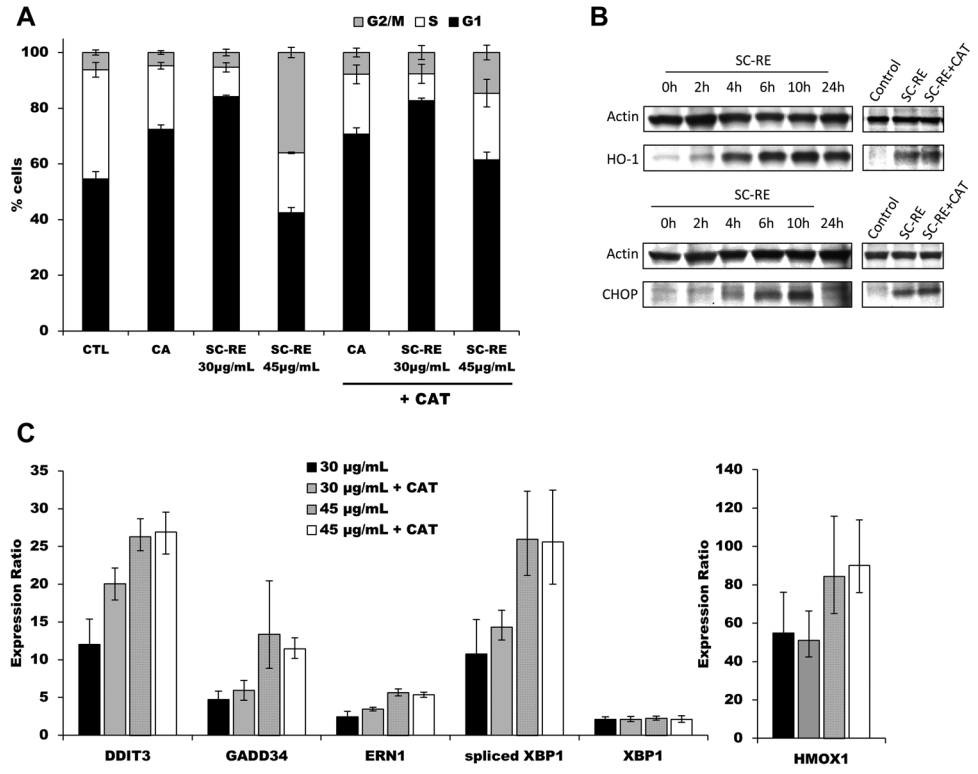

Figure 4. (A) Histograms of cell cycle distribution. Control and treated cells with 12.5 μg/mL of CA, and 30 μg/mL and 45 μg/mL of SC-RE, with and without 30 U/mL catalase, for 24 h were analyzed by flow cytometry. (B) Western blot analysis of HO-1 and CHOP in SC-RE-treated cells (30 μg/mL) at different time points (left panels), and in SC-RE-treated cells (45 μg/mL) with and without catalase for 6 h (right panels); (C) Expression ratios (relative to control) of relevant gene biomarkers in HT-29 cells exposed to 30 and 45 μg/mL of SC-RE, with and without 30 U/mL catalase, for 6 h. Error bars are given as the 95% CI of three independent experiments.

possible contribution to the anti-proliferative and molecular effects attributed to these polyphenols.

Our results demonstrate that H_2O_2 produced by individual rosemary diterpenes and rosemary extract under culture conditions is influenced by the type of polyphenol, concentration and incubation time. A previous study performed in cell free systems demonstrated that CA underwent rapid oxidation to generate H_2O_2 in a concentration-dependent manner [5]. Although our results also suggest that CA produces H_2O_2 in culture media, the H_2O_2 concentrations produced by this diterpene in culture media appear to be comparatively lower than those reported in PBS at the same time point. It is also interesting to note that H_2O_2 generation mediated by CS follows a kinetic that does not exert apparent strong prooxidant effects at the cytostatic concentration assayed in the present study. On the other hand, H_2O_2 generated by CA and SC-RE showed similar trend as that reported for other catechol-type compounds [35]. Higher H_2O_2 concentrations formed in the medium in presence of SC-RE were only partially decomposed in presence of cells. Thus, considering that H_2O_2 may migrate into cells across the cell membrane, and it may exert biological effects on cells, the potential influence of H_2O_2 generated by cytostatic concentrations of rosemary polyphenols in the intracellular redox status was evaluated. The influence of polyphenols in intracellular ROS levels is highly heterogeneous in the available literature since it depends on a variety of factors. Cells adapt to oxidative stress increasing levels of antioxidant defenses [31]. In this regard, glutathione is the most abundant endogenous antioxidant in eukaryotic cells. Owing to its reactivity and high intracellular concentrations (within the millimolar range), GSH is involved in cell protection against free radicals and conjugates with toxic electrophiles [36]. According to our observations, CA induces only a mild prooxidant effect that was mediated by H_2O_2 generated from CA autooxidation, and accounted for the modest intracellular ROS observed in CA-treated cells. However, CA was found to rapidly stimulate GSH synthesis supporting previous results by ours and others regarding the indirect antioxidant activity of this diterpene [14] and [17]. As stated above, the H_2O_2-producing properties of CS under the experimental conditions of this study did not contribute to the anti-proliferative activity of this diterpene. These observations were in good agreement with the unaltered intracellular ROS levels observed after exposure with CS. However, intracellular glutathione oxidation by CS was strikingly high after incubation for 6 h. Apparently, this effect could cause some stress in cells, rapidly stimulating synthesis of GSH to counteract GSSG elevation.

Several articles have reported on the effects of CA and CS on intracellular ROS levels in different cell models. In general, high concentrations of both diterpenes are associated with ROS generation. For instance, it has been demonstrated that CA at concentrations higher that 30 μM (~10 μg/mL) induced significant levels of ROS during the first six hours incubation in neuroblastoma [37] and renal carcinoma cells [16]. However, contrasting results have been reported in reports evaluating the in vitro chemoprotective activity of CA at low concentrations (<10 μM; ~3μg/mL). For instance, 10 μM and 1 μM CA were found to increase total glutathione levels in a neuronal HT22 [6] and SH-SY5Y

cell lines [38]. CS has been also subject of study and low concentrations of this diterpene have been found to increase the levels of GSH in human hepatoma HepG2 [39] and C6 glial cells [40]. In a recent report, however, Al Dhaheri et al. [41] have demonstrated that CS concentrations higher than 25 μM (~8 μg/mL) induced generation of ROS and G2 arrest in breast cancer cells after short-term incubations. In a separate study, Ishida et al. [15] observed that incubations for 3 and 6 h of leukemia cells with 40 μM CS (~13 μg/mL) induced apoptosis and glutathione depletion by an unknown mechanism that was independent of extracellular H_2O_2 generation. Our results indicate that after incubation for 6 h, the concentration of GSSG increases over fourfold in CS-treated cells with respect to untreated cells. These findings together with those reported in the literature point out that CS might exert part of its anti-proliferative effect through altering glutathione metabolism. Our data also suggests that SC-RE induced prooxidant effects that were somewhat related with the H_2O_2 formed by autooxidation of the extract constituents. Such effects were partially responsible for the anti-proliferative activity observed in MTT assays, and also in part, accounted for the elevated (over threefold with respect to control) ROS detected in HT-29 cells. SC-RE also induced fast and sustained intracellular glutathione oxidation. Although SC-RE treatment stimulated GSH synthesis, the stimulation was not as substantial as with the individual diterpenes. Under these intracellular metabolic conditions, it is plausible that the alteration of the redox status in the cell occurs after short-term exposures to high SC-RE concentrations, compromising the cellular redox homeostasis and increasing the possibilities for damage by oxidative stress. Furthermore, GSH depletion by BSO, an inhibitor of GSH synthesis, sensitized cells against SC-RE. This potentiating effect of GSH depletion on the anti-proliferative effect of SC-RE treatment suggests a pivotal role of GSH in the response of the cell to SC-RE exposure, underscoring the prooxidant effect of the extract as an additional contributing factor of its activity.

Interestingly, SC-RE showed a differential effect on cell cycle distribution depending on the assayed concentration. Our data are in the same line of evidence reported by Visanji et al. [24] who suggested divergences on the effect of CA on cell cycle distribution as a function of the assayed cell type and polyphenol concentration. In our study, part of the cytostatic effect, supported by cell cycle arrest in G2/M phase and induced by a relatively high concentration of the extract (45 μg/mL), was attributable to H_2O_2 generated in extracellular medium. By contrast, H_2O_2 formed in culture medium by 12.5 μg/mL of CA or 30 μg/mL of SC-RE was not involved in cell cycle effects. Interestingly, neither antioxidant- nor ER-stress biomarkers were affected by H_2O_2 generated by SC-RE at any of the assayed concentrations, suggesting that H_2O_2 generated by polyphenol autooxidation plays an irrelevant role during the transcriptional activation of these important biomarkers.

In our previous work, it was demonstrated that SC-RE treatment induced substantial metabolic and transcriptional changes headed by ROS generation and coordinated unfolded protein response signaling triggered by ER stress in HT-29 cells [17]. It has been recently highlighted the relevant role of glutathione on the oxidant control in the ER [36]. Then, these results provide a new hypothesis that suggests that the unbalanced oxidation and synthesis of glutathione observed in SC-RE-treated HT-29 cells might be a causative factor or the result of ER stress and unfolded protein response.

In conclusion, the investigated rosemary polyphenols generated H_2O_2 under culture conditions and its production was influenced by the type of polyphenol, concentration and incubation time. In addition, large part of the H_2O_2-producing potency of the extract could not be explained by the sum of CA and CS potencies, suggesting that other constituents in the extracts are substantially contributing to the formation of H_2O_2, and consequently to some of the observed effects. Our results indicate that high extracellular H_2O_2 concentrations, resulting of using high (45 μg/mL) SC-RE concentration in culture media, exerted some artifactual effects related with cell cycle distribution and ROS generation, but they did not influence the expression of relevant genes and proteins typically modulated by the extract. These results collectively invite to be cautious in the evaluation of the in vitro cytostatic and cytotoxic effects of high concentrations of polyphenols.

This work was supported by the project AGL2014-53609-P (Ministerio de Economía y Competitividad, Spain) and S2013/ABI-2728 (Comunidad de Madrid). A.V. thanks the Ministerio de Economía y Competitividad for his FPI predoctoral fellowship. E.K. thanks the Scientific and Technological Research Council of Turkey for his grant (TUBITAK-2214A-1059B140065).

The authors declare that they have no conflict of interests.

5 References

[1] Aruoma, O. I., Halliwell, B., Aeschbach, R., Loligers, J., *Xenobiotika* 1992, *22*, 257–268.

[2] Masuda, T., Inaba, Y., Takeda, Y. J., *Agric. Food Chem.* 2001, *49*, 5560–5565.

[3] Masuda, T., Kirikihira, T., Takeda, Y. J., *Agric. Food Chem.* 2005, *53*, 6831–6834.

[4] Slameňová, D., Kubošková, K., Horváthova, E., Robichová, S., *Cancer Lett.* 2002, *177*, 145–153.

[5] Xiang, Q., Liu, Q., Xu, L., Qiao, Y., Wang, Y., Liu, X., *Food Sci. Biotechnol.* 2013, *22*, 1381–1388.

[6] Satoh, T., Kosaka, K., Itoh, K., Kobayahi, A., Yamamoto, M., Shimojo, Y., Kitajima, C., Cui, J., Kamins, J., Okamoto, S., Izumi, M., Shirasawa, T., Lipton, S. A., *J. Neurochem.* 2008, *104*, 1116–1131.

[7] Tamaki, Y., Tabuchi, T., Takahshi, T., Kosaka, K., Satoh, T., *Planta Med.* 2010, *76*, 683–688.

[8] Petiwala, S. M., Puthenveetil, A. G., Johnson J. J., *Front. Pharmacol.* 2013, *4*, 1–4.

[9] Giovannini, C., Masella, R., *Nutr. Neurosci.* 2012, *15*, 134–149.

[10] Ibáñez, C., Valdés, A., García-Cañas, V., Simó, C., Celebier, M., Romamora-Reverte L, Gómez-Martínez, A., Herrero, M., Castro-Puyana, M., Segura-Carretero, A., Ibáñez, E., Ferragut, J. A., Cifuentes A., *J. Chromatogr. A* 2012, *1248*, 139–153.

[11] Valdés, A., García-Cañas, V., Simó, C., Ibáñez, C., Micol, V., Ferragut, J. A., Cifuentes, A., *Anal. Chem.* 2014, *86*, 9807–9815.

[12] Khan, H. Y., Zubair, H., Ullah, M. F., Ahmad, A., Hadi, S. M., *Curr. Drug Targets* 2012, *13*, 1738–1749.

[13] Xiang, Q., Ma, Y., Dong, J., Shen, R., *Int. J. Food Sci. Nutr.* 2015, *66*, 76–84.

[14] Yan, M., Li, G., Petiwala, S. M., *J. Funct. Foods* 2015, *13*, 137–147.

[15] Ishida, Y., Yamasaki, M., Yukizaki, C., Nishiyama, K., Tsubouchi, H., Okayama, A., Kataoka, H., *Human Cell* 2014, *27*, 68–77.

[16] Min, K. J., Jung, K. J., Kwon, T. K., *J. Cancer Prev.* 2014, *19*, 170–178.

[17] Valdés, A., Sullini, G., Ibáñez, E., Cifuentes, A., García-Cañas, V., *J. Funct. Foods* 2015, *15*, 429–439.

[18] Saeidnia, S., Abdollahi, M., *Toxicol. Appl. Pharmacol.* 2013, *271*, 49–63.

[19] Hadi, S. M., Bhat, S. H., Azmi, A. S., Hanif, S., Shamim, U., Ullah, M. F., *Sem. Cancer Biol.* 2007, *17*, 370–376.

[20] Long, L. H., Hoi, A., Halliwell, B., *Arch. Biochem. Biophys.* 2010, *501*, 162–169.

[21] Forester, S. C., Lambert, J. D., *Mol. Nutr. Food Res.* 2011, *55*, 844–854.

[22] Sánchez-Camargo, A. P., Valdés, A., Sullini, G., García-Cañas, V., Cifuentes, A., Ibáñez, E., Herrero, M., *J. Funct. Foods* 2014, *11*, 293–303.

[23] Senft, A. P., Dalton, T. P., Shertzer, H. G., *Anal. Biochem.* 2000, *280*, 80–86.

[24] Visanji, J. M., Thompson, D. G., Padfield, P. J., *Cancer Lett.* 2006, *237*, 130–166.

[25] Glasauer, A., Chandel, N. S., *Biochem. Pharmacol.* 2014, *92*, 90–101.

[26] Knoll, N., Ruhe, C., Veeriah, S., Sauer, J., Glei, M., Gallagher, E. P., Pool-Zobel, B. L., *Toxicol. Sci.* 2005, *86*, 27–35.

[27] Burhans, W. C., Heintz, N. H., *Free Radic. Biol. Med.* 2009, *47*, 1282–1293.

[28] Sarsour, E. H., Kumar, M. G., Chaudhuri, L., Kalen, A. L., Goswami, P. C., *Antiox. Redox Signal.* 2009, *11*, 2985–3011.

[29] Gupta, S. C., Hevia, D., Patchva, S., Park, B., Koh, W., Aggarwal, B. B., *Antiox. Redox Signal.* 2012, *16*, 1295–1322.

[30] Khalil, H. S., Goltsov, A., Langdon, S. P., Harrison, D. J., Bown, J., Deeni, Y., *J. Biotechnol.* 2015, *202*, 12–30.

[31] Jaramillo, M. C., Zhang, D. D., *Genes Dev.* 2014, *27*, 2179–2191.

[32] Wondrak, G. T., *Antiox. Redox Signal.* 2009, *11*, 3013–3069.

[33] Hail, N., Cortes, M., Drake, E. N., Spallholz, J. E., *Free Rad. Biol. Med.* 2008, *45*, 97–110.

[34] Halliwell, B., *Biomed. J.* 2014, *37*, 99–105.

[35] Mendes, V., Costa, V., Mateus, N., *RSC Adv.* 2015, *5*, 1–9.

[36] Appenzeller-Herzog, C., *J. Cell Sci.* 2011, *124*, 843–855.

[37] Tsai, C. W., Lin, C. Y., Lin, H. H., Chen, J. J., *Neurochem. Res.* 2011, *36*, 2442–2451.

[38] Chen, J. H., Ou, H. P., Lin, S. Y., Lin, F. J., Wu, C. R., Chang, S. W., Tsai, C. W., *Chem. Res. Toxicol.* 2012, *25*, 1893–1901.

[39] Chen, C. C., Chen, H. L., Hsieh, C. W., Yang, Y. L., Wung, B. S., *Acta Pharm. Sinica.* 2011, *32*, 62–69.

[40] Kim, S. Y., Park, E., Park, J. A., Choi, B. S., Kim, S., Jeong, G., Kim, C. S., Kim do K., Kim, S. J., Chun, H. S., *J. Agr. Food Chem.* 2010, *58*, 1543–1550.

[41] Al Dhaheri, Y., Attoub, S., Ramadan, G., Arafat, K., Bajbouj, K., Karuvantevida, N., AbuQamar, S., Eid, A., Iratni, R., *PLOS one.* 2014, *9*, e109630, 1–14.

3.2.6 Comprehensive proteomic study of the antiproliferative activity of a polyphenol-enriched rosemary extract on colon cancer cells using nano-liquid chromatography-orbitrap MS/MS

Valdés, A., Artemenko, K. A., *García-Cañas, V., *Bergquist, J., Cifuentes, A. *J. Proteome Res.* 2016 (en prensa).

DOI: http://dx.doi.org/doi:10.1021/acs.jproteome.6b00154

Journal of proteome research

Article

pubs.acs.org/jpr

Comprehensive Proteomic Study of the Antiproliferative Activity of a Polyphenol-Enriched Rosemary Extract on Colon Cancer Cells Using Nanoliquid Chromatography−Orbitrap MS/MS

Alberto Valdés,[†] Konstantin A. Artemenko,[‡] Jonas Bergquist,[*,‡] Virginia García-Cañas,[*,†] and Alejandro Cifuentes[†]

[†]Laboratory of Foodomics, Institute of Food Science Research (CIAL, CSIC), Calle Nicolás Cabrera 9, 28049 Madrid, Spain

[‡]Analytical Chemistry, Department of Chemistry-BMC and SciLifeLab, Uppsala University, Husargatan 3, 75124 Uppsala, Sweden

Supporting Information

ABSTRACT: In this work, a proteomics strategy based on nanoliquid chromatography−tandem mass spectrometry (nano-LC−MS/MS) using an Orbitrap high-resolution mass spectrometer together with stable isotope dimethyl labeling (DML) is applied to quantitatively examine relative changes in the protein fraction of HT-29 human colon cancer cells treated with different concentrations of a polyphenol-enriched rosemary extract over the time. The major objective of this study was to gain insights into the antiproliferative mechanisms induced by rosemary polyphenols. Using this methodology, 1909 and 698 proteins were identified and quantified in cell extracts. The polyphenol-enriched rosemary extract treatment changed the expression of several proteins in a time- and concentration-dependent manner. Most of the altered proteins are implicated in the activation of Nrf2 transcription factor and the unfolded protein response. In conclusion, rosemary polyphenols induced proteomic changes that were related to the attenuation of aggresome formation and activation of autophagy to alleviate cellular stress.

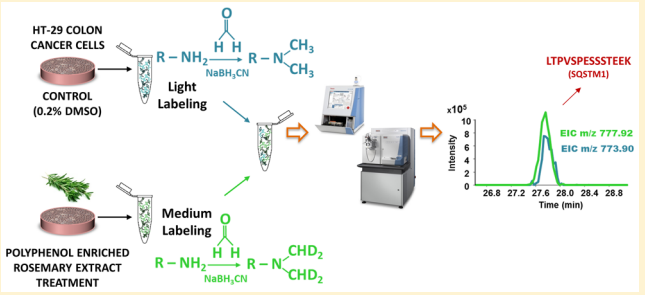

KEYWORDS: *antiproliferative activity, foodomics, colon cancer, dimethyl labeling, HT-29 cells, mass spectrometry, quantitative proteomics, rosemary extract*

INTRODUCTION

The aromatic plant *Rosmarinus officinalis* L. (rosemary) has been used for thousands of years for medicinal purposes due to its health benefits.[1] Among the most relevant properties attributed to rosemary extracts are the antioxidant, anti-inflammatory, chemoprotective, antiadipogenic, and antiproliferative activities.[2−4] The antioxidant activity of rosemary may be attributed to its phenolic constituents: carnosic acid, carnosol, rosmarinic acid, rosmanol, methyl carnosate, and betulinic acid, among others.[3,5] Due to this high antioxidant activity, rosemary has been recently approved as an additive for food preservation by the FDA in the USA and the EFSA in the European Union.[6,7] Several studies have demonstrated that certain rosemary diterpenes, such as carnosic acid and carnosol, can activate in vitro and in vivo nuclear transcription factor Nrf2, a relevant regulator of the response against oxidative stress.[8] Because this response usually enhances xenobiotic detoxification and antioxidant function, rosemary diterpenes and enriched extracts have been suggested to exert chemoprotective activities.[9] In addition, the antiproliferative effect of rosemary polyphenols has been demonstrated in different cancer cell models.[10] Carnosic acid, carnosol, and enriched rosemary extracts exert a broad range of effects at the different molecular levels (mRNA, proteins, and metabolites) causing a variety of responses and outcomes in cancer cells, suggesting that the effect of these compounds is dependent on the cell type and context.[11−14] Recent studies report that concentrations above 25 μM of these compounds induce intracellular redox imbalance[15] and endoplasmic reticulum (ER) stress.[16,17] The study of the biological activity of rosemary compounds have been also approached by the application of novel Foodomics strategies.[18] Thus, comprehensive transcriptomic and metabolomic analyses helped identify global changes induced by rosemary polyphenols on colon cancer and leukemia cells.[11,16,19] As an example, previous results obtained in our laboratory have shown that rosemary polyphenols transcriptionally trigger a strong Nrf2-mediated antioxidant response in addition to the unfolded protein response (UPR) to alleviate ER stress.[16] The findings allowed the establishing of the link between UPR and the observed changes in cholesterol metabolism in colon cancer cells exposed to rosemary polyphenols. Because ER stress can result in distinct and contrasting outputs, it is essential to monitor the amplitude and kinetics of UPR signaling, as well as the crosstalk with other signaling pathways, to understand the underlying mechanisms

Received: February 19, 2016

DOI: 10.1021/acs.jproteome.6b00154
J. Proteome Res. XXXX, XXX, XXX−XXX

of the effects of rosemary polyphenols in cancer cells. In this work, we intend to add another layer of molecular information to the current knowledge of rosemary polyphenols activity against cancer cells. Namely, a proteomic study of the antiproliferative effect of rosemary polyphenols in HT-29 colon cancer cells is presented.

The objectives of this study were to identify: (i) changes in amplitude and kinetics of proteins altered by a rosemary extract enriched in polyphenols using supercritical fluid extraction over the time; and (ii) proteomic differences between the cytostatic and cytotoxic effect of the mentioned supercritical rosemary extract (SC-RE) to gain insights into the antiproliferative mechanisms induced by rosemary polyphenols. To achieve these goals, we have applied a proteomics strategy based on nanoliquid chromatography−tandem mass spectrometry (nano-LC−MS/MS) together with stable isotope dimethyl labeling (DML) to quantitatively examine relative changes in the protein abundance in HT-29 colon cancer cells in response to different SC-RE concentrations over the time. Several stable isotope-labeling-based quantification strategies, such as isobaric tags for relative and absolute quantitation,[20] stable isotope labeling by amino acids in cell culture,[21] and DML,[22] have been developed for MS-based analysis of differential protein expression avoiding the use of tedious 2-DE separations. Among these isotope-labeling strategies, DML is a simple and cost-effective labeling method, and recent studies have demonstrated its robustness and reliability to identify changes in protein levels,[23,24] which makes it suitable to use in large-scale comparative proteomic studies. To our knowledge, this is the first proteomic study on the bioactivity of rosemary polyphenols using high-resolution mass spectrometry profiling and stable isotope labeling.

EXPERIMENTAL SECTION

Chemicals

ACN, methanol (MeOH), formic acid (FA), NaCl, and urea were obtained from Merck (Darmstadt, Germany). Acetone, EDTA, protease inhibitor cocktail, PBS, *n*-octyl-β-D-glucopyranoside (BOG), triethylammonium bicarbonate (TEAB), sodium metavanadate ($NaVO_4$), NaF, β-glycerophosphate, sodium pyrophosphate, CH_2O (37%, v/v), iodoacetamide (IAA), DTT, and chloroquine diphosphate (CQ) were purchased from Sigma-Aldrich (St. Louis, MO). Trypsin/Lys-C mix (Mass Spec grade V5072) was purchased from Promega (Madison, WI), and deuterated formaldehyde CD_2O (20%, v/v) was obtained from ISOTEC (Miamisburg, OH). Sodium cyanoborohydride ($NaBH_3CN$) was purchased from Fluka (Buchs, Switzerland). Ultrapure water was prepared by Milli-Q water purification system (Millipore, Bedford, MA). The SC-RE tested along this work was obtained using supercritical fluid extraction, as described elsewhere.[13]

Cell Culture

Colon adenocarcinoma HT-29 cells obtained from ATCC (American Type Culture Collection, LGC Promochem, UK) were grown in McCoy's 5A supplemented with 10% (v/v) heat-inactivated FBS, 50 U/mL penicillin G, and 50 U/mL streptomycin at 37 °C in humidified atmosphere and 5% CO_2. When cells reached ∼50% confluence, they were trypsinized, neutralized with culture medium, seeded at 10 000 cells/cm^2, and allowed to adhere overnight at 37 °C. Inhibition of cell proliferation was performed using MTT (3-(4,5-dimethyl-2-thiazolyl)-2,5-diphenyl-2H-tetrazolium bromide) assay. Thus, cells were treated with the vehicle (0.2% (v/v) DMSO) regarded as untreated controls or with different SC-RE concentrations for different times, depending on the experiment. In the experiments performed with the autophagy inhibitor CQ, cells were coincubated with different SC-RE concentrations and 10 μM of CQ for 24 and 48 h. After treatments, cells were incubated with 0.5 mg/mL of MTT solution at 37 °C for 3 h. The medium was removed, and the purple formazan crystals were dissolved in DMSO. Then, the absorbance at 570 nm was measured in a microplate reader (Synergy HT, BioTek Instruments, Winooski, VT). The results are provided as the mean ± SEM of at least three independent experiments, each performed in triplicate. According to the NIH definitions,[25] the percentage of growth (PG) was calculated with the formula $PG = 100[(T - T_0)/(C - T_0)]$ when $T \geq T_0$, or $PG = 100[(T - T_0)/C]$ when $T < T_0$, T being the optical density of treated cells, C the optical density of control cells, and T_0 the optical density at time zero. The parameters related with cell proliferation after 24 h of treatment (GI50, 50% growth inhibition; TGI, total growth inhibition; and LC50, 50% lethal concentration) were calculated using SigmaPlot (version 12.5) software (Systat Software Inc., Erkrath, Germany). For proteomic experiments, cells were treated with GI50, TGI, and LC50 of the SC-RE, and the vehicle (0.2% (v/v) DMSO) for different times (2, 6, and 24 h) in 78 cm^2 cell culture dishes. The experiments were performed in triplicate, obtaining a total of 36 samples. After incubation, the growth medium from culture plates was removed by aspiration, and cells were trypsinized and pelleted.

Flow Cytometry Analysis

For the annexin V/7-AAD assay, HT-29 cells were plated in 78 cm^2 cell culture dishes and incubated with a lethal concentration of SC-RE for 24 and 48 h. Cells were trypsinized and incubated with phycoerythrin (PE)-conjugated annexin V (annexin V-PE) and 7-aminoactinomycin D (7-AAD) (BD Pharmingen, San Jose, CA) for 15 min at room temperature in the dark. Experiments were performed in triplicate using a Gallios flow cytometer equipped with a blue (488 nm) laser (Beckman Coulter, FL), and a total of 10 000 events were recorded.

To estimate the aggresome formation, we plated HT-29 cells in 78 cm^2 cell culture dishes and treated them with different SC-RE concentrations with or without 10 μM of CQ for 24 and 48 h. At the end of the treatment, cells were trypsinized and resuspended in PBS at 1×10^6 cells/mL. Cells were washed with PBS, fixed in 4% (v/v) formaldehyde in PBS for 30 min, and then permeabilized with 0.5% (v/v) Triton X-100, 3 mM EDTA, pH 8 on ice for 30 min. Cells were washed, resuspended in 500 μL of ProteoStat (Enzo Life Sciences, Plymouth Meeting, PA) dye (prepared according to kit instructions), and incubated for 30 min at room temperature and protected from light. Experiments were performed in triplicate using a Gallios flow cytometer, and a total of 20 000 events were recorded with a blue laser.

Sample Preparation for LC−MS/MS-Based Proteomics

Cell pellets were washed with 1 mL of cold PBS and counted in a Neubauer counting chamber using a light microscope (ID3,Carl Zeiss, Jena, Germany). After being counted, 1×10^6 cells were lysed with 300 μL of lysis buffer (6 M urea, 1% (m/v) BOG, 0.15 M NaCl, 1.3 mM EDTA, 1 mM $NaVO_4$, 5 mM NaF, 2.5 mM sodium-pyrophospate, and 5 mM β-glycerophosphate in PBS) supplemented with 10 μL of

DOI: 10.1021/acs.jproteome.6b00154
J. Proteome Res. XXXX, XXX, XXX−XXX

protease inhibitor cocktail to prevent protein degradation. The samples were incubated for 60 min at 4 °C during mild agitation, sonicated for 30 min at 0 °C in a water bath (Elma, Germany), and then centrifuged at 10000*g* at 4 °C for 15 min (Sigma, Germany). The supernatants were collected, and protein concentration in the cell lysates was measured using Biorad DC (Bio-Rad Laboratories, Hercules, CA) assay. Then, 10 μg of proteins were mixed with 500 μL of an ice-cold tributylphosphate/acetone/methanol mixture (1:12:1, v/v/v) and incubated at 4 °C for 90 min. The precipitate was pelleted by centrifugation for 15 min (3000*g* at 4 °C), washed with 1 mL of cold acetone, and finally air-dried. Pellets were dissolved in 20 μL of 1% (m/v) BOG with 20% (v/v) ACN in 0.1 M TEAB, and the proteins were reduced with 10 μL of 45 mM DTT at 56 °C for 15 min, cooled down to room temperature and alkylated with 10 μL of 100 mM IAA for 15 min in the dark. Samples were then digested with 0.5 μg of LysC/trypsin solution (5% m/m, of total protein content) and incubated at 37 °C overnight in darkness. The digests were dried in SpeedVac to remove ACN and resuspended in 70 μL of 0.1 M TEAB, and BOG was extracted with water-saturated ethyl-acetate according to the protocol of Yeung et al.[26] Dimethyl labeling was performed according to Boersema et al.[22] The tryptic peptide mixtures were reconstituted in 70 μL of 0.1 M TEAB. Control samples were mixed with 4 μL of regular formaldehyde CH_2O (4%, v/v), and treated samples were mixed with 4 μL of deuterated formaldehyde CD_2O (4%, v/v), marking them as light and medium, respectively. After a brief vortexing, 4 μL of freshly prepared 0.6 M $NaBH_3CN$ solution was added to each sample, and the vials were incubated for 60 min at room temperature with mild agitation. The reaction was terminated by adding 16 μL of 1% (v/v) ammonia solution (Merck, Germany), after which 8 μL of 5% (v/v) FA (Merck, Germany) was added to consume the excess labeling reagents. Finally, the samples, labeled with light and medium isotopes, were mixed together. The mixed samples were desalted on Isolute C18 solid-phase extraction columns (1 mL, 50 mg capacity, Biotage, Uppsala, Sweden) using the following schedule: the column was washed three times with 500 μL of ACN and equilibrated three times with 500 μL of 1% (v/v) FA. The tryptic peptides were adsorbed to the media using three repeated cycles of loading. The column was washed using 3 × 500 μL 1% (v/v) FA, and finally, the peptides were eluted in 300 μL of 50% (v/v) ACN, 1% (v/v) FA. After being desalted, peptides were dried in a SpeedVac and redissolved in 0.1% (v/v) FA to a concentration of 1 μg/μL prior to nano-LC−MS/MS.

LC−MS/MS Analysis

Aliquots (5 μL) containing ∼1 μg of tryptic peptides were injected into a nano-LC−MS/MS system consisting of EASY-nLC II (Thermo Fisher Scientific, Bremen, Germany) coupled via a nanoelectrospray ionization ion source to Orbitrap Velos Pro mass spectrometer (Thermo Fisher Scientific, Bremen, Germany). The peptide separations were performed on in-house packed uncoated fused silica emitters (PicoTip emitter, length 150 mm, 75 μm i.d., 375 μm o.d., tip opening 5 ± 1 μm, New Objective, Woburn, MA). The emitters were packed with a methanol slurry of reverse-phase, fully end-capped Reprosil-Pur C18-AQ 3 μm resin (Dr. Maisch GmbH, Ammerbuch-Entringen, Germany) using a PC77 pressure injection cell (Next Advance, Averill Park, NY). The separations were performed at a flow rate of 250 nL/min with mobile phases A (water with 0.1% (v/v) formic acid) and B (acetonitrile with 0.1% (v/v) formic acid). A 97 min gradient from 4% B to 30% B followed by 8 min from 30% B to 48% B, 6 min from 48% B to 75% B, and a washing step with 75% B for 3 min was used. The mass spectrometer was operated in positive-ion mode with unattended data-dependent acquisition mode, in which the mass spectrometer automatically switches between acquiring a high-resolution survey mass spectrum in the Orbitrap (resolving power 60000 fwhm) and consecutive low-resolution, collision-induced dissociation fragmentation of up to 10 of the most abundant ions in the ion trap using a normalized collision energy of 35.0 eV. Ions that were once selected for acquisition were dynamically excluded for 30 s for further fragmentation.

MaxQuant Analysis

All MS raw files were collectively processed with MaxQuant (version 1.5.2.8)[27] applying the Andromeda search engine[28] with the following adaptions. The false discovery rate (FDR) was set to 1% for both proteins and peptides, and we specified a minimum length of seven amino acids. MaxQuant scored peptides for identification based on a search with a maximal mass deviation of precursor and fragment masses of up to 20 ppm and 0.5 Da. The Andromeda search engine was used for the MS/MS spectra search against a concatenated forward and reversed version of the Uniprot human database (downloaded on February 11, 2015, containing 89 909 entries and 245 frequently detected contaminants) for quantitative study. Enzyme specificity was set as C-terminal to Arg and Lys, also allowing cleavage at proline bonds and a maximum of two missed cleavages. Carbamidomethylation of cysteine residues was set as the fixed modification, and the oxidation of methionine; the phosphorylation of serine, threonine, and tyrosine; and protein *N*-acetylation were allowed as variable modifications. For dimethyl labeling, DimethylLys0 and DimethylNter0 were set as light labels, and DimethylLys4 and DimethylNter4 were set as medium labels. A minimum peptide ratio count of two and at least one "razor peptide" was required for quantification. After protein quantification, each data set was normalized to the median of the ratios to correct for the mixing of medium- and light-labeled cells at 1:1 ratios and to enable a better comparison between the different conditions.

Statistical and Bioinformatics Analysis

Prior to any statistical analysis using Perseus software (http://141.61.102.17/perseus_doku/doku.php?id=start), identifications flagged as reverse, potential contaminants, or proteins identified only by site modification were excluded for further analysis, and the relative protein abundance was transformed to the $\log_2$ scale. For principal component analysis (PCA), proteins present in all biological replicates across the nine data sets were considered to avoid imputation of missing values. However, to be less restrictive in the identification of proteins with altered relative abundance in treated cells with respect to the control group, a protein was included in the analysis when it was identified in at least two biological replicates. In this case, a 1.5-fold cutoff in relative protein abundance and a p value of <0.05 (one sample t test) were applied. When data sets obtained in two different incubation times were compared, a two-group t test was performed, and a permutation-based FDR was applied to calculate the p values by randomly permuting samples within each group, considering statistically significant when $p < 0.05$.[29]

DOI: 10.1021/acs.jproteome.6b00154
J. Proteome Res. XXXX, XXX, XXX−XXX

For upstream regulator (UR) analysis, the lists of proteins passing the established thresholds were uploaded in the bioinformatics tool Ingenuity Pathway Analysis (IPA; Qiagen, Redwood City, CA). In UR analysis, upstream regulators are considered as those molecules, such as transcription factors, that can affect the expression of another molecule. The activation state for each regulator was predicted based on global direction of changes in the different experimental condition for previously published targets of this regulator. Significance of the activation or deactivation of molecules predicted by UR analysis was tested by the Fisher Exact test p value, considering only the predictions with significant p value of <0.05 and a regulation z-score of <− 2 or >2 for deactivation and activation, respectively.

RESULTS

In Vitro Characterization of the Antiproliferative Effect of Rosemary Extract (SC-RE) on HT-29 Colon Cancer Cells

The cytostatic and cytotoxic effects of SC-RE depending on its concentration were investigated in exponentially growing HT-29 cells. To attain this, we analyzed various concentrations of the SC-RE ranging from 0 to 60 μg/mL on HT-29 for 24 h by MTT assay. PG values were calculated based on data obtained at beginning (time zero) and after 24 h of each treatment. In Figure 1, PG values above zero are indicative of cytostatic activity because they represent the percentage of growth relative to control cell number at the beginning of the treatment. However, PG values lower than zero indicates cytotoxicity (i.e., lower cell numbers than those at the start of treatment). Based on PG data, the response parameters, GI50 and TGI, as indicators for cytostaticity, and LC50, indicative of cytotoxicity, were also determined for 24 h incubation time (Figure 1A). As can be seen, the obtained values were GI50 = 16.2 ± 1.4 μg/mL; TGI = 26.3 ± 0.9 μg/mL, and LC50 = 38.7 ± 1.4 μg/mL.

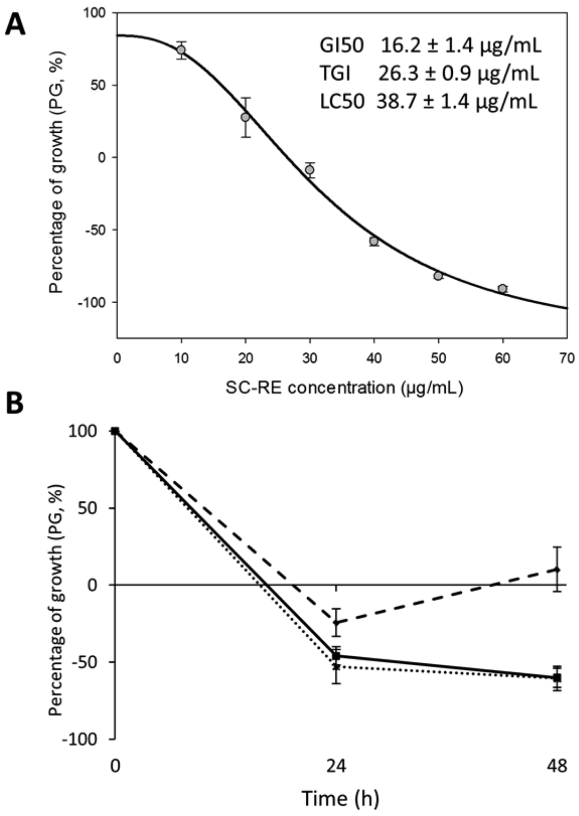

Figure 1. Percentage of growth of HT-29 cells incubated for 24 h with different SC-RE concentrations (A) or incubated with LC50 concentration of SC-RE for 6 h (dashed line), 12 h (dotted line), and 24 h (solid line) and analyzed at 24 and 48 h after the beginning of the treatment (B). Error bars are given as the 95% confidence interval of three independent experiments, each performed in triplicate.

To characterize in more detail the activity of the SC-RE, we investigated the dependency of its cytotoxic effect on the incubation time within the first 24 h of treatment. Thus, exponentially growing HT-29 cells were incubated with a concentration of the extract equal to LC50 for different times (6, 12, and 24 h). After 6, 12, and 24 h incubations with SC-RE, the culture medium was removed, and cells were refreshed with complete medium. Inhibition of cell proliferation was analyzed by MTT assay after 24 and 48 h of the SC-RE treatment. As is shown in Figure 1B, the incubation of cells with the extract for 6 h was enough to induce effects that were mostly cytostatic. On withdrawal of the extract, such an effect was reversed and cells partially recovered. In contrast, longer exposures (12 and 24 h) to the same extract concentration had stronger cytotoxic effects, and extract withdrawal did not recover the remaining cells. Taken together, these results suggest that irreversible mechanisms of cytotoxicity mediated by SC-RE in HT-29 cells take place after 12 h of continuous exposure.

Next, to investigate whether the cytotoxic effect was mediated through apoptosis or necrosis, treated and control cells were stained with Annexin V-PE and 7-AAD and subjected to flow cytometry analysis (Figure 2). Annexin V-PE binds to cells in early apoptosis and the fluorescent dye 7-AAD stains cells in late stages of apoptosis or cells that are already dead. As shown in the representative replicates of this analysis in Figure 2B, the percentage of Annexin V-PE positive (D2 + D4) cells was similar at 24 h between the SC-RE treatment (9.6%) and the untreated cells (11.2%), indicating the absence of apoptosis. However, the percentage of cells staining negative for Annexin V-PE and positive for 7-AAD (D1), indicative of necrosis, increased over time, reaching 19.2 and 32.7% for the SC-RE after 24 and 48 h, respectively.

Proteomic Profiles of HT-29 Colon Cancer Cells Treated with SC-RE

To gain insights into the molecular mechanisms altered by the SC-RE treatment, we employed dimethyl labeling combined with nano-LC−MS/MS to assess the SC-RE-induced differential expression of the proteome of HT-29 cells. In particular, we aimed at investigating temporal changes in protein levels in HT-29 cells in response to different cytostatic and cytotoxic concentrations of the extract. To attain this, we incubated HT-29 cells with three different concentrations of the SC-RE corresponding to the three different response parameters (GI50, TGI, and LC50) for 2, 6, and 24 h, with each experiment done in triplicate (Figure 3). In parallel, HT-29 cells were incubated with the vehicle (0.2% (v/v) DMSO) for the same time periods as the controls. To enable quantitative proteome comparisons, we performed stable isotope dimethyl labeling on the nine sets of experiments, using "light" and "medium" labels for control and SC-RE-treated cells, respectively. Equal protein amounts of light-labeled and medium-labeled lysates were mixed to generate 27 samples for further analysis. All mixtures were then subjected to nano-LC−MS/MS analysis. MS raw data files were then collectively

DOI: 10.1021/acs.jproteome.6b00154
J. Proteome Res. XXXX, XXX, XXX−XXX

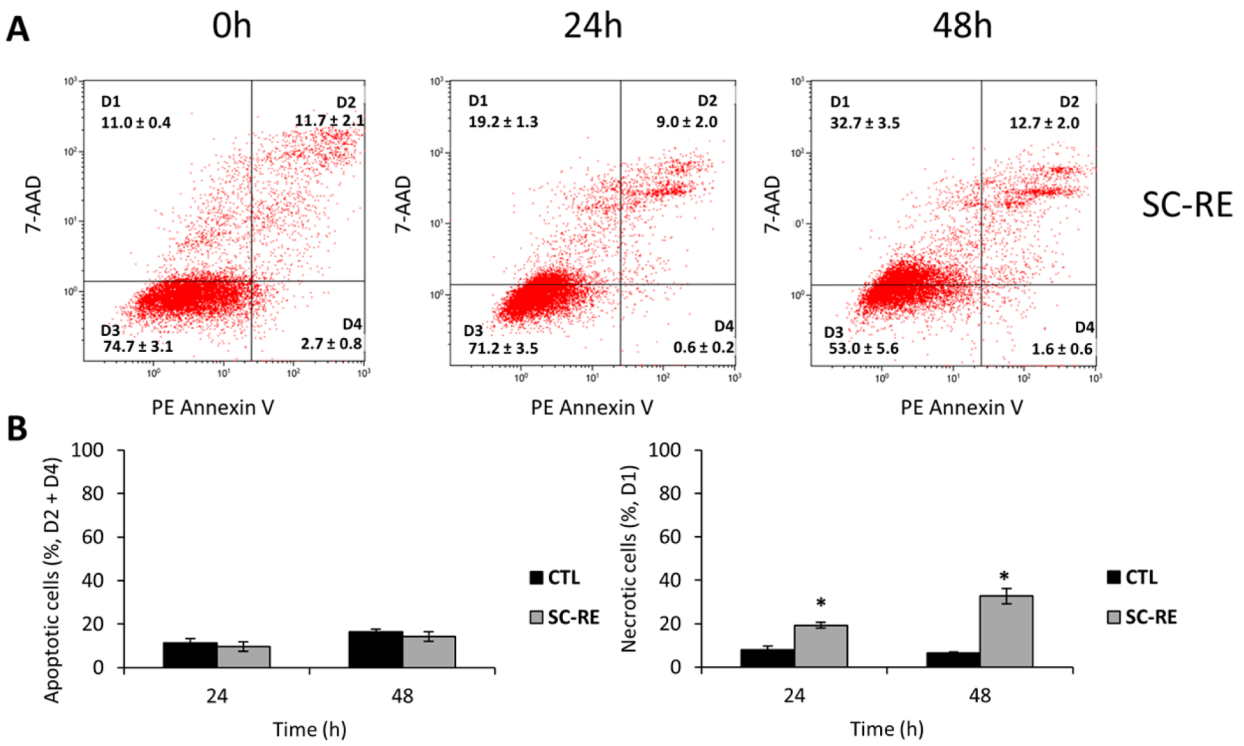

Figure 2. (A) Representative graphs obtained by flow cytometric analysis after double-staining with Annexin V-PE/7-AAD of HT-29 cells exposed to the LC50 concentration of SC-RE for 0, 24, and 48 h. (B) Percentage of apoptotic (D2 + D4) and necrotic (D1) cells detected in the SC-RE treatment and control cells after 24 and 48 h (n = 3; * indicates significant differences between the treated and control samples as determined by t test, P < 0.01).

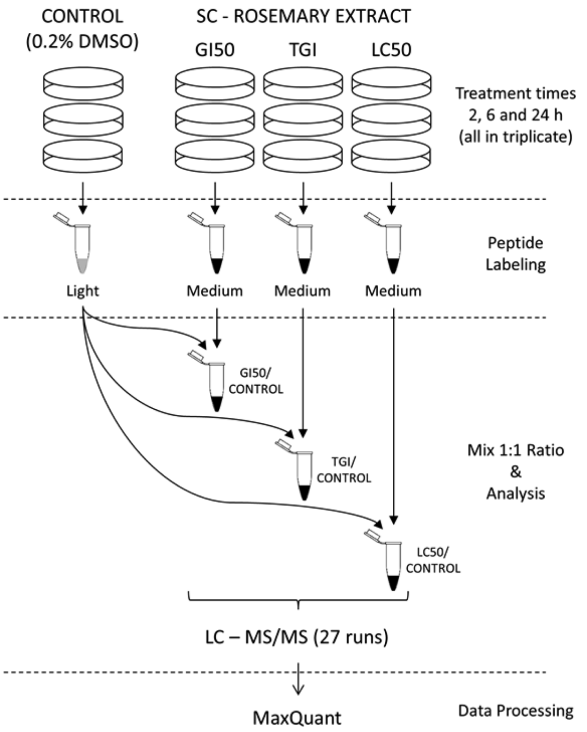

Figure 3. Experimental design of the DML method combined with nano-LC–Orbitrap MS/MS analysis used in the present study. HT-29 cells were incubated with GI50, TGI, and LC50 concentrations of SC-RE or 0.2% DMSO (control) for 2, 6, and 24 h, all in triplicate, and the proteins were extracted and digested with trypsin. Tryptic peptides from control and treated samples were labeled as "light" and "medium", respectively, and mixed 1:1 prior to LC–MS/MS analysis.

processed with the MaxQuant software for FDR-controlled peptide and protein identification and dimethyl labeling-based quantification. A total of 1909 distinct proteins were identified (protein level FDR < 1%) with an average of 718 quantified proteins after performing all of the analyses (see Table S1). Among them, 323 proteins were present in all biological replicates across the nine data sets, and on average, 698 proteins were quantified in at least two replicates for each experimental condition.

Then, to gain further insights into these data, we evaluated the concordance of a protein data set obtained in the present study and microarray data obtained under identical cell culture conditions in previous work.[16] Namely, the selected conditions for correlation analysis were the untreated and treated cells with the TGI concentration of the extract for 24 h. DNA microarray analysis identified 2211 mRNAs (about 5% of the total genes on the array) as differentially expressed (FDR< 5%) in HT-29 cells under the same treatment conditions.[20] The correlation between both omics data sets was investigated in terms of the direction and amplitude of the statistically significant mRNA and protein changes. Cross-referencing gene and protein identifiers was performed by retrieving gene names from Uniprot human database using Maxquant (version 1.5.2.8). Transcriptomics data overlapped 89.9% of proteomic data, representing 771 proteins for which mRNA and protein changes were compared, providing a correlation coefficient of 0.699 (Figure 4A). Of these proteins, 66.9% were not altered with statistical significance in any of the data sets, whereas 15.2% and 8.9% statistically were significantly altered at the protein or mRNA level, respectively. Then, considering only the statistically significant mRNA and protein changes (9.0%),

DOI: 10.1021/acs.jproteome.6b00154
J. Proteome Res. XXXX, XXX, XXX–XXX

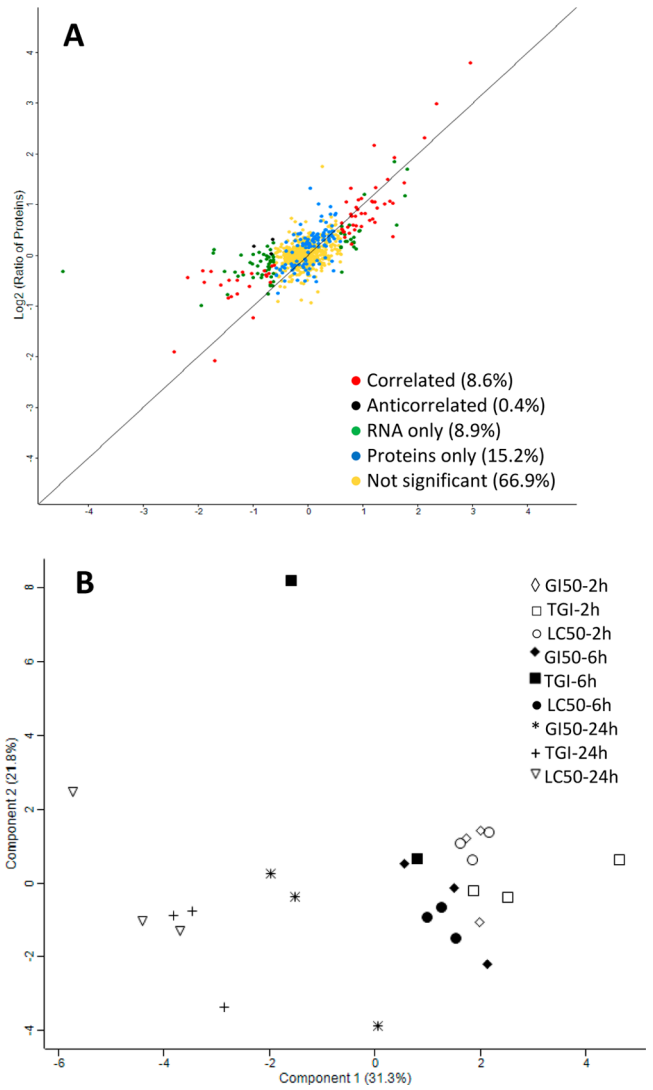

Figure 4. (A) Scatter plot of mRNA versus protein expression ratios (log_2) of HT-29 cells exposed to TGI concentration of SC-RE for 24 h. (B) Principal component analysis of HT-29 cells incubated with GI50, TGI, and LC50 concentrations of SC-RE for 2, 6, and 24 h.

the correlation coefficient between 69 mRNAs and proteins was calculated to be 0.891.

Next, PCA was carried out to determine and compare the overall relation among the three different concentrations of SC-RE (GI50, TGI, and LC50) and the three different incubation times (2, 6, and 24 h). When the combination of the first and the second principal component was represented, capturing together more than 50% of the variance in the data, most of the samples obtained at time points 2 and 6 h were grouped in the PCA plot (Figure 4B). In addition, samples obtained at time point 24 h were more scattered, but TGI and LC50 samples were closer to one another than to GI50 samples.

Effect of SC-RE Concentration on HT-29 Cell Proteome

Initial examination of the nine data sets separately indicated that the number of the statistically significant altered proteins and the magnitude of the changes increased with the extract concentration and incubation time (Table S2). Thus, none of the significantly altered proteins (p value <0.05) after 2 h of treatment with GI50 and TGI concentrations passed the fold-change threshold of 1.5, and only one protein, SLC25A6, was significantly down-regulated by using the LC50 concentration of the extract. In contrast, according to the same statistical criteria, 17, 50, and 55 proteins were found to be significantly altered after 24 h of treatment with GI50, TGI, and LC50 concentrations, respectively (Table 1). The comparison of the data showed 13 proteins that were shared among the three data sets, whereas 18 proteins were shared only between TGI and LC50 data. To identify transcriptional factors potentially involved in the observed protein changes induced by the extract, we subjected the three lists of significantly altered proteins at the 24 h time point to UR analysis using the IPA bioinformatics tool (Table 2). In consonance with previous studies, UR analysis predicted activation of Nrf2 (encoded by NFE2L2 gene) and C/EBPα (encoded by CEBPA) transcription factors in SC-RE-treated cells at any of the concentrations assayed.[8,16] This prediction of Nrf2 activation was experimentally supported by the up-regulation of sequestosome (SQSTM1/p62) and proteins related with the antioxidant response (GCLM and TXNRD1), NADPH generation (ME1, UGDH, and SLC2A1), detoxification (AKR1C3, AKR1C1, and AKR1B10), and other functions (PSAT1) that were common to all three concentrations (downstream targets supporting the activation of the transcription regulators summarized in Table 2 are cross-referenced in Table 1). The analysis also revealed that TGI and LC50 treatments activated two common transcription factors, Atf4 and Xbp1, which are tightly linked to the UPR. The same applies to the activation of the Sp1 transcription factor with a role in modulating the cellular response to DNA damage. In general, the magnitude of the changes in the relative abundance of proteins involved in UPR increased, with the SC-RE concentration reflecting higher ER stress.

To further explore the similarities and differences between TGI and LC50 data sets, we compared the patterns of UPR-related proteins (namely, those transcriptionally controlled by Atf4 and Xbp1). We observed that common UPR proteins in both data sets included relevant ER chaperones (HSPA5 and HYOU1); amino-acyl tRNA synthetases involved with protein synthesis (AARS, WARS, and GARS); proteins involved in targeting and translocation of nascent polypeptides into the ER (SEC61B); vesicle trafficking (SEC23B); and proteins involved in essential amino-acid influx (SLC3A2) and metabolism (ASNS). Interestingly, there were other UPR-related proteins whose abundances were specifically altered in LC50 data, which reinforced the involvement of amino acid uptake (SLC1A5 and SLC7A5) and protein synthesis (YARS, EPRS, and EIF5) functions in cells treated with the lethal SC-RE concentration. Other contrasting differences between data sets were identified with respect to the protein degradation and aggregation processes, represented by altered levels of chaperones HSP90B1 (endoplasmin) and HSP1A1 (hsp70) after LC50 treatment. In contrast, examination of TGI data set indicated the down-regulation of cell-cycle and proliferation markers (MKI67, MCM7, and TOP2A) as well as changes in proteins related to cytoskeleton organization (STMN1 VIL1, CAPN2, ACTA1, and CALB2).

Temporal Changes in the Relative Abundance of Proteins in Response to SC-RE Treatment in HT-29 Cells

To investigate the protein expression dynamics and prevailing molecular pathways underlying the response of HT-29 cells to SC-RE treatment, we performed comparative analyses of the proteomic profiles obtained at different times for the three

DOI: 10.1021/acs.jproteome.6b00154
J. Proteome Res. XXXX, XXX, XXX−XXX

Table 1. Significantly Altered Proteins after the Incubation of HT-29 Cells with GI50, TGI, and LC50 Concentrations of SC-RE for 24 h

	cross-reference	GI50		TGI		LC50	
gene names	from Table 2	$\log_2$ ratio	p value	$\log_2$ ratio	p value	$\log_2$ ratio	p value
SQSTM1	1	1.704	0.0001	2.165	0.0014	2.613	0.0014
CTSD	1, 5, 6			0.906	0.0099	0.604	0.0028
GCLM	1	1.307	0.0382	1.427	0.0025	1.809	0.0004
GCLC	1					1.267	0.0155
TXNRD1	1, 5	1.030	0.0121	1.320	0.0028	1.315	0.0004
TXN	1,4	0.630	0.0299	0.819	0.0185		
SRXN1	1					2.659	0.0065
HMOX1	1, 4, 5, 6			3.802	0.0205	4.292	0.0182
SLC2A1	1, 5, 6	0.763	0.0449	0.967	0.0427	1.245	0.0490
UGDH	1, 5, 6	0.900	0.0145	1.070	0.0082	1.103	0.0135
ME1	1, 6	0.715	0.0469	1.075	0.0005	1.086	0.0063
IDH1	1, 6			0.697	0.0046	0.802	0.0393
PGD	1, 2			0.723	0.0326	0.869	0.0144
G6PD	1, 6			0.809	0.0281		
AKR1B10	1, 2	1.632	0.0191	1.933	0.0026	1.712	0.0132
AKR1C1	1, 2	1.965	0.0075	2.985	0.0003	2.586	0.0025
AKR1C3	1, 2	1.572	0.0069	1.500	0.0027	1.465	0.0049
EPHX1	1, 2, 6			0.946	0.0270		
PSAT1	1, 3	0.908	0.0088	1.337	0.0034	1.359	0.0195
HSP90B1	1, 3, 4					0.616	0.0092
MT2A	2	3.413	0.0051				
ANXA1	2, 6	0.717	0.0147	1.129	0.0005	1.586	0.0069
ASNS	2, 3, 5, 6			2.314	0.0031	2.157	0.0015
SLC3A2	3	1.017	0.0492	1.319	0.0067	2.036	0.0129
SLC1A5	3					0.642	0.0067
SLC7A5	3					0.851	0.0333
AARS	3			0.821	0.0190	1.053	0.0048
WARS	3			1.023	0.0093	0.830	0.0279
GARS	3			1.055	0.0002	1.361	0.0210
SARS	3			0.935	0.0187		
YARS	3					0.749	0.0018
EPRS	3					0.695	0.0252
EIF5	3					0.653	0.0399
HSPA5	2, 3, 4, 5			0.648	0.0143	1.014	0.0040
HYOU1	4			0.775	0.0054	1.155	0.0052
SEC61B	4, 6			0.639	0.0047	0.761	0.0046
SEC23B	4, 6			1.017	0.0315	0.650	0.0298
SRPRB	4					0.736	0.0151
RANBP1	5					−0.604	0.0274
NAMPT	6	0.781	0.0146	1.054	0.0013	1.408	0.0129
HSPA1A	6	0.602	0.0175			1.002	0.0087
SFN	6			1.016	0.0050	1.364	0.0095
SERPINB5	6			0.831	0.0239	0.733	0.0232
PSAP	6			0.646	0.0132	0.896	0.0297
KPNA2	6			−1.230	0.0008	−1.122	0.0009
BCAP31	6			0.767	0.0181		
STMN1	6			−0.612	0.0281		
CNN2	6			−0.743	0.0245		
RRM1	6			−0.807	0.0098		
MCM7	6			−0.838	0.0262		
TOP2A	6			−1.908	0.0032		
MKI67	6			−2.082	0.0046		
CRIP1		−0.588	0.0107				
S100P				1.050	0.0020	1.165	0.0058
EIF1; EIF1B				0.801	0.0314	0.822	0.0382
ANXA10				1.092	0.0381		
AGR2				0.824	0.0467		
CALB2				0.772	0.0199		

DOI: 10.1021/acs.jproteome.6b00154
J. Proteome Res. XXXX, XXX, XXX−XXX

Table 1. continued

	cross-reference	GI50		TGI		LC50	
gene names	from Table 2	log_2 ratio	p value	log_2 ratio	p value	log_2 ratio	p value
RTN4				0.685	0.0412		
ACTA1				0.606	0.0469		
CAPN2				0.601	0.0220		
TMPO				−0.587	0.0096		
VIL1				−0.754	0.0039		
GFPT1						1.064	0.0097
ASPH						0.967	0.0299
ANXA5						0.820	0.0302
LRRC59						0.684	0.0475
HSPH1						0.644	0.0150
GDI1						0.616	0.0232
RBBP4						−0.587	0.0097
GMDS						−0.604	0.0416
NASP						−0.620	0.0076
CBX3						−0.634	0.0220
ALDH18A1						−0.710	0.0180
SLC12A2						−0.806	0.0024
DCTPP1						−0.900	0.0038
POF1B						−1.655	0.0295

Table 2. Prediction of Transcription Factors by UR Analysis (IPA Software) in HT-29 Cells Treated with GI50, TGI, and LC50 Concentrations of SC-RE for 24 h

		GI50		TGI		LC50	
ref for Table 1	transcription regulator	Z score	p value	Z score	p value	Z score	p value
1	NFE2L2	2.891	$2.47{\cdot}10^{-12}$	3.617	$7.86{\cdot}10^{-14}$	3.585	$4.43{\cdot}10^{-13}$
2	CEBPA	2.177	$9.38{\cdot}10^{-6}$	2.630	$2.30{\cdot}10^{-7}$	2.449	$6.69{\cdot}10^{-6}$
3	ATF4			2.414	$2.45{\cdot}10^{-10}$	2.779	$4.00{\cdot}10^{-13}$
4	XBP1			2.388	$4.41{\cdot}10^{-6}$	2.574	$5.16{\cdot}10^{-7}$
5	SP1			2.214	$1.33{\cdot}10^{-4}$	2.214	$3.79{\cdot}10^{-5}$
6	TP53			2.712	$1.14{\cdot}10^{-16}$		

concentrations of the SC-RE assayed. For these analyses, only those proteins overlapping across different time points were retained, and a FDR of 5% was used to determine statistically significant proteins differentially regulated between data sets (Table S3). As anticipated by PCA results, data sets obtained at 2 and 6 h of incubations with GI50 and TGI concentrations of the extract were too similar, and their comparison did not show any significant difference. However, the relative abundance of six proteins revealed statistically significant differences (FDR < 5%) between 2 and 6 h incubations with LC50 treatment; however, only SQSTM1 passed the 1.5-fold change threshold considered in this study, increasing the fold change from 0.9 to 1.8. As shown in Figure 5A, LC50 treatment for 24 h resulted in a significant temporal increase of various proteins regulated by Nrf2 transcription factor, such as those involved in NADPH generation (UGDH, PGD, and IDH1), detoxification (AKR1B10 and AKR1C3), and antioxidant proteins (TXNRD1). Also, the relative abundance of several RE and cytosolic chaperones involved in protein folding also increased over the time. As expected in cells affected by UPR signaling, amino-acids transporters (SLC3A2 and SLC1A5) and amino-acyl tRNA synthetases implicated in protein synthesis (GARS, AARS, and EPRS) accumulated from 6 to 24 h in treated cells, as well as other proteins with different functions. In contrast, two proteins involved in nucleocytoplasmic trafficking (KPNA2 and RANBP1) were down-regulated by the treatment. In addition to all these variations detected in cells under LC50 treatment, the most noticeable temporal change was observed for the autophagy receptor SQSTM1/p62 that steadily increased over the time course. Also, the abundance of other proteins involved in regulation of autophagic degradation (ANXA1) and in lysosomal protein degradation (CTSD) was significantly increased over the time. The changes in relative protein abundance in cells under cytostatic treatment were similar to those observed in the more severe LC50 treatment for 24 h (Figure 5B). However, the relative abundance of two cytosolic chaperones, HSP90AA1 and HSPA1A, with reported roles in protein folding and degradation, showed different dynamics between TGI and LC50 treatments. As can be seen in Figure 5A, these two proteins reached a plateau after 6 h of exposure to TGI concentration, whereas a gradual increase under LC50 treatment was observed, showing maximum levels at 24 h (see Figure 5B). Another interesting difference was that although proteins involved in amino-acids uptake and protein synthesis were identified and quantified, no changes in their relative abundance were detected in most of them over the time with TGI treatment. Altogether, these results are indicative that both TGI and LC50 treatments exert similar Nrf2-mediated antioxidant responses. In contrast, the changes related to UPR were in general more obvious in LC50 exposure. Considering the idea that UPR can integrate the intensity of the stimulus and reflect this in the signals that it transduces, our results suggest that the treatment with a LC50 concentration of SC-RE

DOI: 10.1021/acs.jproteome.6b00154
J. Proteome Res. XXXX, XXX, XXX−XXX

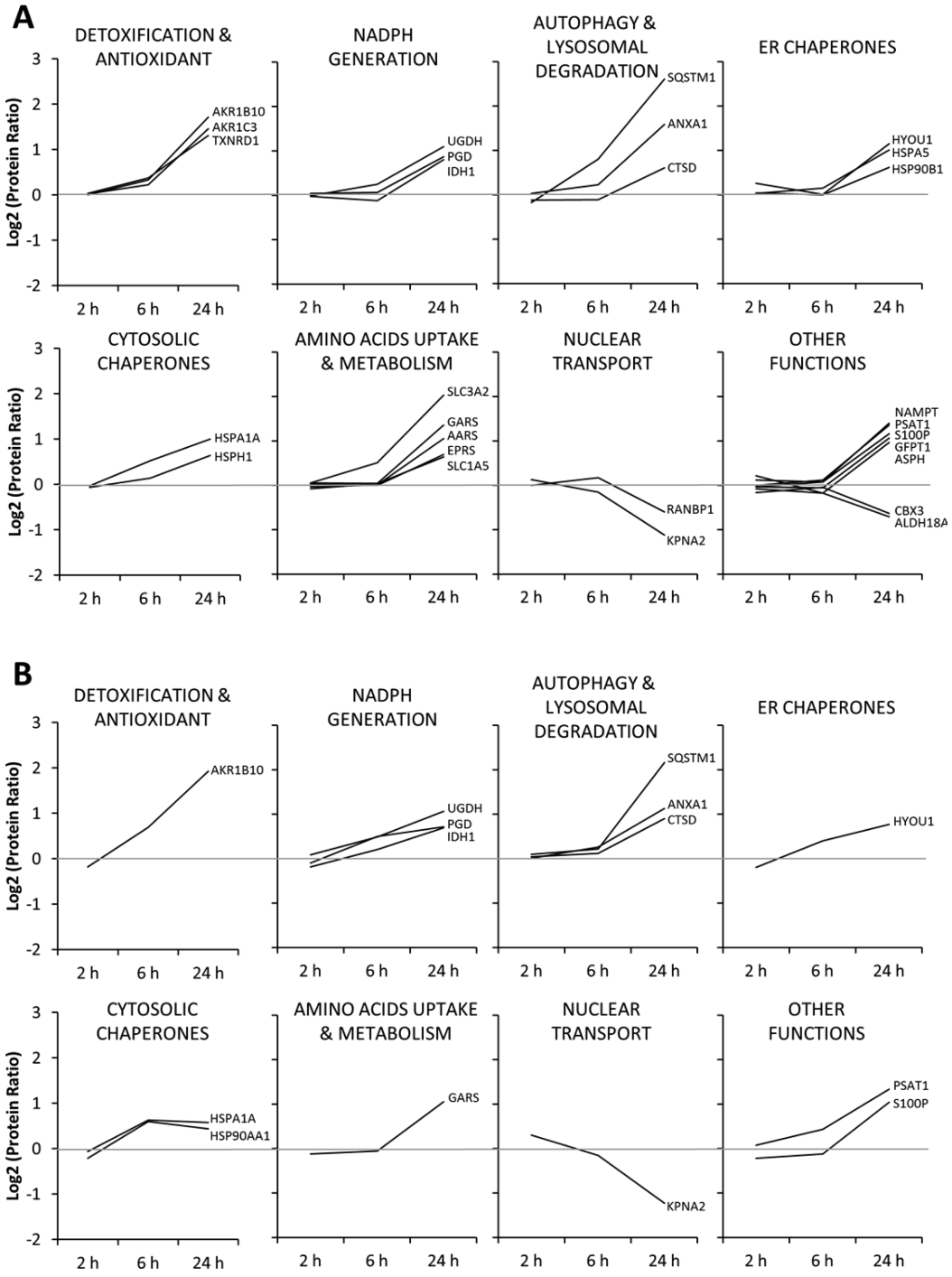

Figure 5. Temporal expression (log_2 ratio) of the differentially expressed proteins after the treatment of HT-29 cells with LC50 (A) and TGI (B) concentrations of SC-RE for 24 h.

induces more severe and sustained ER stress than with TGI. In addition, the observed differences in some of the cytosolic chaperones suggest that LC50 could induce effects on the protein folding efficiency in the ER and degradation capacity for a longer time.

Role of Autophagy and Protein Aggregation in the Response of HT-29 Cells to SC-RE

The autophagy−lysosome pathway and protein aggregation are of particular interest given their connection with some of the proteins detected in our study (SQSTM1/p62, HSPA1A, HSP90B1, HSP90AA, HSPH1, and ANXA1). Autophagy is thought to be activated by ER stress, possibly to eliminate damaged ER (also referred to as ER-phagy) and abnormal protein aggregates through the lysosomal pathway.[30] To investigate the potential impact of autophagy activation in the survival of cells treated with SC-RE, we coincubated HT-29 cells with a nontoxic dose (10 μM) of the autophagy inhibitor CQ and either LC50 or TGI concentration of the SC-RE for 24 and 48 h. After incubation, the effect of the cotreatments on cell viability was measured by MTT assay. As shown in Figure 6A, no differences on cell viability were observed at 24 h with and without CQ. However, a longer coincubation time (48 h) with

DOI: 10.1021/acs.jproteome.6b00154
J. Proteome Res. XXXX, XXX, XXX−XXX

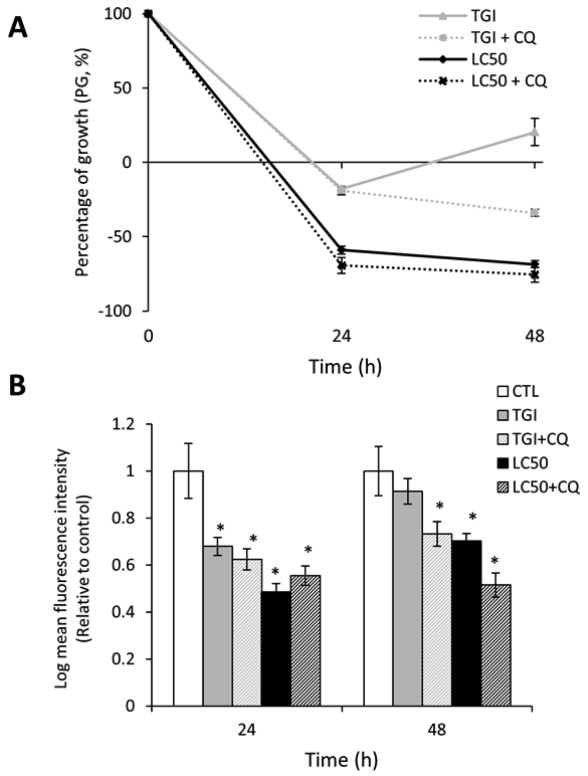

Figure 6. Percentage of growth (A) and aggresome formation (B) of HT-29 cells incubated for 24 and 48 h with TGI and LC50 concentrations of SC-RE, with or without 10 μM of CQ (n = 3; * indicates significant differences between the treated and control samples as determined by the t test; $P < 0.05$).

CQ aggravated significantly (p value < 0.05) the effect of TGI concentration on cell growth, suggesting that autophagy activation exerts cytoprotection by alleviating the stress induced by the long-term exposure to SC-RE. Co-incubation with the autophagy inhibitor and the lethal concentration LC50 of the extract did not cause any further effect on cell viability.

Aggresome formation is an active and highly regulated process by which misfolded protein substrates aggregate and are assembled to form a structure known as an aggresome that can be eliminated by autophagy.[31] Given the link between aggresome formation and two of the proteins altered with the treatments, SQSTM1/p62 and HSPA1A, it appeared reasonable to investigate the presence of aggresome in treated cells using flow cytometry and the ProteoStat dye, a reagent that enables the quantification of aggregated protein within aggresomes and other inclusion bodies.[32] As it is shown in Figure 6B, aggregates formation decreased proportionally with the extract concentration compared to proliferating control cells within the first 24 h of incubation. In contrast, after 48 h of TGI treatment, aggresome levels increased and were closer to those observed in control cells (Figure 6B), which was coincident with the observed cell-growth recovery (Figure 6A). Interestingly, cells co-treated with the inhibitor CQ showed no significant effects on protein aggresome levels compared to those observed in cells treated only with the extract, suggesting that autophagy is not specifically involved in aggresome clearance in treated cells. Altogether, these results suggest that regardless of the high relative abundance of SQSTM1/p62, aggresome formation is marginal in cells treated with the extract, which substantiates the idea that the elevated levels of molecular chaperones in treated cells may effectively improve their folding capacity and, therefore, hamper protein aggregation.

DISCUSSION

Rosemary polyphenols and extracts have been shown to exert cytostatic and cytotoxic activities at higher concentrations than those that typically promote cytoprotection, suggesting that the effects of these compounds are cell-type- and dose-dependent.[11,12,15,17,33] The antiproliferative effect of rosemary polyphenols on HT-29 colon cancer cells has been previously studied on the transcriptional and metabolic levels.[11−13,16] It was demonstrated that the cytostatic concentrations of rosemary polyphenols alter cell-cycle distribution and exert ER stress, triggering UPR and affecting expression of numerous genes.[16] In the present study, we include an additional level of molecular characterization of the effect of rosemary polyphenols on colon cancer cells by performing high-resolution quantitative proteomic profiling using nano-LC, high-resolution MS/MS and DML labeling.

It is well-recognized that protein abundance depends not only on transcription rates of the gene but also on additional regulatory mechanisms, such as translational regulation, mRNA stability, and protein degradation.[34] Moreover, several sources of variability associated with the global measurement of proteins and transcripts, such as differences in sensitivity, dynamic range, ambiguity in identification, etc., may contribute to the potential discordance between mRNA and protein abundances. In the present study, a good correlation between proteomic data (obtained in the present work) and transcriptomic data from previous published work was observed. Thus, the current proteomic study provides extra confirmation for microarray data and new valuable data that allows the gaining of more insight into the biological processes orchestrating the response of HT-29 cells to SC-RE exposure. Indeed, the analyses revealed a number of proteins critically involved in responses against stress. Moreover, the causal analytic tool, UR analysis, based on the IPA algorithm and the Ingenuity Knowledge Base, helped on elucidating the upstream regulatory molecules and associated mechanism to the observed protein changes. The predictive analysis revealed that all the assayed extract concentrations induce Nrf2 transcriptional activity, whereas the higher extract concentrations induce the activation of two relevant transcription factors (Atf4 and Xbp1) related with UPR induction. UPR is a coordinated response that the cell activates when there is an imbalance between the amount of misfolded or unfolded proteins in the ER lumen and the capacity of the ER machinery to refold these proteins, a condition referred to as ER stress.[35] Protein misfolding can be promoted by particular mutations, misincorporation during translation, or unequal biosynthesis of individual subunits of multimeric proteins, but it can be also due to other factors such as redox environment, temperature, ionic strength, and pH.[36] The primary aim of UPR is to sustain cell survival by temporarily attenuating the translational rate and restoring cellular homeostasis via the orchestrated activation of various transcription factors.[37] Such transcriptional activity modulates the expression of genes encoding for components of the ER-associated degradation (ERAD) system, chaperones to enhance the folding capacity in ER, and components of the autophagy machinery.[35] When unfolded or misfolded proteins cannot be refolded by chaperones, they are directed to the ERAD system for retrotranslocation to the cytoplasm and degradation by the

DOI: 10.1021/acs.jproteome.6b00154
J. Proteome Res. XXXX, XXX, XXX−XXX

ubiquitin−proteasome system. If these misfolded proteins fail to fold correctly and are not degraded by the proteasome, they are transported in a microtubule-dependent manner to the perinuclear microtubule-organizing center together with ubiquitin, chaperones, and form aggresomes that eventually can be cleared by autophagy.[36] Macroautophagy (hereafter referred to as autophagy) is a bulk degradation mechanism in which cytosolic proteins, protein aggregates, and organelles are sequestered into autophagosomes and degraded by lysosomes.[38−40] Although the activation of autophagy after ER stress has been assigned a protective role, it can also promote cell death.[38,41] This opposite role, as well as the cell fate, will depend on the intensity of the stimulus, the cell type, and the cellular context.[42] Our data indicate that the SC-RE alters the levels of signature proteins of ER stress and autophagy degradation function in the HT-29 cells. To explore the possible contribution of autophagy in the cellular response to SC-RE exposure, we used CQ, a lysosomotropic agent that blocks lysosome function by increasing lysosomal pH and is commonly used to inhibit autophagy. Under our experimental conditions, autophagy inhibition resulted in decreased viability of cells treated with a cytostatic dose of the extract. These findings implicate autophagy in the alleviation of ER stress induced by the extract. In line with this, a recent report has demonstrated the link between ER stress and autophagy activation by the involvement of the UPR sensor IRE1α and the transcriptional factor CHOP in HT-29 cells treated with thapsigargin.[43]

In recent years, rising evidence suggests that autophagy is a selective and regulated process.[44] There are several proteins that have been identified to be required for the selective removal of specific substrates. Among them, the autophagy receptor SQSTM1/p62 has been shown to be required for the selective degradation of a variety of substrates.[45] This multifunctional protein has been implicated in the binding and transfer of polyubiquitinated proteins to proteasomes,[46] aggresomes,[47] and autophagosomes,[48] as well as in aggresome-like induced structure formation.[49] It has been reported that the removal of SQSTM1/p62 results in augmented aggregate formation, whereas the overexpression of SQSTM1/p62 reflects increased autophagic flux and aggregate clearance,[50] leading to the idea that this protein can function in garbage packing for the eventual disposal of toxic proteins.[51] A number of studies suggest that SQSTM1/p62 accumulates when autophagy is impaired or blocked. In such a cellular context, SQSTM1/p62 accumulation directly enhances the formation of protein aggregates.[52] In the present work, SQSTM1/p62 increased significantly as early as after 6 h of treatment and was strikingly high with the highest extract concentration and longest incubation (2.61-log fold increase). Interestingly, according to our flow cytometry data, aggresome abundance was inversely related to SQSTM1/p62 relative amount, which could be suggestive of increased autophagic flux and enhanced degradation capacity in treated cells. However, autophagy inhibition by CQ in treated cells did not induce aggresome accumulation, excluding authophagy as the causative mechanism for aggresome reduction and pointing to the idea that aggresome formation appear to be limited regardless elevated levels of SQSTM1/p62 in treated cells.

A novel autophagy-independent role for SQSTM1/p62 has been recently evidenced.[53] It has been demonstrated that the overexpression (or accumulation) of SQSTM1/p62 affects the clearance of ubiquitin−proteasome pathway substrates, regardless of the autophagy status. Such a dependence on SQSTM1/p62 for the accumulation of these substrates can be due to that SQSTM1/p62 prevents ubiquitinated proteins from binding to the machineries that shuttle them to or into the proteasome. The cytotoxicity associated with the inhibitory effect of SQSTM1/p62 accumulation can be explained by the deleterious effect of the reduced clearance of many ubiquitinated proteins.[53] To elucidate whether SQSTM1/p62 up-regulation exerts this or other functions was not the goal of this work and remains to be investigated; however, in agreement with our data, previous reports also showed that SQSTM1/p62 is a stress response gene strongly induced at the mRNA level by the exposure to SC-RE,[20] supporting that, at least in part, SQSTM1/p62 accumulation is transcriptionally regulated. Nrf2 induces the expression of the SQSTM1/p62 gene upon exposure to electrophiles and reactive oxygen species.[54] In addition, autophagy and Nrf2-mediated antioxidant response were recently shown to intersect through the direct interaction between SQSTM1/p62 and Keap1 (reviewed by Jiang et al.).[55] In the canonical antioxidant pathway, Keap1 binds Nrf2 and constantly promotes its degradation by proteasome.[56] Modification of Keap1 cysteine residues promotes the translocation of Nrf2 from the cytoplasm to the nucleus, where it activates the transcription of genes containing antioxidant response elements (AREs) in their regulatory regions. It has been proposed that SQSTM1/p62 sequesters Keap1 into the autophagosomes, impairing Nrf2 degradation, leading to a positive feedback loop that sustains the transcription of Nrf2-inducible genes.[57] Different works have recently evidenced that SQSTM1/p62-mediated non-canonical mechanism of prolonged Nrf2 activation has been associated with the accumulation of protein aggregation and toxicity in vivo and in vitro.[58] Furthermore, excessive Nrf2 activity induces reductive stress by the exaggerated accumulation of highly energy-reducing equivalents in the form of NAD(P)H and GSH, leading to proteotoxicity and detrimental effects in animal models of cardiac dysfunction.[59]

In our study, the patterns of Nrf2-regulated proteins observed in treated cells indicate that the SC-RE enhances Nrf2 activation in a time-dependent fashion. Such an activation affects the up-regulation of proteins that promote NAD(P)H generation (ME1, UGDH, IDH1, and SLC2A1), among others. Accumulating evidence from in vitro studies with different cell models suggests that catechol-type electrophilic compounds such as carnosic acid and carnosol initiate the *S*-alkylation of cysteine thiol of the Keap1 protein, inducing cytoprotective effects by promoting the translocation of NRF2 from the cytoplasm to the nucleus.[8,9] It is also well-accepted that UPR induces the production of reactive oxygen species in the ER due to increased protein folding function, and it also triggers *Nrf2*-mediated antioxidant response to restore cellular redox homeostasis.[60] In line with this, previous work have shown that the expression patterns of the *Nrf2*-mediated antioxidant responsive genes follow the same kinetics as those genes regulated by *Perk*/*Atf4* signaling, a major axis in UPR, in response to the rosemary extract.[13,16] With these considerations in mind and the findings obtained in the present work, it seems reasonable that Nrf2 transcriptional activity is enhanced and prolonged by different mechanisms in SC-RE-treated cells.

As mentioned above, upon ER stress, UPR signaling temporarily attenuates protein synthesis. In general, this inhibition apparently occurs at the earliest time point during UPR, followed by the induction of chaperones and the

DOI: 10.1021/acs.jproteome.6b00154
J. Proteome Res. XXXX, XXX, XXX−XXX

stimulation of ERAD.[61] Besides up-regulating classic UPR targets, ER stress have also been reported to induce the expression of genes involved in amino acid import and metabolism.[62] In the present work, changes in the relative levels of these proteins, and also in various amino-acyl tRNA synthetases, involved in protein synthesis were more evident in LC50 treatment. Interestingly, recent evidence suggest that, on the event of prolonged or unresolved ER stress, premature activation of de novo protein synthesis before restoration of ER homeostasis induces cell death.[63]

Another interesting finding in our present study was that the SC-RE raised the abundance of molecular chaperones. These inducible molecules assist in the proper folding and stabilization of nascent polypeptides and misfolded proteins accumulated during cellular stress, preventing their aggregation and proteolytic cleavage by proteasome.[64] In consonance with this, our data indicated that the increased abundance of chaperones was inversely related with the protein aggregation propensity observed in treated cells. However, HSPA1A has been also suggested to have an active role in the autophagic degradation of proteins when unfolding or aggregation cannot be prevented.[65] This protein helps on delivering defective proteins to different degradation pathways including proteasome, chaperone-assisted selective autophagy, and chaperone-mediated autophagy. Interestingly, HSPA1A displayed different expression patterns between treatments; its relative amount was higher and more prolonged with LC50 concentration than with sublethal TGI treatment, correlating the former with more intense stress and, therefore, a more obvious need for alleviating it. In addition to the HSPA1A changes that prevents protein aggregation,[65] the elevation of ANXA1 levels in treated cells promotes selective degradation by autophagy or proteasome.[66] According to these observations, it seems plausible that a mechanism involving proteasome or autophagy degradation might be contributing to alleviate excessive protein misfolding in treated cells, preventing aggresome formation. In line with this, current evidence implicates Nrf2 signaling in the elevation of proteasome activation in colon cancer cells, which leads to an increased removal of potentially harmful proteins.[67]

The importance of ER protein homeostasis for each cancer subtype is heterogeneous.[68] However, according to the high proliferation and metabolic rates of most types of cancer, the rate of protein synthesis and turnover is expected to be elevated. Thus, interference of this function by inhibitors of proteolytic pathways and or inducers of ER stress has been exploited to kill cancer cells.[69]

CONCLUSIONS

In conclusion, our findings indicate that a link between UPR activation, Nrf2 induction, and degradative processes exists in the response of HT-29 cells to high cytostatic and lethal concentrations of the SC-RE. Rosemary polyphenols induced proteomic changes that seem to elicit adaptive responses to alleviate the stress. Connected to the adaptive responses, autophagy activation operates as pro-survival mechanism if the stress is moderate. Also, degradative processes mediated by cytoplasmic chaperones might attenuate aggresome formation, suggesting that effective proteolytic pathways might be operating to relieve overabundant intracellular unfolded or misfolded proteins. However, it is conceivable that when the stress reaches a certain threshold, the adaptive compensatory mechanisms cannot cope with the cellular damage, leading to cell death. Nrf2 signaling has a reported antitumor protective activity; however, Nrf2 has been also assigned a "dark side" that underlies on its persistent activation in certain cancers that promotes cancel cell proliferation and chemoresistance.[70,71] The SC-RE-induced changes in typical Nrf2-responsive proteins, however, these changes were accompanied by other stress response that reflects loss of protein homeostasis and, depending on the severity of the stress, leads to cytostatic or cytotoxic outcomes. Whether Nrf2 activation is contributing (or not) to such outcomes is unclear at present. However, novel concepts based on the emerging idea in which hyperactivation of the Nrf2 system leads to a reductive stress with detrimental effects for the cell metabolism[72] open new possibilities for the study of Nrf2-inducing agents against cancer.

ASSOCIATED CONTENT

Supporting Information

The Supporting Information is available free of charge on the ACS Publications website at DOI: 10.1021/acs.jproteome.6b00154. The mass spectrometry proteomics data have been deposited to the ProteomeXchange Consortium via the PRIDE partner repository with the data set identifier PXD003623.

Document containing index and captions. (PDF)

Table S1: Protein identification and expression ratio (log_2) of all DML−nano LC−MS/MS experiments performed in HT-29 cells after the treatment with different concentrations of SC-RE at different times. (XLSX)

Table S2: Expression ratio (log_2) of significant altered proteins (p value of <0.05) in HT-29 cells after the treatment with different concentrations of SC-RE at different times. (XLSX)

Table S3: Protein expression ratio (log_2) and statistical significance (permutation-based FDR of <0.05) in HT-29 cells after the treatment with different concentrations of SC-RE at different times. (XLSX)

AUTHOR INFORMATION

Corresponding Authors

*Telephone: +34 910-017-950; fax: +34 910-017-905; e-mail: virginia.garcia@csic.es.

*E-mail: jonas.bergquist@kemi.uu.se.

Notes

The authors declare no competing financial interest.

ACKNOWLEDGMENTS

This work was supported by the projects AGL2014-53609-P (Ministerio de Economía y Competitividad, Spain) and S2013/ABI-2728 (Comunidad de Madrid). A.V. thanks the Ministerio de Economía y Competitividad for his FPI predoctoral fellowship (BES-2012-057014). The Swedish Research Council (2011-4423 and 2015-4870; J.B.) is acknowledged for financial support.

ABBREVIATIONS:

7-AAD, 7-aminoactinomycin D; CQ, chloroquine; DML, dimethyl labeling; ERAD, ER-associated degradation; FDR, false discovery rate; GI50, 50% growth inhibition; IPA, Ingenuity Pathway Analysis; LC50, 50% lethal concentration; MTT, 3-(4,5-dimethyl-2-thiazolyl)-2,5-diphenyl-2H-tetrazo-

DOI: 10.1021/acs.jproteome.6b00154
J. Proteome Res. XXXX, XXX, XXX−XXX

lium bromide; nano-LC−MS/MS, nanoliquid chromatography−tandem mass spectrometry; PE, phycoerythrin; PCA, principal component analysis; PG, percentage of growth; SCRE, supercritical rosemary extract; TGI, total growth inhibition; UPR, unfolded protein response; UR, upstream regulator

REFERENCES

(1) Holmes, P. Rosemary oil. Int. *Int. J. Aromather.* **1999**, *9*, 62−66.
(2) Moreno, S.; Scheyer, T.; Romano, C. S.; Vojnov, A. A. Antioxidant and antimicrobial activities of rosemary extracts linked to their polyphenol composition. *Free Radical Res.* **2006**, *40*, 223−231.
(3) Peng, C. H.; Su, J. D.; Chyau, C. C.; Sung, T. Y.; Ho, S. S.; Peng, C. C.; Peng, R. Y. Supercritical fluid extracts of rosemary leaves exhibit potent anti-inflammation and anti-tumor effects. *Biosci., Biotechnol., Biochem.* **2007**, *71*, 2223−2232.
(4) Ibarra, A.; Cases, J.; Roller, M.; Chiralt-Boix, A.; Coussaert, A.; Ripoll, C. Carnosic acid-rich rosemary (Rosmarinus officinalis L.) leaf extract limits weight gain and improves cholesterol levels and glycaemia in mice on a high-fat diet. *Br. J. Nutr.* **2011**, *106*, 1182−1189.
(5) Herrero, M.; Plaza, M.; Cifuentes, A.; Ibáñez, E. Green processes for the extraction of bioactives from Rosemary: Chemical and functional characterization via ultra-performance liquid chromatography-tandem mass spectrometry and in-vitro assays. *J. Chromatogr. A* **2010**, *1217*, 2512−2520.
(6) U.S. Food and Drug Administration. Code of federal regulations (CFR). Title 21: Food and drugs; Chapter I: Food and Drug Administration, Department of Health and Human Services; subchapter B: Food for Human Consumption; Part 182: Substances Generally Recognized As Safe (GRAS); subpart a−e: General Provisions; subpart 182.10: Spices and Other Natural Seasonings and Flavorings; Office of the Federal Register: Washington, DC, 2014.
(7) European Commission.. Commission Directive 2010/69/EU Annexes to European Parliament and Council Directive. *Off. J. Eur. Communities: Legis.* **2010**, *279*, 22−31.
(8) Satoh, T.; Kosaka, K.; Itoh, K.; Kobayashi, A.; Yamamoto, M.; Shimojo, Y.; Kitajima, C.; Cui, J.; Kamins, J.; Okamoto, S.; Izumi, M.; Shirasawa, T.; Lipton, S. A. Carnosic acid, a catechol-type electrophilic compound, protects neurons both in vitro and in vivo through activation of the Keap1/Nrf2 pathway via S-alkylation of targeted cyteines on Keap1. *J. Neurochem.* **2008**, *104*, 1116−1131.
(9) Martin, D.; Rojo, A. I.; Salinas, M.; Diaz, R.; Gallardo, G.; Alam, J.; De Galarreta, C. M.; Cuadrado, A. Regulation of heme oxygenase-1 expression through the phosphatidylinositol 3-kinase/Akt pathway and the Nrf2 transcription factor in response to the antioxidant phytochemical carnosol. *J. Biol. Chem.* **2004**, *279*, 8919−8929.
(10) González-Vallinas, M.; Reglero, G.; Ramírez de Molina, A. Rosemary (Rosmarinus officinalis L.) extract as a potential complementary agent in anticancer therapy. *Nutr. Cancer* **2015**, *67*, 1223−1231.
(11) Valdés, A.; Simó, C.; Ibáñez, C.; Rocamora-Reverte, L.; Ferragut, J. A.; García-Cañas, V.; Cifuentes, A. Effect of dietary polyphenols on K562 leukemia cells: a Foodomics approach. *Electrophoresis* **2012**, *33*, 2314−2327.
(12) Valdés, A.; García-Cañas, V.; Rocamora-Reverte, L.; Gómez-Martínez, A.; Ferragut, J. A.; Cifuentes, A. Effect of rosemary polyphenols on human colon cancer cells: Transcriptomic profiling and functional enrichment analysis. *Genes Nutr.* **2013**, *8*, 43−60.
(13) Valdés, A.; García-Cañas, V.; Simó, C.; Ibáñez, C.; Micol, V.; Ferragut, J. A.; Cifuentes, A. Comprehensive foodomics study on the mechanisms operating at various molecular levels in cancer cells in response to individual rosemary polyphenols. *Anal. Chem.* **2014**, *86*, 9807−9815.
(14) Ishida, Y.; Yamasaki, M.; Yukizaki, C.; Nishiyama, K.; Tsubouchi, H.; Okayama, A.; Kataoka, H. Carnosol, rosemary ingredient, induces apoptosis in adult T-cell leukemia/lymphoma cells via glutathione depletion: proteomic approach using fluorescent two-dimensional differential gel electrophoresis. *Hum. Cell* **2014**, *27*, 68−77.
(15) Xiang, Q.; Ma, Y.; Dong, J.; Shen, R. Carnosic acid induces apoptosis associated with mitochondrial dysfunction and AKT inactivation in HepG2 cells. *Int. J. Food Sci. Nutr.* **2015**, *66*, 76−84.
(16) Valdés, A.; Sullini, G.; Ibáñez, E.; Cifuentes, A.; García-Cañas, V. Rosemary polyphenols induce unfolded protein response and changes in cholesterol metabolism in colon cancer cells. *J. Funct. Foods* **2015**, *15*, 429−439.
(17) Petiwala, S. M.; Berhe, S.; Li, G.; Puthenveetil, A. G.; Rahman, O.; Nonn, L.; Johnson, J. J. Rosemary (Rosmarinus officinalis) extract modulates CHOP/GADD153 to promote androgen receptor degradation and decreases xenograft tumor growth. *PLoS One* **2014**, *9*, e89772.
(18) García-Cañas, V.; Simó, C.; Herrero, M.; Ibáñez, E.; Cifuentes, A. Present and future challenges in food analysis: Foodomics. *Anal. Chem.* **2012**, *84*, 10150−10159.
(19) Ibáñez, C.; Valdés, A.; García-Cañas, V.; Simó, C.; Celebier, M.; Rocamora-Reverte, L.; Gómez-Martínez, A.; Herrero, M.; Castro-Puyana, M.; Segura-Carretero, A.; Ibáñez, E.; Ferragut, J. A.; Cifuentes, A. Global Foodomics strategy to investigate the health benefits of dietary constituents. *J. Chromatogr. A* **2012**, *1248*, 139−153.
(20) Ross, P. L.; Huang, Y. N.; Marchese, J. N.; Williamson, B.; Parker, K.; Hattan, S.; Khainovski, N.; Pillai, S.; Dey, S.; Daniels, S.; Purkayastha, S.; Juhasz, P.; Martin, S.; Bartlet-Jones, M.; He, F.; Jacobson, A.; Pappin, D. J. Multiplexed protein quantitation in Saccharomyces cerevisiae using amine-reactive isobaric tagging reagents. *Mol. Cell. Proteomics.* **2004**, *3*, 1154−1169.
(21) Ong, S. E.; Blagoev, B.; Kratchmarova, I.; Kristensen, D. B.; Steen, H.; Pandey, A.; Mann, M. Stable isotope labeling by amino acids in cell culture, SILAC, as a simple and accurate approach to expression proteomics. *Mol. Cell. Proteomics* **2002**, *1*, 376−386.
(22) Boersema, P. J.; Raijmakers, R.; Lemeer, S.; Mohammed, S.; Heck, A. J. Multiplex peptide stable isotope dimethyl labeling for quantitative proteomics. *Nat. Protoc.* **2009**, *4*, 484−494.
(23) Sui, P.; Watanabe, H.; Ossipov, M. H.; Porreca, F.; Bakalkin, G.; Bergquist, J.; Artemenko, K. Dimethyl-labeling-based protein quantification and pathway search: a novel method of spinal cord analysis applicable for neurological studies. *J. Proteome Res.* **2013**, *12*, 2245−2252.
(24) Sjödin, M. O.; Wetterhall, M.; Kultima, K.; Artemenko, K. Comparative study of label and label-free techniques using shotgun proteomics for relative protein quantification. *J. Chromatogr. B: Anal. Technol. Biomed. Life Sci.* **2013**, *928*, 83−92.
(25) Monks, A.; Scudiero, D.; Skehan, P.; Shoemaker, R.; Paull, K.; Vistica, D.; Hose, C.; Langley, J.; Cronise, P.; Vaigro-Wolff, A.; Gray-Goodrich, M.; Campbell, H.; Mayo, J.; Boyd, M. Feasibility of a high-flux anticancer drug screen using a diverse panel of cultured human tumor cell lines. *J. Natl. Cancer Inst.* **1991**, *83*, 757−766.
(26) Yeung, Y. G.; Stanley, E. R. Rapid detergent removal from peptide samples with ethyl acetate for mass spectrometry analysis. *Curr. Protoc. Protein Sci.* **2010**, *16*, 16.12.110.1002/0471140864.ps1612s59
(27) Cox, J.; Mann, M. MaxQuant enables high peptide identification rates, individualized p.p.b.-range mass accuracies and proteome-wide protein quantification. *Nat. Biotechnol.* **2008**, *26*, 1367−1372.
(28) Cox, J.; Neuhauser, N.; Michalski, A.; Scheltema, R. A.; Olsen, J. V.; Mann, M. Andromeda: a peptide search engine integrated into the MaxQuant environment. *J. Proteome Res.* **2011**, *10*, 1794−1805.
(29) Hubner, N. C.; Bird, A. W.; Cox, J.; Splettstoesser, B.; Bandilla, P.; Poser, I.; Hyman, A.; Mann, M. Quantitative proteomics combined with BAC TransgeneOmics reveals in vivo protein interactions. *J. Cell Biol.* **2010**, *189*, 739−754.
(30) Kroemer, G.; Mariño, G.; Levine, B. Autophagy and the integrated stress response. *Mol. Cell* **2010**, *40*, 280−293.
(31) Yao, T. The role of ubiquitin in autophagy-dependent protein aggregate processing. *Genes Cancer* **2010**, *1*, 779−786.
(32) Shen, D.; Coleman, J.; Chan, E.; Nicholson, T. P.; Dai, L.; Sheppard, P. W.; Patton, W. F. Novel cell- and tissue-based assays for

DOI: 10.1021/acs.jproteome.6b00154
J. Proteome Res. XXXX, XXX, XXX−XXX

detecting misfolded and aggregated protein accumulation within aggresomes and inclusion bodies. *Cell Biochem. Biophys.* **2011**, *60*, 173−185.
(33) Barni, M. V.; Carlini, M. J.; Cafferata, E. G.; Puricelli, L.; Moreno, S. Carnosic acid inhibits the proliferation and migration capacity of human colorectal cancer cells. *Oncol. Rep.* **2012**, *27*, 1041−1048.
(34) Waters, K. M.; Pounds, J. G.; Thrall, B. D. Data merging for integrated microarray and proteomic analysis. *Briefings Funct. Genomics Proteomics* **2006**, *5*, 261−272.
(35) Lafleur, M. A.; Stevens, J. L.; Lawrence, J. W. Xenobiotic perturbation of ER stress and the unfolded protein response. *Toxicol. Pathol.* **2013**, *41*, 235−262.
(36) Garcia-Mata, R.; Gao, Y. S.; Sztul, E. Hassles with taking out the garbage: aggravating aggresomes. *Traffic* **2002**, *3*, 388−396.
(37) Urra, H.; Dufey, E.; Lisbona, F.; Rojas-Rivera, D.; Hetz, C. When ER stress reaches a dead end. *Biochim. Biophys. Acta, Mol. Cell Res.* **2013**, *1833*, 3507−3517.
(38) Ding, W. X.; Ni, H. M.; Gao, W.; Yoshimori, T.; Stolz, D. B.; Ron, D.; Yin, X. M. Linking of autophagy to ubiquitin-proteasome system is important for the regulation of endoplasmic reticulum stress and cell viability. *Am. J. Pathol.* **2007**, *171*, 513−524.
(39) Benbrook, D. M.; Long, A. Integration of autophagy, proteasomal degradation, unfolded protein response and apoptosis. *Exp. Oncol.* **2012**, *34*, 286−297.
(40) Cheng, X.; Liu, H.; Jiang, C. C.; Fang, L.; Chen, C.; Zhang, X. D.; Jiang, Z. W. Connecting endoplasmic reticulum stress to autophagy through IRE1/JNK/beclin-1 in breast cancer cells. *Int. J. Mol. Med.* **2014**, *34*, 772−781.
(41) Ullman, E.; Fan, Y.; Stawowczyk, M.; Chen, H. M.; Yue, Z.; Zong, W. X. Autophagy promotes necrosis in apoptosis-deficient cells in response to ER stress. *Cell Death Differ.* **2008**, *15*, 422−425.
(42) Verfaillie, T.; Salazar, M.; Velasco, G.; Agostinis, P. Linking ER stress to autophagy: potential implications for cancer therapy. *Int. J. Cell Biol.* **2010**, *2010*, 1.
(43) Shimodaira, Y.; Takahashi, S.; Kinouchi, Y.; Endo, K.; Shiga, H.; Kakuta, Y.; Kuroha, M.; Shimosegawa, T. Modulation of endoplasmic reticulum (ER) stress-induced autophagy by C/EBP homologous protein (CHOP) and inositol-requiring enzyme 1α (IRE1α) in human colon cancer cells. *Biochem. Biophys. Res. Commun.* **2014**, *445*, 524−533.
(44) Johansen, T.; Lamark, T. Selective autophagy mediated by autophagic adapter proteins. *Autophagy* **2011**, *7*, 279−296.
(45) Deegan, S.; Saveljeva, S.; Gorman, A. M.; Samali, A. Stress-induced self-cannibalism: on the regulation of autophagy by endoplasmic reticulum stress. *Cell. Mol. Life Sci.* **2013**, *70*, 2425−2441.
(46) Korolchuk, V. I.; Menzies, F. M.; Rubinsztein, D. C. Mechanisms of cross-talk between the ubiquitin-proteasome and autophagy-lysosome systems. *FEBS Lett.* **2010**, *584*, 1393−1398.
(47) Nagaoka, U.; Kim, K.; Jana, N. R.; Doi, H.; Maruyama, M.; Mitsui, K.; Oyama, F.; Nukina, N. Increased expression of p62 in expanded polyglutamine-expressing cells and its association with polyglutamine inclusions. *J. Neurochem.* **2004**, *91*, 57−68.
(48) Kirkin, V.; McEwan, D. G.; Novak, I.; Dikic, I. A role for ubiquitin in selective autophagy. *Mol. Cell* **2009**, *34*, 259−269.
(49) Liu, X. D.; Ko, S.; Xu, Y.; Fattah, E. A.; Xiang, Q.; Jagannath, C.; Ishii, T.; Komatsu, M.; Eissa, N. T. Transient aggregation of ubiquitinated proteins is a cytosolic unfolded protein response to inflammation and endoplasmic reticulum stress. *J. Biol. Chem.* **2012**, *287*, 19687−19698.
(50) Paine, M. G.; Ramesh Babu, J.; Seibenhener, M. L.; Wooten, M. W. Evidence for p62 aggregate formation: role in cell survival. *FEBS Lett.* **2005**, *579*, 5029−5034.
(51) Moscat, J.; Diaz-Meco, M. T. p62 at the crossroads of autophagy, apoptosis, and cancer. *Cell* **2009**, *137*, 1001−1004.
(52) Komatsu, M.; Waguri, S.; Koike, M.; Sou, Y. S.; Ueno, T.; Hara, T.; Mizushima, N.; Iwata, J.; Ezaki, J.; Murata, S.; Hamazaki, J.; Nishito, Y.; Iemura, S.; Natsume, T.; Yanagawa, T.; Uwayama, J.; Warabi, E.; Yoshida, H.; Ishii, T.; Kobayashi, A.; Yamamoto, M.; Yue, Z.; Uchiyama, Y.; Kominami, E.; Tanaka, K. Homeostatic levels of p62 control cytoplasmic inclusion body formation in autophagy-deficient mice. *Cell* **2007**, *131*, 1149−1163.
(53) Korolchuk, V. I.; Mansilla, A.; Menzies, F. M.; Rubinsztein, D. C. Autophagy inhibition compromises degradation of ubiquitin-proteasome pathway substrates. *Mol. Cell* **2009**, *33*, 517−527.
(54) Jain, A.; Lamark, T.; Sjøttem, E.; Bowitz Larsen, K.; Atesoh Awuh, J.; Øvervatn, A.; McMahon, M.; Hayes, J. D.; Johansen, T. p62/SQSTM1 is a target gene for transcription factor NRF2 and creates a positive feedback loop by inducing antioxidant response element-driven gene transcription. *J. Biol. Chem.* **2010**, *285*, 22576−22591.
(55) Jiang, T.; Harder, B.; Rojo de la Vega, M.; Wong, P. K.; Chapman, E.; Zhang, D. D. p62 links autophagy and Nrf2 signaling. *Free Radical Biol. Med.* **2015**, *88*, 199−204.
(56) Kansanen, E.; Kuosmanen, S. M.; Leinonen, H.; Levonen, A. L. The Keap1-Nrf2 pathway: Mechanisms of activation and dysregulation in cancer. *Redox Biol.* **2013**, *1*, 45−49.
(57) Inami, Y.; Waguri, S.; Sakamoto, A.; Kouno, T.; Nakada, K.; Hino, O.; Watanabe, S.; Ando, J.; Iwadate, M.; Yamamoto, M.; Lee, M. S.; Tanaka, K.; Komatsu, M. Persistent activation of Nrf2 through p62 in hepatocellular carcinoma cells. *J. Cell Biol.* **2011**, *193*, 275−284.
(58) Dodson, M.; Redmann, M.; Rajasekaran, N. S.; Darley-Usmar, V.; Zhang, J. KEAP1-NRF2 signalling and autophagy in protection against oxidative and reductive proteotoxicity. *Biochem. J.* **2015**, *469*, 347−355.
(59) Brewer, A. C.; Mustafi, S. B.; Murray, T. V. A.; Rajasekaran, N. S.; Benjamin, I. J. Reductive stress linked to small HSPs, G6PD, and Nrf2 pathways in heart disease. *Antioxid. Redox Signaling* **2013**, *18*, 1114−1127.
(60) Cao, S. S.; Kaufman, R. J. Endoplasmic reticulum stress and oxidative stress in cell fate decision and human disease. *Antioxid. Redox Signaling* **2014**, *21*, 396−413.
(61) Hetz, C.; Chevet, E.; Harding, H. P. Targeting the unfolded protein response in disease. *Nat. Rev. Drug Discovery* **2013**, *12*, 703−719.
(62) Harding, H. P.; Zhang, Y.; Zeng, H.; Novoa, I.; Lu, P. D.; Calfon, M.; Sadri, N.; Yun, C.; Popko, B.; Paules, R.; Stojdl, D. F.; Bell, J. C.; Hettmann, T.; Leiden, J. M.; Ron, D. An integrated stress response regulates amino acid metabolism and resistance to oxidative stress. *Mol. Cell* **2003**, *11*, 619−633.
(63) Han, J.; Back, S. H.; Hur, J.; Lin, Y. H.; Gildersleeve, R.; Shan, J.; Yuan, C. L.; Krokowski, D.; Wang, S.; Hatzoglou, M.; Kilberg, M. S.; Sartor, M. A.; Kaufman, R. J. ER-stress-induced transcriptional regulation increases protein synthesis leading to cell death. *Nat. Cell Biol.* **2013**, *15*, 481−490.
(64) Brüning, A.; Jückstock, J. Misfolded proteins: from little villains to little helpers in the fight against cancer. *Front. Oncol.* **2015**, *5*, 47.
(65) Lamark, T.; Johansen, T. Aggrephagy: Selective disposal of protein aggregates by macroautophagy. *Int. J. Cell Biol.* **2012**, *2012*, 736905.
(66) Kang, J. H.; Li, M.; Chen, X.; Yin, X. M. Proteomics analysis of starved cells revealed Annexin A1 as an important regulator of autophagic degradation. *Biochem. Biophys. Res. Commun.* **2011**, *407*, 581−586.
(67) Arlt, A.; Bauer, I.; Schafmayer, C.; Tepel, J.; Müerköster, S. S.; Brosch, M.; Röder, C.; Kalthoff, H.; Hampe, J.; Moyer, M. P.; Fölsch, U. R.; Schäfer, H. Increased proteasome subunit protein expression and proteasome activity in colon cancer relate to an enhanced activation of nuclear factor E2-related factor 2 (Nrf2). *Oncogene* **2009**, *28*, 3983−3996.
(68) Clarke, H. J.; Chambers, J. E.; Liniker, E.; Marciniak, S. J. Endoplasmic reticulum stress in malignancy. *Cancer Cell* **2014**, *25*, 563−573.
(69) Sovolyova, N.; Healy, S.; Samali, A.; Logue, S. E. Stressed to death - mechanisms of ER stress-induced cell death. *Biol. Chem.* **2014**, *395*, 1−13.
(70) Jaramillo, M. C.; Zhang, D. D. The emerging role of the Nrf2-Keap1 signaling pathway in cancer. *Genes Dev.* **2013**, *27*, 2179−2191.

DOI: 10.1021/acs.jproteome.6b00154
J. Proteome Res. XXXX, XXX, XXX−XXX

(71) Gañán-Gómez, I.; Wei, Y.; Yang, H.; Boyano-Adánez, M. C.; García-Manero, G. Oncogenic functions of the transcription factor Nrf2. *Free Radical Biol. Med.* **2013**, *65*, 750−764.
(72) Levonen, A. L.; Hill, B. G.; Kansanen, E.; Zhang, J.; Darley-Usmar, V. M. Redox regulation of antioxidants, autophagy, and the response to stress: implications for electrophile therapeutics. *Free Radical Biol. Med.* **2014**, *71*, 196−207.

DOI: 10.1021/acs.jproteome.6b00154
J. Proteome Res. XXXX, XXX, XXX−XXX

3.2.7 Nano-liquid chromatography-orbitrap MS-based quantitative proteomics reveals differences between the mechanisms of action of carnosic acid and carnosol in colon cancer cells

Valdés, A., *García-Cañas, V., Artemenko, K. A., *Bergquist, J., Cifuentes, A.

Enviado para su publicación a la revista *Molecular and Cellular Proteomics*

Manuscript Title:	Nano-Liquid Chromatography-Orbitrap MS -Based Quantitative Proteomics Reveals Differences Between the Mechanisms of Action of Carnosic Acid and Carnosol in Colon Cancer Cells
Manuscript No:	MCP/2016/061481
Manuscript Type:	Research Article
Date Submitted by the Author:	2 Jun 2016
Complete List of Authors:	Alberto Valdés, Virginia García-Cañas, Konstantin A. Artemenko, Jonas Bergquist, and Alejandro Cifuentes
Keywords:	Cancer Biology*; Colorectal cancer; Mass Spectrometry; Proliferation* ; Quantification; HT-29 cells; carnosic acid; carnosol; dimethyl labeling ; foodomics

NANO-LIQUID CHROMATOGRAPHY-ORBITRAP MS-BASED QUANTITATIVE PROTEOMICS REVEALS DIFFERENCES BETWEEN THE MECHANISMS OF ACTION OF CARNOSIC ACID AND CARNOSOL IN COLON CANCER CELLS

Alberto Valdés[1], Virginia García-Cañas[1]*, Konstantin A. Artemenko[2], Jonas Bergquist[2]*, Alejandro Cifuentes[1]

[1] Laboratory of Foodomics, Institute of Food Science Research (CIAL, CSIC), Calle Nicolás Cabrera 9, 28049 Madrid, Spain.

[2] Analytical Chemistry, Department of Chemistry-BMC and SciLifeLab, Uppsala University, Husargatan 3, 75124 Uppsala, Sweden.

***Correspondence: Dr. V. García-Cañas**

E-mail: virginia.garcia@csic.es

Telephone: +34 910-017-950

Fax: +34 910-017-905

***Correspondence: Prof. Jonas Bergquist**

E-mail: jonas.bergquist@kemi.uu.se

Telephone: +46 (0)18 471 3675

Fax: +46 (0)18 471 3692

Running title: Proteomics profiling of CA and CS effects in cancer cells

Abbreviations

AMC, 7-amino-4-methylcoumarin

BOG, n-octyl-β-D-glucopyranoside

CA, carnosic acid

CS, carnosol

DML, dimethyl labeling

ER, endoplasmic reticulum

ERAD, ER-associated degradation

FDR, false discovery rate

GI50, 50% growth inhibition

IC50, 50% inhibitory concentration

IPA, Ingenuity Pathway Analysis

LC50, 50% lethal concentration

nano-LC-MS/MS, nano-liquid chromatography-tandem mass spectrometry

Rb, retinoblastoma

Suc-LLVY-AMC, N-Succinyl-Leu-Leu-Val-Tyr-AMC

TGI, total growth inhibition

UPR, unfolded protein response

UR, upstream regulator

SUMMARY

Carnosic acid (CA) and carnosol (CS) are two structurally related diterpenes present in rosemary herb (*Rosmarinus officinalis)*. Although several studies have demonstrated that both diterpenes can scavenge free radicals and interfere in cellular processes such as cell proliferation, they may not necessarily exert the same effects at the molecular level. In this work, a shotgun proteomics study based on stable isotope dimethyl labeling (DML) and nano-liquid chromatography-tandem mass spectrometry (nano-LC-MS/MS) has been performed to identify the relative changes in proteins and to gain some light on the specific molecular targets and mechanisms of action of CA and CS in HT-29 colon cancer cells. Protein profiles revealed that CA and CS induce different Nrf2-mediated response. Furthermore, examination of our data revealed that each diterpene affects protein homeostasis by different mechanisms. CA treatment induced the expression of proteins involved in the unfolded protein response in a concentration dependent manner reflecting accumulation of misfolded proteins in the ER, whereas CS directly inhibits chymotrypsin-like activity of the 20S proteasome. In conclusion, the unbiased proteomics-wide method applied in the present study has demonstrated to be a powerful tool to reveal differences on the mechanisms of action of two related bioactive compounds in the same biological model.

INTRODUCTION

Carnosic acid (CA) and carnosol (CS) are two structurally related phenolic compounds belonging to the abietanes family of naturally occurring diterpenes in the popular Lamiaceae herbs, rosemary (*Rosmarinus officinalis*), and sage (*Salvia officinalis*) (1). CS has a lactone moiety across the B ring, while CA has a free carboxylic acid group. Both diterpenes are capable of directly scavenging free radicals (2) and are also regarded as "pro-electrophilic" compounds that become active electrophiles after oxidation to their quinone forms. It has been recognized that CA and CS quinones react with a critical thiol in Keap1, causing it to release Nrf2 transcription factor that may enter the nucleus for subsequent activation of ARE (antioxidant-response element)-mediated transcription of an array of proteins that protect against oxidative stress (3,4). In fact, this effect has been considered as the predominant cause for the observed protective activity of both diterpenes in studies on their role in central nervous system (5). Besides their well-known property for indirectly increasing endogenous cellular antioxidant defenses via activation of the Keap1/Nrf2/ARE cascade, these compounds have a potential to modulate other multiple mechanisms causing a broad range of effects in cellular functions and biological outcomes depending on the cell model under study and the experimental conditions (6). For instance, CA and CS may interfere with a range of different cellular processes related to cell proliferation, invasiveness, tumorigenesis, and survival of cancer cells. Although CA and CS seem to share comparable antiproliferative potency they may not necessarily exert the same exact effects at the molecular level (7-11). Indeed, the wide spectrum of molecular targets of CA and CS in cancer cells has been recently reviewed by Petiwala and Johnson (12). For instance, CS has been shown to target Bcl-2 (13), CREB-binding protein/p300 (14), NF-kB and c-Jun (15), β-catenin (16), p21 (9), ERK1/2 (17), Jak2/Src-STAT3 (18), AMPK-mTOR (19), androgen receptor and estrogen receptor α (20,21), among others. In the case of CA, its anti-cancer activity has also been linked to different molecular targets. For example, CA blocked the epithelial to mesenchymal transformation by inhibiting Akt phosphorylation and the secretion of several proteins involved in the invasiveness of melanoma (18) and colon adenocarcinoma cells (22). In another work, CA induced apoptosis through reactive oxygen species mediated p38 activation

in neuroblastoma cells (4). In human prostate carcinoma cells, CA increased PP2A activity, leading to Akt and NF-kB signaling inhibition and induction of apoptosis (23). In addition, CA has been shown to sensitize human renal carcinoma Caki cells to TRAIL-induced apoptosis through down-regulation of c-FLIP and Bcl-2 at the post-translational levels and induction of DR5, Bim and PUMA transcription, events that were attributed to the up-regulation of CHOP and ATF4 typically observed in cells under ER stress (24). Recent works have reported the involvement of autophagy cell death in the anti-proliferative activity of CS and CA in different cancer cell lines (17,25). In this regard, CA-induced autophagic cell death has been closely linked to negative regulation of the Akt/mTOR pathway in human hepatoma cells (25). Furthermore, blockage of Akt signaling by PTEN expression seems to be a part of the causative mechanism for the anti-proliferative effect of CA in leukemia cells (27). CS has been also implicated in the inhibition of PI3K/Akt and mTOR signaling pathway mediated by AMPK activation in G2 phase-arrested prostate cancer cells (19). Taken together, all the reported pleiotropic cellular and molecular effects conferred to these rosemary diterpenes support the notion that the underlying mechanisms of action of these compounds are complex and diverse. Recently, foodomics has demonstrated to be a useful strategy to cover the identification of a wide range of molecular changes induced by rosemary compounds in *in vitro* cell models. In this line of work, comprehensive transcriptomic and metabolomic analyses helped on identifying global changes induced by rosemary polyphenols on colon cancer and leukemia cells (28-30). As an example, previous results obtained in our laboratory have shown that a CA-enriched rosemary extract transcriptionally trigger a strong Nrf2-mediated antioxidant response in addition to the unfolded protein response (UPR) to alleviate ER stress (30). Furthermore, the recent application of comprehensive proteomics based on nano-liquid chromatography-tandem mass spectrometry (nano-LC-MS/MS) combined with stable isotope dimethyl labeling (DML) has generated new insights regarding the role of autophagy and proteostasis in the cellular response to rosemary polyphenols, demonstrating the suitability of this proteomics strategy for the investigation of the mechanisms of action of dietary compounds in cancer cells (31). In the present work, we have applied DML and nano-LC-MS/MS to investigate global protein changes in HT-29 colon cancer cells in response to individual rosemary diterpenes, CA and CS. The objectives of this study were to: (i)

identify changes in relative abundance of proteins altered by CA and CS exposures over the time; and (ii) detect differences between the protein profiles obtained in CA- and CS-treated cells in order to shed light on the specific molecular targets and mechanisms of action of each diterpene in colon cancer cells.

EXPERIMENTAL PROCEDURES

Chemicals

ACN, methanol (MeOH), formic acid (FA), NaCl and urea were obtained from Merck (Darmstadt, Germany). Ethanol was provided by VWR Chemicals (Fontenay-sous-Bois, France). Acetone, EDTA, protease inhibitor cocktail, PBS, n-octyl-β-D-glucopyranoside (BOG), triethyl ammonium bicarbonate (TEAB), sodium metavanadate ($NaVO_4$), NaF, β-Glycerophosphate, sodium pyrophosphate, (37%, v/v), iodoacetamide (IAA), DTT, CA, CS, sucrose, $MgCl_2$, KCl, adenosine 5′-triphosphate disodium salt hydrate (ATP), digitonine and MG-132 were purchased from Sigma Aldrich (St. Louis, MO, USA). Trypsin/Lys-C Mix (Mass Spec Grade V5072) was purchased from Promega (Madison, USA) and deuterated formaldehyde CD_2O (20% (v/v)) was obtained from ISOTEC (Miamisburg, Ohio, USA). Sodium cyanoborohydride ($NaBH_3CN$) was purchased from Fluka (Buchs, Switzerland). Ultrapure water was prepared by Milli-Q water purification system (Millipore, Bedford, MA, USA). N-Succinyl-Leu-Leu-Val-Tyr-7-amino-4-methylcoumarin (Suc-LLVY-AMC) chymotrypsin-like substrate and purified human erythrocytes 20S proteasome were purchased from Enzo Life Sciences (Plymouth Meeting, PA, USA).

Cell Culture

Colon adenocarcinoma HT-29 cells obtained from ATCC (American Type Culture Collection, LGC Promochem, UK) were grown in McCoy's 5A supplemented with 10% (v/v) heat-inactivated FBS, 50 U/mL penicillin G, and 50 U/mL streptomycin at 37 ºC in humidified atmosphere and 5% CO_2. When cells

reached ~50% confluence, they were trypsinized, neutralized with culture medium, seeded at 10, 000 cells/cm^2 in 78 cm^2 cell culture dishes and allowed to adhere overnight at 37 ºC for 24 h.

Flow cytometry analysis

To study the cell cycle distribution, HT-29 cells were treated with cytostatic concentrations of CA or CS in complete culture medium for 24 h. After the treatment, cells were trypsinized, washed with PBS, and fixed with 70% (v/v) cold ethanol at −20 °C for at least 24 h. Then, fixed cells were resuspended in 0.5 mL of PI/RNase staining buffer (BD Pharmingen), incubated for 15 min in the dark, and analyzed on a Gallios flow cytometer equipped with a blue (488nm) laser (Beckman Coulter, FL, USA). Events were gated for peak width and area to exclude subcellular debris and aggregates. A total of 10, 000 events were recorded for each sample and a frequency histogram of peak area was generated and analyzed using Cylchred (V.1.0.0.1) software (University of Wales College of Medicine, Cardiff, U.K.). Results are provided as the mean ± SEM of three independent experiments.

Determination of 26S and 20S proteasome activity

To determine the 26S and 20S proteasome chymotrypsin-like activity after diterpene treatment, HT-29 cells were incubated with cytostatic concentrations of CA, CS or vehicle (0.2% (v/v) DMSO) for different times. As a positive control, cells were incubated with 1 μM of MG-132, a specific inhibitor of the proteasome activity. After the treatment, the 20S and 26S proteasome activities were measured as previously described (32). Cells were trypsinized, washed with PBS and divided equally into two aliquots. To evaluate the 20S proteasome activity, one aliquot was resuspended in 300 μL of lysis buffer (50 mM Tris titrated by HCl to pH 7.5, 250 mM sucrose, 5 mM $MgCl_2$, 1 mM DTT, 0.5 mM EDTA and 0.025% digitonin). To evaluate the 26S activity, the second aliquot was resuspended in lysis buffer containing 2 mM ATP. ATP prevents

dissociation of the 26S proteasome into its components and ensures its maximal activity. Cells were incubated on ice for 5 minutes, followed by centrifugation at 20,000×g for 15 minutes at 4°C. The supernatants were collected and the protein concentration in the cell lysates was determined using Bio-rad DC™ (Bio-Rad Laboratories, Hercules, CA). To measure the 20S proteasome chymotrypsin-like activity, 4 µg of protein extract were incubated in 200 µL of assay buffer (50 mM Tris titrated by HCl to pH 7.5, 40 mM KCl, 5 mM $MgCl_2$, 1 mM DTT), for 45 min at 37°C with 100 µM fluorogenic peptide substrate Suc-LLVY-AMC. The ATP-dependent 26S proteasome chymotrypsin-like activity was estimated using the same procedure as for the 20S, but 2 mM ATP was added to the reaction mixtures. After incubation, hydrolyzed 7-amino-4-methylcoumarin (AMC) was measured in a microplate reader (Synergy HT, BioTek Instruments, Winooski, Vermont), using an excitation filter of 360 nm and an emission filter of 460 nm. Results are provided as the mean ± SEM of the proteasome activity relative to the control of three independent experiments, and ANOVA with Fisher LSD post hoc test was applied considering significant differences when $p < 0.05$.

To determine the inhibitory chymotrypsin-like activity of diterpenes in purified 20S proteasome, 200 ng of purified human erythrocytes 20S proteasome were incubated with 100 µM Suc-LLVY-AMC in 200 µL of assay buffer (50 mM Tris titrated by HCl to pH 7.5), for 45 min at 37°C with or without different concentrations of CA, CS or MG-132. Hydrolyzed AMC was quantified as described above, and IC50 (50% inhibitory concentration) was calculated from three independent experiments using SigmaPlot (version 12.5) software (Systat Software Inc., Erkrath, Germany).

Experimental Design and sample preparation for proteomics analysis

For proteomic experiments, HT-29 cells were incubated with different concentrations (GI50, 50% growth inhibition; TGI, total growth inhibition, LC50, 50% lethal concentration) of two polyphenols (CA, CS) or vehicle (0.2% (v/v) DMSO), for 2, 6 or 24 h. Three biological replicates were used in the experiments,

obtaining a total of 63 samples. After incubation, cells were trypsinized and washed with 1 mL of cold PBS, and 1×10^6 cells were lysed with 300 µL of lysis buffer (6 M urea, 1% BOG, 0.15 M NaCl, 1.3 mM EDTA, 1 mM $NaVO_4$, 5 mM NaF, 2.5 mM sodium-pyrophospate and 5 mM β-Glycerophosphate in PBS) supplemented with 10 µL of protease inhibitor cocktail. The samples were incubated for 60 min at 4 ºC during mild agitation, sonicated for 30 min at 0 ºC in water bath (Elma, Germany) and centrifuged at 10,000×g at 4 ºC for 15 min (Sigma, Germany). Protein concentration was measured using Bio-rad DC™ assay and 10 µg of proteins were incubated at 4 ºC for 90 min in 500 µL of ice-cold tributylphosphate:acetone:methanol mixture (1:12:1, v/v/v). The precipitate was centrifuged for 15 min (3,000×g at 4 ºC), washed with 1 mL cold acetone, and finally air-dried. The resulting pellets were dissolved in 20 µL of 1% (w/v) BOG with 20% (v/v) ACN in 0.1 M TEAB, and the proteins were reduced with 10 µL of 45 mM DTT at 56 ºC for 15 min and alkylated with 10 µL of 100 mM IAA for 15 min in the dark. For protein digestion, samples were incubated at 37 ºC overnight in darkness with 0.5 µg of LysC/trypsin solution (5% w/w, of total protein content). Samples were dried in SpeedVac to remove ACN, resuspended in 70 µL of 0.1 M TEAB and water saturated ethyl-acetate was used to extract BOG (33). The tryptic peptide mixtures were reconstituted in 70 µL of 0.1 M TEAB and dimethyl labeling was performed as previously described (34). Briefly, 4 µL of regular formaldehyde CH_2O (4%, v/v) was added to control samples and 4 µL of deuterated formaldehyde CD_2O (4%, v/v) was added to treated samples, marking them as light and medium respectively. After vortexing, 4 µL of freshly prepared 0.6 M $NaBH_3CN$ solution was added to each sample and incubated for 60 min at room temperature with mild agitation. The reaction was finished by adding 16 µL of 1% (v/v) ammonia solution (Merck, Germany) and 8 µL of 5% (v/v) FA (Merck, Germany) was added to consume the excess of the labeling reagents. Finally, light and medium samples were mixed together and desalted on Isolute C18 solid phase extraction columns (1 mL, 50 mg capacity, Biotage, Uppsala, Sweden). After desalting, peptides were dried in a SpeedVac and redissolved in 0.1% (v/v) FA to a concentration of 1 µg/µL prior to nano-LC−MS/MS.

Nano-LC-MS/MS analysis and protein database searches

Five-µL aliquots containing ~ 1 µg of tryptic peptides were injected into a nano-LC-MS/MS system consisting of EASY-nLC II (Thermo Fisher Scientific, Bremen, Germany) coupled via nanoelectrospray ionization ion source to Orbitrap Velos Pro™ mass spectrometer (Thermo Fisher Scientific, Bremen, Germany). The peptide separations were performed on in-house packed uncoated fused silica emitters (PicoTip™ emitter, length 150 mm, 75 µm i.d., 375 µm o.d., tip opening 5±1 µm, New Objective, Woburn, USA). The emitters were packed with a methanol slurry of reversed-phase, fully end-capped Reprosil-Pur C18-AQ 3 µm resin (Dr. Maisch GmbH, Ammerbuch-Entringen, Germany) using a PC77 pressure injection cell (Next Advance, Averill Park, NY, USA). The separations were performed at a flow rate of 250 nL/min with mobile phases A (water with 0.1% (v/v) formic acid) and B (acetonitrile with 0.1% (v/v) formic acid). A 97-min gradient from 4% B to 30% B followed by 8 min from 30% B to 48% B, 6 min from 48% B to 75% B and a washing step with 75% B for 3 min was used. The mass spectrometer was operated in positive ion mode with unattended data-dependent acquisition mode, in which the mass spectrometer automatically switches between acquiring a high resolution survey mass spectrum in the Orbitrap (resolving power 60000 fwhm) and consecutive low-resolution, collision-induced dissociation fragmentation of up to ten of the most abundant ions in the ion trap using normalized collision energy of 35.0 eV. Ions that were once selected for acquisition were dynamically excluded for 30 s for further fragmentation. The mass spectrometry proteomics data have been deposited to the ProteomeXchange Consortium (35) via the PRIDE partner repository with the dataset identifier PXD004253.

All MS raw files were collectively processed with MaxQuant (version 1.5.2.8) (36) applying the Andromeda search engine with the following adaptions (37). The false discovery rate (FDR) was set to 1% for both proteins and peptides and we specified a minimum length of seven amino acids. MaxQuant scored peptides for identification based on a search with a maximum mass deviation of precursor and fragment masses of up to 20 ppm and 0.5 Da. The Andromeda search engine was used for the MS/MS spectra search against a concatenated forward and reversed version of the Uniprot human database (downloaded on

February 11, 2015, containing 89,909 entries and 245 frequently detected contaminants) for quantitative study. Enzyme specificity was set as C-terminal to Arg and Lys, also allowing cleavage at proline bonds and a maximum of two missed cleavages. Carbamidomethylation of cysteine residues was set as fixed modification while oxidation of methionine, phosphorylation of serine/threonine/tyrosine and protein N-acetylation were allowed as variable modifications. For dimethyl labeling, DimethylLys0 and DimethylNter0 were set as light labels, and DimethylLys4 and DimethylNter4 were set as medium labels. A minimum peptide ratio count of two and at least one "razor peptide" was required for quantification. After protein quantification, each data set was normalized to the median of the ratios to correct for mixing of medium and light labeled cells at 1:1 ratios, and to enable a better comparison between the different conditions.

Statistical and bioinformatics analysis

Prior to any statistical analysis using Perseus software (http://141.61.102.17/perseus_doku/doku.php?id=start), identifications flagged as reverse, potential contaminants, or proteins identified only by site modification were excluded for further analysis, and the relative protein abundance was transformed to the $\log_2$ scale. To identify the differentially expressed proteins in treated cells with respect to the control group, a 1.5-fold cutoff in relative protein abundance and a p-value < 0.05 (one sample t-test) were applied in those proteins identified in at least two biological replicates. The lists of differentially expressed proteins were uploaded in the bioinformatics tool Ingenuity Pathway Analysis (IPA; Qiagen, Redwood City, CA, USA) to perform a causal upstream regulator (UR) analysis. In UR analysis, the activation state of each regulator (such as transcription factors) is predicted based on global direction of changes in the different experimental condition for previously published targets of this regulator. Significance of the activation or deactivation of molecules predicted by UR analysis was

tested by the Fisher Exact test p-value, considering only the predictions with significant p-value < 0.05, and regulation z-score < −2 or > 2, for deactivation and activation, respectively.

RESULTS AND DISCUSSION

CA and CS treatments, protein identification and quantification

The anti-proliferative activity of CA and CS was previously determined and reported in (10). The response parameters GI50 and TGI, indicators for cytostaticity, and LC50, indicative for cytotoxicity, were used as reference to prepare the working concentrations in the proteomics experiments. Based on reported data, GI50, TGI and LC50 were 33.3 ± 2.8, 47.7 ± 2.9, and 69.1 ± 3.9 μg/mL for CA, and 41.6 ± 1.7, 52.7 ± 3.0, and 70.6 ± 4.0 μg/mL for CS, respectively.

The study of cell cycle distribution can provide useful information to determine the mechanism by which both diterpenes induce growth inhibition. The effect of rosemary diterpenes in cell cycle progression has shown to be cell type- and concentration-dependent. For instance, it has been reported that CA and CS induce G2/M phase arrest in Caco-2 cells (9), but CA and CS block cell cycle before and after prometaphase, respectively. A recent study in our laboratory suggested that the effects of a CA-enriched rosemary extract on cell cycle distribution are highly dependent on the extract concentration (11). In the present work, we used the maximum cytostatic concentration (TGI) calculated for CA and CS to investigate the possible changes on HT-29 cell cycle distribution exerted by these compounds using flow cytometry analysis. As shown in **Figure 1**, incubation of exponentially growing HT-29 cells with TGI concentrations of each diterpene for 24 h resulted in a substantial inhibition of cell cycle progression at different cell cycle phases. Namely, CA induced an obvious G1 arrest on HT-29 cells, represented by the accumulation of cells in the G1 phase (67.6% ± 1.2) with a concomitant decrease in the percentage of cells in the G2/M phase (10.5% ± 1.5) with respect to untreated control cells (57.0% ± 1.5 and 17.3% ± 1.6, respectively). On the other side, CS caused G2/M arrest as observed by the significant increase in the cell population in that phase

(42.8% ± 3.9), with a simultaneous decrease in the percentage of cells in the G1 (46.5% ± 3.6) and S phases (10.8% ± 0.3). These results give evidences that the molecular and cellular mechanisms underlying the antiproliferative activity of CA and CS are potentially distinct in HT-29 cell line.

To study in depth the molecular mechanisms underlying the antiproliferative activity of CA and CS, the impact of both diterpenes was investigated on the HT-29 proteome using quantitative proteomics platform based on DML combined with nano-LC-MS/MS. We aimed at identifying temporal changes in protein levels in HT-29 cell lysates in response to different cytostatic and cytotoxic concentrations of the extract. To achieve this, cells were incubated with three different concentrations of the CA and CS corresponding to the three different response parameters, GI50, TGI, and LC50, as well as with the vehicle (0.2% (v/v) DMSO, as controls) for different times (2, 6 and 24 h). In these proteomic experiments, quantitative comparison based on stable isotope dimethyl labeling was performed on the eighteen sets of experiments, using "light" for control cells and "medium" labels and CA- or CS-treated cells (**Figure 2**). Using three biological replicates per group, equal protein amounts of light-labeled and medium-labeled samples were mixed to generate 54 samples for further analysis. All mixtures were then analyzed using nano-LC-MS/MS analysis. MS raw data files were then simultaneously processed with the MaxQuant software for FDR-controlled peptide and protein identification and dimethyl labeling-based quantification (the identification and quantification of the peptides and proteins are found in **Supplemental Material Tables S1 and S2**, respectively). A total of 1,952 distinct proteins were identified (protein level FDR < 1%) with an average of 697 quantified proteins after performing all the analyses (see **Supplemental Material, Table S3**). The number of proteins identified in common across the 18 experimental conditions was 248. Relative abundance ratios were calculated for all proteins to screen the significantly altered proteins in each experimental condition, considering all the combinations of three variables (diterpene type, concentration and exposure time; see **Supplemental Material, Tables S4 and S5**). In this study, the restrictive criterion to consider a protein as significantly changed upon diterpene exposure included a 1.5-fold change cutoff in relative protein abundance, equivalent to $\log_2$ fold change of ± 0.585; and a p-value < 0.05 (one sample t-

test). According to this, the total number of proteins displaying significant changes upon CA and CS treatments was 76 and 57, respectively. Among them, a cluster of 26 proteins were common to both treatments.

Early changes in HT-29 proteome upon diterpene exposure

In order to study the dynamic of protein expression in HT-29 cells during the course of CA and CS treatments, the ratio of the significantly changed proteins obtained at different incubation times were examined. Three exposure duration times of 2, 6 and 24 h were chosen in order to analyze very early, early and late proteomic perturbations, respectively, occurring in treated cells with different concentrations of individual diterpenes (**Table 1 and Table 2)**. Most of the changes were detected after 24 h incubations with CA and CS. Indeed, none of the significantly altered proteins (p-value < 0.05) after 2 h treatment with GI50 concentration of CA passed the log fold change threshold established in the present study, and only EFHD2 and SLC25A3 were significantly altered by using the TGI and LC50 concentrations of CA, respectively. Interestingly, CS did not induce detectable significant changes in the relative abundance of any protein after 2 h; however, after 6 h of treatment, all the tested CS concentrations up-regulated the protein markers for the Nrf2-mediated antioxidant response (HMOX1 and SQSTM1), as well as three cytosolic chaperones, DNAJB1, HSPH1, and HSPA1A, being the latter accumulated in a concentration-dependent fashion (**Table 1**). In contrast, only the highest concentration of CA altered the levels of the oxidative stress markers, HMOX1 and SQSTM1 in HT-29 cells. Altogether, these results suggest that HT-29 cells trigger the antioxidant response upon exposure to both diterpenes, CA and CS; however, the observed different temporal and concentration effect of CS versus CA on markers for Nrf2-signaling might be accounted for a faster activation in cells treated with CS. In addition, the early up-regulation of different cytosolic chaperones in CS-treated cells may be indicative of proteotoxic stress at very early exposure times.

CA and CS induce different pattern of Nrf2-dependent proteins in HT-29 cells

Next, causal upstream regulator analyses of the protein profiles obtained after 24 h exposures to CA and CS were performed using IPA bioinformatics tool to obtain a broader picture of the potential transcriptional regulators that could be operating in the response of HT-29 cells to diterpenes. In agreement with the well-known ability of CA and CS to activate Nrf2 signaling (3,4), causal analysis predicted significant activation of Nrf2 under most of the tested conditions with both diterpenes (**Table 3**). To further determine whether Nrf2 activation by CA and CS follows the same transcriptional program, the relative abundance of the proteins that support Nrf2 activation by both diterpenes was examined (**Table 2**). In general, CA exerted changes that were slightly higher in SQSTM1 (also known as p62), as well as in molecules related with the antioxidant response and detoxication metabolism. In addition, a greater number of proteins related with NADPH generation were altered by CA treatments when compared with those affected by CS. On the other side, only CS-treated cells showed altered levels of eight different proteins belonging to 19S and 20S proteasome complexes. The results obtained suggest that although both diterpenes appear to affect antioxidant endogenous defenses, CA and CS induce different Nrf2-mediated response, revealing potential relevant differences in their mode of action. Nrf2 signaling pathway has become the subject of an intense research in last years (38). Recent evidences highlight the complexity of Nrf2 signaling pathway, such as for example the crosstalk with other pathways such as UPR or autophagy (39,40). Thus, depending on the cellular context and type of activation, Nrf2 signaling can be prolonged by different mechanisms other than the classical Nrf2-Keap1, such as for example Keap1 sequestration by p62, that may have profound biological consequences (41).

CA activates UPR proteins and down-regulates proteins transcriptionally controlled by E2F1

A detailed examination of the proteomic profiles obtained after 24 h treatments and IPA results (**Tables 2** and **3**) showed other interesting differences on the cellular response to both diterpenes. Specifically, CA

treatment caused up-regulation of proteins transcriptionally controlled by ATF4 and XBP1, along with ER chaperones. These observations corroborate previously reported transcriptomic data and suggest that only CA treatment exerts ER stress and activation of the UPR, which are indicative of perturbation of proteostasis within ER (30). Proteins supporting UPR signaling by XBP1 and ATF4 included relevant molecules involved in ER-associated degradation (ERAD) system, ER chaperones with key role in UPR, amino-acyl tRNA synthetases related with tRNA charging function, and molecules involved in essential amino acid uptake and metabolism (**Table 2**). Numerous environmental, physiological and pathological insults, as well as nutrient fluctuations, disrupt the ER protein-folding environment to cause protein misfolding and accumulation of misfolded proteins, referred to as ER stress (42). Prolonged UPR activation owing to severe or unresolved ER stress leads to cell death. In addition, it has been demonstrated that activation of UPR results in growth arrest in G1 phase of the cell cycle (43) and that ER stress triggers G1 phase cell cycle arrest in various cancer cells (44). Recent studies carried out in our laboratories have demonstrated that polyphenol-enriched rosemary extract also induce UPR activation in colon cancer cells (30,31). Our present results suggest that CA is one of the bioactive compounds in the extract contributing to the activation of such response to stress.

Furthermore, IPA causal analysis predicted deactivation of E2F1 transcription factor in cells treated with TGI concentration of CA (**Table 3**). E2F1 belongs to the E2F family of transcription factors that, in combination with retinoblastoma (Rb) family tumor suppressor proteins, controls DNA replication and cell cycle progression. The Rb/E2F pathway plays a pivotal role in regulating the initiation of DNA replication, and disruption of the pathway is common in virtually all human cancers (45). Although E2F is involved in a variety of cellular activities, the best understood function of E2F is to regulate transcription of genes involved in the transition from G1 to S phase, regulators of S phase entry and components of the DNA replication machinery. Our observations indicate that transcriptional targets of E2F1 essential for DNA synthesis (RRM1, TOP2A) and cell cycle progression (COPS8, RBBP4) were down-regulated in CA-treated cells (**Table 2**). In support of a decreased E2F1 transcriptional activity, our data shows that the

tumor suppressor SERPINB5 (also known as maspin) was up-regulated in CA-treated cells. Published data suggest that maspin controls cell cycle; specifically, it has been shown that maspin down-regulation by E2F1 activation accelerates cell cycle progression in gastric cancer (46). CA treatment additionally induced down-regulation of various proteins directly involved in the generation of pyrimidine (CAD) and purine (GMPS, HPRT1) nucleotides needed for DNA synthesis, as well as proteins involved in DNA replication (NAP1L1, NASP) and cell proliferation maintenance (MKI67), suggesting that CA treatment attenuates all these cellular processes. In agreement with previous transcriptomic studies carried out on CA-enriched extracts (30), our data show that the response mediated by down-regulation of E2F1 transcriptional activity constitutes a reasonable link to the G1 phase arrest observed in CA-treated cells, and provides a potential explanation for the inhibitory effect of this diterpene on HT-29 cell proliferation. Also, connected with some of these observations, the expression levels of TOP2A, MKI67 and E2F1 have recently shown to provide valuable prediction in the prognosis of cancer (47). Our data also showed that CS down-regulated various proteins, such as CBX3, HIST1H2AJ and HMGN2, with recognized key roles in epigenetic control of chromatin structure and gene expression. Particularly, CBX3 has recently shown to promote colon cancer growth by directly repressing expression of p21, an inhibitor of cellular proliferation in response to DNA damage (48).

Rosemary diterpenes altered cell adhesion and cytoskeletal proteins

Other findings of our present study revealed the alteration of proteins with a key role in cell adhesion and colorectal cancer (**Table 2**). For instance, LC50 CA treatment caused substantial increase in the relative abundance of GCNT3, a protein that has been shown to suppress cell adhesion, motility, and invasion of colon cancer cells (49). GCNT3 is frequently expressed at low levels in the majority of colorectal carcinomas whereas its overexpression dramatically inhibits colon cancer cell growth *in vitro* and *in vivo*. Such effects have been associated with its ability to induce carbohydrate changes on the cells surface

affecting cell-extracellular matrix interactions. In last years, GCNT3 expression has gained relevance and it has been recently proposed as a promising biomarker for colon cancer to monitor the response to chemotherapy (50). The GCNT3 up-regulation in CA-treated cells observed in the present study is coincident with other published data associating the GCNT3-inducing effect of CA and CA-enriched rosemary extracts with their antitumor effect on colon and pancreatic cancer cell lines (50). In contrast, the relative abundance of CD44 and MUC5AC proteins significantly decreased in CS-treated cells with LC50. CD44 is a cell surface marker for cancer stem cells in various tumors and a major adhesion molecule for the extracellular matrix. It has been implicated in tumor cell invasion and metastasis (51) and its ablation triggers growth arrest in proliferative tumor cells (52). *De novo* synthesis of MUC5AC, a secreted gel-forming mucin normally found in the stomach, has been reported in colon carcinomas (53). This mucin is involved in the formation of a biological inhibitory complex towards E-cadherin, a key component for the maintenance of cell-cell adhesion. In HT-29 cells, the loss of MUC5AC expression has been linked with a gain of function of E-cadherin, resulting in the loss of their invasiveness (54). Among the altered cytoskeletal proteins, it is interesting to note the down-regulation of SLC9A3R1 by CA and CS treatments. This protein is a known scaffold for epidermal growth factor receptor (EGF-R), and has also been suggested as marker of colorectal cancer progression on the basis of its expression and subcellular localization (55). Specifically, this marker appears to play a central role in maintaining the integrity and capacity of EGF-R proliferative signaling pathways in HT-29 cells (56). SLC9A3R1 down-regulation has been reported to shutdown the entire pathway and the cells revert to a less proliferative phenotype. Taken together, our results show that CA and CS treatments modulate proteomic changes that affect cytoskeleton, cell-surface and secreted molecules. The observed changes suggest that rosemary diterpenes affect cell adhesion to extracellular matrix, and therefore, reduce the invasive potential of HT-29 cells. Similarly, Barni et al. have demonstrated that CA inhibited the cell adhesion and migration functions in Caco-2 cells; although in that case the effects were associated to the decreased activity of secreted proteases and down-regulation of COX-2 expression (22).

CS inhibits proteasome activity in HT-29 cells

As mentioned above, our data obtained at 24 h indicate that CS modulates the levels of various protein subunits which are critical for 26S proteasome functions. The 26S proteasome is a multi-enzymatic protease complex with a central role in the ubiquitin-proteasome system, which is responsible for turnover and removal of intracellular abnormal proteins (57) and has a pivotal role in the regulation of many cellular processes including signal transduction, transcription, stress responses, cell differentiation, and metabolic adaptation (58-60). The 26S proteasome consists of one 20S core proteasome with multicatalytic activity and two 19S regulatory caps (61-63). The 19S regulatory caps contain the lid, which is responsible for recognition and docking of polyubiquitinated proteins into the 20S complex, and the base, which has ATPase activity needed for the unfolding and linearization of proteins (64). The 20S core can also exist in a free form that is often referred to as the 20S proteasome, and in contrast with the 26S proteasome, the 20 proteasome functions independently of ATP and is unable of degrading polyubiquitinylated proteins (65).

Unlike normal cells, several cancer cells show aberrant increased proteasomal activity that promotes the degradation of tumor suppressor proteins and cell cycle proteins favoring cancer cell survival, high proliferation rates, and development of drug resistance (66-76). In our present work, to further examine whether the changes in the relative abundance of proteasome subunits induced by CS accounted for changes in the proteasome activity, the chymotrypsin-like activity of the proteasome was assessed in cells after diterpenes exposure for different times (2, 6 and 24 h). MG-132, a well-known proteasome inhibitor was used as positive control. After incubations, 26S and 20S proteasome activities were assayed in cell extracts with the Suc-LLVY-AMC labelled peptide under ATP-stimulated and ATP-independent conditions, respectively. Data revealed that CS treatment decreased both proteasome activities at the earliest time assayed (2 h) in HT-29 cells (**Figure 3A** and **B**). Proteasome activity further decreased down to 50.5% upon exposure to CS for 6 h, but it increased in the window from 6 to 24 hours to levels close below those

detected in untreated control cells. In contrast, CA treatment did not induce significant changes in either 26S or 20S proteasome activity. We therefore hypothesize that CS directly inhibits the 20S proteasome catalytic activity. To test this hypothesis, rosemary diterpenes were tested for their capacity to inhibit chymotrypsin-like activity in 20S purified proteasome. As shown in **Figure 3C**, the profile of proteasome inhibition shows that CA failed to inhibit proteasome activity when tested to concentrations up to 50 µM whereas CS inhibited proteasomal function with an IC50 value of 16.5 µM (**Figure 3D**). Compared with the stronger inhibitory activity of MG-132 (IC50~70 nM, **Figure 3E**), CS was ~200-fold less potent, suggesting that CS is a weak inhibitor of 20S proteasome activity. The inhibitory activity of CS observed in HT-29 cells and the successive activity recovery correlated with proteasome subunit up-regulation detected at 24 h. These results are in full agreement with other recent works evidencing that cells increase the expression of proteasome subunits in response to partial proteasome inhibition as a compensatory mechanism to raise proteasome content (77,78). In this regard, different reports suggest that Nrf1 and Nrf2 transcription factors control the induction of proteasome subunits genes in several cell types (79,80). However, it appears that only Nrf1 up-regulates proteasome genes upon proteasome inhibition (81). It has been recently observed that the compensatory response mediated by proteasome inhibition and Nrf1 also involves the up-regulation of VCP (also known as p97), a protein with a key role in the Nrf1 translocation for subsequent processing and activation (78,82). Consistent with Nrf1 activation, our proteomic data indicated increased levels of VCP/p97 suggesting that up-regulation of proteasome subunits in CS-treated cells could be potentially mediated by Nrf1 transcriptional activity. Proteasome inhibition frequently results in G2/M phase cell-cycle arrest and, ultimately, in cell death (66,83-85), which is in good agreement with the observed effects induced by CS in our present study. Such deleterious effects induced by proteasome inhibition, are frequently more significant in neoplastic cells than in normal cells (86). In last years, the proteasome has emerged as an attractive therapeutic target for the treatment of cancer (87). Some proteasome inhibitors have shown to be particularly effective in the sensitizing drug-resistant tumors (72,88). However, their clinical use is limited by their typical elevated toxicity. It has been suggested that proteasome inhibitors from natural food sources with low toxicity can be potential anticancer agents (88).

According to our results, CS could be a promising proteasome inhibitor of comparable potency to other dietary polyphenols, such as genistein, kaempferol, quercetin, and myricetin, with reported inhibitory effects on the 20S proteasome proteolytic activity (89,90). Our proteomics data also indicated a strong pattern of HSPA1A and HSP90AA1 accumulation in CS-treated cells compared to control (**Table 1** and **2**), suggesting the activation of cytoprotective heat shock response to alleviate loss of protein homeostasis in the cytosolic compartment. Interestingly, HSPA1A gene expression is controlled via rapid activation of heat shock factor-1 (HSF1) and is normally induced by proteasome inhibitors (91). Recent data suggest that HSPA1A overexpression protects cancer cells from proteasome inhibitors toxicity by promoting lysosomal integrity (92). To target this survival response, chaperone inhibitors alone or in combination with proteasome inhibitors have been widely investigated as a therapeutic strategy in some cancers; however, due to the induction of other chaperones as compensatory mechanisms, this approach has not progressed to clinical trials. This is in line with recent strategies that highlight the advantage of targeting the master transcription factor HSF1 to enhance the impact of proteasome inhibition (93).

CONCLUSIONS

Collectively, our results suggest that although both CA and CS activate the Nrf2 pathway, they induce distinct Nrf2-mediated transcriptional programs that may potentially constitute different mechanisms of action. The proteomic study carried out in the present work suggests that CA and CS cause cellular stress by negatively altering cell proteostasis. However, a detailed examination of our data reveals that each diterpene affects protein homeostasis by different mechanisms. Thus, cellular response to CA involved UPR activation, a typical mechanism triggered by the accumulation of misfolded proteins in the ER. On the other hand, HT-29 cells activated the cytoprotective heat shock response, constituted by increased levels of cytosolic chaperones that potentially alleviate the loss protein homeostasis upon CS-mediated proteasome inhibition. In our present work, we have successfully demonstrated that CS directly inhibits

chymotrypsin-like activity of the 20S proteasome. Other concurrent protein changes affecting DNA synthesis and replication, cell cycle progression, cell adhesion and cytoskeleton functions, among others, corroborate the "pleiotropic" character of the effects exerted by both diterpenes at the molecular level. In summary, our unbiased proteome-wide strategy has proven to be a powerful tool to reveal differences on the mechanisms of action of two related bioactive compounds in the same biological model.

ACKNOWLEDGMENTS

This work was supported by the project AGL2014-53609-P (Ministerio de Economía y Competitividad, Spain) and S2013/ABI-2728 (Comunidad de Madrid). A.V. thanks the Ministerio de Economía y Competitividad for his FPI pre-doctoral fellowship (BES-2012-057014). The Swedish Research Council (2011-4423 and 2015-4870; J.B.) is acknowledged for financial support.

CONFLICT OF INTEREST

The authors declare that there is no conflict of interest.

REFERENCES

1. González, M. A. (2015) Aromatic abietane diterpenoids: their biological activity and synthesis. *Nat. Prod. Rep.* **32**, 684-704.

2. Aruoma, O. I., Halliwell, B., Aeschbach, R., and Löligers, J. (1992) Antioxidant and pro-oxidant properties of active rosemary constituents: carnosol and carnosic acid. *Xenobiotica* **22**, 257-268.

3. Satoh, T., Kosaka, K., Itoh, K., Kobayashi, A., Yamamoto, M., Shimojo, Y., Kitajima, C., Cui, J., Kamins, J., Okamoto, S., Izumi, M., Shirasawa, T., and Lipton, S. A. (2008) Carnosic acid, a catechol-type electrophilic compound, protects neurons both in vitro and in vivo through activation of the Keap1/Nrf2 pathway via S-alkylation of targeted cyteines on Keap1. *J. Neurochem.* **104**, 1116−1131.

4. Tsai, C. W., Lin, C. Y., Lin, H. H., and Chen, J. H. (2011) Carnosic acid, a rosemary phenolic compound, induces apoptosis through reactive oxygen species-mediated p38 activation in human neuroblastoma IMR-32 cells. *Neurochem. Res.* **36**, 2442-2451.

5. Satoh, T., McKercher, S. R. and Lipton, S. A. (2013) Nrf2/ARE-mediated antioxidant actions of pro-electrophilic drugs. *Free Radic. Biol. Med.* **65**, 645-657.

6. González-Vallinas, M., Reglero, G., and Ramírez de Molina, A. (2015) Rosemary (Rosmarinus officinalis L.) extract as a potential complementary agent in anticancer therapy. *Nutr. Cancer* **67**, 1221-1229.

7. Takahashi, T., Tabuchi, T., Tamaki, Y., Kosaka, K., Takikawa, Y., and Satoh, T. (2009) Carnosic acid and carnosol inhibit adipocyte differentiation in mouse 3T3-L1 cells through induction of phase2 enzymes and activation of glutathione metabolism. *Biochem. Biophys. Res. Commun.* **382**, 549-554.

8. Tamaki, Y., Tabuchi, T., Takahashi, T., Kosaka, K., and Satoh, T. (2010) Activated glutathione metabolism participates in protective effects of carnosic acid against oxidative stress in neuronal HT22 cells. *Planta Med.* **76**, 683-688.

9. Visanji, J. M., Thompson, D. G., and Padfield, P. J. (2006) Induction of G2/M phase cell cycle arrest by carnosol and carnosic acid is associated with alteration of cyclin A and cyclin B1 levels. *Cancer Lett.* **237**, 130-136.

10. Valdés, A., García-Cañas, V., Simó, C., Ibáñez, C., Micol, V., Ferragut, J. A. and Cifuentes, A. (2014) Comprehensive Foodomics study on the mechanisms operating at various molecular levels in cancer cells in response to individual rosemary polyphenols. *Anal. Chem.* **86**, 9807-9815.

11. Valdés, A., García-Cañas, V., Koçak, E., Simó, C., and Cifuentes, A. (2016) Foodomics study on the effects of extracellular production of hydrogen peroxide by rosemary polyphenols on the anti-proliferative activity of rosemary polyphenols against HT-29 cells. *Electrophoresis* **0**, 1-10.

12. Petiwala, S. M., and Johnson, J. J. (2015) Diterpenes from rosemary (Rosmarinus officinalis): Defining their potential for anti-cancer activity. *Cancer Lett.* **367**, 93-102.

13. Dörrie, J., Sapala, K., and Zunino, S. J. (2001) Carnosol-induced apoptosis and downregulation of Bcl-2 in B-lineage leukemia cells. *Cancer Lett.* **170**, 33-39.

14. Subbaramaiah, K., Cole, P. A., and Dannenberg, A. J. (2002) Retinoids and carnosol suppress cyclooxygenase-2 transcription by CREB-binding protein/p300-dependent and -independent mechanisms. *Cancer Res.* **62**, 2522-2530.

15. Huang, S. C., Ho, C. T., Lin-Shiau, S. Y. and Lin, J. K. (2005) Carnosol inhibits the invasion of B16/F10 mouse melanoma cells by suppressing metalloproteinase-9 through down-regulating nuclear factor-kappa B and c-Jun. *Biochem. Pharmacol.* **69**, 221-232.

16. Moran, A. E., Carothers, A. M., Weyant, M. J., Redston, and Bertagnolli, M. M. (2005) Carnosol inhibits beta-catenin tyrosine phosphorylation and prevents adenoma formation in the C57BL/6J/Min/+ (Min/+) mouse. *Cancer Res.* **65**, 1097-1104.

17. Al Dhaheri, Y., Attoub, S., Ramadan, G., Arafat, K., Bajbouj, K., Karuvantevida, AbuQamar, S., Eid, A., and Iratni R. (2014) Carnosol induces ROS-mediated beclin1-independent autophagy and apoptosis in triple negative breast cancer. *PLoS One.* **9**, e109630.

18. Park, K. W., Kundu, J., Chae, I. G., Kim, D. H., Yu, M. H., Kundu, J. K. and Chun, K. S. (2014) Carnosol induces apoptosis through generation of ROS and inactivation of STAT3 signaling in human colon cancer HCT116 cells. *Int. J. Oncol.* **44**, 1309-1315.

19. Johnson, J. J., Syed, D. N., Heren, C. R., Suh, Y., Adhami, V. M. and Mukhtar, H., (2008) Carnosol, a dietary diterpene, displays growth inhibitory effects in human prostate cancer PC3 cells leading to G2-phase cell cycle arrest and targets the 5'-AMP-activated protein kinase (AMPK) pathway. *Pharm. Res.* **25**, 2125-2134.

20. Johnson, J. J., Syed, D. N., Suh, Y., Heren, C. R., Saleem, M., Siddiqui, I. A., Mukhtar, H. D. (2010) Disruption of androgen and estrogen receptor activity in prostate cancer by a novel dietary diterpene carnosol: implications for chemoprevention. *Cancer Prev. Res.* **3**, 1112-1123.

21. Petiwala, S. M., Berhe, S., Li, G., Puthenveetil, A. G., Rahman, O., Nonn, L., and Johnson, J. J. (2014) Rosemary (Rosmarinus officinalis) extract modulates CHOP/GADD153 to promote androgen receptor degradation and decreases xenograft tumor growth. *PLoS One* **9**, e89772.

22. Barni, M. V., Carlini, M. J., Cafferata, E. G., Puricelli, L., and Moreno, S. (2012) Carnosic acid inhibits the proliferation and migration capacity of human colorectal cancer cells. *Oncol. Rep.* **27**, 1041-1048.

23. Kar, S., Palit, S., Ball, W. B., and Das, P. K. (2012) Carnosic acid modulates Akt/IKK/NF-κB signaling by PP2A and induces intrinsic and extrinsic pathway mediated apoptosis in human prostate carcinoma PC-3 cells. *Apoptosis* **17**, 735-747.

24. Min, K. J., Jung, K. J., and Kwon, T. K. (2014) Carnosic acid induces apoptosis through reactive oxygen species-mediated endoplasmic reticulum stress induction in human renal carcinoma Caki cells. *J. Cancer Prev.* **19**, 170-178.

25. Gao, Q., Liu, H., Yao, Y., Geng, L., Zhang, X., Jiang, L., Shi, B., and Yang, F. (2015) Carnosic acid induces autophagic cell death through inhibition of the Akt/mTOR pathway in human hepatoma cells. *J. Appl. Toxicol.* **35**, 485-492.

26. Yan, M., Li, G., Petiwala, S. M., Householter, E. and Johnson, J. J. (2015) Standardized rosemary (Rosmarinus officinalis) extract induces Nrf2/sestrin-2 pathway in colon cancer cells. *J. Func. Foods* **13**, 137–147.

27. Wang, R., Cong, W. H., Guo, G., Li, X. X., Chen, X. L., Yu, X. N., and Li, H. (2012) Synergism between carnosic acid and arsenic trioxide on induction of acute myeloid leukemia cell apoptosis is associated with modulation of PTEN/Akt signaling pathway. *Chin. J. Integr. Med.* **18**, 934-941.

28. Valdés, A., Simó, C., Ibáñez, C., Rocamora-Reverte, L., Ferragut, J. A., García-Cañas, V., and Cifuentes, A. (2012). Effect of dietary polyphenols on K562 leukemia cells: A Foodomics approach. *Electrophoresis* **33**, 2314-2327.

29. Ibáñez, C., Valdés, A., García-Cañas, V., Simó, C., Celebier, M., Rocamora-Reverte, L., Gómez-Martínez, A., Herrero, M., Castro-Puyana, M., Segura-Carretero, A., Ibáñez, E., Ferragut, J. A., and Cifuentes, A. (2012) Global Foodomics strategy to investigate the health benefits of dietary constituents. *J. Chromatogr. A* **1248**, 139-153.

30. Valdés, A., Sullini, G., Ibáñez, E., Cifuentes, A., and García-Cañas, V. (2015) Rosemary polyphenols induce unfolded protein response and changes in cholesterol metabolism in colon cancer cells. *J. Funct. Foods* **15**, 429-439.

31. Valdés, A., Artemenko, K. A., Bergquist, J., García-Cañas, V., Cifuentes, A. (2016) Comprehensive Proteomic Study of the Antiproliferative Activity of a Polyphenol-Enriched Rosemary Extract on Colon Cancer Cells Using Nanoliquid Chromatography-Orbitrap MS/MS. *J. Proteome Res.* DOI: 10.1021/acs.jproteome.6b00154.

32. Kisselev, A. F., Goldberg, A. L. (2005) Monitoring activity and inhibition of 26S proteasomes with fluorogenic peptide substrates. *Methods Enzymol.* **398**, 364-378.

33. Yeung, Y. G., and Stanley, E. R. (2010) Rapid detergent removal from peptide samples with ethyl acetate for mass spectrometry analysis. *Curr. Protoc. Protein Sci.* **16**, 16.12.

34. Boersema, P. J., Raijmakers, R., Lemeer, S., Mohammed, S., and Heck, A. J. (2009) Multiplex peptide stable isotope dimethyl labeling for quantitative proteomics. *Nat. Protoc.* **4**, 484-494.

35. Vizcaíno, J. A., Deutsch, E. W., Wang, R., Csordas, A., Reisinger, F., Ríos, D., Dianes, J. A., Sun, Z., Farrah, T., Bandeira, N., Binz, P. A., Xenarios, I., Eisenacher, M., Mayer, G., Gatto, L., Campos, A., Chalkley, R. J., Kraus, H. J., Albar, J. P., Martinez-Bartolome, S., Apweiler, R., Omenn, G. S., Martens, L., Jones, A. R., and Hermjakob, H. (2014) ProteomeXchange provides globally coordinated proteomics data submission and dissemination. *Nat. Biotechnol.* **32**, 223–226.

36. Cox, J. and Mann, M. (2008) MaxQuant enables high peptide identification rates, individualized p.p.b.-range mass accuracies and proteome-wide protein quantification. *Nat. Biotechnol.* **26**, 1367–1372.

37. Cox, J., Neuhauser, N., Michalski, A., Scheltema, R. A., Olsen, J. V., and Mann, M. (2011) Andromeda: a peptide search engine integrated into the MaxQuant environment. *J. Proteome Res.* **10**, 1794–1805.

38. Suzuki, T., and Yamamoto, M. (2015) Molecular basis of the Keap1-Nrf2 system. *Free Radic. Biol. Med.* **88**, 93-100.

39. Eletto, D., Chevet, E., Argon, Y., and Appenzeller-Herzog, C. (2014) Redox controls UPR to control redox. *J. Cell Sci.* **127**, 3649-3658.

40. Levonen, A. L., Hill, B. G., Kansanen, E., Zhang, J., and Darley-Usmar, V. M. (2014) Redox regulation of antioxidants, autophagy, and the response to stress: implications for electrophile therapeutics. *Free Radic. Biol. Med.* **71**, 196-207.

41. Dodson, M., Redmann, M., Rajasekaran, N. S., Darley-Usmar, V., and Zhang, J. (2015) KEAP1-NRF2 signalling and autophagy in protection against oxidative and reductive proteotoxicity. *Biochem. J.* **469**, 347-355.

42. Wang, M., and Kaufman, R. J. (2014). The impact of the endoplasmic reticulum protein-folding environment on cancer development. *Nat. Rev. Cancer* **14**, 581-597.

43. Brewer, J. W., Hendershot, L. M., Sherr, C. J., and Diehl, J. A. (1999) Mammalian unfolded protein response inhibits cyclin D1 translation and cell-cycle progression. *Proc. Natl. Acad. Sci. USA* **96**, 8505-8510.

44. Puthalakath, H., O'Reilly, L. A., Gunn, P., Lee, L., Kelly, P. N., Huntington, D., Hughes, P. D., Michalak, E. M., McKimm-Breschkin, J., Motoyama, N., Gotoh, T., Akira, S., Bouillet, P., Strasser, and A. (2007) ER stress triggers apoptosis by activating BH3-only protein Bim. *Cell* **129**, 1337-1349.

45. Nevins, J. R. (2001) The Rb/E2F pathway and cancer. *Hum. Mol. Genet.* **10**, 699-703.

46. Kim, M., Ju, H., Lim, B., and Kang, C. (2012) Maspin genetically and functionally associates with gastric cancer by regulating cell cycle progression. *Carcinogenesis* **33**, 2344-2350.

47. Malhotra, S., Lapointe, J., Salari, K., Higgins, J. P., Ferrari, Montgomeryet, K., van de Rijn, M., Brooks, J. D., and Pollack, J. R. (2011) A tri-marker proliferation index predicts biochemical recurrence after surgery for prostate cancer. *PLoS One* **6**, e20293.

48. Liu, M., Huang, F., Zhang, D., Ju, J., Wu, X. B., Wang, Y., Wang, Y., Wu, Y., Nie, M., Li, Z., Ma, C., Chen, X., Zhou, J. Y., Tan, R., Yang, B. L., Zen, K., Zhang, C. Y., Chen, Y. G., and Zhao, Q. (2015) Heterochromatin protein HP1γ promotes colorectal cancer progression and is regulated by miR-30a. *Cancer Res.* **75**, 4593-4604.

49. Huang, M. C., Chen, H. Y., Huang, H. C., Huang, J., Liang, J. T., Shen, T. L., Lin, N. Y., Ho, C. C., Cho, I. M., and Hsu, S. M. (2006) C2GnT-M is downregulated in colorectal cancer and its re-expression causes growth inhibition of colon cancer cells. *Oncogene* **25**, 3267-3276.

50. González-Vallinas, M., Molina, S., Vicente, G., Zarza, V., Martín-Hernández, R., García-Risco, M. R., Fornari, T., Reglero, G., and Ramírez de Molina, A. (2014) Expression of microRNA-15b and the glycosyltransferase GCNT3 correlates with antitumor efficacy of Rosemary diterpenes in colon and pancreatic cancer. *PLoS One* **9**, e98556.

51. Xu, H., Tian, Y., Yuan, X., Wu, H., Liu, Q., Pestell, R. G., and Wu, K. (2015) The role of CD44 in epithelial-mesenchymal transition and cancer development. *Onco Targets Ther.* **8**, 3783-3792.

52. Ishimoto, T., Nagano, O., Yae, T., Tamada, M., Motohara, T., Oshima, H., Oshima, M., Ikeda, T., Asaba, R., Yagi, H., Masuko, T., Shimizu, T., Ishikawa, T., Kai, K., Takahashi, E., Imamura, Y., Baba, Y., Ohmura, M., Suematsu, M., Baba, H., and Saya H. (2011) CD44 variant regulates redox status in cancer cells by stabilizing the xCT subunit of system xc(-) and thereby promotes tumor growth. *Cancer Cell* **19**, 387-400.

53. Bara, J., Chastre, E., Mahiou, J., Singh, R. L., Forgue-Lafitte, M. E., Hollande, E., and Godeau, F. (1998) Gastric M1 mucin, an early oncofetal marker of colon carcinogenesis, is encoded by the MUC5AC gene. *Int. J. Cancer* **75**, 767-773.

54. Truant, S., Bruyneel, E., Gouyer, V., De Wever, O., Pruvot, F. R., Mareel, M., and Huet, G. (2003) Requirement of both mucins and proteoglycans in cell-cell dissociation and invasiveness of colon carcinoma HT-29 cells. *Int. J. Cancer* 104, 683-694.

55. Hayashi, Y., Molina, J. R., Hamilton, S. R., and Georgescu, M. M. (2010) NHERF1/EBP50 is a new marker in colorectal cancer. *Neoplasia* **12**, 1013-1022.

56. Kruger, W. A., Monteith, G. R., and Poronnik, P. (2013) NHERF-1 regulation of EGF and neurotensin signalling in HT-29 epithelial cells. *Biochem. Biophys. Res. Commun.* **432**, 568-573.

57. Glickman, M. H., and Cienchanover, A. (2002) The ubiquitin-proteasome proteolytic pathway: Destruction for the sake of construction. *Physiol. Rev.* **82**, 373-428.

58. Schmidt, M., and Finley, D. (2014) Regulation of proteasome activity in health and disease. *Biochim. Biophys. Acta* **1843**, 13-25.

59. Sengupta, S., and Henry, R. W. (2015) Regulation of the retinoblastoma-E2F pathway by the ubiquitin-proteasome system. *Biochim. Biophys. Acta* **1849**, 1289-1297.

60. Demasi, M., Netto, L. E., Silva, G. M., Hand, C.L. de Oliveira, C. L., Bicev, R. N., Gozzo, F., Barros, M. H., Leme, J. M., and Ohara, E. (2013) Redox regulation of the proteasome via S-glutathionylation. *Redox Biol.* **2**, 44-51.

61. Peters, J. M. (1994) Proteasomes: protein degradation machines of the cell. *Trends Biochem. Sci.* **19**, 377-382.

62. Peters, J. M., Franke, W. W., and Kleinschmidt, J. A. (1994) Distinct 19 S and 20 S subcomplexes of the 26 S proteasome and their distribution in the nucleus and the cytoplasm. *J. Biol. Chem.* **269**, 7709-7718.

63. McDougall, G. J., Ross, H. A., Ikeji, M., and Stewart, D. (2008) Berry extracts exert different antiproliferative effects against cervical and colon cancer cells grown in vitro. *J. Agric. Food Chem.* **56**, 3016-3023.

64. Shen, M., Schmitt, S., Buac, D., and Dou, Q. P. (2013) Targeting the ubiquitin-proteasome system for cancer therapy. *Expert Opin. Ther. Targets* **17**, 1091-1108.

65. Coux, O., Tanaka, K., and Goldberg, A. L. (1996) Structure and functions of the 20S and 26S proteasomes. *Annu. Rev. Biochem.* **65**, 801-847.

66. Adams, J. (2002) Proteasome inhibition: a novel approach to cancer therapy. *Trends Mol. Med*. **8**, S49-S54.

67. An, B., Goldfarb, R. H., Siman, R., and Dou, Q. P. Novel dipeptidyl proteasome inhibitors overcome Bcl-2 protective function and selectively accumulate the cyclin-dependent kinase inhibitor p27 and induce apoptosis in transformed, but not normal, human fibroblasts. *Cell Death Differ.* **5**, 1062-1075.

68. Lopes, U. G., Erhardt, P., Yao, R., and Cooper, G. M. (1997) p53-dependent induction of apoptosis by proteasome inhibitors. *J. Biol. Chem.* **272**, 12893-12896.

69. Nam, S., Smith, D. M., and Dou, Q. P. Tannic acid potently inhibits tumor cell proteasome activity, increases p27 and Bax expression, and induces G1 arrest and apoptosis. *Cancer Epidemiol. Biomarkers Prev.* **10**, 1083-1088.

70. Wada, M., Kosaka, M., Saito, S., Sano, T., Tanaka, K., and Ichihara, A. (1993) Serum concentration and localization in tumor cells of proteasomes in patients with hematologic malignancy and their pathophysiologic significance. *J. Lab. Clin. Med.* **12**, 215–231.

71. Kumatori, A., Tanaka, K., Inamura, N., Sone, S., Ogura, T., Matsumoto, T., Tachikawa, T., Shin, S., and Ichihara, A. (1990) Abnormally high expression of proteasomes in human leukemic cells. *Proc. Natl. Acad. Sci. USA* **87**, 7071-7075.

72. Kisselev, A.F., and Goldberg, A. L. (2001) Proteasome inhibitors: from research tools to drug candidates, *Chem. Biol.* **8**,739-758.

73. Afjehi-Sadat, L., Gruber-Olipitz, M., Felizardo, M., Slavc, I., and Lubec, G. (2004) Expression of proteasomal proteins in ten different tumor cell lines. *Amino Acids* **27**, 129-140.

74. Ishibashi, Y., Hanyu, N., Suzuki, Y., Yanai, S., Tashiro, K., Usuba, T., Iwabuchi, S., Takahashi, T., Takada, K., Ohkawa, K., Urashima, M., and Yanaga, K. (2004) Quantitative analysis of free ubiquitin and multi-ubiquitin chain in colorectal cancer. *Cancer Lett*. **211**, 111-117.

75. Marfella, R., D'Amico, M., Esposito, K., Baldi, A., Di Filippo, C., Siniscalchi, M., Sasso, F. C., Portoghese, M., Cirillo, F., Cacciapuoti, F., Carbonara, O., Crescenzi, B., Baldi, F., Ceriello, A., Nicoletti, G. F., D'Andrea, F., Verza, M., Coppola, L., Rossi, F., and Giugliano, D. (2006) The ubiquitin-proteasome system and inflammatory activity in diabetic atherosclerotic plaques: effects of rosiglitazone treatment. *Diabetes* **55**, 622-632.

76. Deng, J., Carlson, N., Takeyama, K., Dal Cin, P., Shipp, M., and Letai, A. (2007) BH3 Profiling Identifies Three Distinct Classes of Apoptotic Blocks to Predict Response to ABT-737 and Conventional Chemotherapeutic Agents. *Cancer Cell* **12**, 171-185.

77. Bugno, M., Daniel, M., Chepelev, N. L., and Willmore, W. G. (2015) Changing gears in Nrf1 research, from mechanisms of regulation to its role in disease and prevention. *Biochim. Biophys. Acta* **1849**, 1260-1276.

78. Sha, Z., and Goldberg, A. L. (2014) Proteasome-mediated processing of Nrf1 is essential for coordinate induction of all proteasome subunits and p97. *Curr. Biol.* **24**, 1573-1583.

79. Kwak, M. K., Cho, J. M., Huang, B., Shin, S., and Kensler, T. W. (2007) Role of increased expression of the proteasome in the protective effects of sulforaphane against hydrogen peroxide-mediated cytotoxicity in murine neuroblastoma cells. *Free Radic. Biol. Med.* **43**, 809-817.

80. Steffen, J., Seeger, M., Koch, A., and Krüger, E. (2010) Proteasomal degradation is transcriptionally controlled by TCF11 via an ERAD-dependent feedback loop. *Mol. Cell.* **40**, 147-158.

81. Radhakrishnan, S. K., Lee, C. S., Young, P., Beskow, A., Chan, J. Y., and Deshaies, R. J. (2010) Transcription factor Nrf1 mediates the proteasome recovery pathway after proteasome inhibition in mammalian cells. *Mol. Cell.* **38**, 17-28.

82. Radhakrishnan, S. K., den Besten, W., and Deshaies, R. J. (2014) p97-dependent retrotranslocation and proteolytic processing govern formation of active Nrf1 upon proteasome inhibition. *Elife* **3**, e01856.

83. Dou, Q. P., and Li, B. (1999) Proteasome inhibitors as potential novel anticancer agents. *Drug Resist. Updat.* **2**, 215-223.

84. Gottesman, S., Wickner, S., and Maurizi, M. R. (1997) Protein quality control: triage by chaperones and proteases. *Genes Dev.* **11**, 815-823.

85. Bence, N. F., Sampat, R. M., and Kopito, R. R. (2001) Impairment of the ubiquitin-proteasome system by protein aggregation. *Science* **292**, 1552-1555.

86. Kazi, A., Daniel, K. G., Smith, D. M., Kumar, N. B., and Dou, Q. P. (2003) Inhibition of the proteasome activity, a novel mechanism associated with the tumor cell apoptosis-inducing ability of genistein. *Biochem. Pharmacol.* **66**, 965-976.

87. Landis-Piwowar, K. R., Milacic, V., Chen, D., Yang, H., Zhao, Y., Chan, T. H., Yan, B., and Dou, Q. P. (2006) The proteasome as a potential target for novel anticancer drugs and chemosensitizers. *Drug Resist. Updat.* **9**, 263-273.

88. Shen, M., Chan, T. H., and Dou, Q. P. (2012) Targeting tumor ubiquitin-proteasome pathway with polyphenols for chemosensitization. *Anticancer Agents Med. Chem.* **12**, 891-901.

89. Chen, D., Daniel, K. G., Chen, M. S., Kuhn, D. J., Landis-Piwowar, K. R., and Dou, Q. P. (2005) Dietary flavonoids as proteasome inhibitors and apoptosis inducers in human leukemia cells. *Biochem. Pharmacol.* **69**, 1421-1432.

90. Shim, S. H. (2011) 20S proteasome inhibitory activity of flavonoids isolated from Spatholobus suberectus. *Phytother. Res.* **25**, 615-618.

91. Akerfelt, M., Trouillet, D., Mezger, V., and Sistonen, L. (2007) Heat shock factors at a crossroad between stress and development. *Ann. N. Y. Acad. Sci.* **1113**, 15-27.

92. Qi, W., White, M. C., Choi, W., Guo, C., Dinney, C., McConkey, D. J., Siefker-Radtke, A. (2013) Inhibition of inducible heat shock protein-70 (hsp72) enhances bortezomib-induced cell death in human bladder cancer cells. *PLoS One* **8**, e69509.

93. Shah, S. P., Lonial, S., and Boise, L. H. (2015) When Cancer Fights Back: Multiple Myeloma, Proteasome Inhibition, and the Heat-Shock Response. *Mol. Cancer Res.* **13**, 1163-1173.

SUPPLEMENTAL DATA RELATED TO THIS ARTICLE

The mass spectrometry proteomics data have been deposited to the ProteomeXchange Consortium via the PRIDE partner repository with the dataset identifier PXD004253.

Reviewer account details:

Username: reviewer60469@ebi.ac.uk

Password: OXSxgvZ8

Supplemental Material Table S1. Identification and quantification of the peptides obtained after MaxQuant data processing.

Supplemental Material Table S2. Identification and quantification of the proteins obtained after MaxQuant data processing.

Supplemental Material Table S3. Expression ratio (Log_2) of all DML-nano LC-MS/MS experiments performed in HT-29 cells after the treatment with different concentrations of CA and CS at different times.

Supplemental Material Table S4. Expression ratio (Log_2) of significant altered proteins (p -value < 0.05) in HT-29 cells after the treatment with different concentrations of CA at different times.

Supplemental Material Table S5. Expression ratio (Log_2) of significant altered proteins (p -value < 0.05) in HT-29 cells after the treatment with different concentrations of CS at different times.

FIGURE LEGENDS

Figure 1. Cell cycle distribution determined by flow cytometry of HT-29 cells incubated with or without TGI concentration of CA or CS for 24 h (* indicates significant differences between the treated and control samples as determined by t-test, $P < 0.05$).

Figure 2. Scheme of the DML method and nano-LC-MS/MS analysis followed for the proteomics study. HT-29 cells were incubated with different concentrations (GI50, TGI, LC50) of two polyphenols (CA, CS) or vehicle, for 2, 6 or 24 h. After protein extraction and enzymatic digestion, peptides from control and treated samples were labeled as “light” and “medium” respectively, and mixed 1:1 prior to nano-LC-MS/MS analysis.

Figure 3. Inhibition of the proteasome activity in HT-29 cells after incubation with TGI concentration of CA or CS for 2, 6 and 24 h. A, 26S proteasome activity; B, 20S proteasome activity. Concentration dependent inhibition of the chymotrypsin-like activity of the purified 20S proteasome. C, Carnosic acid; D, Carnosol; E, MG-132.

.

Table 1. Log_2 ratio of the significantly altered proteins after the incubation of HT-29 cells with GI50, TGI and LC50 concentrations of CA and CS for 2 and 6 hours.

	2h				6h					
	TGI		LC50		GI50		TGI		LC50	
	Gene name	log_2 ratio	Gene name	log_2 ratio	Gene name	log_2 ratio	Gene name	log_2 ratio	Gene name	log_2 ratio
CA	EFHD2	-0.63	SLC25A3	0.59	MISP	-0.61	SDHA	0.80	HMOX1	2.26
							RPS24	0.68	SQSTM1	0.68
							RPS26	0.63		
CS					HMOX1	3.46	HMOX1	3.54	HMOX1	3.04
					HSPA1A	1.22	DNAJB1	1.70	HSPA1A	1.73
					SQSTM1	0.67	HSPA1A	1.53	HSPH1	0.92
					PSMC4	0.63	HSPH1	0.88	SQSTM1	0.91
					POF1B	-0.88	SLC2A1	0.63		
							SLC3A2	0.60		

Table 2. Significantly altered proteins after the incubation of HT-29 cells with GI50, TGI and LC50 concentrations of CA and CS for 24 hours.

Name	CA			CS		
	GI50	TGI	LC50	GI50	TGI	LC50
Antioxidant defence						
GCLC[1]	0.92	1.23	1.29	--	--	--
GCLM[1]	--	1.37	1.53	n.s.	1.11	1.54
TXNRD1[1]	1.08	1.41	1.41	0.85	1.13	1.28
TXN[1]	0.61	n.s.	n.s.	n.s.	n.s.	n.s.
SRXN1[1]	--	--	2.63	--	--	--
MT2A[1]	n.s.	n.s.	1.48	n.s.	n.s.	1.04
NADPH generation						
SLC2A1	n.s.	0.94	n.s.	n.s.	n.s.	n.s.
ME1[1]	0.85	0.91	0.94	n.s.	--	0.91
IDH1[1]	n.s.	n.s.	0.75	n.s.	n.s.	n.s.
PGD[1]	0.69	0.77	0.79	n.s.	n.s.	n.s.
G6PD[1]	n.s.	0.68	n.s.	n.s.	n.s.	n.s.
Detoxification metabolism						
AKR1B10[1]	1.52	1.82	1.61	1.37	1.58	n.s.
AKR1C1	1.83	2.24	2.94	1.79	n.s.	1.30
AKR1C3	1.26	1.37	1.31	n.s.	n.s.	0.71
Ubiquitin-proteasomal degradation						
PSMC1[1]	n.s.	n.s.	n.s.	n.s.	0.73	0.76
PSMC2[1]	n.s.	n.s.	n.s.	n.s.	0.67	0.72
PSMC3[1]	n.s.	n.s.	n.s.	n.s.	0.72	n.s.
PSMC5[1]	n.s.	--	n.s.	n.s.	--	0.87
PSMA4[1]	n.s.	n.s.	n.s.	n.s.	n.s.	0.69
PSMA7[1]	n.s.	n.s.	n.s.	n.s.	0.63	n.s.
PSMD1[1]	n.s.	n.s.	n.s.	--	--	0.62
PSMD2[1]	n.s.	--	--	--	--	0.75
VCP	n.s.	n.s.	n.s.	n.s.	n.s.	0.64
Chaperones						
HSP90AA1	n.s.	n.s.	n.s.	n.s.	0.78	0.81
HSPH1	n.s.	n.s.	n.s.	0.87	0.96	1.33
HSPA1A	n.s.	n.s.	0.68	1.18	1.48	2.29
SQSTM1	1.42	1.78	2.52	1.59	1.74	1.77
Unfolded Protein Response (ERAD)						
SEC61B[2]	n.s.	n.s.	0.83	--	n.s.	n.s.
HYOU1[2]	n.s.	0.59	1.21	n.s.	n.s.	n.s.
SSR1[2]	n.s.	n.s.	0.65	--	--	n.s.
SSR4[2]	n.s.	n.s.	0.64	--	--	n.s.
HSPA5[2,3]	n.s.	0.65	1.21	n.s.	n.s.	0.59
HSP90B1[2,3]	n.s.	n.s.	0.65	n.s.	n.s.	n.s.
HSPA9[2]	n.s.	n.s.	0.59	n.s.	n.s.	n.s.
Unfolded Protein Response (tRNA charging and AAs metabol.)						
AARS[3]	n.s.	0.62	0.96	--	n.s.	n.s.
WARS[3]	0.88	n.s.	1.15	--	--	n.s.
GARS[3]	0.63	0.99	1.21	n.s.	n.s.	n.s.
SARS[3]	n.s.	0.94	1.17	--	--	--
YARS[3]	n.s.	--	0.60	--	--	n.s.
SLC3A2[3]	0.82	1.49	1.78	n.s.	0.72	1.02
SLC1A5[3]	n.s.	n.s.	n.s.	n.s.	0.59	n.s.
ASNS[3]	1.63	--	2.47	--	--	1.62
PSAT1[3]	0.59	0.98	1.09	--	n.s.	0.80
E2F-targets						
RRM1[4]	n.s.	-0.88	--	n.s.	n.s.	n.s.
COPS8[4]	n.s.	-0.71	n.s.	n.s.	n.s.	n.s.
TOP2A[4]	n.s.	-1.33	-2.46	n.s.	n.s.	n.s.
RBBP4[4]	n.s.	n.s.	-0.85	n.s.	n.s.	n.s.
CSDE1[4]	n.s.	n.s.	-0.66	n.s.	n.s.	n.s.
Pyrimidine and purine nucleotides biosynthesis						
CAD	n.s.	n.s.	-0.64	n.s.	-0.67	n.s.
GMPS	n.s.	n.s.	-0.61	n.s.	n.s.	n.s.
HPRT1	n.s.	n.s.	-0.61	--	--	n.s.
DNA replication / cell proliferation						
NASP	n.s.	n.s.	-0.80	n.s.	n.s.	n.s.
NAP1L1	n.s.	n.s.	-0.60	n.s.	n.s.	n.s.
MKI67	n.s.	-1.32	n.s.	--	n.s.	-1.07
SERPINB5	0.60	--	n.s.	--	--	--
Cellular adhesion						
GCNT3	--	--	1.79	--	--	--
CD44	n.s.	n.s.	n.s.	n.s.	n.s.	-0.92
MUC5AC	n.s.	n.s.	n.s.	n.s.	n.s.	-0.69
CNN2	n.s.	-1.04	-1.40	n.s.	n.s.	-1.05
POF1B	n.s.	-0.96	-1.65	n.s.	-0.96	--
Cytoskeleton						
SLC9A3R1	n.s.	n.s.	-0.69	n.s.	n.s.	-0.59
MSN	n.s.	n.s.	n.s.	n.s.	0.64	n.s.
VIL1	n.s.	n.s.	n.s.	n.s.	-0.73	n.s.
TUBA1C	n.s.	n.s.	n.s.	n.s.	--	0.59
Chromatine						
HMGN2	--	n.s.	n.s.	-1.16	--	n.s.
HIST1H2AJ	n.s.	n.s.	n.s.	--	-1.42	n.s.
CBX3	n.s.	n.s.	n.s.	n.s.	n.s.	-0.61
Other functions						
TMEM109	n.s.	n.s.	-0.71	n.s.	n.s.	n.s.
GLG1	n.s.	--	-0.90	n.s.	n.s.	n.s.
TMPO	n.s.	n.s.	-0.65	n.s.	n.s.	n.s.
KPNA2	n.s.	-0.83	-1.19	n.s.	n.s.	n.s.
STMN1	n.s.	-0.65	-0.78	n.s.	n.s.	n.s.
GMDS	-0.60	n.s.	n.s.	--	--	--
HN1L	n.s.	--	n.s.	n.s.	n.s.	-0.69
RAB1A	n.s.	n.s.	n.s.	--	--	-0.97
SLC12A2	--	n.s.	--	--	--	-1.87
ALDH18A1	n.s.	n.s.	-0.59	n.s.	--	-0.66
S100P	n.s.	n.s.	1.40	n.s.	n.s.	n.s.
GFPT1	n.s.	n.s.	1.06	n.s.	n.s.	n.s.
TOP1[3]	n.s.	n.s.	0.60	n.s.	n.s.	n.s.
LRRC59	n.s.	n.s.	0.59	n.s.	n.s.	n.s.
ANXA5	n.s.	n.s.	0.62	n.s.	n.s.	n.s.
GOT1	n.s.	--	0.74	n.s.	n.s.	n.s.
RCN1	0.66	--	n.s.	--	--	n.s.
CAPN2	0.62	--	n.s.	--	--	--
CLIC4	--	--	0.72	--	--	--
UGDH[1]	0.97	1.06	1.06	n.s.	n.s.	n.s.
SERPINH1	--	n.s.	--	--	--	0.87
ACSL5	n.s.	--	--	--	--	0.83
CD59	n.s.	n.s.	n.s.	n.s.	n.s.	0.80
CALB2	n.s.	n.s.	n.s.	0.70	n.s.	n.s.
S100A14	n.s.	n.s.	n.s.	n.s.	0.82	n.s.
C1QBP	n.s.	n.s.	n.s.	--	0.61	n.s.
NAMPT	0.65	1.10	1.41	n.s.	0.93	0.96
SFN	0.61	0.64	1.39	n.s.	1.07	1.23
ANXA1	0.81	1.07	1.52	n.s.	n.s.	0.79
PSAP	0.73	n.s.	1.19	n.s.	n.s.	1.27
RAB10	n.s.	n.s.	0.64	--	n.s.	0.84

Proteins whose expression is regulated by: 1) Nrf2; 2) XBP1; 3) ATF4; 4) E2F1. n.s., not significant

Table 3. Prediction of transcription factors by UR analysis (IPA software) in HT-29 cells treated with GI50, TGI and LC50 concentrations of CA and CS for 24 hours

	GI50			TGI			LC50		
	Transcription regulator	**Z-score**	**P-value**	**Transcription regulator**	**Z-score**	**P-value**	**Transcription regulator**	**Z-score**	**P-value**
CA	NFE2L2	2.889	$7.72 \cdot 10^{-11}$	NFE2L2	3.193	$1.33 \cdot 10^{-12}$	NFE2L2	3.028	$1.80 \cdot 10^{-11}$
				E2F1	-2.000	$5.83 \cdot 10^{-8}$	ATF4	2.611	$3.27 \cdot 10^{-11}$
							XBP1	2.417	$7.52 \cdot 10^{-7}$
CS				NFE2L2	2.756	$1.80 \cdot 10^{-9}$	NFE2L2	2.799	$4.84 \cdot 10^{-11}$

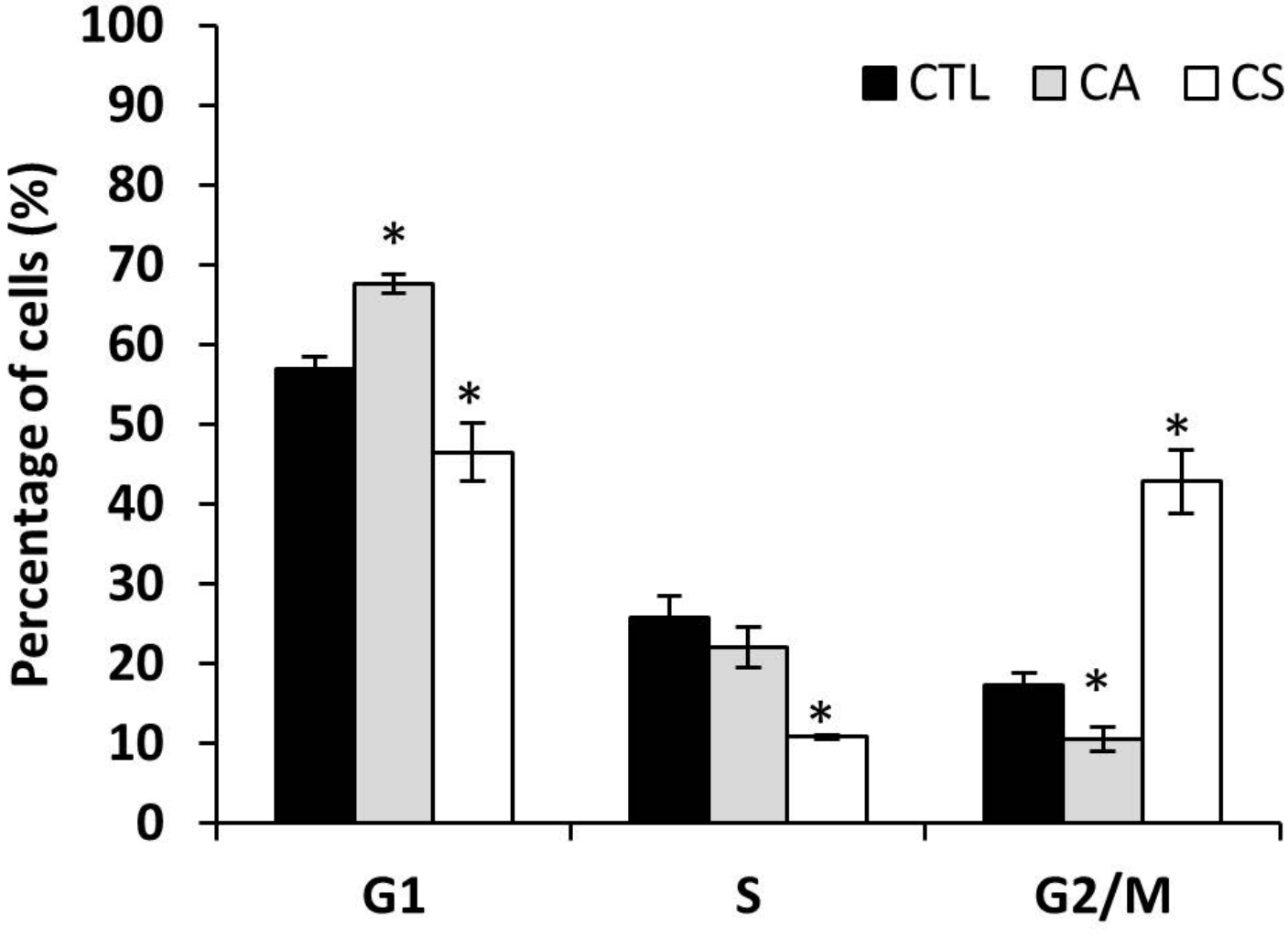
100
90
80
70
60
50
40
30
20
10
0
Percentage of cells (%)
CTL
CA
CS
*
*
*
*
*
G1
S
G2/M

Figure 1

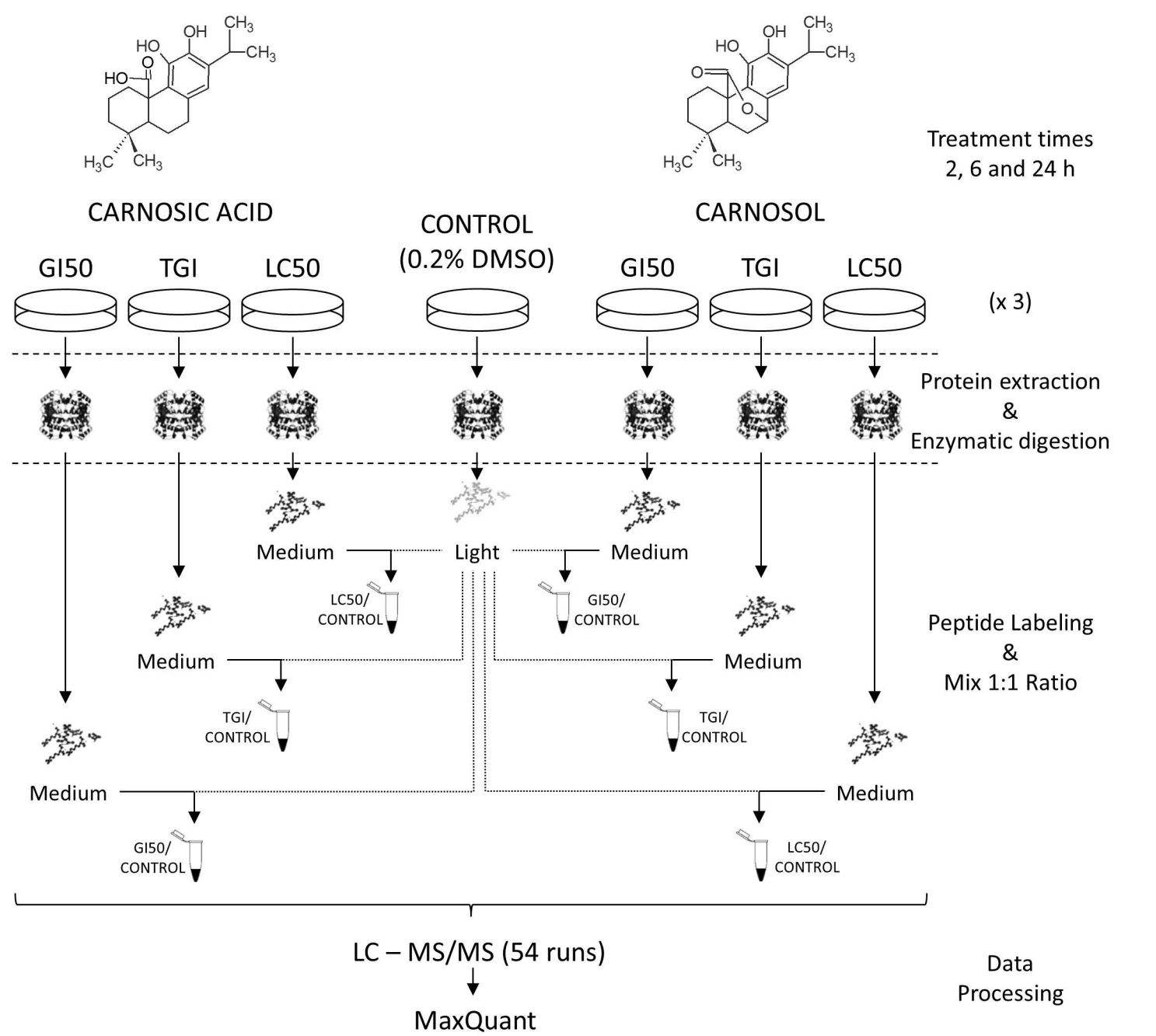
CARNOSIC ACID
CARNOSOL
Treatment times
2, 6 and 24 h
CONTROL
(0.2% DMSO)
GI50
TGI
LC50
GI50
TGI
LC50
(x 3)
Protein extraction
&
Enzymatic digestion
Medium
Light
Medium
LC50/
CONTROL
GI50/
CONTROL
Medium
Medium
TGI/
CONTROL
TGI/
CONTROL
Peptide Labeling
&
Mix 1:1 Ratio
Medium
Medium
GI50/
CONTROL
LC50/
CONTROL
LC – MS/MS (54 runs)
MaxQuant
Data
Processing

Figure 2

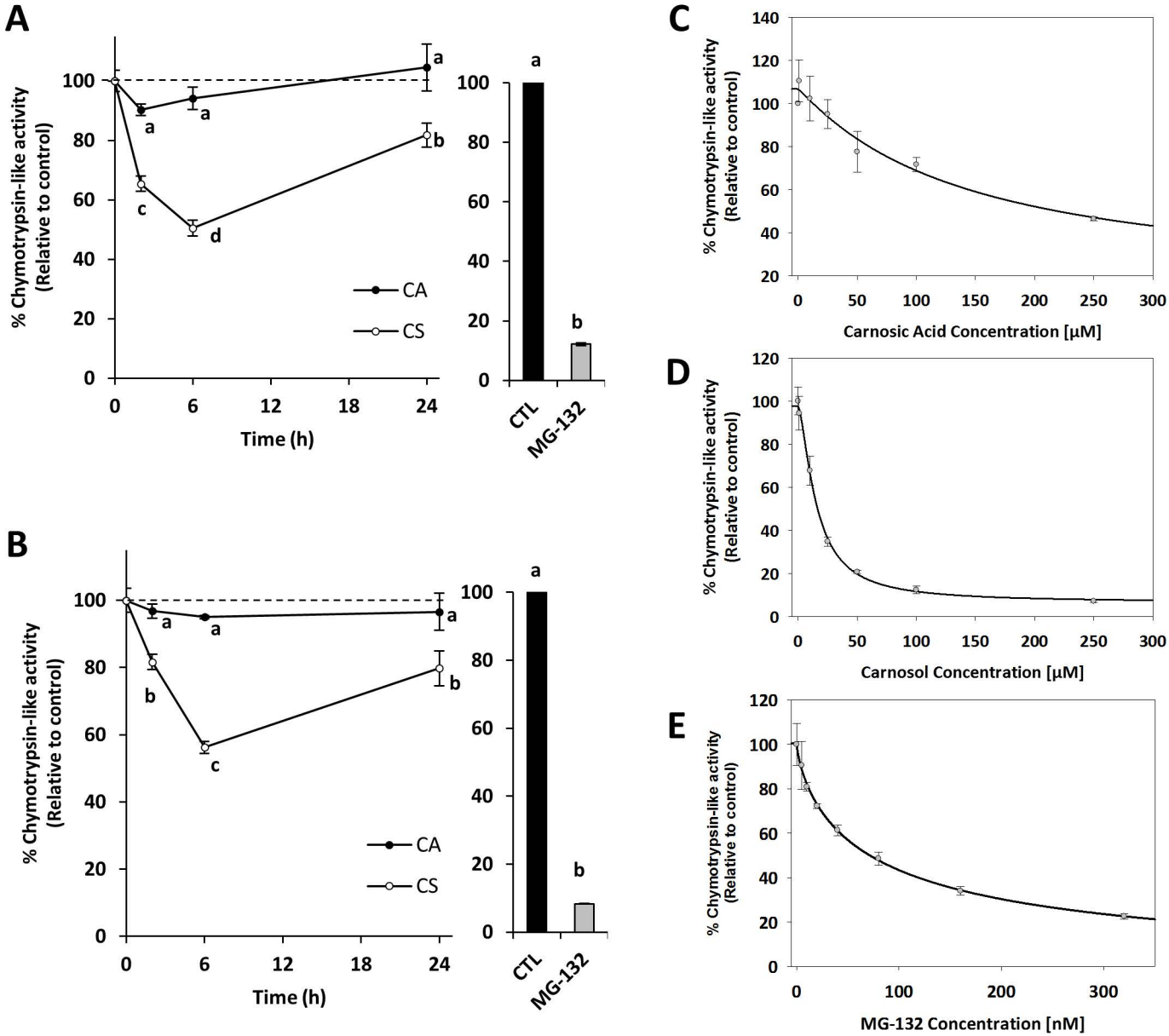
A
% Chymotrypsin-like activity (Relative to control)
Time (h)
CA
CS
CTL
MG-132
B
C
Carnosic Acid Concentration [μM]
D
Carnosol Concentration [μM]
E
MG-132 Concentration [nM]

Figure 3

4. DISCUSIÓN GENERAL

4. DISCUSIÓN GENERAL

Como se ha indicado anteriormente, el objetivo de esta Tesis doctoral es el estudio del efecto antiproliferativo de polifenoles de origen alimentario desde un punto de vista alimentómico. Concretamente, en los trabajos presentados en esta Memoria se han estudiado varios extractos de romero enriquecidos en compuestos fenólicos, así como los polifenoles mayoritarios determinados en los extractos más activos, ácido carnósico y carnosol. Los extractos se seleccionaron de una colección de extractos obtenidos y caracterizados químicamente en el laboratorio en el que se ha desarrollado la presente Tesis doctoral.

4.1. Actividad antiproliferativa de los polifenoles de romero

Los dos estudios iniciales presentados en esta Memoria demuestran que, de todos los extractos de romero ensayados, aquellos obtenidos mediante SFE muestran una actividad antiproliferativa superior, tanto en las líneas celulares de leucemia (sección 3.1.2) como en las líneas de cáncer de colon (sección 3.2.2). En concreto, el extracto de romero obtenido mediante SFE empleando CO_2 a 40 ºC, 150 bares de presión y 7% de etanol es el que presenta un efecto antiproliferativo mayor. Este extracto se caracteriza por su elevado contenido en ácido carnósico (151.5 µg/mg de extracto) y carnosol (226.4 µg/mg de extracto), lo cual aportaría nuevas evidencias del efecto inhibitorio de estos compuestos en la proliferación celular de varios modelos de cáncer. En el caso de las células de leucemia, el efecto antiproliferativo del extracto de romero es más acusado en la línea con el fenotipo sensible (K562) que en la línea resistente a fármacos (K562/R), observándose valores de inhibición de la proliferación de 46 y 74%, respectivamente, en los tratamientos con una

concentración de extracto equivalente a 5 µM de polifenoles totales durante 48 horas (equivalente a 7.03 µg/mL de extracto de romero). En el caso de las células de cáncer de colon, los mayores efectos antiproliferativos se observan tras el tratamiento con una concentración de extracto de 10 µM de polifenoles totales (equivalente a 14.06 µg/mL de extracto de romero), siendo la línea HT-29 más refractaria al efecto inhibitorio del extracto. Estos resultados indican que las células de leucemia son más sensibles al extracto de romero que las células de cáncer de colon y, además, están en consonancia con lo observado en otros estudios realizados con este tipo de compuestos en otras líneas celulares (Guerrero y col., 2006). Varios trabajos publicados en los últimos años también sugieren que el efecto antiproliferativo de los extractos de romero enriquecidos en polifenoles varía considerablemente en función de la composición del extracto y la línea celular ensayada (González-Vallinas y col., 2015a; Petiwala y Johnson, 2015), lo cual indica que tanto el patrón mutacional como el contexto celular podrían influir en la efectividad de estos compuestos para inhibir la proliferación celular

Para el desarrollo de los trabajos de las secciones 3.2.3-3.2.7, fue necesaria la preparación de un nuevo extracto de romero en las mismas condiciones de extracción, pero utilizando un equipo de SFE que permite escalar el proceso de extracción. Es preciso indicar que el nuevo extracto mostró algunas diferencias en composición con respecto al primer extracto, como por ejemplo el contenido en ácido carnósico (256.0 y 151.5 µg/mg de extracto, respectivamente) y carnosol (37.1 y 226.4 µg/mg de extracto, respectivamente). El trabajo recogido en la sección 3.2.3 de la Memoria permitió confirmar la actividad antiproliferativa del nuevo extracto en la línea HT-29 y, además, se observó que la actividad del extracto era superior a la de cualquiera de sus constituyentes mayoritarios, ácido carnósico y carnosol. Este estudio permitió determinar que el ácido carnósico y el carnosol presentan actividad antiproliferativa dependiente del tiempo y de la

concentración y que, dada su abundancia en el extracto y actividad, el ácido carnósico es el principal responsable de la actividad del extracto. Además, el estudio de los posibles efectos sinérgicos, antagónicos y aditivos indicó que ambos diterpenos tienen un efecto aditivo en la proporción a la que se encuentran en el extracto y que la suma de ambos no puede explicar la totalidad del efecto observado con el extracto de romero. Estos resultados sugieren que además de los dos diterpenos mayoritarios, existen otros compuestos en el extracto de romero que pueden tener efectos antiproliferativos aditivos o sinérgicos y que, por tanto, pueden contribuir a la actividad antiproliferativa del extracto de romero.

4.2 Efecto de los polifenoles de romero en el ciclo celular

Los resultados presentados en esta Tesis doctoral también demuestran que los polifenoles de romero presentan actividad citostática en los tipos celulares estudiados, ya que bloquean la progresión del ciclo celular en algunas de sus fases (secciones 3.1.2 y 3.2.2). En general, el bloqueo del ciclo celular varía en función del tipo celular, el tipo de polifenol (extracto de romero, ácido carnósico y carnosol), la concentración, y el tiempo de incubación (secciones 3.1.2, 3.2.2, 3.2.3, 3.2.5 y 3.2.7). En el caso de las dos líneas celulares de leucemia, el bloqueo se observa en la fase G2/M del ciclo celular con una concentración de 5 μM de polifenoles totales a las 48 horas de tratamiento, indicando que el primer extracto de romero estudiado en esta Tesis doctoral ejerce un efecto citostático similar en ambas líneas. En el caso de las líneas de cáncer de colon, el mismo extracto induce la parada del ciclo en la fase G2/M a una concentración de 10 μM de polifenoles totales. La línea HT-29, además de ser más refractaria al efecto del extracto que la línea SW480, mostró un bloqueo más tardío (72 h vs. 24 h) del ciclo celular en respuesta al extracto. Por otro lado, el segundo extracto de romero (con un mayor contenido en ácido

carnósico y un menor contenido en carnosol), mostró un efecto citostático notablemente diferente al observado con el primer extracto. Por ejemplo, concentraciones del segundo extracto próximas a la TGI (26.3 µg/mL) indujeron un bloqueo las células HT-29 en la fase G1 del ciclo celular en tan solo 24 horas de tratamiento (sección 3.2.3), mientras que una concentración superior a la LC50 (38.7 µg/mL) bloqueó la progresión del ciclo celular en la fase G2/M (sección 3.2.5). Estas diferencias observadas en relación al efecto citostático del extracto sugieren la activación de mecanismos y respuestas celulares distintos en función de la concentración de extracto empleada. En línea con nuestras observaciones, Visanji y col. (2006), y más recientemente, Einbond y col. (2012) han descrito diferencias en el efecto citostático de algunos polifenoles de romero en función del modelo celular empleado. Además, es necesario indicar que las discrepancias encontradas en cuanto al efecto en el ciclo celular de los dos extractos de romero utilizados en el desarrollo de esta Tesis doctoral pueden deberse a las diferencias observadas en la composición química de los extractos. Dada su superior actividad antiproliferativa, especialmente en la línea de cáncer de colon HT-29, se seleccionó el segundo extracto, enriquecido en ácido carnósico, para continuar el desarrollo de los trabajos de esta Tesis. El estudio del ciclo celular de las células HT-29 también indicó diferencias entre los polifenoles principales en el extracto, ácido carnósico y carnosol. Mientras que una concentración de ácido carnósico equivalente a la TGI (47.7 µg/mL) bloqueó las células en la fase G1, una concentración de carnosol con un efecto inhibitorio similar (52.7 µg/mL) bloqueó las células en G2/M (sección 3.2.7).

4.3 Activación de la *Respuesta al Estrés Oxidativo*

La adopción de la estrategia Alimentómica en esta Tesis doctoral ha permitido obtener una visión global del efecto de los polifenoles de romero frente a varios tipos

celulares de cáncer a nivel molecular. Una de las observaciones más frecuentes en todos los estudios ómicos llevados a cabo es la alteración de la expresión de genes, proteínas y metabolitos relacionados con la *Respuesta al Estrés Oxidativo* en respuesta al tratamiento con polifenoles de romero. La *Respuesta al Estrés Oxidativo* está gobernada a nivel transcripcional por el factor de transcripción NRF2 (Gorrini y col., 2013) (ver Figuras 4.1 y 4.2). En condiciones normales, el factor de transcripción NRF2 se encuentra unido a la proteína KEAP1 en el citoplasma, que favorece su ubiquitinación y posterior degradación por el proteasoma. Sin embargo, cuando se produce una situación de estrés oxidativo, la proteína KEAP1 se oxida y se disocia de NRF2, permitiendo que éste último se transloque al núcleo y se una a las secuencias ARE de los promotores de un gran número de genes efectores. El factor NRF2 controla la expresión de: 1) genes involucrados en la respuesta antioxidante, como por ejemplo, los genes que codifican para proteínas antioxidantes (SRXN1, TXNRD1) y proteínas que regulan la síntesis, regeneración y utilización de glutatión (GCLC, GCLM, GSR1); 2) genes que codifican para proteínas implicadas en procesos de detoxificación, como por ejemplo, los genes que codifican para enzimas de fase I (AKR1C1, NQO1) y de fase II (GSTM1, GSTP1); y 3) genes que codifican para proteínas involucradas en la generación de potencial reductor, como por ejemplo, las que regeneran NADPH (G6PD, IDH1, ME1) (Hayes y Dinkova-Kostova, 2014).

Se ha demostrado que el ácido carnósico (en su forma quinona) interacciona mediante una reacción de S-alquilación con un residuo de cisteína de la proteína KEAP1, permitiendo la liberación de NRF2, y su translocación al núcleo (Satoh y col., 2008). Los resultados presentados en esta Tesis doctoral demuestran que tanto el extracto de romero (en las células de leucemia y cáncer de colon), como el ácido carnósico y el carnosol (en las células HT-29 de cáncer de colon), activan la respuesta transcripcional mediada por NRF2. Los resultados del análisis causal (de factores de transcripción) de los datos

transcriptómicos y proteómicos efectuado con la herramienta bioinformática IPA indican que la activación de NRF2 depende de la composición fenólica (extracto de romero, ácido carnósico o carnosol), de la concentración y del tiempo ensayado. Además, los resultados del análisis proteómico han permitido corroborar que el extracto de romero y el ácido carnósico inducen la activación de NRF2, observándose un máximo en la expresión de proteínas reguladas por NRF2 a las 24 horas. Sin embargo, comparativamente y en base a la expresión relativa de las proteínas controladas por NRF2, la activación de NRF2 producida por el ácido carnósico es menos intensa a la producida por el extracto de romero. El análisis proteómico también nos ha permitido establecer que la activación de NRF2 tras el tratamiento con carnosol sigue un patrón diferente, mostrando un máximo de inducción prematuro (6 horas) de la expresión de las proteínas reguladas por NRF2. Además, los resultados también indican que, en general, el extracto de romero y el ácido carnósico inducen cambios más evidentes en la expresión de proteínas relacionadas con la respuesta antioxidante, con procesos de detoxificación y con la generación de potencial reductor que el carnosol.

Los resultados obtenidos en los estudios metabolómicos también aportan información de gran utilidad, demostrando que los polifenoles de romero inducen cambios en los niveles del antioxidante endógeno glutatión, cuya síntesis está regulada transcripcionalmente por NRF2. El glutatión es el principal metabolito antioxidante intracelular y juega un papel fundamental en la defensa celular frente a las especies reactivas del oxígeno. Como se muestra en los resultados de la sección 3.2.5, la inhibición de su síntesis mediante la pre-incubación con el fármaco BSO sensibilizó las células HT-29 de cáncer de colon frente al extracto de romero. Estos resultados corroboran la activación de la *Respuesta al Estrés Oxidativo* tras el tratamiento con el extracto de romero,

e indican que el glutatión es un metabolito esencial en la respuesta adaptativa de las células tratadas con el extracto de romero.

Además de la activación de NRF2 mediada por la interacción del ácido carnósico con KEAP1, existen otros mecanismos moleculares que regulan la activación de NRF2 y, por consiguiente, la transcripción de sus genes efectores. Concretamente, la activación de la *Respuesta a Proteínas Desplegadas*, la inducción de la proteína p62 (SQSTM1, sequestosoma) y la inhibición del complejo macromolecular denominado proteasoma, regulan positivamente la activación de NRF2. La conexión entre estos procesos y NRF2 se discutirá en las secciones siguientes.

4.4 Activación de la *Respuesta a Proteínas Desplegadas*

La *Respuesta a Proteínas Desplegadas* es un proceso adaptativo y coordinado que la célula activa cuando se produce un desequilibrio entre la cantidad de proteínas desplegadas y la capacidad de degradación y plegamiento del retículo endoplasmático. La activación de esta respuesta está mediada por tres proteínas que actúan como sensores de proteínas mal plegadas en la membrana del retículo endoplasmático y activan tres rutas distintas que a su vez están interconectadas (Boyce y Yuan, 2006) (ver Figuras 4.1 y 4.2). La primera ruta es la iniciada por la proteína PERK. La activación de PERK se ha relacionado con la activación de EIF2A, un factor de transcripción que regula negativamente la síntesis proteica (Harding y col., 1999). El factor de transcripción EIF2A también se ha relacionado con la activación del factor de transcripción ATF4, que junto con DDIT3 controla la expresión de un número importante de genes relacionados con el transporte y el metabolismo de aminoácidos (Han y col., 2013a). La segunda ruta es la iniciada por la proteína ERN1, una proteína transmembrana que tiene un dominio sensor

dirigido hacia el retículo endoplasmático y un dominio con actividad endoribonucleasa dirigido al citosol (Zhang y Kaufman, 2004). La activación de ERN1 desencadena la activación XBP1, un factor de transcripción que regula la expresión de genes que codifican para proteínas chaperonas (proteínas de plegamiento). La tercera ruta está controlada por la proteína ATF6. Esta proteína transmembrana también tiene un dominio sensor dirigido hacia el retículo endoplasmático, y cuando se activa, permite que sea transportada al Golgi para su procesado. Una vez procesada, la proteína ATF6 se transloca al núcleo, donde induce la expresión de XBP1 y de otras proteínas con capacidad degradativa. Todos estos cambios moleculares desencadenados por la *Respuesta a Proteínas Desplegadas* tienen como objetivo el restablecimiento de la homeostasis proteica (o proteostasis) en el retículo endoplasmático. Para ello, los primeros efectos derivados de la activación de esta respuesta adaptativa son la reducción de la tasa de traducción de proteínas, y el aumento de la capacidad degradativa y de plegamiento de proteínas del retículo endoplasmático. Como se ha mencionado anteriormente, un efecto interesante de la *Respuesta a Proteínas Desplegadas* es la activación del factor NRF2. Algunos estudios han demostrado que la proteína PERK tiene la capacidad de fosforilar NRF2, lo que permite su disociación de la proteína KEAP1 y su translocación al núcleo (Cullinan y col., 2003).

Los resultados transcriptómicos y proteómicos obtenidos en esta Tesis doctoral demuestran que el extracto de romero y el ácido carnósico inducen la activación de la *Respuesta a Proteínas Desplegadas* en las células HT-29 durante las primeras 24 horas de tratamiento. Esto se puede deducir de la inducción de un número significativo de transcritos y proteínas específicamente asociadas con la activación de PERK y ERN1. Concretamente, los datos transcriptómicos obtenidos del análisis con microarrays de expresión génica y confirmados mediante RT-qPCR, indican que el extracto de romero y el ácido carnósico inducen significativamente la expresión de los genes PPP1R15A y DDIT3 (relacionados

con la activación de PERK), y ERN1 y XBP1 (relacionados con la activación de ERN1). Además, el análisis de los patrones temporales de expresión de estos genes mediante RT-qPCR indica que tanto el extracto de romero, como el ácido carnósico inducen la expresión temprana (6 horas) de la *Respuesta a Proteínas Desplegadas*. En cuanto a la expresión de los genes relacionados con la activación de ERN1, los análisis demuestran que la expresión de ERN1 y XBP1 es máxima a las 12 horas, siendo mayor la expresión tras el tratamiento con el extracto de romero. Por otro lado, los datos proteómicos además de corroborar que el extracto y el ácido carnósico activan la *Respuesta a Proteínas Desplegadas*, revelan diferencias interesantes en la respuesta celular frente a los distintos polifenoles. El extracto de romero y el ácido carnósico inducen la expresión de proteínas del retículo endoplasmático cuyo papel es asistir en el plegamiento de las proteínas translocadas (como, por ejemplo, HYOU1, HSPA9 y HSP90B1), mientras que con el carnosol no se observa este efecto. Estos datos sugieren que únicamente el extracto de romero y el ácido carnósico desencadenan la activación de la *Respuesta a Proteínas Desplegadas* para recuperar la homeostasis en el retículo endoplasmático.

Además, el análisis de los patrones de expresión de marcadores moleculares de la *Respuesta a Proteínas Desplegadas* y la *Respuesta al Estrés Oxidativo* indicó que ambas respuestas siguen una dinámica de activación similar en cada uno de los tratamientos con polifenoles, lo que sugiere que la *Respuesta a Proteínas Desplegadas* podría contribuir significativamente en la activación de NRF2. Generalmente, la activación de la *Respuesta a Proteínas Desplegadas* está asociada al estrés en el retículo endoplasmático, y se ha demostrado que los cambios en los niveles de las especies reactivas del oxígeno intracelulares pueden inducir este estrés (Cao y Kaufman, 2014). Algunos trabajos publicados recientemente sugieren que el ácido carnósico induce estrés en el retículo endoplasmático como consecuencia de la generación de especies reactivas del oxígeno, y

atribuyen su actividad antiproliferativa a este efecto (Min y col., 2014). Los resultados presentados en esta Tesis doctoral demuestran que el extracto de romero, y en menor medida el ácido carnósico, presentan efecto prooxidativo ya que inducen la generación de especies reactivas del oxígeno al inicio del tratamiento, aunque los niveles se restablecen a las 12 horas de tratamiento. En la bibliografía, numerosos estudios atribuyen la actividad antiproliferativa de los compuestos fenólicos a su actividad prooxidante (Saeidnia y Abdollahi, 2013). Sin embargo, un número importante de trabajos científicos también sugieren que en algunos casos la actividad antiproliferativa de algunos polifenoles de plantas (como por ejemplo el ácido gálico o el resveratrol) podría ser un resultado artefactual consecuencia de la propia autooxidación de polifenol en el medio de cultivo, generando niveles de especies del oxígeno reactivas que pueden llegar a ser tóxicos (Long y col., 2010; Forester y Lambert, 2011).

Dada la posible implicación de las especies reactivas del oxígeno en la activación de la *Respuesta a Proteínas Desplegadas* y de la *Respuesta al Estrés Oxidativo*, y la posibilidad de que éstas fueran producto de la autooxidación de los polifenoles en el medio de cultivo, resultó pertinente estudiar este fenómeno. Los resultados del estudio indicaron que tanto el extracto de romero como el ácido carnósico inducen la generación de peróxido de hidrógeno en el medio extracelular, y que al menos parte del peróxido de hidrógeno está relacionado con la generación intracelular de las especies reactivas del oxígeno. Sin embargo, este trabajo también demuestra que el peróxido de hidrógeno del medio de cultivo no interfiere en la expresión de algunos marcadores moleculares involucrados en la *Respuesta al Estrés Oxidativo* y la *Respuesta a Proteínas Desplegadas*, por lo que se puede descartar la generación de peróxido de hidrógeno y de las especies reactivas del oxígeno como desencadenantes de estas respuestas.

4.5 Cambios en los niveles del colesterol

Además de activar la *Respuesta a Proteínas Desplegadas*, el estrés en el retículo endoplasmático puede inducir la activación de los factores de transcripción SREBP1 y SREBP2, relacionados con el metabolismo de lípidos (Rutkowski y col., 2008). La alteración del metabolismo de lípidos es una característica frecuente durante los procesos de reprogramación metabólica en células de cáncer, y un requisito para mantener la tasa de proliferación elevada. Los análisis transcriptómicos iniciales llevados a cabo en las líneas de cáncer de colon tratadas con extracto de romero y ácido carnósico indican que el extracto de romero altera la expresión de varios genes relacionados con el metabolismo del colesterol (sección 3.2.2). Por ello, resultó interesante determinar si los cambios observados en el transcriptoma en respuesta a los tratamientos también se traducían en cambios en los niveles de colesterol. Los resultados del análisis de colesterol libre y colesterol total realizado mediante GC-MS (sección 3.2.4) indican que el extracto de romero, y en menor medida el ácido carnósico, inducen un aumento de los niveles de colesterol total en las células HT-29 de cáncer de colon a partir de las primeras 24 horas de incubación. Con el objetivo de identificar el mecanismo molecular por el cual se producen los cambios observados en los niveles de colesterol, se llevó a cabo un estudio transcriptómico en células HT-29 tratadas durante 24 horas con el extracto y ácido carnósico. El análisis causal llevado a cabo con la herramienta IPA reveló que ambos tratamientos inducen la activación de los factores de transcripción SREBP1 y SREBP2. Sin embargo, el análisis mediante RT-qPCR de la expresión del gen HMGCR, controlado por SREBP2 y con un papel clave en la síntesis de colesterol, indicó que los tratamientos no inducen cambios significativos a nivel transcripcional en genes de síntesis de colesterol. Por otro lado, el estudio de los patrones temporales de expresión de otros genes también asociados al metabolismo del colesterol y controlados por otros factores de transcripción, indica que el extracto de romero

y en menor medida el ácido carnósico inducen un cambio significativo en la expresión del gen VLDLR. El producto de este gen es el receptor de la lipoproteína de muy baja densidad, y dada su implicación en la absorción de colesterol, podría ser el responsable de la acumulación del colesterol en las células tratadas con el extracto y el ácido carnósico.

4.6 Mantenimiento de la homeostasis proteica

La *Respuesta a Proteínas Desplegadas* también implica la activación de mecanismos degradativos específicos, como por ejemplo el sistema ERAD (del inglés, *Endoplasmic-Reticulum-Associated Protein Degradation*) que permiten restablecer la homeostasis en el retículo endoplasmático (Lafleur y col., 2013). Este sistema ERAD se activa cuando las chaperonas del retículo endoplasmático, proteínas encargadas del plegamiento de las proteínas desplegadas, son incapaces de restaurar la proteostasis. El proceso general de degradación consiste en la retrotranslocación de las proteínas desplegadas del retículo al citoplasma, su marcaje con la proteína ubiquitina para su degradación final a través de un complejo macromolecular, denominado proteasoma (Lafleur y col., 2013). Cuando las proteínas desplegadas se acumulan en el retículo endoplasmático, se puede producir una acumulación de proteínas desplegadas en el citoplasma que puede superar la capacidad degradativa del proteasoma con el consiguiente efecto tóxico. Otro mecanismo celular que permite mitigar el estrés proteotóxico consiste en la agregación de las proteínas ubiquitinadas que no son degradadas por el proteasoma en complejos proteicos denominados agresomas, que pueden después ser eliminados del citoplasma celular mediante autofagia (Garcia-Mata y col., 2002). Recientemente, una serie de estudios sugieren que la proteína SQSTM1 participa activamente en la selección de sustratos proteicos para su posterior transferencia a agresomas y autofagosomas para su

posterior degradación (Korolchuk y col., 2010). Además, algunos estudios sugieren que la inducción de la expresión de esta proteína refleja el aumento del flujo autofágico y la eliminación de agregados tóxicos del citoplasma (Paine y col., 2005). La autofagia es un mecanismo de degradación global que permite a la célula eliminar porciones grandes del citoplasma (incluyendo proteínas citosólicas, agregados de proteínas y orgánulos) mediante su encapsulamiento en autofagosomas, y su eliminación posterior mediante los lisosomas. En los últimos años se ha demostrado que la autofagia es un proceso selectivo y regulado (Johansen y Lamark, 2011).

Los resultados de los análisis transcriptómicos efectuados en esta Tesis doctoral demuestran que el extracto de romero y el ácido carnósico inducen la expresión de SQSTM1 (sección 3.2.4). Además, los estudios proteómicos confirman esta observación (secciones 3.2.6 y 3.2.7), lo cual podría indicar que las células activan la autofagia en respuesta al tratamiento con el extracto de romero y el ácido carnósico. El estudio de inhibición de la autofagia con el inhibidor cloroquina y el co-tratamiento con el extracto de romero, permitió confirmar esta hipótesis y observar que la inhibición de la autofagia sensibiliza las células HT-29 frente al extracto, lo cual es indicativo de que la autofagia se activa en las células tratadas como mecanismo adaptativo. Por otro lado, el análisis de la formación de agresomas en células tratadas indicó que, en contra de lo esperado, la formación de agresomas disminuye en respuesta tanto al tratamiento con romero como al co-tratamiento con cloroquina, lo cual descarta la activación de formación de agresomas como posible vía de eliminación de proteínas desplegadas del citoplasma.

Algunos estudios recientes evidencian que la proteína SQSTM1, además de tener una función clave en los mecanismos de formación de agresomas y degradación por autofagia, tiene un papel fundamental en la regulación de la activación del factor NRF2 y, por consiguiente, de la *Respuesta al Estrés Oxidativo.* Su expresión está regulada

transcripcionalmente por NRF2, pero además, SQSTM1 tiene la capacidad de interaccionar con la proteína KEAP1 y dirigirla hacia el autofagosoma para su degradación mediante autofagia (ver Figuras 4.1 y 4.2). Este proceso genera un circuito de retroalimentación positiva que mantiene activado NRF2 y, en consecuencia, se produce una inducción de la expresión génica sostenida de los genes de la *Respuesta al Estrés Oxidativo* (Jiang y col., 2015). Recientemente, Dodson y col (2015) han demostrado que la activación prolongada del factor NRF2 por este mecanismo se ha asociado con el aumento excesivo de NADPH y glutatión, que desencadena proteotoxicidad y efectos adversos. Es interesante mencionar que los datos proteómicos indican que las células tratadas con el extracto de romero y el ácido carnósico mantienen elevados los niveles de expresión de varias proteínas involucradas en la generación de potencial reductor (como, por ejemplo, ME1, UGDH y IDH1), la proteína SQSTM1, y de un número importante de proteínas también controladas por NRF2 después de 24 horas de tratamiento. Esta observación sirve de base para formular una nueva hipótesis, todavía sin demostrar, que considera la posibilidad de que la activación excesiva y sostenida de NRF2 por los polifenoles cause un estrés reductivo y un efecto proteotóxico en la célula.

El proteasoma (o proteasoma 26S) es un complejo multi-enzimático que está implicado, entre otros procesos celulares, en el replegamiento y la degradación de proteínas no funcionales (Glickman y Ciechanover, 2002). Este complejo está formado por dos unidades, la unidad 20S (o catalítica), y la unidad 19S (o reguladora). La unidad 19S (o proteasoma 19S) esta a su vez dividida en dos regiones, la "tapa" (encargada del reconocimiento y la transferencia de las proteínas poliubiquitinadas a la unidad 20S), y la "base" (responsable del desplegamiento de las proteínas y la linearización). La unidad 20S también puede encontrarse de forma libre en el citoplasma (denominándose proteasoma 20S), y se ha demostrado que su actividad es independiente de ATP y más estable en

condiciones de estrés oxidativo que la actividad del 26S (Ben-Nissan y Sharon, 2014). Tanto la unidad 19S como la 20S están formadas por subunidades que están reguladas transcripcionalmente por NRF2, lo que refleja la estrecha relación entre los mecanismos de degradación de la célula y la *Respuesta al Estrés Oxidativo*. Además de NRF2, el factor de transcripción NRF1 también regula transcripcionalmente la expresión de las subunidades del proteasoma y otras proteínas, como por ejemplo VCP, que juega un papel importante en el procesado y la translocación de NRF1 al núcleo (ver Figuras 4.1 y 4.2).

Los datos obtenidos del análisis proteómico que se presentan en esta Memoria demuestran que el carnosol induce la expresión de varias subunidades del proteasoma y de la proteína VCP. Estos resultados sugieren que el carnosol induce la activación del factor NRF1. Recientemente, los trabajos de Radhakrishnan y col. (2014) y Sha y Goldberg (2014), demuestran que NRF1 se activa cuando se produce una inhibición parcial del proteasoma. Los resultados del estudio de la inhibición *in vitro* del proteasoma confirman que el carnosol (pero no el ácido carnósico) disminuye la actividad del proteasoma de las células HT-29. Además, también se ha podido demostrar por primera vez que el carnosol inhibe de forma directa la actividad catalítica del proteasoma 20S. La inhibición del proteasoma se ha asociado con el bloqueo de las células en la fase G2/M (Adams, 2004), un efecto que también se observa en el estudio del ciclo celular en células tratadas con carnosol.

4.7 Regulación de E2F1

El estrés en el retículo endoplasmático y la activación de la *Respuesta a Proteínas Desplegadas* también se han relacionado con el bloqueo en la fase G1 del ciclo celular de varias líneas de cáncer (Brewer y col., 1999; Puthalakath y col., 2007). La regulación del

ciclo celular es muy compleja y en ella participan numerosos factores de transcripción como, por ejemplo, la familia de factores de transcripción E2F. Aunque estos factores están involucrados en varios procesos celulares, su función más conocida es la regulación transcripcional de genes implicados en la transición G1-S y en la replicación del DNA (Wong y col., 2011). Por ejemplo, el factor de transcripción E2F1 controla la expresión del gen RBBP4 (implicado en la progresión del ciclo celular) y de los genes RRM1 y TOP2A (implicados en la síntesis de DNA). Al igual que el resto de los factores E2F, E2F1 está regulado principalmente por el supresor tumoral RB (retinoblastoma). Un artículo publicado recientemente ha demostrado que la *Respuesta a Proteínas Desplegadas* regula negativamente la actividad de E2F1 con el consiguiente efecto en la progresión del ciclo celular (Pagliarini y col., 2015) (ver Figuras 4.1 y 4.2).

En esta Tesis doctoral, los resultados del análisis causal de los datos transcriptómicos indican que el extracto de romero y el ácido carnósico inactivan E2F1 tras 24 horas. Esta predicción se apoya en que el extracto de romero y el ácido carnósico inhiben la expresión de algunos genes controlados por E2F1 como, por ejemplo, RRM1, TOP2A y RBBP4. Además, el estudio proteómico ha permitido confirmar que las proteínas codificadas por estos genes se reprimen con el extracto de romero y con el ácido carnósico, pero no con el carnosol. Estos resultados sugieren que la inactivación de E2F1 en respuesta a los tratamientos con el extracto de romero y el ácido carnósico podría estar regulada por la *Respuesta a Proteínas Desplegadas*, permitiendo establecer un nexo de unión entre la *Respuesta a Proteínas Desplegadas* y el efecto cistostático observado en las células HT-29.

4.8 Otros efectos: adhesión celular, citoesqueleto y metabolismo de poliaminas

Además de los efectos ya comentados, las estrategias Alimentómicas adoptadas en estos trabajos también revelan que los polifenoles de romero ejercen otros cambios a nivel molecular. Por ejemplo, los datos proteómicos indican que el ácido carnósico induce la expresión de la proteína GCNT-3, una proteína involucrada en los procesos de adhesión e invasión celular de las células de cáncer de colon (Huang y col., 2006). Esta proteína está poco expresada en las células de cáncer de colon y se ha demostrado que su inducción reduce la proliferación celular. Además, un estudio reciente ha relacionado la inducción de GCNT3 con el efecto antiproliferativo de un extracto de romero enriquecido en ácido carnósico (González-Vallinas y col., 2015b). Los datos proteómicos también demuestran que la expresión de la proteína SLC9A3R1 disminuye con el tratamiento con ácido carnósico y con carnosol. Esta proteína permite que otras proteínas como, por ejemplo, el factor de crecimiento epidérmico, se mantengan unidas a la membrana plasmática mediante su unión con las proteínas del citoesqueleto. La represión de SLC9A3R1 bloquea la actividad del factor de crecimiento epidérmico, ya que impide la liberación de las señales de crecimiento, por lo que su represión se ha relacionado con la disminución de la proliferación de las células HT-29 (Kruger y col., 2013). Los estudios metabolómicos y transcriptómicos también revelan que los polifenoles del romero alteran el metabolismo de las poliaminas. El metabolismo de las poliaminas está relacionado, entre otros procesos, con la proliferación celular (Thomas y Thomas, 2003), y se ha demostrado que la alteración de los niveles de estos metabolitos puede tener efectos citostáticos en las células HT-29 (Witherspoon y col., 2013). El análisis metabolómico indica que el tratamiento de las células HT-29 con ácido carnósico reduce los niveles de N-acetilputrescina, N-acetilcadaverina y ácido-γ-butírico, y el estudio transcriptómico demuestra que este

polifenol induce la expresión de los genes MAOB y ALDH1A3. La disminución de N-acetilputrescina podría estar explicada por la inducción de los genes MAOB y ALDH1A3 (involucrados en su degradación). Por un lado, la N-acetilputrescina puede transformarse en 4-acetamidobutanal mediante la proteína MAOB. Este nuevo metabolito puede, a su vez, transformarse en 4-acetamidobutanoato mediante la proteína ALDH1A3.

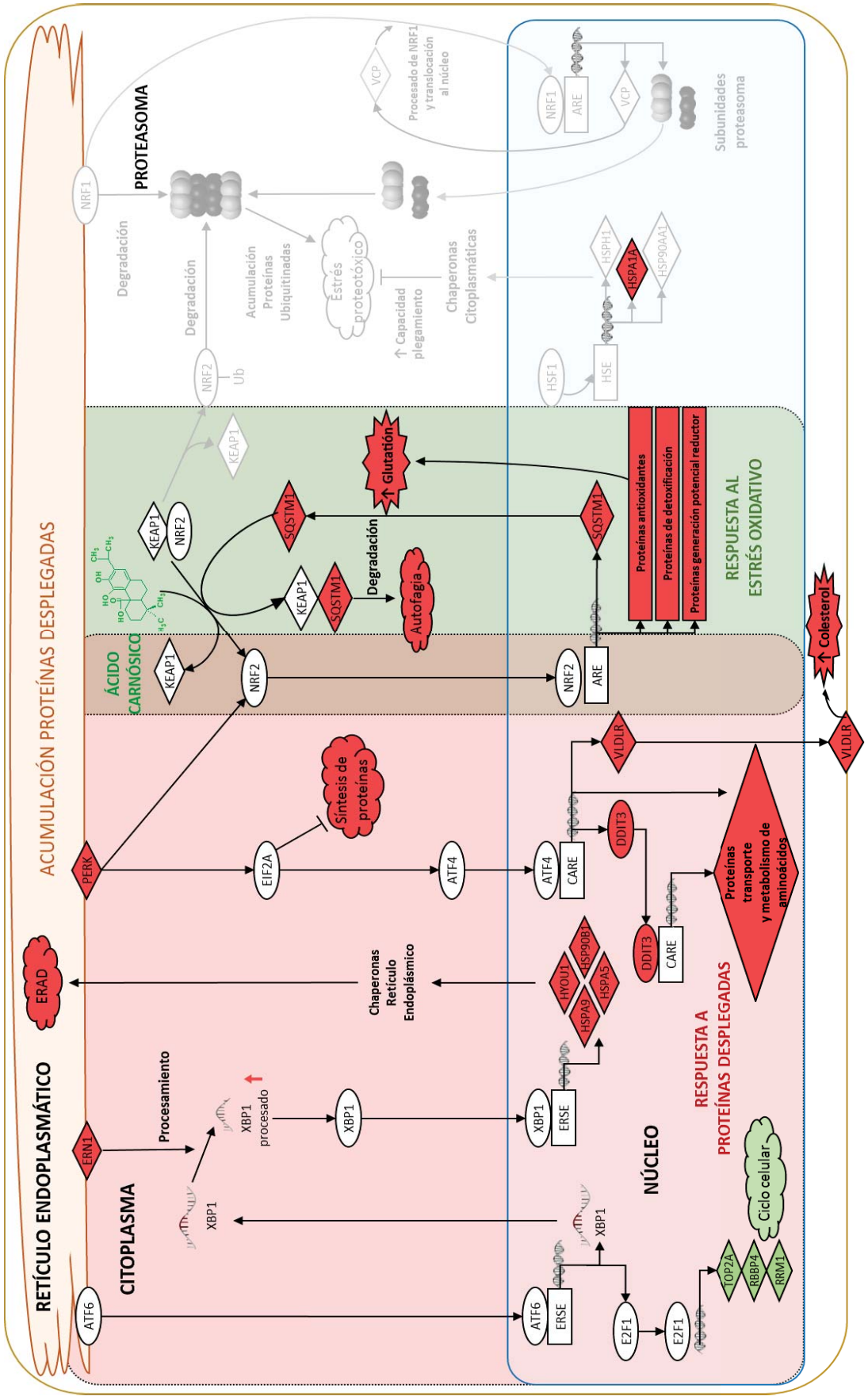

Figura 4.1 Esquema de los efectos producidos a nivel molecular por el ácido carnósico.

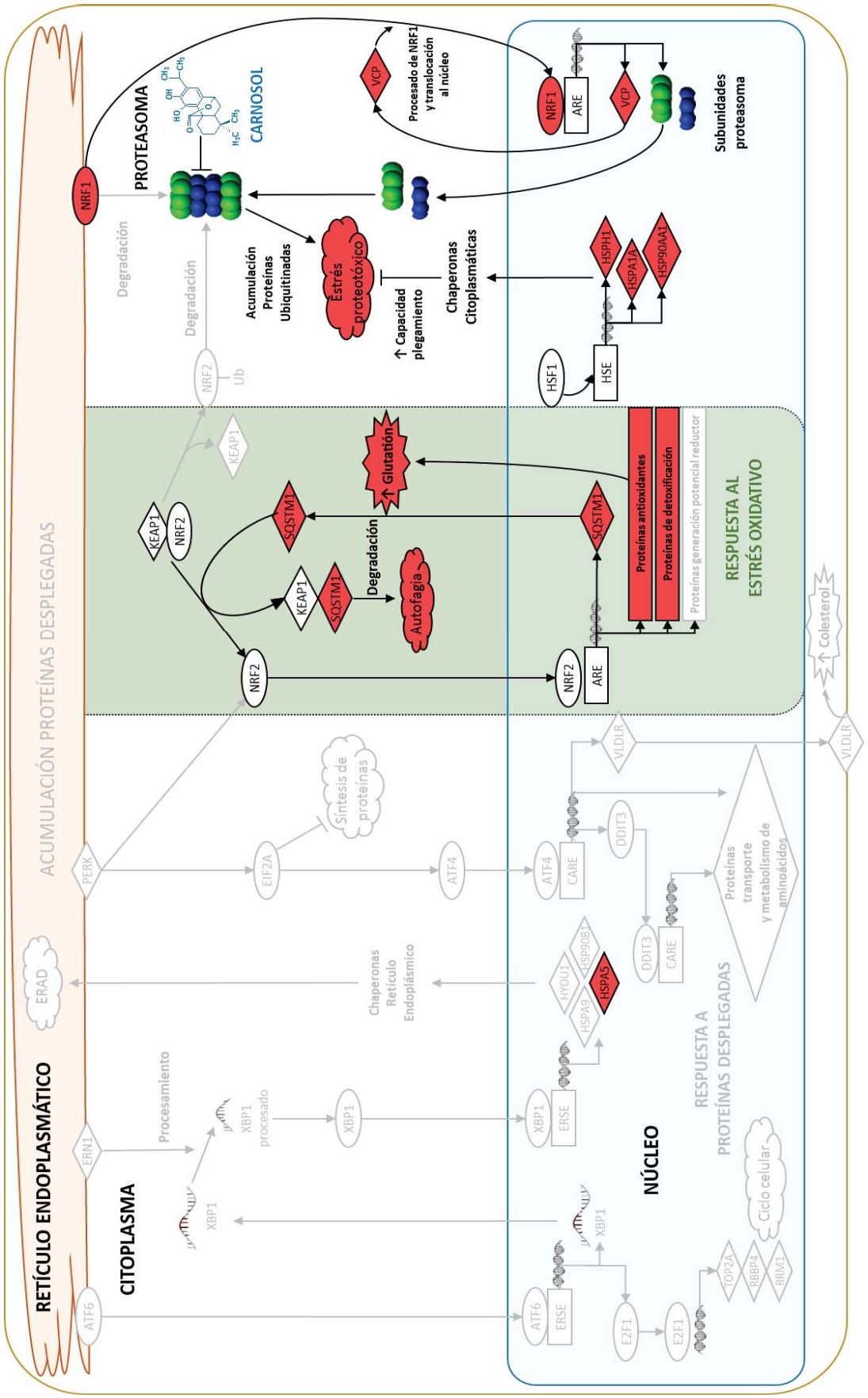

Figura 4.2 Esquema de los efectos producidos a nivel molecular por el carnosol.

Como demuestran los resultados obtenidos durante el desarrollo de la presente Tesis doctoral, la Alimentómica, basada en el uso combinado de tecnologías ómicas y herramientas bioinformáticas, ha permitido estudiar el efecto antiproliferativo de los polifenoles de romero desde un punto de vista global. Esta aproximación también ha permitido generar nuevas hipótesis sobre los posibles mecanismos de acción de estos compuestos, algo difícil de conseguir de haberse llevado a cabo un estudio más clásico centrado en el análisis de un número limitado de marcadores moleculares.

Por otro lado, la falta de herramientas computacionales y métodos estandarizados, así como el existente conocimiento limitado de los procesos celulares a nivel molecular, han sido las principales limitaciones encontradas en el desarrollo de esta Tesis doctoral. Por ello, la interpretación y la integración de la enorme cantidad de datos obtenidos mediante las distintas plataformas ómicas han requerido de un gran esfuerzo, y los resultados presentados en esta Tesis doctoral corresponden a los principales cambios a nivel molecular observados. Los datos ómicos se encuentran almacenados en repositorios públicos, por lo que están a disposición de la comunidad científica para su comprobación y su posible futuro reanálisis.

5. CONCLUSIONES/

CONCLUSIONS

5. CONCLUSIONES

Las conclusiones principales del trabajo realizado se enumeran a continuación:

1. De todos los extractos de romero ensayados, el obtenido mediante SFE empleando CO_2 a 40 ºC, 150 bares de presión y 7% de etanol es el que presenta una actividad antiproliferativa mayor frente a células de leucemia y de cáncer de colon.
2. La actividad antiproliferativa del extracto de romero y de sus polifenoles principales (ácido carnósico y carnosol) es dependiente del tiempo y la concentración. Además, el ácido carnósico y el carnosol tienen actividades antiproliferativas aditivas en la proporción a la que se encuentran en el extracto.
3. El tratamiento con polifenoles de romero bloquea la progresión del ciclo celular en función del tipo celular, la composición fenólica, la concentración y el tiempo de incubación.
4. La estrategia Alimentómica indica que el tratamiento con polifenoles de romero activa la *Respuesta al Estrés Oxidativo* mediante la activación del factor de transcripción NRF2. Además, la activación de NRF2 es dependiente de la composición fenólica, la concentración y el tiempo de incubación.
5. Los estudios transcriptómicos y proteómicos indican que el tratamiento con el extracto de romero y el ácido carnósico induce la activación temprana de la *Respuesta a Proteínas Desplegadas*, y reprime la actividad del factor de transcripción E2F1 en las células HT-29.
6. El extracto de romero y el ácido carnósico inducen la generación de peróxido de hidrógeno en el medio de cultivo, no obstante, esta molécula no interfiere en la expresión de algunos marcadores moleculares involucrados en la *Respuesta al Estrés Oxidativo* y la *Respuesta a Proteínas Desplegadas*.

7. El tratamiento con el extracto de romero y en menor medida con el ácido carnósico induce la acumulación de colesterol en las células HT-29.
8. Se ha demostrado por primera vez que el carnosol inhibe de forma directa la actividad catalítica del proteasoma, con una IC50 de 16.5 μM.

CONCLUSIONS

The following main conclusions are drawn from this PhD Thesis work:

1. Among the tested rosemary extracts, the extract obtained using SFE with CO_2 at 40 ºC, 150 bars and 7% of ethanol shows the highest antiproliferative activity against leukemia and colon cancer cells.
2. The antiproliferative activity of rosemary extract and its main polyphenols (carnosic acid and carnosol) is time and concentration dependent. Moreover, carnosic acid and carnosol show additive antiproliferative activity in the concentration at which they are present in the extract.
3. The rosemary polyphenols stop the cell cycle progression in a manner that depends on the cell model, phenolic composition, concentration and time.
4. The Foodomics strategy indicates that rosemary polyphenols treatment activates the *Oxidative Stress Response* through the activation of NRF2 transcription factor. In addition, NRF2 activation depends on the phenolic composition, the concentration and the time of incubation.
5. The transcriptomics and proteomics studies indicate that rosemary extract and carnosic acid treatment induce the early activation of the *Unfolded Protein Response* and the inactivation of E2F1 transcription factor in HT-29 cells.
6. The rosemary extract and carnosic acid induce hydrogen peroxide production in cell culture medium, however, this molecule does not interfere in the expression of certain molecular biomarkers involved in the *Oxidative Stress Response* and the *Unfolded Protein Response*.
7. The rosemary extract, and in a lesser extent carnosic acid treatment, induces cholesterol accumulation in HT-29 cells.

8. It has been demonstrated for the first time that carnosol directly inhibits the catalytic activity of the proteasome, with an IC50 of 16.5 μM.

6. BIBLIOGRAFÍA

6. BIBLIOGRAFÍA

Adams, J., *Nat. Rev. Cancer* 2004, *4*, 349-360.

Ahmed, F. E., *J. Environ. Sci. Health C. Environ. Carcinog. Ecotoxicol. Rev.* 2004, *22*, 91-147.

Afonso, M. S., de O Silva, A. M., Carvalho, E. B., Rivelli, D. P., Barros, S. B., Rogero, M. M., y col., *Nutr. Metab.* 2013, *10*, 1-19.

Almela, L., Sánchez-Muñoz, B., Fernández-López, J. A., Roca, M. J., Rabe, V., *J. Chromatogr. A* 2006, *1120*, 221-229.

Anand, P., Kunnumakkara, A. B., Sundaram, C., Harikumar, K. B., Tharakan, S. T., Lai, O. S. y col., *Pharm. Res.* 2008, *25*, 2097-2116.

Anđelković, U., Martinović, T., Josić, D., *Curr. Opin. Food Sci.* 2015, *4*, 92–98.

Annadurai, R. S., Neethiraj, R., Jayakumar, V., Damodaran, A. C., Rao, S. N., Katta, M. A., y col., *PLoS One* 2013, *8*, e56217.

Apweiler, R., Bairoch, A., Wu, C. H., Barker, W. C., Boeckmann, B., Ferro, S., y col., *Nucleic Acids Res.* 2004, *32*, 115-119.

Araujo, J. R., Goncalves, P., Martel, F., *Nutr. Res.* 2011, *31*, 77-87.

Arranz, E., Jaime, L., García-Risco, M. R., Fornari, T., Reglero, G., Santoyo, S., *Int. J. Food Sci. Technol.* 2015, *50*, 674–681.

Aruoma, O. I., Halliwell, B., Aeschbach, R., Löliger, J., *Xenobiotica* 1992, *22*, 257–268.

Ashburner, M., Ball, C. A., Blake, J. A., Botstein, D., Butler, H., Cherry, J. M., y col., *Nat. Genet.* 2000, *25*, 25-29.

Aune, D., Chan, D. S. M., Lau, R., Vieira, R., Greenwood, D. C., Kampman, E., y col., *Cancer Causes Control* 2012, *23*, 521-535.

Babovic, N., Zizovic, I., Saicic, S., Ivanovic, J., Petrovic, S., *Chem. Ind. Chem. Eng. Q.* 2010, *16*, 287–293.

Bai, N., He, K., Roller, M., Lai, C. S., Shao, X., Pan, M. H., y col., *J. Agric. Food Chem.* 2010, *58*, 5363-5367.

Bakirel, T., Bakirel, U., Keleş, O. U., Ulgen, S. G., Yardibi, H., *J. Ethnopharmacol.* 2008, *116*, 64-73.

Barczak, A., Rodriguez, M. W., Hanspers, K., Koth, L. L., Tai, Y. C., Bolstad, B. M., y col., *Genome Res.* 2003, *13*, 1775-1785.

Bardou, M., Barkun, A. N., Myriam, M., *Gut* 2013, *62*, 933-947.

Barni, M. V., Carlini, M. J., Cafferata, E. G., Puricelli, L., Moreno, S., *Oncol. Rep.* 2012, *27*, 1041-1048.

Bartels, C., *Biomed. Environ. Mass Spectrom.* 1990, *19*, 363–368.

Bellumori, M., Michelozzi, M., Innocenti, M., Congiu, F., Cencetti, G., Mulinacci, N., *Talanta* 2015, *131*, 81-87.

Benjamini, Y., Hochberg, Y., *J. R. Stat. Soc. B* 1995, *57*, 289–300.

Ben-Nissan, G., Sharon, M., Biomolecules 2014, *4*, 862–884.

Bennink, M. R., en: American Institute for Cancer Research (Ed), *Nutrition and cancer prevention: new insights into the role of phytochemicals*, Springer, New York, 2001, pp.11-17.

Bicchi, C., Binello, A., Rubiolo, P., *Phytochem. Anal.* 2000, *11*, 236–242.

Bobe, G., Murphy, G., Albert, P. S., Sansbury, L. B., Lanza, E., Schatzkin, A., y col., *Int. J. Cancer* 2012, *130*, 1649-1659.

Bousbia, N., Vian, M. A., Ferhat, M. A., Petitcolas, E., Meklati, B. Y., Chemat, F., *Food Chem.* 2009, *114*, 355–362.

Boutron-Ruault, M. C., Senesse, P., Méance, S., Belghiti, C., Faivre, J., *Nutr. Cancer* 2001, *39*, 50-57.

Boyce, M., Yuan, J., *Cell Death. Differ.* 2006, *13*, 363-373.

Brenner, S., Johnson, M., Bridgham, J., Golda, G., Lloyd, D. H., Johnson, D., y col., *Nat. Biotechnol.* 2000, *18*, 630-634.

Brewer, J. W., Hendershot, L. M., Sherr, C. J., Diehl, J. A., *Proc. Natl. Acad. Sci. USA* 1999, *96*, 8505-8510.

Brown, D. W., Butchko, R. A., Busman, M., Proctor, R. H., *Fungal Genet. Biol.* 2012, *49*, 521-532.

Bryant, R. J., McClung, A. M., *Food Chem.* 2011, *124*, 501–513.

Burton, G. R., McGehee, R. E. Jr., *Nutrition* 2004, *20*, 109-114.

Cahan, P., Rovegno, F., Mooney, D., Newman, J. C., St Laurent, G., McCaffrey, T. A., *Gene* 2007, *401*, 12-18.

Cai, F., Dupertuis, Y. M., Pichard, C., *Curr. Opin. Clin. Nutr.* 2012, *15*, 99-106.

Can, G., Cakir, Z., Kartal, M., Gunduz, U., Baran, Y., *Anticancer Res.* 2012, *32*, 2673-2678.

Cao, S. S., Kaufman, R. J., *Antioxid. Redox Signal.* 2014, *21*, 396-413.

Carvalho, B. S., Irizarry, R. A., *Bioinformatics* 2010, *26*, 2363-2367.

Celebier, M., Ibáñez, C., Simó, C., Cifuentes, A., *Methods Mol. Biol.* 2012, *869*, 185-195.

Chaabane, F., Krifa, M., Matera, E., Loussaeif, A., Dijoux-Franca, M. G., Ghedira, K., y col., *Tumour Biol.* 2014, *35*, 8991-8998.

Chen, C. C., Chen, H. L., Hsieh, C. W., Yang, Y. L., Wung, B. S., *Acta Pharmacol. Sin.* 2011, *32*, 62-69.

Chen, G. C., Pang, Z., Liu, Q. F., *Eur. J. Clin. Nutr.* 2012, *66*, 1182-1186.

Cheung, S., Tai, J., *Oncol. Rep.* 2007, *17*, 1525-1531.

Chope, G. A., Cools, K., Hammond, J. P., Thompson, A. J., Terry, L. A., *Ann. Bot.* 2012, *109*, 819-831.

Churchill, G. A., *Nat. Genet.* 2002, *32*, 490-495.

Cifuentes, A., *J. Chromatogr. A* 2009, *1216*, 7109.

Clarkson, B., Strife, A., *Leukemia* 1993, *7*, 1683–1721.

Cox, J., Mann, M., *Nat. Biotechnol.* 2008, *26*, 1367-1372.

Cox, J., Neuhauser, N., Michalski, A., Scheltema, R. A., Olsen, J. V., Mann, M., *J. Proteome Res.* 2011, *10*, 1794-1805.

Crowell, J. A., Steele, V. E., Fay, J. R., *Mol. Cancer Ther.* 2007, *6*, 2139-2148.

Cullinan, S. B., Zhang, D., Hannink, M., Arvisais, E., Kaufman, R. J., Diehl,

J. A., *Mol. Cell. Biol.* 2003, *23*, 7198–7209.

Cunsolo, V., Muccilli, V., Saletti, R., Foti, S., *J. Mass Spectrom.* 2014, *49*, 768-784.

Dodson, M., Redmann, M., Rajasekaran, N. S., Darley-Usmar, V., Zhang, J., *Biochem. J.* 2015, *469*, 347-355.

Dombkowski, A. A., Thibodeau, B. J., Starcevic, S. L., Novak, R. F., *FEBS Lett.* 2004, *560*, 120-124.

Doolaege, E. H. A., Raes, K., Smet, K., Andjelkovic, M., van Poucke, C., de Smet, S., y col., *J. Agric. Food Chem.* 2007, *55*, 7283–7287.

Druker, B. J., Lydon, N. B., *J. Clin. Invest.* 2000, *105*, 3-7.

Dumbravă, D. G., Moldovan, C., Raba, D. N., Popa, M. V., *J. Agroaliment. Proc. Technol.* 2012, *18*, 253–258.

Edgar, R., Domrachev, M., Lash, A. E., *Nucleic Acids Res.* 2002, *30*, 207-210.

Edman, P., *Acta Chem. Scand.* 1950, *4*, 283-293.

Egan, A. N., Schlueter, J., Spooner, D. M., *Am. J. Bot.* 2012, *99*, 175-185.

Einbond, L. S., Wu, H. A., Kashiwazaki, R., He, K., Roller, M., Su, T., y col., *Fitoterapia* 2012, *83*, 1160-1168.

Eng, J. K., McCormack, A. L., Yates III, J. R., *J. Am. Soc. Mass Spectrom.* 1994, *5*, 976-989.

Evans, C., Owen-Lynch, P., Whetton, A. D., Dive, C., *Cancer Res.* 1993, *53*, 1735–1738.

Estruch, R., Ros, E., Salas-Salvadó, J., Covas, M. I., Corella, D., Arós, F., y col., *N. Engl. J. Med.* 2013, *368*, 1279-90.

Faderl, S., Talpaz, M., Estrov, Z., O'Brien, S., Kurzrock, R., Kantarjian, H. M., *New Engl. J. Med.* 1999, *341*, 164–172.

Fatima, T., Snyder, C. L., Schroeder, W. R., Cram, D., Datla, R., Wishart, D., y col., *PLoS One* 2012, *7*, e34099.

Fedirko, V., Tramacere, I., Bagnardi, V., Rota, M., Scotti, L., Islami, F., y col., *Ann. Oncol.* 2011, *22*, 1958-1972.

Fenn, J. B., Mann, M., Meng, C. K., Wong, S. F., Whitehouse, C. M., *Science* 1989, *246*, 64-71.

Ferlay, J., Soerjomataram, I., Ervik, M., Dikshit, R., Eser, S., Mathers, C., y col., *GLOBOCAN 2012 v1.0*, 2013, International Agency for Research on Cancer, Lyon (France) (http://globocan.iarc.fr.)

Fernandes, A. R., Rose, M., Mortimer, D., Carr, M., Panton, S., Smith, F., *J. Chromatogr. A* 2011, *1218*, 9279-9287.

Fiehn, O., *Plant Mol. Biol.* 2002, *48*, 155-171.

Forester, S. C., Lambert, J. D., *Mol. Nutr. Food Res.* 2011, *55*, 844–854

Franke, A. A., Halm, B. M., Kakazu, K., Li, X., en: Fraga, C. G. (Ed), *Plant Phenolics and Human Health*, John Wiley & Sons, Inc., Hoboken, New Jersey, 2013, pp. 165–183.

Freeman, H. J., *World J. Gastroenterol.* 2008, *14*, 1810–1811.

Gallardo, J. M., Carrera, M., Ortea, I., en: Cifuentes, A. (Ed), *Foodomics: Advanced Mass Spectrometry in Modern Food Science and Nutrition*, John Wiley & Sons, Inc., Hoboken, New Jersey, 2013, pp. 125–165.

Gammon, A., Jasperson, K., Kohlmann, W., Burt, R. W., *Best Pract. Res. Clin. Gastroenterol.* 2009, *23*, 219-231.

Ganesh, V., Hettiarachchy, N. S., *Biochim. Biophys. Acta* 2012, *1824*, 1107-1117.

Gao, Q., Liu, H., Yao, Y., Geng, L., Zhang, X., Jiang, L., y col., *J. Appl. Toxicol.* 2015, *35*, 485-492.

García-Cañas, V., Simó, C., Castro-Puyana, M., Cifuentes, A., *Electrophoresis* 2014, *35*, 147-169.

García-Cañas, V., Simó, C., Herrero, M., Ibáñez, E., Cifuentes A., *Anal. Chem.* 2012 *84*, 10150–10159.

García-Cañas, V., Simó, C., León, C., Cifuentes, A., *J. Pharm. Biomed.* 2010, *51*, 290-304.

Garcia-Mata, R., Gao, Y. S., Sztul, E., *Traffic* 2002, *3*, 388-396.

Gerber, M., Hoffman, R., *Br. J. Nutr.* 2015, *113*, 4-10.

Gerber, M., *Br. J. Nutr.* 2012, *107*, S228-S239.

Gerber, S. A., Rush, J., Stemman, O., Kirschner, M. W., Gygi, S., *P. Proc. Natl. Acad. Sci. USA* 2003, *100*, 6940-6945.

Glickman, M. H., Ciechanover, A., *Physiol. Rev.* 2002, *82*, 373-428.

Gomez-Cabrero, D., Abugessaisa, I., Maier, D., Teschendorff, A., Merkenschlager, M., Gisel, A., y col., *BMC Syst. Biol.* 2014, *8*, 1-10.

González-Vallinas, M., Reglero, G., Ramírez de Molina, A., *Nutr. Cancer* 2015a, *67*, 1221-1229.

González-Vallinas, M., Vargas, T., Moreno-Rubio, J., Molina, S., Herranz, J., Cejas, P., y col., *Eur. J. Cancer* 2015b, *51*, 1-8.

Gorham, E. D., Garland, C. F., Garland, F. C., Grant, W. B., Mohr, S. B., Lipkin, M., y col., *J. Steroid. Biochem.* 2005, *97*, 179-194.

Gorrini, C., Harris, I. S., Mak, T. W., *Nat. Rev. Drug Discov.* 2013, *12*, 931-947.

Goss, K. H., Groden, J., *J. Clin. Oncol.* 2000, *18*, 1967-1979.

Groffen, J., Stephenson, J. R., Heisterkamp, N., de Klein, A., Bartram, C. R., Grosveld, G., *Cell* 1984, *36*, 93–99.

Guerrero, I. C., Andrés, L. S., León, L. G., Machín, R. P., Padrón, J. M., Luis, J. G., y col., *J. Nat. Prod.* 2006, *69*, 1803-1805.

Guertin, K. A., Freedman, N. D., Loftfield, E., Stolzenberg-Solomon, R. Z., Graubard, B. I., Sinha, R., *Br. J. Cancer* 2015, *113*, 1081-1085.

Gunderson, K. L., Kruglyak, S., Graige, M. S., Garcia, F., Kermani, B. G., Zhao, C., y col., *Genome Res.* 2004, *14*, 870-877.

Gygi, S. P., Rist, B., Gerber, S. A., Turecek, F., Gelb, M. H., Aebersold R., *Nat. Biotechnol.* 1999, *17*, 994-999.

Hadziabdić, M. O., Bozikov, V., Pavić, E., Romić, Z., *Coll. Antropol.* 2012, *36*, 1427-1434.

Han, J., Back, S. H., Hur, J., Lin, Y. H., Gildersleeve, R., Shan, J., y col., *Nat. Cell Biol.* 2013a, *15*, 481-490.

Han, M. H., Lee, W. S., Jung, J. H., Jeong, J. H., Park, C., Kim, H. J., y col., *Food Chem. Toxicol.* 2013b, *62*, 382-389.

Hansen, L., Skeie, G., Landberg, R., Lund, E., Palmqvist, R., Johansson, I., y col., *Int. J. Cancer* 2012, *131*, 469-478.

Harding, H. P., Zhang, Y., Ron, D., *Nature* 1999, *397*, 271-274.

Hayes, J. D., Dinkova-Kostova, A. T., *Trends Biochem. Sci.* 2014, *39*, 199-218.

Herrero, M., García-Cañas, V., Simó, C., Cifuentes, A., *Electrophoresis* 2010a, *31*, 205-228.

Herrero, M., Plaza, M., Cifuentes, A., Ibáñez, E., *J. Chromatogr. A* 2010b, *1217*, 2512-2520.

Herrero, M., Simó, C., García-Cañas, V., Ibáñez, E., Cifuentes A., *Mass Spectrom. Rev.* 2012, *31*, 49-69.

Hsu, J. L., Huang, S. Y., Chow, N. H., Chen, S. H., *Anal. Chem.* 2003, *75*, 6843-6852.

Huang, M. C., Chen, H. Y., Huang, H. C., Huang, J., Liang, J. T., Shen, T. L., y col., *Oncogene* 2006, *25*, 3267-3276.

Hughes, T. R., Mao, M., Jones, A. R., Burchard, J., Marton, M. J., Shannon, K. W., y col., *Nat. Biotechnol.* 2001, *19*, 342-347.

Hussain, A. I., Anwar, F., Chatha, S. A., Jabbar, A., Mahboob, S., Nigam, P. S., *Braz. J. Microbiol.* 2010, *41*, 1070-1078.

Ibáñez, C., Valdés, A., García-Cañas, V., Simó, C., Celebier, M., Rocamora-Reverte, L., y col., *J. Chromatogr. A* 2012, *1248*, 139-153.

Iriti, M.,Vitalini, S. *Pol. J. Food Nutr. Sci.* 2012, *62*, 71-76.

Ishida, Y., Yamasaki, M., Yukizaki, C., Nishiyama, K., Tsubouchi, H., Okayama, A., y col., *Hum. Cell.* 2014, *27*, 68-77.

Ishihama, Y., Oda, Y., Tabata, T., Sato, T., Nagasu, T., Rappsilber, J., y col., *Mol. Cell. Proteomics* 2005, *4*, 1265-1272.

Iwasaki, R., Ito, K., Ishida, T., Hamanoue, M., Adachi, S., Watanabe, T., y col., *Cancer Sci.* 2009, *100*, 349-356.

Jasperson, K. W., Tuohy, T. M., Neklason, D. W., Burt, R. W., *Gastroenterology* 2010, *138*, 2044-2058.

Jemal, A., Siegel, R., Xu, J., Ward, E., *C. A. Cancer J. Clin.* 2010, *60*, 277-300.

Johansen, T., Lamark, T., *Autophagy* 2011, *7*, 279−296,

Jiang, T., Harder, B., Rojo de la Vega, M., Wong, P. K., Chapman, E., Zhang, D. D., *Free Radic. Biol. Med.* 2015, *88*, 199-204.

Joshi-Tope, G., Vastrik, I., Gopinath, G. R., Matthews, L., Schmidt, E., Gillespie, M., y col., *Cold Spring Harb. Symp. Quant. Biol.* 2003, *68*, 237-243.

Kanehisa, M., *Trends Genet.* 1997, *13*, 375-376.

Katajamaa, M, Oresic, M., *BMC Bioinformatics* 2005, *18*, 6, 1-12.

Key, T. J., Appleby, P. N., Masset, G., Brunner, E. J., Cade, J. E., Greenwood, D. C., y col., *Int. J. Cancer* 2012, *131*, E320-E325.

Khalid, U., Saleem, T., Imam, A. M., Khan, M. R., *World J. Surg. Oncol.* 2011, *9*, 14.

Khan, N., Mukhtar, H., en: Fraga, C. G. (Ed), *Plant Phenolics and Human Health*, John Wiley & Sons, Inc., Hoboken, New Jersey, 2013, pp. 1–49.

Khlifi, D., Sghaier, R. M., Amouri, S., Laouini, D., Hamdi, M., Bouajila, J., *Food Chem. Toxicol.* 2013, *55*, 202-208.

Klaus, S., Pültz, S., Thöne-Reineke, C., Wolfram, S., *Int. J. Obes.* 2005, *29*, 615-623.

Kontogianni, V.G., Tomic, G., Nikolic, I., Nerantzaki, A. A., Sayyad, N., Stosic-Grujicic, S., y col., *Food Chem.* 2013, *136*, 120-129.

Korolchuk, V. I., Menzies, F. M., Rubinsztein, D. C., *FEBS Lett.* 2010, *584*, 1393−1398.

Kruger, W. A., Monteith, G. R., Poronnik, P., *Biochem. Biophys. Res. Commun.* 2013, *432*, 568-573.

Kumar, C., Mann, M., *FEBS Lett.* 2009, *583*, 1703-1712.

Kussmann, M., Panchaud, A., Affolter, M., *J. Proteome Res.* 2010, *9*, 4876-4887.

Lafleur, M. A., Stevens, J. L., Lawrence, J. W., *Toxicol. Pathol.* 2013, *41*, 235−262.

Lamba, G., Ambrale, S., Lee, B., Gupta, R., Rafiyath, S. M., Liu, D., *J. Hematol. Oncol.* 2012, *5*, 21.

Lappe, M., Holm, L., *Nat. Biotechnol.* 2004, *22*, 98-103.

Lee, L. S., Choi, J. H., Sung, M. J., Hur, J. Y., Hur, H. J., Park, J. D., y col., *Mol. Nutr. Food Res.* 2015, *59*, 784-794.

Lee, K. W., Lee, H. J., *Biofactors* 2006, *26*, 105-121.

Levis, S., Strickman-Stein, N., Doerge, D. R., Krischer, J., *Contemp. Clin. Trials* 2010, *31*, 293-302.

Linet, M. S., Cartwright, R. A., en Schottenfeld, D., Fraumeni, J. F. Jr. (Eds), *Cancer epidemiology and prevention*, Oxford University Press, Nueva York, 1996, pp. 841-892.

Liu, H., Sadygov, R. G., Yates III, J. R., *Anal. Chem.* 2004, *76*, 4193-4201.

Liu, R. H., *J. Nutr.* 2004, *134*, 3479-3485.

Lodha, T. D., Basak, J. J., *Mol. Biotechnol.* 2012, *50*, 87–97.

Long, L. H., Hoi, A., Halliwell, B., *Arch. Biochem. Biophys.* 2010, *501*, 162–169.

López-Jiménez, A., García-Caballero, M., Medina, M. Á., Quesada, A. R., *Eur. J. Nutr.* 2013, *52*, 85-95.

Mahbub, A. A., Le Maitre, C. L., Haywood-Small, S. L., McDougall, G. J., Cross, N. A., Jordan-Mahy, N. *Anticancer Agents Med. Chem.* 2013, *13*, 1601-1613.

Maitra, R. D., Kim, J., Dunbar, W. B., *Electrophoresis* 2012, *33*, 3418-3428.

Manach, C., Scalbert, A., Morand, C., Rémésy, C., Jiménez, L., *Am. J. Clin. Nutr.* 2004, *79*, 727-747.

Mangena, T., Muyima, N. Y. O., *Lett. Appl. Microbiol.* 1999, *28*, 291–296.

Mann, M., Hendrickson, R. C., Pandey, A., *Ann. Rev. Biochem.* 2001, *70*, 437-473.

Markus, M. A., Morris, B. J., *Clin. Interv. Aging* 2008, *3*, 331-339.

Marques, F. Z., Markus, M. A., Morris, B. J., *Int. J. Biochem. Cell Biol.* 2009, *41*, 2125-2128.

Martens, L., Hermjakob, H., Jones, P., Adamski, M., Taylor, C., States, D., y col., *Proteomics* 2005, *5*, 3537-3545.

Mayer, B. (Ed), *Bioinformatics for Omics Data*, Springer-Verlag, New York Inc, 2011.

McLafferty, F. W., Fridriksson, E. K., Horn, D. M., Lewis, M. A., Zubarev, R. A. *Science* 1999, *284*, 1289–1290.

Mehrotra, B., Mendes, P., en: Saito, K., Dixon, R. A., Willmitzer, L. (Eds), *Plant Metabolomics*, Springer-Verlag, Heidelberg, Berlin, 2006, pp. 105–111.

Min, K., Jung, K., Kwon, T. K., *J. Cancer Prev.* 2014, *19*, 170–178.

Mirgorodskaya, O. A., Kozmin, Y. P., Titov, M. I., Körner, R., Sönksen, C. P., Roepstorff, P., *Rapid Commun. Mass Spectrom.* 2000, *14*, 1226-1232.

Morin, P. J., Sparks, A. B., Korinek, V., Barker, N., Clevers, H., Vogelstein, B., y col., *Science* 1997, *275*, 1787-1790.

Morozova, O., Marra, M. A. *Genomics* 2008, *92*, 255-264.

Mortazavi, A., Williams, B. A., McCue, K., Schaeffer, L., Wold, B., *Nat. Methods* 2008, *5*, 621-628.

Mulinacci, N., Innocenti, M., Bellumori, M., Giaccherini, C., Martini, V., Michelozzi, M., *Talanta* 2011, *85*, 167-176.

Nakazato, T., Ito, K., Miyakawa, Y., Kinjo, K., Yamada, T., Hozumi, N., y col., *Haematologica* 2005, *90*, 317-325.

Nambiar, P. R., Gupta, R. R., Misra, V., *Mutat. Res.* 2010, *693*, 3-18.

Niculescu, M. D., Pop, E. A., Fischer, L. M., Zeisel, S. H., *J. Nutr. Biochem.* 2007, *18*, 380-390.

Oda, Y., Huang, K., Cross, F. R., Cowburn, D., Chait, B. T., *Proc. Natl. Acad. Sci. USA* 1999, *96*, 6591-6596.

Ojeda-Sana, A. M., van Baren, C. M., Elechosa, M. A., Juarez, M. A., Moreno, S., *Food Control* 2013, *31*, 189–195.

Ong, S. E., Blagoev, B., Kratchmarova, I., Kristensen, D. B., Steen, H., Pandey, A., y col., *Mol. Cell. Proteomics* 2002, *1*, 376-386.

Pagliarini, V., Giglio, P., Bernardoni, P., De Zio, D., Fimia, G. M., Piacentini, M., y col., *J. Cell Sci.* 2015, *128*, 1166-1179.

Paine, M. G., Ramesh Babu, J., Seibenhener, M. L., Wooten, M., W., *FEBS Lett.* 2005, *579*, 5029−5034.

Panchaud, A., Affolter, M., Kussmann, M., *J. Proteomics* 2012, *75*, 3546-3559.

Paniwnyk, L., Cai, H., Albu, S., Mason, T. J., Cole, R., *Ultrasonics Sonochem.* 2009, *16*, 287-292.

Park, S. Y., Song, H., Sung, M. K., Kang, Y. H., Lee, K. W., Park, J. H., *Int. J. Mol. Sci.* 2014a, *15*, 12698-12713.

Park, K. W., Kundu, J., Chae, I. G., Kim, D. H., Yu, M. H., Kundu, J. K., y col., *Int. J. Oncol.* 2014b, *44*, 1309-1315.

Pavlidis, P., Qin, J., Arango, V., Mann, J. J., Sibille, E., *Neurochem. Res.* 2004, *29*, 1213-1222.

Pennazza, G., Fanali, C., Santonico, M., Dugo, L., Cucchiarini, L., Dachà, M., y col., *Food Chem.* 2013, *136*, 668-674.

Peng, C. H., Su, J. D., Chyau, C. C., Sung, T. Y., Ho, S. S., Peng, C. C., y col., *Biosci. Biotechnol. Biochem.* 2007, *71*, 2223-2232.

Peng, M., Taouatas, N., Cappadona, S., van Breukelen, B., Mohammed, S., Scholten, A., y col., *Nat. Methods* 2012, *9*, 524-525.

Perez-Jimenez, F., Alvarez de Cienfuegos, G., Badimon, L., Barja, G., Battino, M., Blanco, A., y col., *Eur. J. Clin. Invest.* 2005, *35*, 421-424.

Perkins, D. N., Pappin, D. J., Creasy, D. M., Cottrell, J. S., *Electrophoresis* 1999, *20*, 3551-3567.

Persidis, A., *Nat. Biotechnol.* 1999, *17*, 94–95.

Petiwala, S. M., Berhe, S., Li, G., Puthenveetil, A. G., Rahman, O., Nonn, L., y col., *PLoS One* 2014, *9*, e89772.

Petiwala, S. M., Johnson, J. J., *Cancer Lett.* 2015, *367*, 93-102

Petiwala, S. M., Puthenveetil, A. G., Johnson, J. J., *Front. Pharmacol.* 2013, *4*, 1-4.

Puthalakath, H., O'Reilly, L. A., Gunn, P., Lee, L., Kelly, P. N., Huntington, N. D., y col., *Cell* 2007, *129*, 1337-1349.

Quintas-Cardama, A., Kantarjian, H. M., Cortes, J. E., *Cancer Control* 2009, *16*, 122-131.

Quiñones, M., Miguel, M., Aleixandre, A., *Pharmacol. Res.* 2013, *68*, 125-131.

Rac, M., Ostric-Matijasevic, B., *Rev. Francaise Corps Gras.* 1955, *2*, 796-803.

Radhakrishnan, S. K., den Besten, W., Deshaies, R. J., *Elife* 2014, *3*, e01856.

Rao, A., Janezic, S., *Nutr. Cancer* 1992, *18*, 43-52.

Ren, R. *Oncogene* 2002, *21*, 8629–8642.

Rogachev, I., Aharoni, A. *Methods Mol. Biol.* 2012, *860*, 129-144.

Roldan-Gutierrez, J. M., Ruiz-Jiménez, J., Luque de Castro, M. D., *Talanta* 2008, *75*, 1369-1375.

Romano, C. S., Abadi, K., Repetto, V., Vojnov, A. A., Moreno, S., *Food Chem.* 2009, *115*, 456–461.

Ross, P. L., Huang, Y. N., Marchese, J. N., Williamson, B., Parker, K., Hattan, S., y col., *Acta Agric. Slov.* 2009, *93*, 51–58.

Rudolf, E., Andelova, H., Cervinka, M., *Anticancer Agent Med. Chem.* 2007, *7*, 559-575.

Rustgi, A. K., *Genes Dev.* 2007, *15*, 2525-2538.

Rutkowski, D. T., Wu, J., Back, S. H., Callaghan, M. U., Ferris, S. P., Iqbal, J., y col., *Dev. Cell* 2008, *15*, 829-840

Saeidnia, S., Abdollahi, M., *Toxicol. Appl. Pharmacol.* 2013, *271*, 49–63.

Salehi, P., Fakhari, A. R., Ebrahimi, S. N., Heydari, R., *Flavour Frag. J.* 2007, *22*, 280-285.

Salido, S., Altarejos, J., Nogueras, M., Sánchez, A, Luque, P., *J. Essent. Oil Res.* 2003, *15*, 10-14.

Sánchez-Camargo, A. P., Mendiola, J. A., Valdés, A., Castro-Puyana, M., García-Cañas, V., Cifuentes, A., y col., *J. Supercrit. Fluids* 2016, *107*, 581-589.

Sánchez-Camargo, A. P., Valdés, A., Sullini, G., García-Cañas, V., Cifuentes, A., Ibáñez, E., y col., *J. Funct. Foods* 2014, *11*, 293-303.

Sant, M., Allemani, C., Sieri, S., Krogh, V., Menard, S., Tagliabue, E., y col., *Int. J. Cancer* 2007, *121*, 911-914.

Santos, F. P., Ravandi, F. Leuk., *Lymphoma* 2009, *50*, 16-26.

Sathe, S. K., Seeram, N. P., Kshirsagar, H. H., Heber D., Lapsle, K. A., *J. Food Sci.* 2008, *73*, 607-614.

Satoh, T., Kosaka, K., Itoh, K., Kobayahi, A., Yamamoto, M., Shimojo, Y., y col., *J. Neurochem.* 2008, *104*, 1116–1131.

Sayd, T., Chambon, C., Laville, E., Lebret, B., Gilbert, H., Gatellier, P., *Food Chem.* 2012, *135*, 2238-2244.

Scalbert, A., Manach, C., Morand, C., Rémésy, C., Jiménez, L., *Crit. Rev. Food Sci. Nutr.* 2005, *45*, 287-306.

Scalbert, A., Williamson, G., *J. Nutr.* 2000, *130*, 2073-2085.

Schmidt, A., Kellermann, J., Lottspeich, F., *Proteomics* 2005, *5*, 4-15.

Schwarz, K., Ternes, W. Z., *Lebensm. Unters. Forsch.* 1992, *195*, 99-103.

Scollard, J., Francis, G. A., O'Beirne, D., *LWT Food Sci. Technol.* 2014, *57*, 16-21.

Sha, Z., Goldberg, A. L., *Curr. Biol.* 2014, *24*, 1573-1583.

Shaffer, J. P., *Annu. Rev. Psychol.* 1995, *46*, 561–584.

Silva, J. C., Gorenstein, M. V., Li, G. Z., Vissers, J. P., Geromanos, S. J., *Mol. Cell. Proteomics* 2006, *5*, 144-156.

Sinha, R., Chow, W. H., Kulldorff, M., Denobile, J., Butler, J., Garcia-Closas, M., y col., *Cancer Res.* 1999, *59*, 4320-4324.

Slamenova, D., Kuboskova, K., Horvathova, E., Robichova, S., *Cancer Lett.* 2002, *177*, 145-153.

Smith, C. A., O'Maille, G., Want, E. J., Qin, C., Trauger, S. A., Brandon, T. R., y col., *Ther. Drug Monit.* 2005, *27*, 747-751.

Smith, C. A., Want, E. J., O'Maille, G., Abagyan, R., Siuzdak, G., *Anal. Chem.* 2006, *78*, 779-787.

Sofi, F., Casini, A., *World J. Gastroenterol.* 2014, *20*, 7339-7346.

Solidoro, A., Salazar, F., de la Flor, J., Sánchez, J., Otero, J., *Cancer* 1981, *48*, 1053-1057.

Stafford, P., en: Hardiman G. (Ed), *Microarray Innovations: Technology and Experimentation*, CRC Press, Boca Raton, 2009, pp. 97–117.

Steijger, T., Abril, J. F., Engström, P. G., Kokocinski, F., Hubbard, T. J., Guigó, R., y col., *Nat. Methods.* 2013, *10*, 1177-1184.

Stewart, B., Wild, C. P., World Cancer Report, 2014, International Agency for Research on Cancer (http://www.thehealthwell.info/node/725845).

Sun, J. M., Jung, H. C., *Korean J. Gastroenterol.* 2004, *44*, 59-65.

Szumny, A., Figiel, A., Gutierrez-Ortiz, A., Carbonell-Barrachina, A. A., *J. Food Eng.* 2010, *97*, 253-260.

Tai, J., Cheung, S., Wu, M., Hasman, D., *Phytomedicine* 2012, *19*, 436-443.

Tanaka, K., Waki, H., Ido, Y., Akita, S., Yoshida, Y., Yoshida, T., y col., *Rapid Commun. Mass Spectrom.* 1988, *2*, 151–153.

Tavani, A., Malerba, S., Pelucchi, C., Dal Maso, L., Zucchetto, A., Serraino, D., y col., *Ann. Oncol.* 2012, *23*, 2737-2742.

Teixeira, B., Marques, A., Ramos, C., Neng, N. R., Nogueira, J. M. F., Saraiva, J. A., y col., *Ind. Crop Prod.* 2013, *43*, 587-595.

Tengstrand, E., Rosén, J., Hellenäs, K. E., Aberg, K. M., *Anal. Bioanal. Chem.* 2013, *405*, 1237-1243.

Thomas, T., Thomas, T. J., *J. Cell Mol. Med.* 2003, *7*, 113-126.

Thompson, A., Schäfer, J., Kuhn, K., Kienle, S., Schwarz, J., Schmidt, G., y col., *Anal. Chem.* 2003, *75*, 1895-1904.

Tirumalai, P. S., Prakash, S., *Afr. J. Microbiol. Res.* 2011, *5*, 5188–5193.

Trachtenberg, A. J., Robert, J. H., Abdalla, A. E., Fraser, A., He, S. Y., Lacy, J. N., y col., *Methods Mol. Biol.* 2012, *802*, 3-17.

Trimigno, A., Marincola, F. C., Dellarosa, N., Picone, G., Laghi, L., *Curr. Opin. Food Sci.* 2015, *4*, 99–104.

Tsiatsiani, L., Heck, A. J., *FEBS J.* 2015, *282*, 2612-2626.

Tuck, K. L., Hayball, P. J., *J. Nutr. Biochem.* 2002, *13*, 636-644.

Udenigwe, C. C., Aluko, R. E., *J. Food Sci.* 2012, *77*, 11-24.

Valdés, A., García-Cañas, V., en Cifuentes, A. (Ed), *Foodomics: Advanced Mass Spectrometry in Modern Food Science and Nutrition*, John Wiley & Sons, Inc., Hoboken, New Jersey, 2013a, pp. 191–220.

Valdés, A., Ibáñez, C., Simó, C., García-Cañas, V., *Trends Anal. Chem.* 2013b, 52, 142–154.

Velculescu, V. E., Zhang, L., Vogelstein, B., Kinzler, K. W., *Science* 1995, *270*, 484-487.

Vergara, D., Simeone, P., Bettini, S., Tinelli, A., Valli, L., Storelli, C., y col., *Food Funct.* 2014, *5*, 1261-1269.

Vicente, G., Molina, S., González-Vallinas, M., García-Risco, M. R., Fornari, T., Reglero, G., y col., *J. Supercrit. Fluids* 2013, *79*, 101–108.

Visanji, J. M., Thompson, D. G., Padfield, P. J., *Cancer Lett.* 2006, *237*, 130-136.

Vizcaíno, J. A., Foster, J. M., Martens, L., *J. Proteomics* 2010, *73*, 2136-2146.

Wang, Z., Gerstein, M., Snyder, M., *Nat. Rev. Genet.* 2009, *10*, 57-63.

Wang, Z. J., Joshi, A. M., Ohnaka, K., Morita, M., Toyomura, K., Kono, S., y col., *Nutr. Cancer* 2012, *64*, 798-805.

Wark, P. A., Lau, R., Norat, T., Kampman, E., *Am. J. Clin. Nutr.* 2012, *96*, 622-631.

Wasinger, V. C., Cordwell, S. J., Cerpa-Poljak, A., Yan, J. X., Gooley, A. A., Wilkins, M. R., y col., *Electrophoresis* 1995, *16*, 1090-1094.

Wasinger, V. C., Zeng, M., Yau, Y., *Int. J. Proteomics* 2013, *2013*, 180605.

Watson, A. J., Collins, P. D., *Dig. Dis.* 2011, *29*, 222-228.

Westerhoff, H. V., Alberghina, L., en Alberghina, L., Westerhoff, H. V. (Eds), *Systems Biology: Definitions and Perspectives*, Springer-Verlag, Heidelberg, Berlin, 2005, pp. 3–9.

WHO, *Cancer Fact sheet N°297* 2015, World Health Organization (http://www.who.int/mediacentre/factsheets/fs297/en/).

Wiener, M. C., Sachs, J. R., Deyanova, E. G., Yates, N. A., *Anal. Chem.* 2004, *76*, 6085-6096.

Wilhelm, B. T., Landry, J. R., *Methods* 2009, *48*, 249-257.

Williams, C. D., Satia, J. A., Adair, L. S., Stevens, J., Galanko, J., Keku, T. O., y col., *Nutr. Cancer* 2010, *62*, 701-709.

Winkler, H., *Verlag Fischer Jena* 1920, *231*.

Wishart, D. S., Knox, C., Guo, A. C., Eisner, R., Young, N., Gautam, B., y col., *Nucleic Acids Res.* 2009, *37*, 603-610.

Witherspoon, M., Chen, Q., Kopelovich, L., Gross, S. S., Lipkin, S. M., *Cancer Discov.* 2013, *3*, 1072-1081.

Wolin, K. Y., Yan, Y., Colditz, G. A., *Br. J. Cancer* 2011, *104*, 882-885.

Wong, J. V., Dong, P., Nevins, J. R., Mathey-Prevot, B., You, L., *Cell Cycle* 2011, *10*, 3086-3094.

Wu, J., Lee, M., Ho, C.T., Chang, S. S., *J. Am. Oil Chem. Soc.* 1982, *59*, 339-345.

Wu, S. J., Feng, B., Li, K., Zhu, X., Liang, S. H., Liu, X. F., y col., *Am. J. Med.* 2012, *125*, 551-559.

Xiang, Q., Liu, Q., Xu, L., Qiao, Y., Wang, Y., Liu, X., *Food Sci. Biotechnol.* 2013, *22*, 1381–1388.

Xiang, Q., Ma, Y., Dong, J., Shen, R., *Int. J. Food Sci. Nutr.* 2015, *66*, 76-84.

Yan, M., Li, G., Petiwala, S. M., Householter, E., Johnson, J. J., *J. Funct. Foods* 2015, *13*, 137-147.

Yates III, J. R., *J. Am. Chem. Soc.* 2013, *135*, 1629–1640.

Yesil-Celiktas, O., Sevimli, C., Bedir, E., Vardar-Sukan, F., *Plant Foods Hum. Nutr.* 2010, *65*, 158–163.

Yu, M. H., Choi, J. H., Chae, I. G., Im, H. G., Yang, S. A., More, K., y col., *Food Chem.* 2013, *136*, 1047-1054.

Zeng, M., Liang, Y., Li, H., Wang, M., Wang, B., Chen, X., y col., *J. Pharm. Biomed. Anal.* 2010, *52*, 265-272.

Zeng, W., Mortazavi, A., *Nat. Immunol.* 2012, *13*, 802-807.

Zhang, B., Powers, R., *Future Med. Chem.* 2012, *4*, 1273-1306.

Zhang, K., Kaufman, R. J., *J. Biol. Chem.* 2004, *279*, 25935-25938.

ANEXO I

LISTA DE PUBLICACIONES

SCI Journals

Valdés, A., Simó, C., Ibáñez, C., Rocamora-Reverte, L., Ferragut, J. A., García-Cañas, V., Cifuentes, A. Effect of dietary polyphenols on K562 leukemia cells: A Foodomics approach. *Electrophoresis* 2012, *33*, 2314-2327.

Ibáñez, C., **Valdés, A.**, García-Cañas, V., Simó, C., Celebier, M., Rocamora-Reverte, L., Gómez-Martínez, A., Herrero, M., Castro-Puyana, M., Segura-Carretero, A., Ibáñez, E., Ferragut, J. A., Cifuentes, A. Global Foodomics strategy to investigate the health benefits of dietary constituents. *J. Chromatogr. A* 2012, *1248*, 139-153.

Valdés, A., García-Cañas, V., Rocamora-Reverte, L., Gómez-Martínez, A., Ferragut, J. A., Cifuentes, A. Effect of rosemary polyphenols on human colon cancer cells: transcriptomic profiling and functional enrichment analysis. *Genes Nutr.* 2013, *8*, 43-60.

Valdés, A., García-Cañas, V., Cifuentes, A. CGE-laser induced fluorescence of double-stranded DNA fragments using GelGreen dye. *Electrophoresis* 2013, *34*, 1555-1562.

Valdés, A., Simó, C., Ibáñez, C., García-Cañas, V. Foodomics strategies for the analysis of transgenic foods. *Trends Anal. Chem.* 2013, *52*, 2-15.

Valdés, A., Ibáñez, C., Simó, C., García-Cañas, V. Recent transcriptomics advances and emerging applications in food science. *Trends Anal. Chem.* 2013, *52*, 142–154.

Ibáñez, C., García-Cañas, V., **Valdés, A.**, Simó, C. Novel MS-based approaches and applications in food metabolomics. *Trends Anal. Chem.* 2013, *52*, 100-111.

Valdés, A., García-Cañas, V., Simó, C., Ibáñez, C., Micol, V., Ferragut, J. A., Cifuentes, A. Comprehensive Foodomics study on the mechanisms operating at various molecular

levels in cancer cells in response to individual rosemary polyphenols. *Anal Chem.* 2014, *86*, 9807-9815.

Sánchez-Camargo, A. P., **Valdés, A.**, Sullini, G., García-Cañas, V., Cifuentes, A., Ibáñez, E., Herrero, M. Two-Step sequential supercritical fluid extracts from Rosemary with enhanced anti-proliferative activity. *J. Funct. Foods* 2014, *11*, 293-303.

Simó, C., Ibáñez, C., **Valdés, A.**, Cifuentes, A., García-Cañas, V. Metabolomics of Genetically Modified Crops. *Int. J. Mol. Sci*. 2014, *15*, 18941-18966.

Valdés, A., Sullini, G., Ibáñez, E., Cifuentes, A., García-Cañas, V. Rosemary polyphenols induce unfolded protein response and changes in cholesterol metabolism in colon cancer cells. *J. Funct. Foods* 2015, *15*, 429-439.

Ibáñez, C., Simó, C., **Valdés, A.**, Campone, L., Piccinelli, A. L., García-Cañas, V., Cifuentes, A. Metabolomics of adherent mammalian cells by capillary electrophoresis-mass spectrometry: HT-29 cells as case study. *J. Pharm. Biomed. Anal.* 2015, *110*, 83-92.

Campone, L., Piccinelli, A. L., Celano, R., Russo, M., **Valdés, A.**, Ibáñez, C., Rastrelli, L. A fully automated method for simultaneous determination of aflatoxins and ochratoxin A in dried fruits by pressurized liquid extraction and online solid-phase extraction cleanup coupled to ultra-high-pressure liquid chromatography-tandem mass spectrometry. *Anal. Bioanal. Chem.* 2015, *407*, 2899-2911.

Valdés, A., García-Cañas, V., Kocak, E., Simó, C., Cifuentes, A. Foodomics study on the effects of extracellular production of hydrogen peroxide by rosemary polyphenols on the anti-proliferative activity of rosemary polyphenols against HT-29 cells. *Electrophoresis* 2016, *0*, 1-10.

Valdés, A., Artemenko, K. A., García-Cañas, V., Bergquist, J., Cifuentes, A. Comprehensive proteomic study of the antiproliferative activity of a polyphenol-enriched rosemary extract on colon cancer cells using nanoliquid chromatography-Orbitrap MS/MS. *J. Proteome Res.* DOI: 10.1021/acs.jproteome.6b00154

Sánchez-Camargo, A. P., Mendiola, J. A., **Valdés, A.**, Castro-Puyana, M., García-Cañas, V., Cifuentes, A., Herrero, M., Ibáñez, E. Supercritical antisolvent fractionation of rosemary extracts obtained by pressurized liquid extraction to enhance their antiproliferative activity. *J. Supercrit. Fluids* 2016, *107*, 581-589.

Valdés, A., García-Cañas, V., Artemenko, K. A., Bergquist, J., Cifuentes, A. Nano-liquid chromatography-Orbitrap MS-based quantitative proteomics reveals differences between the mechanisms of action of carnosic acid and carnosol in colon cancer cells. *Molecular and Cellular Proteomics* (submitted).

Book Chapters and No-SCI Journals

Valdés, A., García-Cañas, V., en Cifuentes, A. (Ed), *Foodomics: Advanced Mass Spectrometry in Modern Food Science and Nutrition*, John Wiley & Sons, Inc., Hoboken, New Jersey, 2013, pp. 191-220.

Valdés, A., Simó, C., Ibáñez, C., García-Cañas, V., en García-Cañas, V., Cifuentes, A., Simó, C. (Eds), *Applications of Advanced Omics Technologies: From Genes to Metabolites*, Elsevier, Oxford, UK, 2014, pp. 107-128.

Valdés, A., Simó, C., Ibáñez, C., García-Cañas, V., en García-Cañas, V., Cifuentes, A., Simó, C. (Eds), *Applications of Advanced Omics Technologies: From Genes to Metabolites*, Elsevier, Oxford, UK, 2014, pp. 349-373.

Ibáñez, C., **Valdés, A.**, García-Cañas, V., Simó, C., en García-Cañas, V., Cifuentes, A., Simó, C. (Eds), *Applications of Advanced Omics Technologies: From Genes to Metabolites*, Elsevier, Oxford, UK, 2014, pp. 249-278.

Ibáñez, C., García-Cañas, V., **Valdés, A.**, Simó, C., en Simó, C., Cifuentes, A., García-Cañas, V. (Eds), *Fundamentals of Advanced Omics Technologies: From Genes to Metabolites*, Elsevier, Oxford, UK, 2014, pp. 235-253.

Valdés, A., Simó, C., Ibáñez, C., García-Cañas, V., en Benkeblia, N. (Eds), *Omics technologies and crops improvement*, Taylor & Francis Group, Broken Sound Parkway, New Jersey, 2015, pp. 15-44.

Valdés, A., García-Cañas, V., Simó, C., Cifuentes, A., Ibáñez, C. Dietary components and their effect in colon cancer: Foodomics evaluation using Tanrsciptomics and Metabolomics. *SECyTA Bulletin* 2012, *33*, 51-68.